



**ROBERT GORDON  
UNIVERSITY•ABERDEEN**

## **OpenAIR@RGU**

### **The Open Access Institutional Repository at Robert Gordon University**

<http://openair.rgu.ac.uk>

#### **Citation Details**

**Citation for the version of the work held in 'OpenAIR@RGU':**

**JOSHI, A. R., 2011. On-line measurement of partial discharges in high voltage rotating machines. Available from *OpenAIR@RGU*. [online]. Available from: <http://openair.rgu.ac.uk>**

#### **Copyright**

Items in 'OpenAIR@RGU', Robert Gordon University Open Access Institutional Repository, are protected by copyright and intellectual property law. If you believe that any material held in 'OpenAIR@RGU' infringes copyright, please contact [openair-help@rgu.ac.uk](mailto:openair-help@rgu.ac.uk) with details. The item will be removed from the repository while the claim is investigated.



# **ON-LINE MEASUREMENT OF PARTIAL DISCHARGES IN HIGH VOLTAGE ROTATING MACHINES**

**ABHIJIT R. JOSHI**

A thesis presented in partial fulfilment of the  
requirements of

The Robert Gordon University  
for the degree of Master of Philosophy

This research programme was carried out  
in collaboration with Dowding & Mills (Aberdeen)

September 2011

## Declaration

I hereby declare that the material presented in this report is the consequence of work undertaken by me at Dowding & Mills in association with The Robert Gordon University.

This report has not been accepted in any previous application for a degree and all the sources of information have been duly acknowledged.

During the course of research, the following training courses were undertaken through an approved Knowledge Transfer Program:

- LabVIEW Basics Course – I (3 days)
- LabVIEW Basics Course – II (2 days)
- Offshore Survival Certificate Course (3 days)
- COMPEX Hazardous Areas Course (5 days)
- Electricity at Work Regulations Course (1 day)

Signature

A handwritten signature in black ink, appearing to read 'A. R. Jones', is written over a horizontal line. The signature is stylized and cursive.

---

September 2011

## **Acknowledgements**

First and foremost I would like to express my sincere gratitude to Prof. John Watson for providing me the opportunity to undertake this project through Knowledge Transfer Programme. His continual support and guidance as my main project supervisor throughout the course of the project was invaluable. I would also like to thank Dr. Dino Kouadria for his valuable inputs and guidance on the various technical aspects and development of this project.

I extend my regards to Mr. Norman Campbell and Dowding & Mills for sponsoring this project. I am also grateful to Mr. Trevor Wilson for his tips on electronic design and for providing me with electronic components from his lab in the time of need.

A special mention of thanks is due to Mr. Steve Elliott of Dowding & Mills without whom the field-testing of this project would have been an impossible task. His co-operation, helpful comments and continuous encouragement to complete my thesis kept me going throughout the project. I am also very grateful to Mrs. Morag Elliott for keeping me motivated and for helping me to proof read the thesis.

I would also like to thank my parents and my sister Akshata, who as always have been an unflinching support in my tough times. Last but not the least I would like to thank my wife Ashwini, for understanding of my days and weekends spent preparing this thesis. Without her support and patience this thesis would have been a distant reality.

## Abstract

The on-line condition monitoring of rotating machines is given paramount importance, particularly in Oils and Gas industries where the financial implications of machine shut-down is very high. This project work was directed towards the on-line condition monitoring of high voltage rotating machines by detection of partial discharges (PD) which are indicative of stator insulation degradation.

Partial discharge manifests itself in various forms which can be detected using various electrical and non-electrical techniques. The electrical method of detecting small current pulses generated by PD using a Rogowski coil as a sensor has been investigated in this work. Dowding & Mills, who are commercially involved in the condition monitoring of rotating machines, currently use a system called StatorMonotor® for PD detection. The research is intended to develop a new partial discharge detection system that will replace the existing system which is getting obsolete.

A three phase partial discharge detection unit was specified, designed and developed that is capable of filtering, amplifying and digitising the discharge signals. The associated data acquisition software was developed using LabVIEW software that was capable of acquiring, displaying and storing the discharge signals. Additional software programs were devised to investigate the removal of external noise. A data compression algorithm was developed to store the discharge data in an efficient manner; also ensuring the backward compatibility to the existing analysis software. Tests were performed in laboratory and on machines on-site and the results are presented. Finally, the data acquisition (DAQ) cards that used the PCMCIA bus was replaced with new USB based DAQ cards with the software modified accordingly.

The three phase data acquisition unit developed as a result of this project has produced encouraging results and will be implemented in an industrial environment to evaluate and benchmark its performance with the existing system. Most importantly, a hardware data acquisition platform for the detection of PD pulses has been established within the company which is easily maintainable and expandable to suit any future requirements.

# Contents

	Page
<b>Declaration</b>	<b>ii</b>
<b>Acknowledgements</b>	<b>iii</b>
<b>Abstract</b>	<b>iv</b>
<b>Contents</b>	<b>v</b>
<b>List of figures</b>	<b>x</b>
<b>List of tables</b>	<b>xiv</b>
<b>Chapter 1 Introduction</b>	<b>1</b>
1.1 Significance of rotating machines	1
1.2 Maintenance strategies	7
1.2.1 Breakdown maintenance	3
1.2.2 Preventive maintenance	3
1.2.3 Predictive maintenance / Condition based maintenance	4
1.2.4 Factors for the implementation of condition monitoring	5
1.3 Faults in high voltage induction motors	7
1.3.1 Bearing faults	7
1.3.2 Rotor faults	8
1.3.3 Stator faults	9
1.4 Condition monitoring methods	10
1.3.1 Vibration monitoring	10
1.3.2 Phase current monitoring	11
1.3.3 Partial discharge monitoring	14
1.5 Objectives of the project	14
<b>Chapter 2 Ageing of Insulation Systems</b>	<b>17</b>
2.1 Introduction	17
2.2 Ageing and stress mechanisms	17
2.2.1 Thermal stress	19
2.2.1.1 Iso-thermal stress	19
2.2.1.2 Thermal cycling	19

2.2.2	Mechanical stress	21
2.2.3	Electrical stress	23
2.2.4	Environmental stress	27
2.2.5	Multifactor stress	28
2.3	Conclusion	30
<b>Chapter 3 Partial Discharge Theory</b>		<b>32</b>
3.1	Introduction	32
3.2	Types of partial discharge	32
3.2.1	Internal discharges	33
3.2.1.1	Analogue discharge circuit	33
3.2.1.2	Discharge sites	36
3.2.2	Surface discharges	37
3.2.3	Corona discharges	38
3.3	Partial discharge theory applied to stator windings	38
3.3.1	Insulation breakdown mechanisms in stator windings	39
3.3.2	Defect locations	40
3.3.3	Slot discharges	41
3.3.4	Endwinding discharges	43
3.3.4.1	Endwinding internal discharges	44
3.3.4.2	Phase – phase discharges	44
3.3.4.3	Surface tracking	45
3.4	Summary	46
<b>Chapter 4 Partial Discharge Detection</b>		<b>47</b>
4.1	Introduction	47
4.2	Non – Electrical detection techniques	47
4.2.1	Chemical detection	48
4.2.2	Acoustic detection	49
4.2.3	Optical detection	50
4.3	Electrical detection techniques	51
4.3.1	Power loss detection methods	51
4.3.2	Detection of current pulses	54
4.3.2.1	Straight detection methods	55
4.3.2.2	Balanced detection method	55
4.3.3	On-line electrical detection systems	56
4.4	Sensors used for electrical PD detection	58
4.4.1	Classification of sensors	58

4.4.1.1	Inductive type sensors	58
4.4.1.2	Capacitive type sensors	59
4.4.2	Rogowski coil	59
4.4.3	Radio frequency current transformer	62
4.4.4	Capacitive coupler	63
4.4.5	Stator slot coupler	64
4.5	Review of commercially available PD detectors	67
4.6	Summary	69
<b>Chapter 5 Single Phase Partial Discharge Monitoring Hardware</b>		<b>70</b>
5.1	Introduction	70
5.2	Hardware specifications	71
5.3	System hardware overview	72
5.4	The Rogowski coil	73
5.4.1	Impulse response of coil	74
5.5	Signal conditioning unit	76
5.5.1	Signal conditioning requirements	76
5.5.2	The Anti-Aliasing Filter (AAF)	79
5.5.2.1	Filter calculations	83
5.5.3	The high-pass filter	87
5.5.4	High gain amplifier	88
5.5.5	Isolation transformer	91
5.5.6	Reference signal generator	92
5.6	Analogue to digital converter	94
5.7	Summary	97
<b>Chapter 6 Single Phase Data Acquisition Software</b>		<b>98</b>
6.1	Introduction	98
6.2	Software specifications	99
6.3	Introduction to LabVIEW software	100
6.4	Data acquisition software	100
6.5	On-site testing of single channel system	102
6.5.1	The test set-up	103
6.5.2	The waveform display	104
6.5.3	Data analysis	105
6.5.3.1	Filtering noise – Method 1	106
6.5.3.2	Filtering noise – Method 2	108
6.6	Summary	112

<b>Chapter 7</b>	<b>Three Phase Partial Discharge Monitoring Hardware</b>	<b>113</b>
7.1	Introduction	113
7.2	Important design considerations	113
7.3	System block diagram	114
7.4	The Rogowski coil	115
7.5	Signal conditioning unit	115
7.5.1	Isolation transformer	115
7.5.2	Input variable gain amplifier	115
7.5.3	High-pass filter	117
7.5.4	Low-pass filter (AAF)	117
7.5.5	Output variable gain amplifier	118
7.6	Analogue to digital converter	120
7.5	Summary	121
<b>Chapter 8</b>	<b>Three Phase Data Acquisition Software</b>	<b>122</b>
8.1	Introduction	122
8.2	Data acquisition software	122
8.3	On-site testing of 3-channel system	125
8.3.1	Comparison of system performance	126
8.3.2	Continuous data acquisition	129
8.3.3	PD and noise	131
8.3.4	Data compression	132
8.4	USB data acquisition system	134
8.5	Summary	137
<b>Chapter 9</b>	<b>Discussion</b>	<b>138</b>
9.1	Software development	138
9.1.1	Noise detection and filtering	138
9.1.2	PD data display methods	139
9.1.3	PD analysis techniques	141
9.2	Remote monitoring system	147
9.3	Summary	148
<b>Chapter 10</b>	<b>Conclusions and Future work</b>	<b>149</b>
10.1	Conclusions	149
10.2	Future work	151
10.2.1	Hardware development	151
10.2.2	Software development	155

<b>References</b>	<b>157</b>
<b>Appendix A-1 Comparison of various available discharge Detectors in the market</b>	<b>169</b>
<b>Appendix A-2 PDC-85 Rogowski coil data sheet</b>	<b>170</b>
<b>Appendix A-3 Circuit diagrams for single channel system</b>	<b>171</b>
Appendix A-3.1 Input amplifier	171
Appendix A-3.2 4 <sup>th</sup> Order high-pass filter	172
Appendix A-3.3 6 <sup>th</sup> Order low-pass filter	173
Appendix A-3.4 Output amplifier	174
Appendix A-3.5 Reference signal circuit	175
Appendix A-3.6 Ground connections	175
<b>Appendix A-4 Circuit diagrams for three channel system</b>	<b>176</b>
Appendix A-4.1 Input amplifier	176
Appendix A-4.4 Output amplifier	177
<b>Appendix A-5 LabVIEW program details</b>	<b>178</b>
Appendix A-5.1 Single channel DAQ program	178
Appendix A-5.2 Amplitude based filtering technique	180
Appendix A-5.3 Frequency based filtering technique	182
Appendix A-5.4 Three phase DAQ program for continuous acquisition	184
Appendix A-5.5 Data compression program	186
Appendix A-5.6 Three phase USB DAQ program	188
<b>Appendix A-6 Printed Circuit Board details</b>	<b>198</b>
Appendix A-6.1 Top silk layer of PCB	198
Appendix A-6.2 Top copper layer (component side) of PCB	199
Appendix A-6.3 Bottom copper layer (solder side) of PCB	200

# List of Figures

## Chapter 1

Figure 1.1	Overview of different maintenance types	2
Figure 1.2	Strengths and weaknesses of different maintenance strategies	6
Figure 1.3	Air gap eccentricity	8
Figure 1.4	Typical test set-up for MCSA	12
Figure 1.5	Sidebands generated due to rotor faults	13

## Chapter 2

Figure 2.1	Typical operating conditions of insulation systems in rotating machines	18
Figure 2.2	Movement of stator bar in relation to stator core	22
Figure 2.3	Multistress ageing	30

## Chapter 3

Figure 3.1	Simplified representation of partial discharge	32
Figure 3.2	Different types of discharges	33
Figure 3.3	Simplified model of a cavity in dielectric	34
Figure 3.4	Sequence of internal discharges under a.c. voltage	35
Figure 3.5	Surface discharges	37
Figure 3.6	Failure modes in 3 phase stator windings	39
Figure 3.7	Form-wound stator coil	40
Figure 3.8	Typical defects in slot section	43
Figure 3.9	Typical defects in endwinding section	45

## Chapter 4

Figure 4.1	Dielectric loss as function of voltage	52
Figure 4.2	The Schering Bridge circuit	53
Figure 4.3	Basic circuit of dielectric loss analyser	54
Figure 4.4	Basic circuit for straight detection method	55
Figure 4.5	Basic balanced detection method	56
Figure 4.6	Rogowski coil PD measurement circuit for rotating machines	60
Figure 4.7	Photograph of Rogowski coil inside motor terminal box	61
Figure 4.8	Capacitive coupler detection circuit	63

## **Chapter 5**

Figure 5.1	General block diagram for computer based PD detection system	70
Figure 5.2	Basic block diagram of single phase monitoring system	72
Figure 5.3	Rogowski coil and installation	74
Figure 5.4	RC circuit for generating pulses	74
Figure 5.5	Set-up for testing response of PDC-85 Rogowski coil	75
Figure 5.6	Pulse response of PDC-85 coil	75
Figure 5.7	Different configuration of DAQ system	78
Figure 5.8	Passive single pole low-pass filter	79
Figure 5.9	Anti-aliasing filter characteristics	81
Figure 5.10	Desired response of AAF filter	82
Figure 5.11	Sallen-Key second order low-pass filter circuit	83
Figure 5.12	Practical frequency response of the AAF	87
Figure 5.13	Frequency response of the combined band-pass filter	88
Figure 5.14	Frequency response of input variable gain amplifier	90
Figure 5.15(a)	Front panel of single channel hardware system	93
Figure 5.15(b)	Internal assembly of single channel hardware system	94
Figure 5.16	Complete block diagram of single phase system	96

## **Chapter 6**

Figure 6.1	Front panel of single phase acquisition program	101
Figure 6.2	Test set-up for single phase data acquisition	103
Figure 6.3	PD data acquired with different gain settings	104
Figure 6.4	Typical banded discharge activity	105
Figure 6.5	FFT spectrum of acquired PD signal	106
Figure 6.6	Amplitude based filtering – time domain waveforms	107
Figure 6.7	Amplitude based filtering – frequency domain waveforms	108
Figure 6.8	Complete frequency spectrum of the acquired signal	109
Figure 6.9	Band-pass filtering – time domain signal	109
Figure 6.10	Band-pass filtering – frequency domain signal	110
Figure 6.11	Band-reject filtering – time domain signal	111
Figure 6.12	Band-reject filtering – frequency domain signal	111

## **Chapter 7**

Figure 7.1	Complete block diagram of three phase PD detection system	115
Figure 7.2	Frequency response of input amplifier (3-phase system)	117
Figure 7.3	Frequency response of band-pass filter (3-phase system)	118

Figure 7.4(a)	Front panel of the 3-channel hardware system	120
Figure 7.4(b)	Internal assembly of 3-channel hardware system	120
Figure 7.5	DAQ card interface box	121
<b>Chapter 8</b>		
Figure 8.1	Front panel of three phase data acquisition program	123
Figure 8.2	Test set-up for three phase data acquisition	125
Figure 8.3(a)	PD data for machine M1 with gain of 1200	127
Figure 8.3(b)	PD data for machine M1 with gain of 2700	127
Figure 8.4(a)	PD data for machine M2 with gain of 310	128
Figure 8.4(b)	PD data for machine M2 with gain of 600	128
Figure 8.5	Single cycle PD data from generator	130
Figure 8.6	Effect of data compression on raw PD data	134
Figure 8.7	Front panel of USB DAQ system	138
<b>Chapter 9</b>		
Figure 9.1	Pulse height distribution graph	140
Figure 9.2	' $\phi$ -q-n' pattern display of PD data	140
Figure 9.3	Typical process diagram for PD data analysis	144
Figure 9.4	Block diagram of an expert PD system	146
Figure 9.5	Generalised scheme of a remote monitoring system	148
<b>Chapter 10</b>		
Figure 10.1	New design for signal conditioning unit	153
Figure 10.2	Standard 8 slot PXI chassis with controller	154
<b>Appendix A-5</b>		
Figure A-1	LabVIEW block diagram – Single channel DAQ program	179
Figure A-2	LabVIEW block diagram – Amplitude based filtering	181
Figure A-3	LabVIEW block diagram – Frequency based filtering	183
Figure A-4	LabVIEW block diagram – Three phase continuous data acquisition	185
Figure A-5	LabVIEW block diagram – Data compression program	187
Figure A-6	Software hierarchy diagram for USB DAQ	188
Figure A-7	LabVIEW block diagram – 'Acquire' state for three phase USB DAQ program	190
Figure A-8	LabVIEW block diagram – 'Save' state for three phase USB DAQ program	192

Figure A-9	LabVIEW block diagram – ‘Read’ state for three phase USB DAQ program	194
Figure A-10	LabVIEW block diagram – <i>Master_DAQ_config.vi</i>	195
Figure A-11	LabVIEW block diagram – <i>Slave_DAQ_config.vi</i>	196
Figure A-12	LabVIEW block diagram – <i>Graph.vi</i>	197

## List of Tables

<b>Chapter 1</b>		
Table 1.1	Distribution of failures on failed motor components	7
<b>Chapter 3</b>		
Table 3.1	Relative permittivity and breakdown strength of HV insulating materials	34
<b>Chapter 4</b>		
Table 4.1	Comparison of various electrical PD detection sensors	66
<b>Chapter 5</b>		
Table 5.1	Data acquisition hardware specifications	71
Table 5.2	Gain matrix for combination of input and output amplifier	91
<b>Chapter 6</b>		
Table 6.1	Software specifications for single channel PD system	99
<b>Chapter 7</b>		
Table 7.1	Gain setting details of 3-phase system	119
<b>Chapter 8</b>		
Table 8.1	Data storage format for StatorMonitor PD analysis software	133
<b>Chapter 10</b>		
Table 10.1	Estimate costing for PXI DAQ system	155

# CHAPTER 1: INTRODUCTION

## 1.1 Significance of Rotating Machines

The importance of rotating machines cannot be overemphasised as it is most widely used in modern industry. They are available in various sizes with powers ranging from a fraction of a watt to hundreds of mega-watts. The applications are numerous, limited only by the capacity of imagination. They are used as motors for driving pumps in water-supply plants, traction motors for electrical trains, generators in power plants, etc. In industry, the motors are used for driving compressors, fans and pumps, machine tools, robots, transport equipment and a multitude of other applications.

With the advancement in material science the modern machines are now designed to tighter margins as economics, and subsequently profit, take on a greater precedence in a very competitive marketplace. In addition to this there is a strong economic incentive to continue running older machines up to and beyond their original design lifetime. Therefore, in a climate of such harsh economic reality, modern industry experiences a small but significant number of faults in their rotating plant, which may eventually lead to failure and subsequent loss of availability. The financial costs of such losses represent a significant percentage of the capital cost of the machine. This is especially applicable to high-cost operational environments, such as offshore oil and gas production, where an entire platform may have to shut down if a particularly crucial machine fails. Hence, the efficient maintenance of such electrical assets has become crucial.

## 1.2 Maintenance strategies

Productivity is a key factor for all manufacturing industries to stay competitive in the ever-growing global market. Increased productivity can be achieved through increased availability and minimal downtime. This has a direct focus on the different maintenance types and maintenance strategies used. Thus the maintenance organisation in the company probably has one of the most important functions, namely looking after the assets and keeping track of equipment in order to secure productivity.

The maintenance costs form a major part of the total operating costs of a manufacturing plant. Depending on the type of industry the maintenance cost can represent between 15 and 60 percent of the cost of goods produced <sup>(1)</sup>. This has put

the maintenance department in all industries under continual pressure to reduce the maintenance costs. With a poor maintenance organisation a company will lose a significant amount due to lost production capacity, cost of keeping spare parts, quality deficiencies, etc. Hence an effective maintenance strategy is a crucial component in any organisation's operations.

Over the past few years the maintenance strategies have undergone remarkable changes. The science of maintenance has evolved from simply reacting to machinery breakdowns (*breakdown maintenance*), to performing time-based preventive maintenance, to today's emphasis on the ability to detect early forms of degradation in predictive maintenance (*condition based maintenance*). Many industries now use the relatively modern condition based maintenance strategies in parallel with conventional maintenance schemes. This has reduced unexpected failures; increase the time between planned shutdowns for standard maintenance and reduced operational costs. An overview of different maintenance strategies is shown in figure 1.1

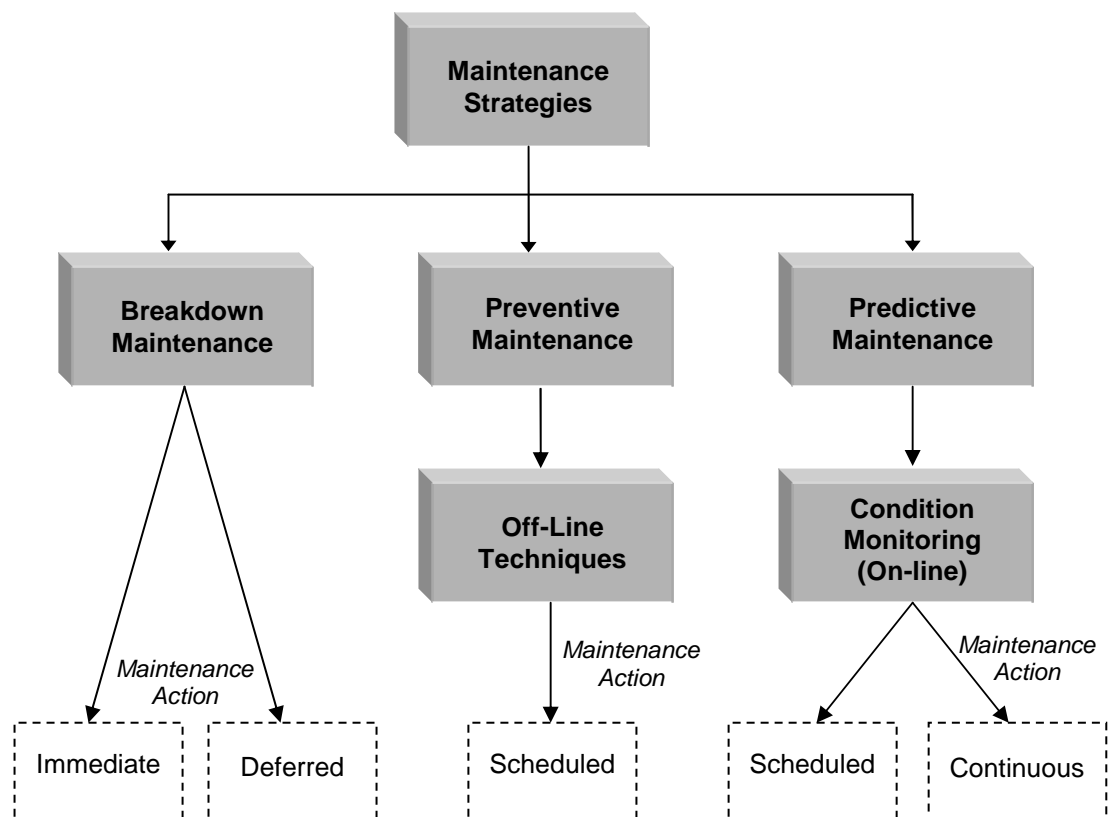


**Figure 1.1 Overview of different maintenance types <sup>(8)</sup>**

### **1.2.1 Breakdown maintenance**

The breakdown maintenance strategy allows the equipment to run until a breakdown occurs and is the simplest approach to maintenance. It is a reactive form of maintenance technique that waits for the machine or equipment to fail before any maintenance action is taken. For some equipment the maintenance action must be performed immediately, for others the maintenance action can be deferred in time, all depending on the equipment's function. A plant using a breakdown maintenance strategy does not invest any money in maintenance until a machine or system fails to operate. Often referred to as '*corrective maintenance*', it is the most expensive form of maintenance strategy. The major expenses associated with this form of strategy are the high spare parts inventory cost, high overtime-labour costs, high machine downtime and low machine availability.

Because no attempt is made to anticipate the maintenance requirements, a plant implementing breakdown maintenance must be able react to all possible failures within the plant. This forces the maintenance department to maintain extensive spare parts inventories, particularly for all the critical equipment in the plant. An alternative is to rely on equipment vendors who can provide immediate delivery for all required spare parts. Even if the latter was possible, premiums for the expedited delivery substantially increase the cost of repair parts and the downtime required to correct machine failure. Such a scenario is of particular relevance to process industries, like the oil and gas industry, where unexplained or unplanned shutdowns can have serious financial consequences in terms of lost production. However, this may be an appropriate strategy in some cases such as, when a failure has no serious cost or safety consequence or is low on the priority list or when implementing a predictive maintenance strategy is not practical. Breakdown maintenance can also be considered as the default maintenance action since the possibility of an unexpected breakdown will always exist.

### **1.2.2 Preventive maintenance**

Preventive maintenance can be defined as a series of predefined and scheduled maintenance activities that are designed to reduce equipment breakdowns, increase equipment reliability and improve productivity <sup>(2)</sup>.

Contrary to breakdown maintenance, preventive maintenance takes steps to prevent and fix problems before a failure occurs. All the preventive maintenance strategies are

time-driven programs and mainly use off-line monitoring techniques. The maintenance is performed on a scheduled basis with scheduled intervals often based on manufacturer's recommendations and past experience with the equipment. The maintenance includes activities like keeping an accurate history of equipment performance and repairs, routine inspections, performing necessary upkeep and servicing, cleaning, lubrication, etc. The main advantage of preventive maintenance is that outages and shutdowns can be planned in advance and the resources can be allocated accordingly, preventing any undue burden on the production activity.

However, there are also disadvantages to this strategy. At times, equipment that is in good condition will be removed from service (off-line) when not necessary, causing loss of production and incurring unnecessary labour and outage costs. In addition, the machine is exposed to the risk of inadvertent damage or incorrect assembly. Failure can still occur between inspections causing unscheduled breakdown.

### **1.2.3 Predictive maintenance / Condition Based Maintenance**

Predictive maintenance can be defined as a "*maintenance technique that applies various technologies and analytical tools to measure and monitor various system and component operating characteristics and to compare these data with established and known standards and specifications in order to predict (forecast) system or component failures*" <sup>(2)</sup>. Another definition describes the strategy as "*the process of identifying production equipment needing maintenance, before its performance gets to a point that quality is reduced or an unplanned shutdown occurs*" <sup>(3)</sup>.

Whereas the breakdown maintenance is applied after the failure and preventive maintenance uses precautionary measures to avert possible problems, predictive maintenance actually evaluates the existing equipment condition based on the recording of measurements to predict the condition of equipment. Hence it is often referred as *condition based maintenance (CBM)*. CBM relies on condition monitoring techniques such as oil analysis, vibration analysis, thermography, phase current analysis, partial discharge analysis and other diagnostic techniques for making maintenance decisions. Most of these techniques are non-invasive on-line monitoring techniques and do not interfere with the normal operation of the equipment. This saves the precious production time and enables the testing to be carried out under stress conditions that are present during normal operation. CBM technique can provide several advantages over other maintenance strategies:

- Improved availability of the equipment
- Improved production quality, reliability and safety
- Improved planning and scheduling of repairs
- Reduced cost of spares and materials

Because of these reasons on-line condition monitoring has gained considerable importance and has become well established in the industry. However there are some disadvantages associated with this strategy. Effective condition monitoring requires the appropriate testing equipment and properly trained staff. Hence the investment cost tends to be high with specialist skills required for assessing the condition of the equipment. There may be a temptation to introduce condition monitoring to areas where the benefits are marginal, such as non-critical equipment. The strengths and weaknesses of different maintenance strategies are shown in figure 1.2.

#### **1.2.4 Factors for the implementation of condition monitoring**

The implementation of an effective condition monitoring system depends on the following factors:

- A clear relationship must exist between the measurements being taken and the condition of the equipment.
- The monitoring system must be reliable and should be able to respond quickly to provide enough warning of deterioration in the condition of the machine for appropriate action to be taken. For example, if a monitoring scheme could only detect a fault one second before the machine fails, then this scheme would not be beneficial for maintenance. If the scheme, however, could progressively monitor the development of a fault over a number of weeks or months, it would be of considerable value for maintenance.
- The benefits of performing condition monitoring to predict equipment condition must outweigh the implementation and running costs.
- The machine should be able to be taken out of service and repaired at a cost substantially less than the likely cost of repairs following failure.
- The result of monitoring produces significantly less production loss due to maintenance scheduling, as opposed to unexpected failures.

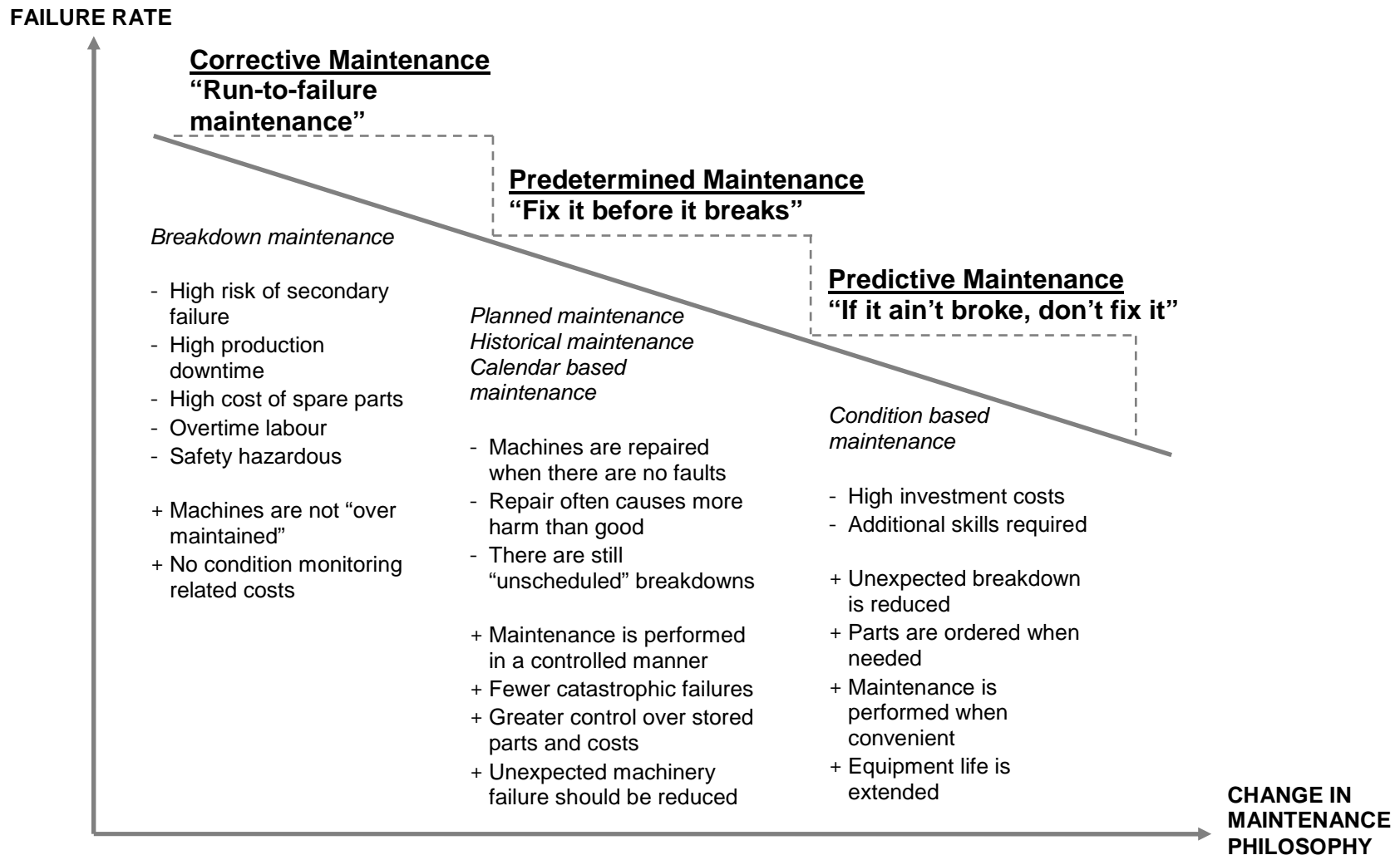


Figure 1.2 Strengths and Weaknesses of different maintenance strategies <sup>(8)</sup>

## 1.3 Faults in high voltage induction motors

The induction motor is the most prevalent machine found in the industry today and is known for its simple construction and ruggedness. Large induction motors are often used in hostile environments such as mines, offshore oil exploration and production platforms. In such environments the machines are exposed to a diverse amount of contamination and operated rigorously which can lead to various faults. For example, direct on-line starting is still prevalent whereby the machine is started at full load causing high mechanical and thermal stresses.

The manifestations of faults can be either mechanical, electrical or a combination of both. Some of the major faults are bearing failure, rotor bar breakages, eccentricity problems and stator winding failure. A survey of failures in high voltage induction motors in the petrochemical industry has been presented Thorsen et al. <sup>(4)</sup>. Table 1.1 shows the details of the failed components along with the number of failures and its percentage.

**Table 1.1 Distribution of failures on failed motor component <sup>(4)</sup>**

Failed component	Number of failures	Percent
Bearing	129	51.6
Stator Windings	62	24.8
Rotor-bars / rings	15	6
Shaft or coupling	8	3.2
External device	34	13.6
Not specified	2	0.8
Total	250	100

The main fault contributors of motor faults are described below:

### 1.3.1 Bearing faults

There are many reasons attributable for bearing faults. Rotor malfunctions and dynamic failures produce a great deal of energy that is dissipated from the system through bearings and their support. Some of the main reasons for failure are improper or insufficient lubrication, heavy radial and axial stresses due to shaft deflection, worn teeth in gearboxes, coupling misalignment and inadequate mounting. This list is not

exhaustive, but is examples of major stresses that may lead to increased vibrations and thereby, increased wear and tear of the motor bearings.

### 1.3.2 Rotor faults

Rotor faults are mainly caused by breaks in the joints between bars and end rings. This can happen for a number of reasons, such as casting problems during the manufacturing process, excessive vibrations caused by pulsating load or stresses due to direct on-line start-ups. When a bar cracks it produces a high resistance joint on the end ring, causing overheating which may eventually lead to bar completely breaking. A broken bar increases the current flowing through the remaining bars, resulting in torque fluctuations which may cause further mechanical damage.

Air-gap eccentricity is another rotor related fault that can lead to severe mechanical problems. Air-gap eccentricity is said to exist when a non-uniform air-gap between the rotor and the stator occurs. There are two types of air-gap eccentricity, namely static and dynamic. In the case of static eccentricity the minimum air-gap between the stator and rotor is fixed in space. This may be caused by the stator core ovality or due to the incorrect positioning of the rotor or stator. In the case of dynamic eccentricity, the minimum air-gap rotates with the rotor. Dynamic eccentricity may be caused due to several factors such as bent rotor shaft, bearing wear or misalignment, etc. Figure 1.3 below shows the air-gap eccentricity.

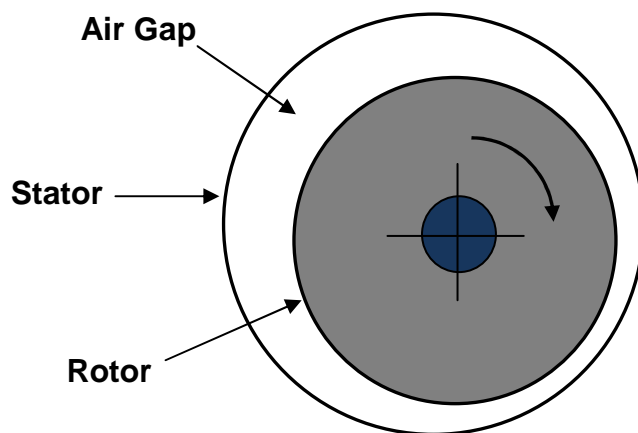


Figure 1.3 Air gap eccentricity

In reality, an inherent level of static and dynamic eccentricity tends to exist even in newly manufactured machines. However, an increase in the air gap eccentricity leads to non-uniformity of the magnetic flux causing abnormal mechanical stresses and vibrations. This can have an adverse effect on the bearings which in turn will lead to higher levels of eccentricity. In severe cases a catastrophic failure can occur if the air gap eccentricity increases to such a level that the resultant unbalanced magnetic pull causes a rotor to stator rub.

### **1.3.3 Stator faults**

Table 1.1 shows that around 25% of all large induction motor failures are attributable to stator faults with the main reason being the breakdown of high voltage (HV) stator insulation <sup>(4)</sup>. The HV insulation breakdown may be result of many factors such as deposits of contamination on insulation, conductor vibration, thermal cycling, repetitive voltage surges and transients, chemical attack or insulation degradation due to internal discharges <sup>(5, 6)</sup>.

For example, winding insulation can become contaminated with oil, carbon dust, cement dust, insects, etc. This contamination mixes with moisture or oil to form a partially conductive coating on the stator winding. This results in electrical tracking affecting the health of the insulation <sup>(6)</sup>. Vibration is probably one of the major causes of premature degradation of HV stator windings. The high electromagnetic forces between the rotor and stator act directly on the coils in the slots. If there is any loosening of the coil in the slot the vibrations will lead to mechanical abrasion of the coil sides in the slot, eroding the insulation. If the insulation breaks down completely, then a short circuit can occur locally between the coils, causing severe damage to the HV stator windings. Severe insulation degradation, if undetected, can propagate through the stator in a very short time.

Whenever degradation occurs in a HV stator insulation system, be it due to electrical, mechanical or environmental conditions, it is generally accompanied by the generation of partial discharges <sup>(7)</sup> which further aids the degradation process. Partial discharges are discussed in detail in the chapter 3. However, it is noteworthy that the HV stator insulation degradation process is usually not a sudden death event. It is a slow process and is more likely to be the end result of progressive degradation over a period of time which can be as short as a few months or as long as tens of years.

## 1.4 Condition monitoring methods

An arsenal of methods, electrical or otherwise, is used for the condition monitoring of rotating machines <sup>(5, 14, 15)</sup>. Condition monitoring is applied as a diagnostic tool, both for fault detection and as a basis for maintenance planning. Various monitoring techniques use different machine variables like magnetic flux, vibration, acoustic noise, temperature, air-gap torque, power, phase current, partial discharge, etc. as monitoring parameters. Some of the most popular methods applied for condition monitoring of rotating machines are as follows:

### 1.4.1 Vibration monitoring

Rotating machines are complex mechanical structures with articulate elements. Each machine will have at least two sets of its own bearings, a possible gear reducer with several bearings and gear sets, a coupling arrangement, etc. These parts, when excited, could oscillate, where joints to other coupled elements transmit such oscillations. The result is a complex frequency spectrum that is characteristic to that equipment and is made up of a combination of all parts of the equipment. Each time the behaviour of the component changes (due to wear or crack), a frequency component of the system will be affected thus changing the vibration patterns <sup>(9)</sup>. Gaps, failures or misalignment of bearings of rotating machines, shaft or coupling misalignment reflect on the change of frequencies or the appearance of new ones.

Vibration monitoring uses vibration transducers, such as accelerometers of piezoresistive types with linear frequency response. The measured parameters are displacement, velocity and acceleration. The transducers are fixed around the bearings of the motor to monitor the varying patterns of vibration. In general the orientation of the sensors follows the three main axis of the machine, i.e. vertical, horizontal and axial.

The acquired signals are normally processed and stored using various analysis methods like spectrum analysis or cepstrum analysis. Vibration monitoring and analysis methods have been discussed in detail in <sup>(10, 11, 12)</sup>. If the condition of the machine deteriorates, the vibration associated with it will generally alter in a predictable way. By measuring and analysing the vibration of a machine, it may be possible to determine the nature and extent of deterioration and predict the machine behaviour in future. The components that are typically monitored using this technique include couplings, bearings, rotors / shafts, and gears. This technique can distinguish several failures

such as imbalance, looseness, misalignment, wear and poor lubrication. Vibration monitoring has been largely adopted by a number of industries, but has the inherent disadvantage of having to affix transducers to the machines being monitored, often in quite inaccessible places.

#### **1.4.2 Phase current monitoring**

Monitoring machine current can provide an indication to various faults developing within rotating machines <sup>(16, 17, 21)</sup>. One of the most popular applications of current monitoring is the detection of rotor faults like broken rotor bars or high resistance joints within the rotor cage <sup>(5, 18, 19, 20, 22)</sup>. Specific spectral components in the current indicate the presence of defects in the rotor. This technique is popularly known in the industry as Motor Current Signature Analysis (MCSA) or Phase Current Signature Analysis (PCSA).

The current drawn by an ideal motor should have a single component at the supply frequency. However, in practice the current flowing in the stator winding doesn't just depend on the power supply and impedance of the windings, but also includes current induced in the stator winding generated by the magnetic field of the rotor. If an asymmetry is created in rotor currents (due to faults like broken rotor bars or broken short-circuit ring), this will be reflected in the stator current. Thus the stator windings act as a probe or transducer for problems occurring in the rotor. The key issue of MCSA is separating the currents that flow through the stator to drive the motor from the currents that the rotor induces back into the stator if there is a problem. This separation is achieved by measuring current component frequencies other than power frequencies.

A suitable current transformer is clamped around one of the phase cables carrying the load current and the data is recorded over a short period of time. The data gathered is then analysed with a spectrum analyser or a customised data signal processing unit. A schematic representation of a typical test set-up is shown in figure 1.4. This technique has the advantage that no direct access to the motor is required as the phase current can be monitored by a simple clip-on type current transformer placed directly around any phase cable feeding motor.

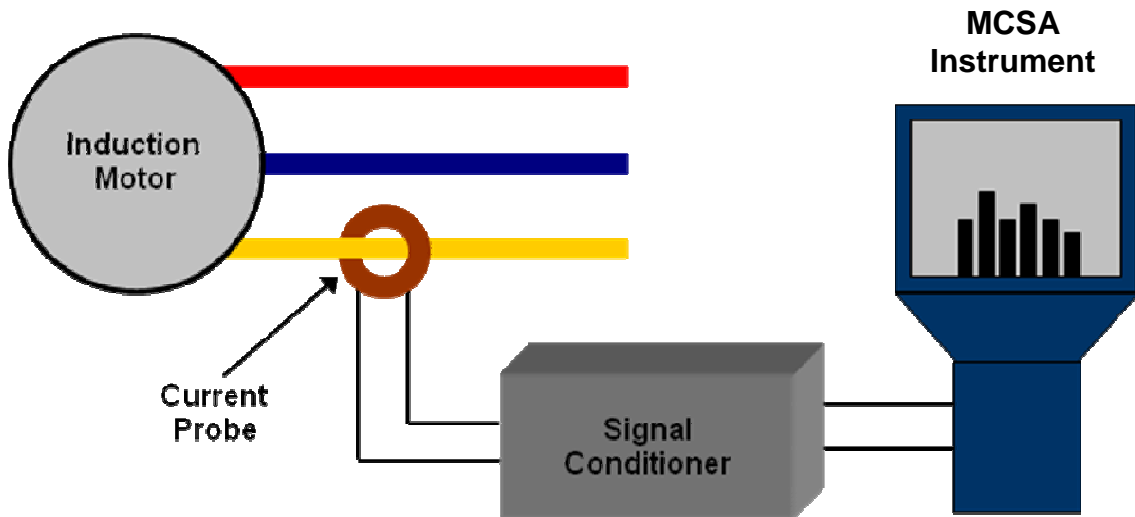


**Figure 1.4 Typical test set-up for MCSA**

If a bar gets broken in the rotor, the two adjacent bars carry the additional current that no longer flows in the broken bar causing a rotor current asymmetry. This asymmetry manifests itself in the form of sidebands around the fundamental frequency and can be viewed when the stator current signal (of any one phase) is viewed in the frequency domain. The detection of these sidebands forms the basis of rotor fault monitoring strategy. The frequency at which the rotor fault sidebands are generated can be calculated by the following formula <sup>(22)</sup>.

$$f_{sb} = f_1 (1 \pm 2s) \text{ Hz} \dots \dots \dots (1.1)$$

where,  $f_{sb}$  = sideband frequency Hz  
 $f_1$  = supply frequency Hz  
 $s$  = per unit slip

These sidebands (as shown in figure 1.5) are called twice slip frequency sidebands, and the relative height of these sidebands with respect to the mains frequency component determines the severity of rotor fault.

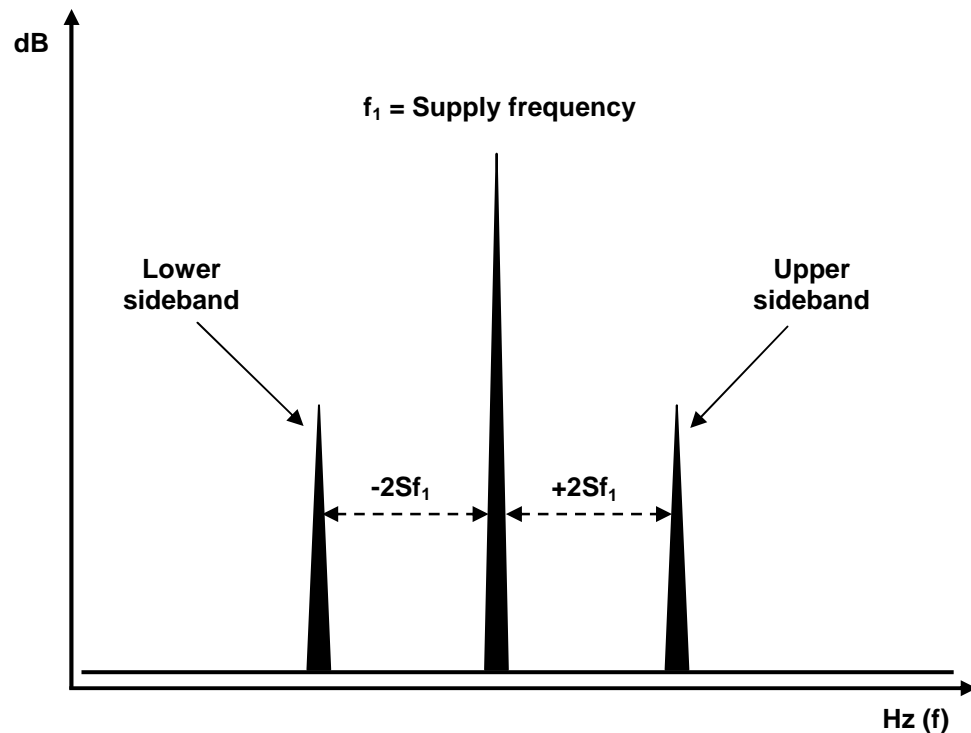


**Figure 1.5 Sidebands generated due to rotor faults**

Typically, the sidebands are approximately 1 Hz or so away from the very large main frequency component and the amplitudes are typically 100-1000 times smaller than the main frequency current <sup>(18)</sup>. If there are no broken bars, there will be no or very low level sidebands. The current imbalance caused by a single broken bar may not affect the machine's performance significantly, but leads to excess heat generation and higher stress in the adjacent bars and consequently may result in several bars breaking. As the fault develops and the rotor damage increases, the relative height of the sidebands with respect to the main peak increases. This technique has been widely accepted by the industry for the effective diagnosis of broken bars in three phase induction motors with many industrial case studies being published <sup>(5, 22)</sup>. However, the tests cannot be performed at low load, as there is insufficient current in the rotor to highlight the faults. The testing is best performed at full load. The minimum load to make a reliable interpretation is typically about 50%.

Yet another important application of MCSA is to detect abnormal air-gap eccentricity in three phase induction motors. It has been shown that both static and dynamic eccentricity give rise to abnormal harmonic frequencies in stator current <sup>(22)</sup>. Similar to the detection of broken bars, the relative height of these frequency components determine the degree of abnormal air-gap eccentricity. However the disadvantage of detecting air-gap eccentricity by phase current analysis is that it requires intimate knowledge of the machine construction like the rotor slot numbers <sup>(16)</sup>.

### **1.4.3 Partial discharge monitoring**

The high voltage stator winding insulation is monitored using various techniques. Partial Discharge monitoring is the most popular technique used for the detection of stator winding insulation faults. As this technique is of particular importance to this project, it will be dealt with in more detail in later chapters.

## **1.5 Objectives of the project**

This project was undertaken as a part of Knowledge Transfer Partnership (KTP) programme. KTP is a UK-wide programme helping businesses to improve their competitiveness and productivity through collaborative projects between business and knowledge base. The source of knowledge base is usually a higher education institution (e.g. university), college or research organisation. Under this programme, The Robert Gordon University (RGU) assumed the role of the knowledge base partner in collaboration with Dowding & Mills (D&M) acting as the company base partner.

The School of Engineering at RGU has a well-established expertise in the field of condition monitoring of electrical machines. D&M is one of the few companies, who are commercially involved in the condition monitoring of electrical machines using partial discharge detection technique. The company manufactures its own partial discharge detection equipment, that was developed in-house (in 1980s) with the association of the expertise available then at RGU. However, in the last few decades, a considerable amount of progress has been made in the field of partial discharge detection and the associated data acquisition hardware. These developments can be adopted to develop a new partial discharge detection system with an improved performance. This development is deemed necessary by the company in order to maintain its position as a market leader and to keep in pace with the modern technology.

Though much is already known about the nature, causes and effects of partial discharges, this knowledge is far from complete and a great deal of work remains to be done before a truly meaningful interpretation of measurements can be made. This is due to the dependency of partial discharge measurements on various factors posing a challenge for analysis. Some of the factors described by Zhu et al. <sup>(143)</sup> are partial discharge calibration problems, location of partial discharge in machine windings, differences between machines and measurement conditions, effect of different types of discharges on the winding insulation, etc. Due to these factors, a significant amount of experience and expertise is involved partial discharge analysis.

Therefore, this research is intended to be a part of a long-term study to build a comprehensive knowledge base from which more accurate diagnosis of motor insulation condition may be derived.

The main objectives of the project within the scope of KTP programme are:

- Carry out a literature search into the following subject areas:
  - Causes of partial discharges and its effect on the machine insulation.
  - Partial discharge detection methods.
  - Modern signal processing techniques used for partial discharge analysis.
  
- Conduct a detailed study of the workings of the existing system used by the company and identify areas of improvement.
  
- Design and develop a computer based on-line data acquisition system capable of detecting and acquiring partial discharge signals, utilising Rogowski coils as detection sensors. This will include the design of signal conditioning hardware unit along with a suitable interface to a data acquisition card.
  
- Develop a platform to enable the application of modern digital signal processing techniques for the analysis of partial discharge data acquired from rotating machines.

The existing partial discharge detection system used by D&M called the 'StatorMONITOR' has been successfully deployed in the north-sea oil and gas sector for more than 2 decades. However, certain drawbacks that have now become apparent will need some consideration for improvement as a part of this project:

- The design is based on the hardware components that were available 20 years ago. Although, some design modifications have been carried out since then, it has now come to a stage where many of the design components have become obsolete making it difficult to manufacture more units. A new design with modern components is essential for sustaining the business demands of the company.

- The existing system is quite bulky as a portable unit, weighing around 12 Kilos including the protective casing. There is a potential for a new modern design to be lighter making it easy to use and transport.
- The signal conditioning hardware (essentially a filtering and amplification unit) is capable of providing a limited number of gain steps (6 different gain settings). Although the minimum and maximum gain settings are sufficient to accommodate the high and low level discharge pulses, addition of intermediate gain steps will provide better visualisation of discharge pulses. This will ultimately aid in making a better analysis.
- The existing acquisition and analysis software was developed using Visual Basic and C++. The use of more modern software like LabVIEW which specifically designed for data acquisition and analysis will provide a platform for sustained development due to its modular approach. Various data compression techniques can be used for storing the raw partial discharge data in an efficient manner.
- At a later stage, the possibility of remote monitoring can be explored which is fast becoming the basis for the maintenance industry, although it will not be a part of this project.

# CHAPTER 2: AGEING OF INSULATION SYSTEMS

## 2.1 Introduction

In any electrical system, the insulation is considered as the passive component as it does not carry any electrical current and does not directly contribute towards the functioning of the electrical system. In other words 'insulation' is an overhead in the system that adds to the cost and increases the conductor size. However, the role of electrical insulation cannot be underestimated. Electrical insulation has combined functions in providing electrical isolation, mechanical support, heat dissipation, energy storage and personal safety. Hence, electrical insulation in any system is of paramount importance.

It is of utmost interest to the manufacturers and the users to know the operating life of any electrical system. From the manufacturer's point of view it is mainly to establish that the product will exceed its guaranteed lifespan. Another equally important reason is to be able to determine the change in lifetime if any alterations are made in the manufacturing process or material used. From a user point of view it is necessary to assess the operating life of the machine for a given load or duty cycle. This is of particular importance to users like electric utilities where the user has to have confidence that a particular machine will remain in an operative condition until the next planned shutdown.

The safety margins in traditional winding designs were very liberal. Precautions like thicker ground-wall insulation for extra insulation, greater cross section of copper to reduce the operating temperature, etc. were used to increase the expected life of the rotating machine. This resulted in insulating systems that outperformed the expected life. However, providing such liberal safety margins meant a significant increase in the manufacturing cost of the machine. The manufacturers are now under constant pressure to reduce the machine cost by reducing design margins and developing better (and thinner) insulating systems with increased stress withstanding capability.

## 2.2 Ageing and Stress Mechanisms

The process of ageing can be described as '*The occurrence of irreversible deleterious changes that affect the performance and shorten useful life*' <sup>(53)</sup>. The ageing of insulation is dependent on various factors like:

- Physical and chemical properties of the material.
- Nature and duration of applied or induced stress mechanisms.
- Material processing and treatment during manufacturing.
- Subsequent use in equipment.

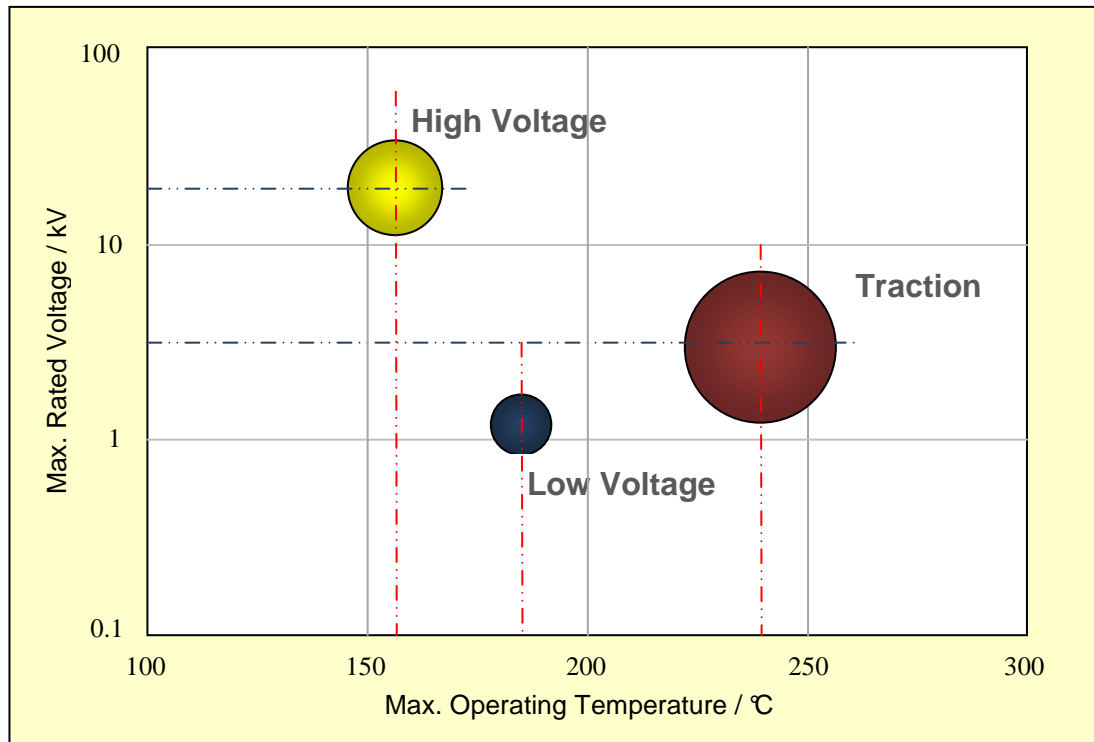


**Fig 2.1 Typical operational conditions of insulation systems in rotating machines (circle diameter corresponds to mechanical stress) <sup>(60)</sup>**

Of the above stated factors, the presence of degrading stresses is the primary reason for the ageing of insulation systems. The insulation system of rotating machines windings are subject to a wide variety of severe stresses with varying intensities depending upon specific application. Figure 2.1 shows the typical operational conditions of insulation systems in rotating electrical machines. The various stresses that affect the integrity of the stator winding insulation system can be classified into thermal stress, mechanical stress, electrical stress and environmental stress.

In any rotating machine, the stated stresses can be present constantly or for a brief period (transients). The constant stresses include the operating temperature (thermal stress), the supply frequency voltage (electrical stress) and the magnetically induced mechanical stresses. The ageing caused due to constant stresses is often referred to as 'intransitive ageing' and is usually a slow degradation process proportional to the number of operating hours of the machine. Transient stresses include direct-on-line starting of motor, out-of-phase synchronisation of generators, lightning strikes,

electrical surge caused due to faults, etc. Ageing caused due to such stresses is referred to as 'transitive ageing' and usually causes rapid degradation of insulation, depending on the number of transients the machine experiences <sup>(31)</sup>.

## 2.2.1 Thermal Stress

Thermal stress is one of the most distinguished causes of the gradual degradation of insulating materials and is often a reason for the failure of stator windings, particularly in air cooled machines. The thermal stress can be described as the ageing process due to a high temperature environment, leading to resistive losses or chemical instability of the insulation. Thermal stress is caused due to a number of reasons like overloading, voltage variations, blocked ventilation ducts, voltage imbalance and ambient temperature <sup>(23)</sup>. The effect of thermal stress on insulation can be described in two forms:

- a) Iso-thermal stress – the dielectric ages in a relatively well established way described by the 'Arrhenius law'.
- b) Thermal cycling – occurs due to sudden load changes or frequent switching operations.

### 2.2.1.1 Iso-thermal stress

In the case of iso-thermal stress the insulation deteriorates gradually over a prolonged time period which is accompanied by the decline in the dielectric strength of insulation. The deterioration is caused as a result of heat generated in the copper conductors, primarily due to  $I^2R$  losses. This heat generated has to be dissipated through the main ground insulation to the iron in the stator core and the air in the end-windings. Additional heat is generated due to core losses, windage and stray load losses adding to the operating temperature of the windings. When the winding insulation is subject to high temperatures above a certain threshold, it results in a chemical reaction (oxidation in case of air-cooled machines) leading to depolymerisation of the binding resin <sup>(24)</sup>. This process makes the insulation brittle resulting in localised cracking and can cause delamination in form wound coil groundwalls.

### 2.2.1.2 Thermal Cycling

The thermal cycling of insulation occurs when a motor in normal service is subjected to a rapid change in loads or frequent starts and stops within a short period of time. During start-up, the motor draws around five to seven times the normal current required

to run under full-load conditions. This problem is of particular relevance to large hydro generators subject to peak duty, large gas turbine generators and pump storage machines. The random-wound stators are unlikely to experience this problem.

A changing load will cause a change in the stator winding temperature. If the temperature changes quickly (due to sudden load changes) the copper conductors will expand axially. However, the stator insulation materials have a lower coefficient of thermal expansion compared to copper. The difference between the thermal expansion coefficients of copper conductors and ground insulation causes the copper to grow more rapidly than the groundwall insulation resulting in relative axial movement between the copper and insulation. These movements from thermal expansion and contraction (after many load cycles) exert a mechanical stress on the insulation. This may eventually result in breaking the bond between the copper and insulation. It has been demonstrated that a duty of arduous nature can result in serious delamination taking place, either within the dielectric structure or between the mainwall insulation and the conductor stack, if the insulation is not properly designed and manufactured<sup>(25, 26)</sup>. The thermoplastic insulation system composed of mica splitting bonded with asphalt or varnish are more prone to thermal cycling failure. Modern insulation systems composed of epoxy resin/mica paper are less prone to thermal cycling as they have a similar thermal expansion coefficient to copper and thus tend to move axially with copper conductors.

The work carried out by Montsinger<sup>(27)</sup> laid the foundation for the empirical relation known as the 10°C rule of ageing which states that for every 10°C increase in temperature the life of insulation would be halved, and conversely, a decrease of 10°C would double the life. Montsinger also stated that the deterioration of insulation was due to the loss of mechanical properties and emphasised that the electrical strength increased with thermal ageing until the material cracked open. However, Montsinger's 10°C rule did not always provide valid results due the fact that the materials age at different rates. This was asserted in an EPRI study<sup>(28)</sup> where the insulation halving intervals varied from 8°C to 14°C for motors ranging from 0.7 kW to 350 kW.

Dakin<sup>(29)</sup> stated that the physical changes during thermal ageing are the result of internal chemical changes in organic material, the theory of chemical reaction rates (governed by Arrhenius rate law) can be applied to study insulation ageing. Dakin proposed that the life of insulation is related to temperature by the following relationship<sup>(29)</sup>.

$$L = Ae^{(B/T)} \dots\dots\dots(2.1)$$

where, 'L' is the life of the insulation, A & B are constants determined by the reaction rate of particular degradation, and T is the temperature in Kelvin. However, the above relation is only valid for high operating temperatures. Every insulation material has a threshold, below which no thermal ageing will occur. As the degradation process is an oxidation chemical reaction, the higher the temperature, the faster the chemical reaction, and the shorter the time to degrade the insulation.

High temperatures do not always have adverse effects in the form of thermal stress. In certain cases, the stator windings at high temperature can be beneficial. High temperatures will prevent moisture from settling on windings, thus reducing the risk of electrical tracking failures. Additionally at high operating temperatures the insulation may swell, reducing the size of any air pockets within the insulation and decreasing the partial discharge activity <sup>(30)</sup>.

### **2.2.2 Mechanical Stress**

The stator windings of a rotating machine are subjected to a large amount of electromagnetic forces. These forces are generated by the interaction of current carried by the stator windings and the magnetic field in which the conductors are located. The resultant electromagnetic forces generated vary sinusoidally at twice the supply frequency. These cyclic forces cause the copper conductors as well as the entire coil to vibrate at twice the supply frequency, primarily up and down in the slot. There is also a force in the circumferential direction caused by the rotor's magnetic field interacting with the current in the stator bar. Figure 2.2 shows the relative movement of a stator bar in relation to the laminated core.

These electromagnetic forces cause mechanical vibrations and is regarded as one of the major causes of premature degradation of stator winding insulation. Maughan et al. <sup>(32)</sup> showed the vibration can cause fretting of insulation which can eventually lead to mechanical failure of the stator winding. If there is any loosening of bars in the stator slots, then the vibration forces will cause a mechanical abrasion of the coil sides and the groundwall insulation. Such friction can cause damage to both the protective corona shield on the coil surface and the groundwall insulation. This may result in an increased partial discharge activity and accelerate the process of insulation degradation. Edwards <sup>(31)</sup> detected the insulation abrasion in the slot region by on-line partial discharge measurements and reported that such abrasion will lead to a

progressive loss of the corona screen and subsequently the main groundwall insulation. Kai Wu et al. <sup>(33)</sup> studied the effect of mechanical vibrations on the partial discharge behaviour and demonstrated the amplitude and frequency of vibrations cause a significant variation in the partial discharge pattern.

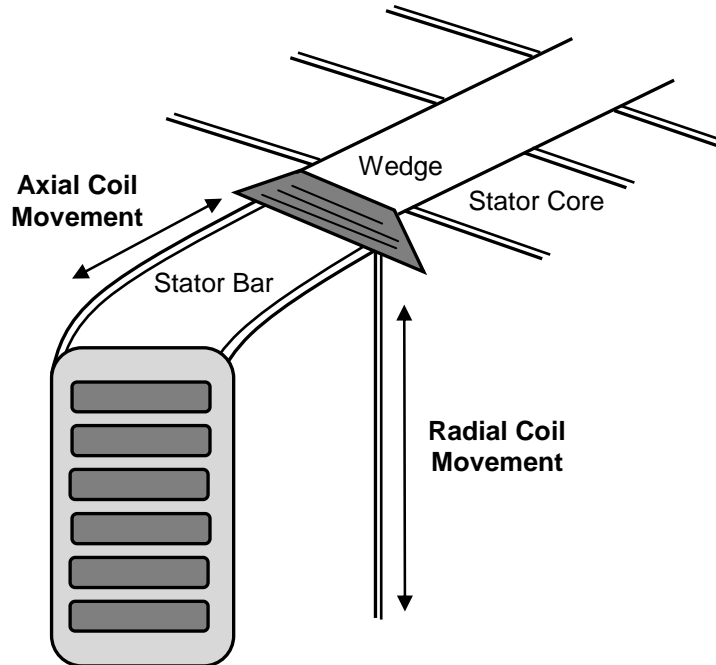


**Figure 2.2 Movement of stator bar in relation to core**

A similar magnetic force occurs in the end-windings region. The movement in the end-winding is more pronounced due to the fact that they are fixed in the slot end and are allowed a number of degrees of freedom. The endwindings in two-pole and four-pole machines are usually longer hence are more prone to the effects of vibration. As shown in figure 2.2 the movement from vibration can be in radial and axial directions. The end-winding bracing is designed to prevent excessive movement in the presence of electromagnetic forces. However, the mechanical stress in the end-windings from vibrations is significant during the start-up of the machine. It is a known fact that during the start-up a machine draws up to 7 times the normal running current resulting in electromagnetic forces that can be 49 times ( $F \propto I^2$ ) the magnitude experienced during normal service. After a large number of starts or frequent transients the endwindings may gradually loosen over time allowing movements between the endwinding components. Such vibrations can also cause fatigue cracking of copper connections.

Other external vibration caused due to mechanical problems such as bearing failure, shaft or coupling deflection and rotor-to-stator misalignment can cause mechanical

damage to the endwinding insulation <sup>(23)</sup>. In an extreme case the rotor can strike the stator and the rotor force can cause the stator laminations to puncture the coil insulation, resulting in a grounded coil.

In order to minimise vibration the bar is supported continuously along the length of the slot by wedges to prevent the radial motion of the bar in the slots. A packing material is used to prevent motion between the insulation and core surfaces. This is necessary in the case of hard thermosetting insulated bars as they do not provide a uniform fit within the core slot. In the case of thermoplastic insulated coils, they are made to conform to the contour of the slot and provide a wedge tight fit as the insulation expands at service temperatures <sup>(34)</sup>. The organic materials in insulation tend to shrink as they thermally age and this may lead to loosening of the stator bars. In order to deal with the problem of insulation shrinkage, many machine manufacturers use ripple springs (warped epoxy-glass composites) under the wedges as side packing material. The springs expand and occupy the space created by shrinkage of other slot components and hold the bars firmly in place <sup>(28)</sup>.

### **2.2.3 Electrical Stress**

If alternating voltage applied to the insulator exceeds a certain threshold value, it causes electrical stress and can lead to the ageing of the insulating material. This type of ageing process is known as electrical fatigue. In low voltage machines (< 1000 Volts) the thickness of the insulation in the stator windings is mainly determined by the mechanical demands of the machine. At such low voltages the electric stress on the insulation is relatively low, but the insulation still has to be thick enough to withstand the harsh mechanical forces applied on the stator windings during normal operation. However, at higher voltages the thickness of the winding insulation is primarily dependent on the applied electric stress i.e. power frequency voltage. It is quite common today to find machines with normal operating electrical stress levels of 2500-3000 V/mm <sup>(43)</sup>.

The power frequency voltage can contribute significantly to the ageing of high voltage insulation, particularly in the presence of partial discharges. In the electrically overstressed regions like voids and cavities within the insulating material, internal partial discharges can occur. The high voltage insulation is usually made of organic materials containing polyesters, asphalts, epoxies, etc. The sparks caused by partial discharges contain electrons and ions which react with the chemical bonds of the organic material, thus accelerating the chemical and thermal ageing process. It can be

said that electrical stress plays a paramount role in the process of insulation degradation, while the other stress mechanisms such as thermal, mechanical and environmental stresses are mostly the inception factors for the formation of defects in the insulation system. It has been shown that the electrical stress can cause partial discharges in defects, which erode the insulating materials and can lead to electrical treeing, often referred to as the most important degradation mechanism in solid insulation <sup>(44)</sup>.

The ability of the insulation to withstand partial discharges over a prolonged period of time is of course essential. Some insulating materials can better withstand partial discharges when compared to others. Partial discharge can be described as small electrical sparks that occur within the air pockets of the insulation or on the surface of an insulating system. It can occur at various locations in the stator windings along the slot region and in the endwindings. The partial discharges are classified into three basic types in machine:

1. Internal discharges occurring in the cavities of dielectric material
2. Surface discharges occurring on the surface of the coils
3. Point discharges occurring in strong electrical fields around sharp points or edges.

The above different types of discharges are discussed in detail in chapter 3.

A significant number of motors are often exposed to transient voltage conditions, which can result in reduced winding life or premature failures (either in form of turn-to-turn or turn to ground). The transient voltages can be caused due to various reasons like line-to-line or line-to-ground faults, opening and closing of circuit breakers, capacitor switching, rapid bus transfers and lightning <sup>(23)</sup>.

Repetitive voltage surges are caused by inverter fed drives that incorporate switching devices. These switches are driven by various pulse width modulation (PWM) techniques that can create a high number of fast rise-time surges per second. Although the rate of rise of the voltage surges is not generally fast enough to cause an uneven voltage distribution throughout the turns of the coil, it is the very high repetition rate and the magnitude of the spikes that affect the life of the insulation system. The effect of these voltage surges is more relevant to the insulation of low voltage motors as they have a relatively weaker insulation. Persson <sup>(45)</sup> carried out a study of PWM inverters on low voltage induction motors and reported that a short rise-time can be potentially

hazardous for motor insulation and it is recommended to have a minimum rise-time of approximately 5  $\mu$ s.

Gupta et al. <sup>(46)</sup> published some data on the effect of repetitive surges on epoxy-impregnated turn insulation in large motor coils which had been operational in normal service. At surge voltages close to the single surge breakdown voltage, results indicated an ageing effect; however no surge ageing was observed at lower voltages. There was some uncertainty in the data as there was a high variability from specimen to specimen, and only a limited number of coils were tested.

The work carried out by Bartnikas et al. <sup>(47)</sup> showed that epoxy insulation can gradually age under the action of repetitive voltage surges of either polarity, even in the absence of partial discharge. Even well made epoxy turn insulation in motor windings may be aged by the repetitive surges created by vacuum switchgear and electronic type power supplies. The insulation that is most likely to age is the turn insulation in the stator winding coils connected to the phase terminals. Although the electric stress across the turn insulation is dependent on the design of the coil and rise-time of the surge, it can be generalised that the faster the rise-time, the greater is the stress across the turn insulation. Due to the fact that electrical stress is one of the primary factors causing the deterioration of electrical insulation, there are methods to determine the ability of insulation to withstand voltage. The industry has adopted accelerated ageing test methods that result in a time-to-failure of days or weeks, rather than years or decades that the insulation is expected to last at normal voltages. The most commonly used test methods are:

- *Short-term breakdown strength*  
In this method the voltage is rapidly increased across an insulating material up to a point when there will be sufficient voltage to puncture the insulation.
- *Voltage endurance test*  
In this method a voltage is applied to an insulation system that is higher than expected during normal operation and the time to failure is measured. The voltage endurance tests are typically performed at four times service voltage levels and the method has been detailed by Ward et al. <sup>(48)</sup> and Stone et al. <sup>(26)</sup>.

The above methods were developed as a result of numerous studies carried out by various researchers who developed empirical models relating the test stress with time to failure. Cygan and Laghiri <sup>(49)</sup> studied various models developed by several

researchers, providing a critical analysis of each method. However, the most commonly used models for ageing studies under electrical stress only are the 'inverse power law' and the 'exponential law'.

- *Inverse Power Law:*

The inverse power model is one of the most frequently used in the ageing studies under electrical stress only. As summarised in <sup>(48)</sup> is described by the following relationship:

$$L = k.V^n \dots\dots\dots(2.2)$$

where  $L$  is the appropriate unit of time (in hours or years),  $V$  is the applied voltage or electrical stress, and  $k$  and  $n$  are constants to be determined based on the characteristics of a given material and the operation conditions of voltage and temperature. If various data points of the above equation are plotted on a log-log paper, it will result in a straight line <sup>(49)</sup>.

- *The Exponential law:*

Next to the inverse power model, the exponential representation is the most commonly used. The basic form of exponential law as reported in <sup>(49)</sup> is given by the following relation:

$$L = c \exp (-kV) \dots\dots\dots(2.3)$$

where,  $L$  is the appropriate unit of time (in hours or years),  $V$  is the applied voltage, and  $c$  and  $k$  are constants to be determined based on experimental data. Various data points of the above equation, if plotted on a semi-log paper will result in a straight line.

The industry has developed over the years, various empirical relations for the prediction of insulation life of electrical systems and most relationships are variations of the above two models. Brancato published a paper <sup>(50)</sup> summarising the various voltage endurance relations and stated the belief of many researchers that there is no deterioration of insulation below discharge inception voltage, thus increasing the insulation life significantly. Modified versions of the above equations have been developed <sup>(51, 52)</sup> that provide a better approximation of insulation life.

## 2.2.4 Environmental Stress

There are many environmental factors that can influence the insulation ageing of stator windings. Some of the factors are moisture condensed on windings, oil from bearings, high humidity, aggressive chemicals leading to reaction, abrasive particles, dirt and debris such as coal dust, cement, sand etc. and radiation if the machine is used in the space environment or nuclear reactor. Of all the above factors the contamination and pollution of insulation surfaces is the most common cause of degradation.

Surface contamination, usually associated with deposits of grime, salt or dampness on the insulation surface can lead to intense surface discharge and tracking. As explained by Dymond et al. <sup>(35)</sup> the process of tracking is accelerated in humid conditions. A moisture film on the polluted surface will permit a localised flow of leakage current. The nature and extent of pollution determines the magnitude of the leakage current. The flow of leakage current causes the conductive film to heat non-uniformly. The heating causes uneven evaporation and distorts the voltage distribution over the surface. The resultant dry-bands create regions of very high resistivity between the edges of the remaining wet film. Almost the entire surface voltage will appear across this dry band and can cause a flashover of the gap. Such localised high energy surface discharge has sufficient energy to decompose and carbonise the underlying insulation. This process continues in a relatively random manner, growing in a tree-like pattern. Eventually, a continuous conducting path may be formed between two live parts resulting in a failure. Practical on-field investigation <sup>(36)</sup> has shown that the presence of contamination (oil and pollution) in the endwindings led to intensive endwinding partial discharge activity affecting the insulation integrity.

Conductive surface contamination may also effectively act as an extension to the earth structure resulting in an increase in the electric field intensity. A clean insulating surface has high resistivity and the discharges therefore have low energy and are incapable of causing rapid erosion of the insulating surface. However, if the surface resistivity at the point of discharge has been compromised due to the deposition of contamination, then the effective surface area feeding current to the discharge and the discharge energy are correspondingly increased <sup>(37)</sup>.

Humidity is another important factor that can influence the insulation ageing process. If the endwindings are clean and dry with no surface contamination and there is sufficient spacing between the coils/bars, there will be no partial discharges. Under such circumstances humidity will have a minimal effect on the insulation. However if the coils are contaminated and are suffering from surface tracking or insufficient spacing, partial

discharges will occur and can be strongly affected by humidity. Stone & Frenger <sup>(38)</sup> showed the significant influence of humidity on partial discharge activity in high voltage stator windings suffering from surface insulation degradation and emphasised the practical importance of humidity measurement along with partial discharge measurement as a trending parameter. Naprasert et al. and Binder et al. <sup>(39, 40)</sup> have shown that the lower the relative humidity, the higher the partial discharge activity and conversely the discharge activity diminishes or are even extinct at higher humidity. Nawawi et al. <sup>(41)</sup> explained the phenomenon stating at humid conditions, the partial discharge inception voltage decreases and the partial discharge extinction voltage increases, leading to a decrease in discharge magnitude. The study conducted by Slotani et al. <sup>(42)</sup> showed that humidity can have different effects on different types of partial discharges. For coils with insulation containing asphalt (more hygroscopic material), humidity amplified the internal discharges. In the case of an epoxy insulation bar, which had more surface discharges, the application of humidity caused a noticeable decrease in surface discharge.

In certain cases the above stated environmental factors in themselves do not cause deterioration, but when combined with other stress mechanism can lead to degradation. For example, the oil, moisture and dirt combination can get collected in the stator ventilation passages and in the endwindings to block the cooling airflow, thus increasing the risk of thermal deterioration. The presence of oil can act as lubrication and facilitate increased movement of the stator bars within the slot leading to insulation abrasion. Chemicals such as acids, paints and solvents can decompose the insulation and reduce its mechanical strength.

### **2.2.5 Multifactor Stress**

The stress mechanisms described above will be present in any harsh operating environment and may operate singularly or in combination to deteriorate the insulation system. For example, the operating voltage of a rotating machine not only causes electrical stress but the winding insulation is also subject to thermal stress as a result of conductor heating due to current flowing through it. Thus the insulation system undergoes ageing due to a combination of electrical stress and its associated thermal effects. In addition, mechanical stress may be present due to induced vibration or the difference in expansion coefficients. The simultaneous presence of various stress mechanisms subjects the machine insulating material to 'multifactor stressing'. The whole insulation degradation process is made more complex as the interaction between ageing factors is not simply additive but synergistic in nature <sup>(53)</sup>. This means

the interaction of various ageing factors produce an effect that is different from the sum of ageing effects produced by each factor individually.

The simultaneous presence of electrical and thermal stresses has been investigated extensively. The presence of these two stresses is almost unavoidable in most applications and various ageing models have been proposed <sup>(49, 54)</sup>. Mazzanti et al. <sup>(55)</sup> made an attempt to quantify the synergistic effect of electrical and thermal stresses on insulation life. They proposed a synergism factor, a ratio between multi-stress ageing rate and the sum of single-stress ageing rates. The tests carried out on polypropylene capacitors and ethylene propylene rubber (EPR) insulated cable models suggested that the synergism between electrical and thermal stress is negligible only if one stress is very low. However, when the action of both the stresses is comparable, the synergism increases and the factor can reach high values.

Several papers have reported multi-stress models combining the electrical, thermal & mechanical stresses for the life prediction of insulation materials. A simple multi-stress ageing model can be developed assuming that the combined-stress ageing rate is the product of the single stress ageing rates. But this leads to an overestimation of synergism between stresses as observed for combined electro-thermal life <sup>(54)</sup>. This results in an underestimation of insulation life, particularly when the stresses are high. The electro-thermo-mechanical life model suggested by Simoni et al. <sup>(56)</sup> was also derived from a suitable combination of the three individual single stress models, but they introduced a correction factor in order to achieve a better fit of the experimental life data. Bartnikas and Morin <sup>(57)</sup> demonstrated the ageing behaviour of stator bars subjected simultaneously to electrical, thermal and mechanical stresses and reported the effect on the ageing rate by increasing each of the three ageing stress factors above the normal operating conditions. They also reported the intricate behaviour of partial discharge process as a function of temperature and electromagnetically induced mechanical forces over a thermal load cycle and stated that the presence of partial discharge is an indication of progressive ageing, the intensity level at any given specific time cannot be used to predict failure.

Paloniemi <sup>(58)</sup> critically assessed the various methods for endurance testing and stated that an exact reproduction of the ageing process in an accelerated ageing test is probably not possible due to the numerous possible paths of degradation reactions. He proposed the theory of 'equalised ageing process' in which all the relevant stresses are accelerated to such an extent that the ageing rate due to each stress is about the same, thus moving a step closer to the reproduction of the true ageing process.

Various stresses interact with each other in a cyclic fashion and this is illustrated in figure 2.3. It must be noted that thermal stress cannot lead to any electrical stress. The electrical, thermal and mechanical stresses represent one side each, whereas the combination of radiation and environmental stresses represent the fourth side. The majority of equipment and systems undergo electrical, mechanical and thermal stresses in practical applications but are not always subjected to radiation or environmental stress. Ageing due to radiation is considered to be critical in space-based systems and nuclear systems.

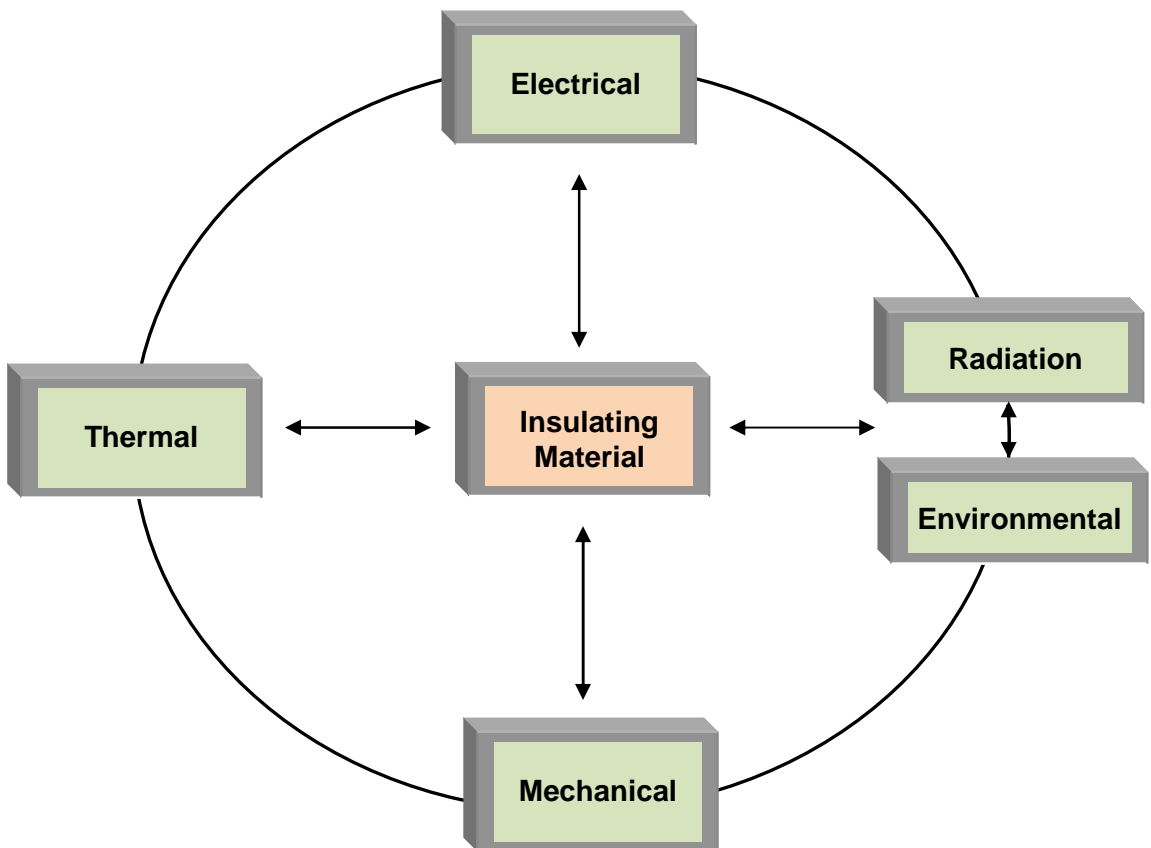


**Figure 2.3 Multistress Ageing** <sup>(53)</sup>

## 2.3 Conclusion

Although the individual stress models provide a good understanding of the effect of stress on insulating material, the multi-stress model approach provides a better approximation of real life insulation degradation process. The multi-stress ageing models take into account the synergistic interaction between various stress mechanisms and are based on the cumulative damage caused by all acting stresses; hence it offers a better approximation of insulation ageing under real conditions.

However, the subject of multi-stress ageing is considered complicated and difficult. The laboratory simulation of various operating conditions may come close to real life conditions, but insulation life predictions based on those data analyses are questionable. With every additional stress the complexity of conducting studies and deriving appropriate ageing models increases. Kimura <sup>(59)</sup> acknowledges the fact stated by Simoni that the ageing curves change complicatedly according to the amplitude of multiple stresses and will require numerous samples to be tested with various combinations of stress amplitudes and application modes. This is one of the reasons why the multifactor ageing models lack sufficient real life experimental evidence.

# CHAPTER 3: PARTIAL DISCHARGE THEORY

## 3.1 Introduction

IEC 60270 (PD measurements) defines partial discharge as 'a localised electrical discharge that only partially bridges the insulation between conductors and which may or may not occur adjacent to a conductor'. If the insulation is completely bridged then the insulation breaks down. Figure 3.1 shows a simplified representation of a discharge occurring within an insulating material. These discharges can occur internally or externally to the insulation.

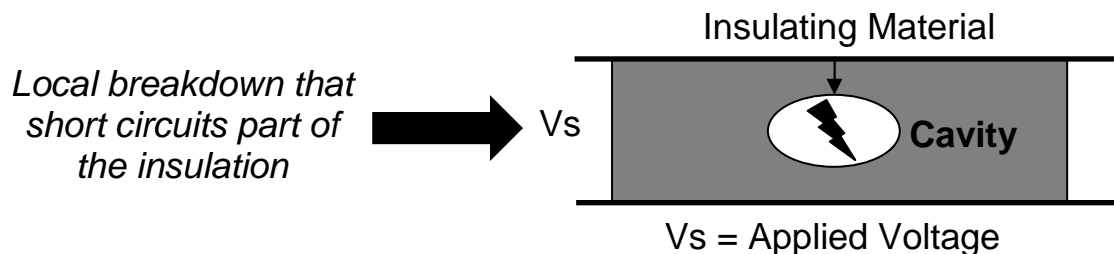


Figure 3.1 Simplified representation of partial discharge

## 3.2 Types of partial discharge

Based on the location and nature of partial discharges, they can be classified into the following four categories <sup>(61)</sup>:

1. Internal discharges - usually occurs within gas filled cavities called voids in liquid and solid insulating materials.
2. Surface discharges – occurs on the surface of an insulating material or at the interface of different insulating materials.
3. Corona discharges – tends to occur on sharp edges or thin conductors that are connected to high or ground potential.
4. Electric treeing

Figure 3.2 shows the different types of discharges along with their locations.

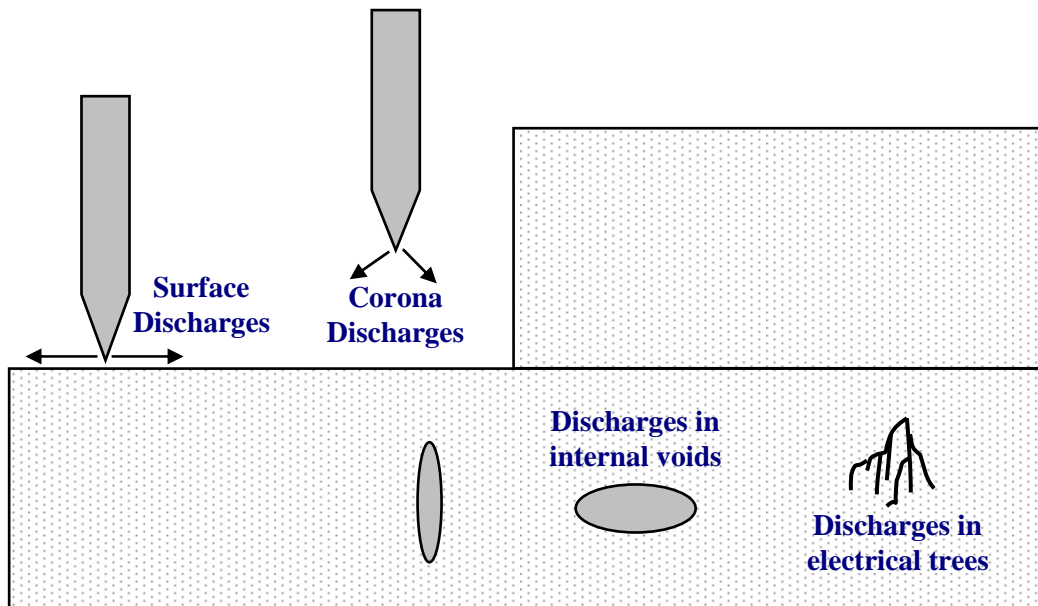


**Figure 3.2 Different Types of Discharges** <sup>(61)</sup>

### 3.2.1 Internal Discharges

Internal discharges take place in inclusions or cavities (voids) within the insulation. It is not practically possible to completely eliminate the occurrence of small faults like voids in an insulating material. A practical insulation structure of a high voltage stator will invariably contain small voids or cavities, often due to inhomogeneities in the insulating material used for the manufacturing. Natural resin based coils and synthetic resin based coils contain gaseous inclusions and are formed due to small quantities of air that become trapped in the insulation during the curing and pressing stages.

These cavities filled with air usually have a lower permittivity and a lower breakdown strength compared to the insulating material. This causes the field intensity to be higher within the cavity than in the dielectric material and may cause a breakdown even under normal working stress affecting the long term integrity of the insulating material.

#### 3.2.1.1 Analogue discharge circuit

The behaviour of internal partial discharges under a.c. voltage stress can be described conveniently with an equivalent analogue circuit representation, often referred to as the 'abc' circuit <sup>(61)</sup>. Figure 3.3 shows a simplified diagram of a cavity within a section of solid insulating material along with its 'abc' equivalent circuit.

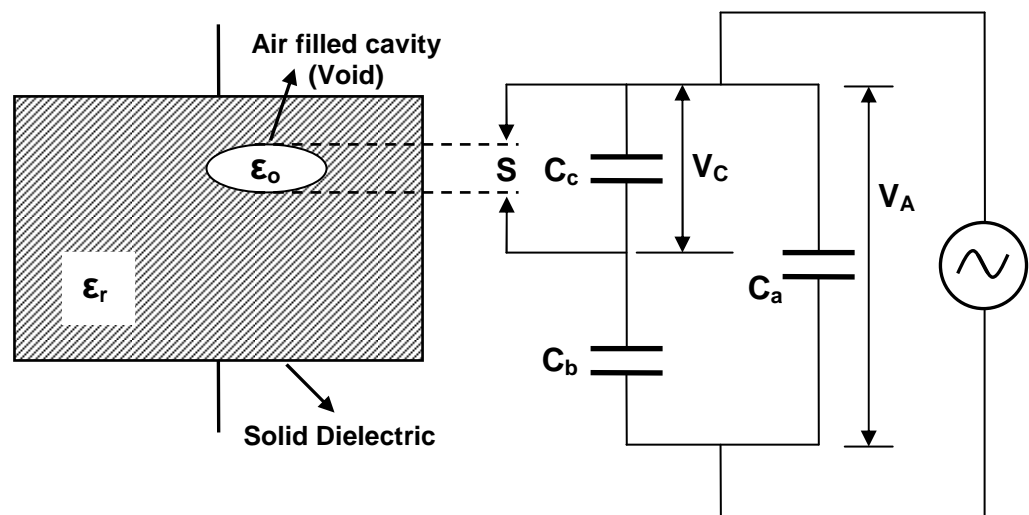


**Figure 3.3 Simple model of a cavity in dielectric <sup>(61)</sup>**

In figure 3.3 the capacitor  $C_c$  represents the capacitance of the cavity;  $C_b$  represents the capacitance of the dielectric material in series with the cavity and  $C_a$  represents the capacitance of the rest of the dielectric material. 'S' represents the spark gap which breaks down when the voltage across it reaches the void breakdown level.

The table 3.1 shows relative permittivity and breakdown strengths of some typical high voltage insulating materials.

**Table 3.1 Relative permittivity and breakdown strength of HV insulating materials**

Material	Relative permittivity	Breakdown strength kV/mm
Air (atmospheric pressure)	1.006	2
Transformer Oil	2.2	28
Polyethylene	2.3	24
Polyurethane	4.0	10
Paper	3.0	9
Mica	6.0	42
Epoxy	4.7	12

The relative permittivity of air ' $\epsilon_o$ ' is equal to unity, whereas the permittivity of solid dielectric (e.g. insulated epoxy mica) given by ' $\epsilon_r$ ' varies between 4 and 6. When the given solid dielectric is subjected to high voltage ( $E_s$ ), the electric stress developed across the cavity ( $E_C$ ) is given by:

$$E_C = (\epsilon_r / \epsilon_o) . E_s \dots\dots\dots (3.1)$$

where,  $\epsilon_r$  = relative permittivity of air  
 $\epsilon_o$  = relative permittivity of solid dielectric

Therefore, from equation 3.1 and table 3.1 it is clear that the electric stress across the cavity is substantially increased. The extent of stress concentration within the cavity will depend on various other factors like the shape and size of the cavity. Kang et al. <sup>(62)</sup> showed that the discharge parameters like magnitude, repetition rate, average discharge power and average discharge current in specimens with larger size voids were greater than in others. As the breakdown strength of air at atmospheric pressure is about 3KV/mm, it can be seen that discharges are likely to occur at normal high voltage operating stress.

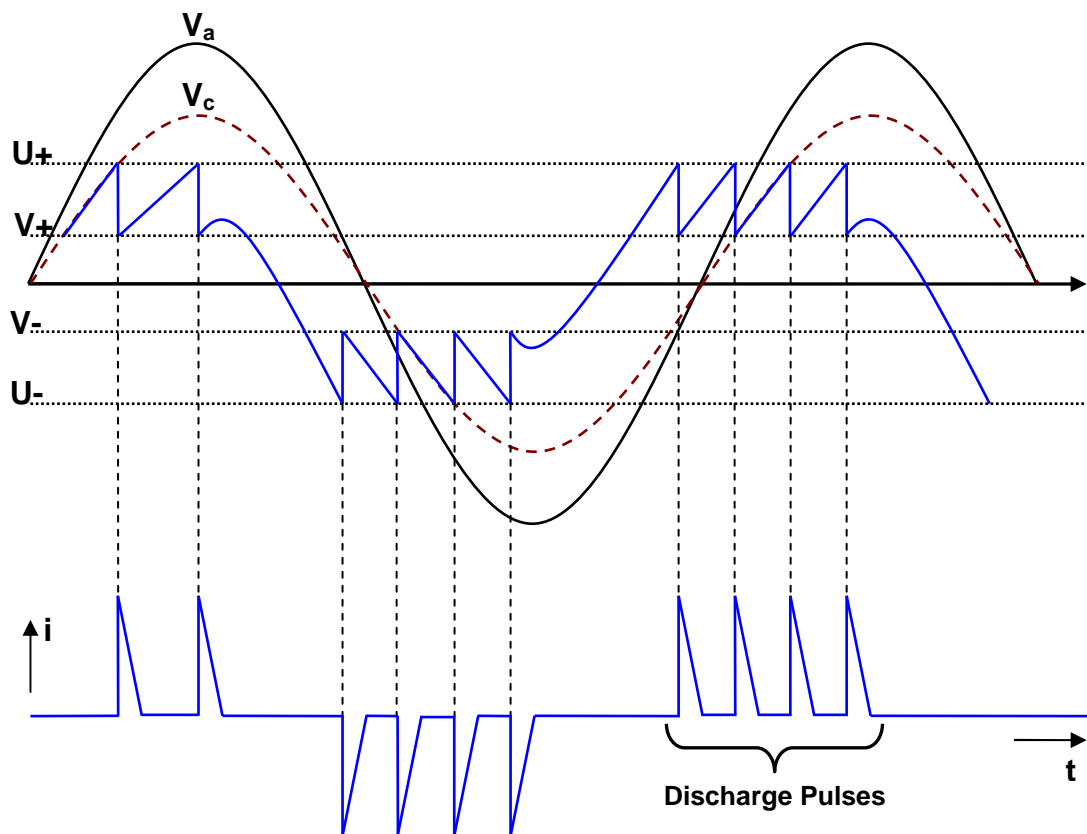


**Figure 3.4 Sequence of internal discharges under a.c. voltage <sup>(61)</sup>**

Referring to figure 3.4, the high voltage across the dielectric is represented by  $V_a$  and the voltage across the cavity is represented by  $V_c$ . When voltage  $V_c$  exceeds the positive breakdown voltage  $U+$  (*inception voltage*) of the cavity a discharge occurs. The breakdown voltage  $U+$  is determined by the Paschen curve that relates the breakdown voltage of air to the product of pressure and electrode spacing <sup>(61)</sup>. When the discharge occurs, the voltage across the cavity drops to  $V+$  volts (*extinction voltage*) and the discharge extinguishes. This typically happens in a time less than

0.1 $\mu$ S. The voltage does not reduce to zero because a residual voltage remains across the cavity.

After the extinction of discharges, the voltage across the cavity increases again along with the applied voltage  $V_a$ . Another discharge occurs when the voltage across the cavity reaches  $U_-$ . This sequence of discharges repeats several times until the applied voltage  $V_a$  begins to decrease and the discharges cease. Thus a number of discharges are produced during the rising portion of the positive half cycle. A similar process takes place in the negative half cycle in which the discharges occur when the voltage across the cavity exceeds  $U_-$ . In this way groups of regularly occurring positive and negative discharges will be produced. Each discharge will cause a current pulse as shown in figure 3.4, and these can be detected by electrical means. The electrical detection of discharges is discussed later.

#### 3.2.1.2 Discharge sites

When a breakdown occurs, there is a net charge transfer from one cavity surface to the opposite one. However, due to the high surface resistivity of the cavity, not all the charge on the surface will be discharged. The remnant charge acts as a localised protective zone and alters the electric field in the cavity. The next discharge therefore is most likely to occur farthest from the previous discharge site. Thus, multiple discharges per cavity are possible. Mason <sup>(63)</sup> clearly showed the development of multiple discharge sites along with the photographs of the void surface taken at different intervals after the start of experiment.

It is important to emphasise that the analogue 'abc' circuit and the resulting sequence of discharges is a simplified model of the actual process within a cavity. In practical conditions a discharge cavity can contain multiple discharge sites, and these sites may be considered as many discharging capacitances, each having its own discharge sequence. This causes a tangential stress along the surface of the cavity and is probable that a discharge site can get partly recharged by a neighbouring discharge site. This transverse leakage affects the discharge sequence <sup>(61)</sup>. The discharge activity is also affected by the surface conductivity of a cavity. The bi-products generated during discharge like the ozone 'O<sub>3</sub>' or nitric oxide 'NO' can attack the surface of the cavity <sup>(64)</sup>.

All these factors can affect the discharge rate and it is most likely that in the presence of any of the above stated mechanisms the discharge rate will be higher than that predicted by the 'abc' circuit. However, the net effect of all these degrading

mechanisms is a slow erosion of cavity surfaces present within the insulating material, thus reducing the overall dielectric strength of the insulation.

### 3.2.2 Surface Discharges

Surface discharges may occur when there is a stress component parallel to a dielectric surface as shown in figure 3.5. Once the discharge has been initiated, it affects the electric field in such a way that the discharge extends beyond the region where there was originally sufficient electric stress to cause the discharge. They are commonly found in bushings, ends of cables and overhang of machine windings. Surface discharges depend on several factors <sup>(65)</sup>:

- Physical properties of the environment in which discharge takes place (gas, liquid).
- Physical properties of solid dielectrics (permittivity, surface resistance, conductivity).
- Distribution of electric field in the site between electrodes.
- Type of voltage and time of operation.
- State of surface of solid dielectrics (polluted, sodden).

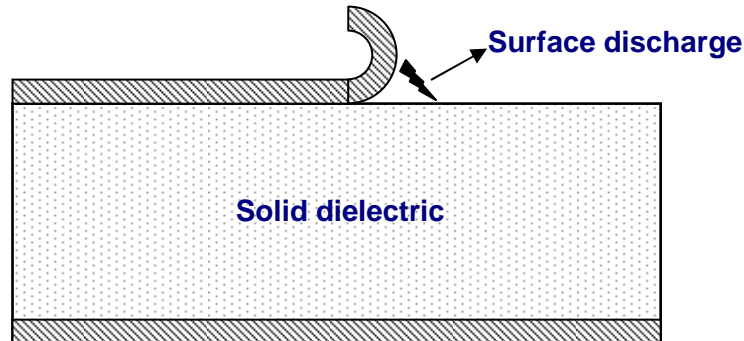


**Figure 3.5 Surface Discharges**

Pollution is one of the main causes of surface discharges and tends to occur between the particles of a contaminant. Salt deposits or dampness can form semiconducting layer and can permit the flow of current. Very often moisture combines with nitrous gases to form Nitric acid and can seriously affect the insulation surface. Insulation surfaces affected by such an acid attack are an ideal surface for tracking to occur <sup>(66)</sup>. Tracking is the result of carbonisation of the surface of the insulation and the carbon tracks tend to electrically short the insulation causing the process to accelerate to an eventual failure.

### **3.2.3 Corona Discharges**

Corona discharges are electrical discharges caused by the ionisation of the medium surrounding the conductor. They tend to occur around sharp points or edges at high voltage because of a high concentration of charge on a small surface area. The inception voltage of corona discharges is difficult to state as it is dependent on various factors like surface smoothness and environmental conditions which affect the space charge near the conductor. They appear sooner at negative than at positive voltage; with a.c. voltage they occur often during the negative half-cycle only <sup>(61)</sup>.

In rotating machines, the end-windings are more susceptible to corona type discharges as the electric stress is intensified in the overhang portion due to its characteristic shape. The gas adjacent to the insulation in the immediate vicinity of the slot exit breaks down and can lead to the development and propagation of discharges over end-windings <sup>(67, 68)</sup>. Hence, the application of stress grading systems along the end-windings is considered essential for high voltage machines. The end-winding discharge is described later in section 3.3.4.

## **3.3 Partial discharge theory applied to stator windings**

A stator comprises of three main components i.e. copper conductors, the stator core and the insulation. The copper acts as the medium to carry the stator winding current and should have a large enough cross section to carry the rated current without overheating. The stator core is made from thin sheets of laminated magnetic steel. It provides a low impedance path for the magnetic fields (from the stator to rotor in the case of the motor and from the rotor to stator in the case of a generator) and prevents the magnetic field from escaping outside the stator core.

The last major component of a stator winding is the electrical insulation. It is considered to be a passive component of the system as it does not produce any magnetic field or guide its path. It does not help to produce any torque or current. It increases the machine size and cost and reduces efficiency; thus acting as an overhead in the system. However, the insulation plays an important role of preventing short circuits between conductors or to ground. In the case of indirectly cooled machines, it also acts as a thermal conductor preventing the overheating of copper windings. It also helps in holding the copper conductors tightly within the stator slots to prevent any movement.

As discussed in chapter 2, the stator winding insulation system contains organic materials as a main constituent. Organic materials soften at a much lower temperature and have a lower mechanical strength compared to copper windings or the steel core. Thus, the electrical insulation is the weakest component in the stator and the life of stator windings is limited by the life of the electrical insulation rather than the copper conductors or the steel core.

### 3.3.1 Insulation breakdown mechanisms in stator windings

Regardless of the cause of failure, it is possible to identify five modes of failures in a three phase stator winding as shown in figure 3.6. Each of these faults will result in a flow of short circuit current in the machine winding from a breakdown in the turn or ground insulation.

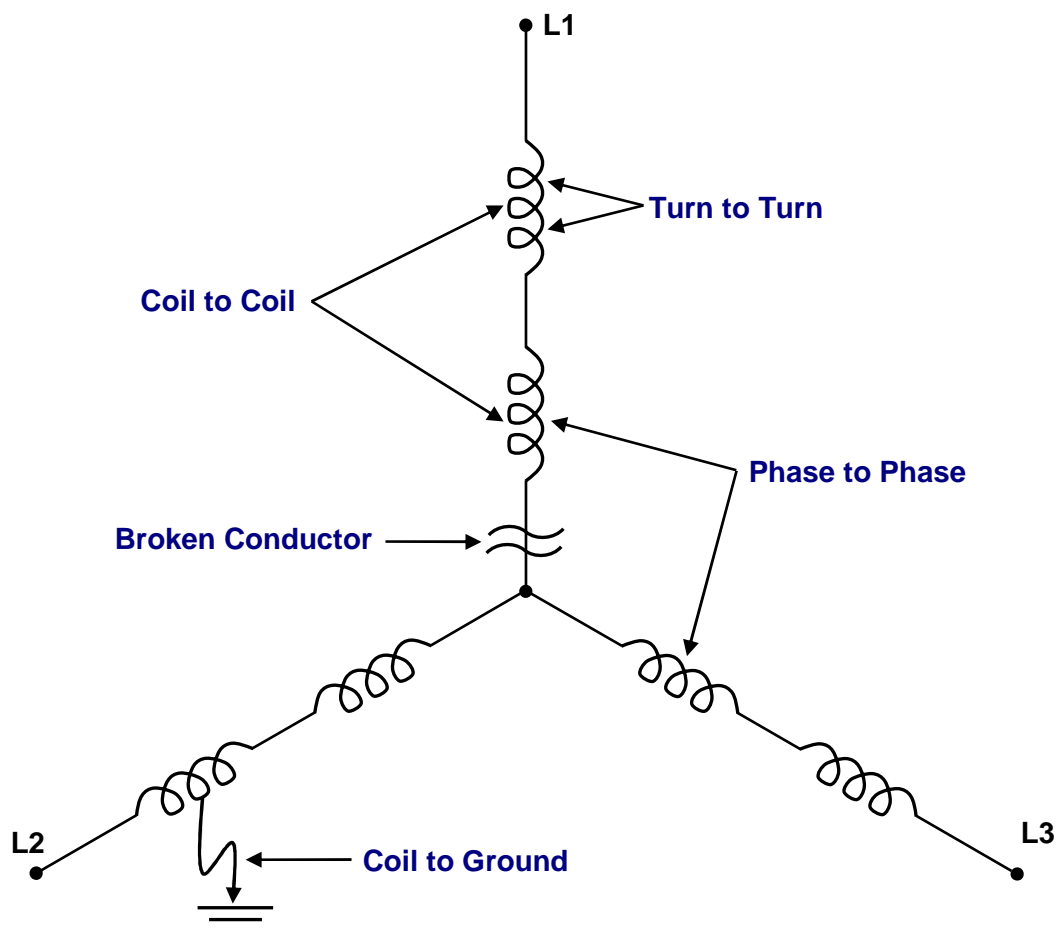


Figure 3.6 Failure modes in 3 phase stator windings <sup>(69)</sup>

For example, a random wound motor started frequently can result in a minor turn-to-turn short within a coil. This short will lead to localised excessive heating resulting in insulation degradation. As this condition progresses more heat is generated in the damaged area until the phase or ground insulation is destroyed. At this point, either a phase-to-phase fault can occur or a phase-to-ground fault can occur eventually leading to a machine failure.

### 3.3.2 Defect locations

The above stated insulation breakdown mechanisms can occur at different locations in a stator winding; hence it is necessary to look at the stator winding construction. The construction of stator winding structures varies depending on the operating voltages and rated power of the machine. The two main types of stator winding structures are *random wound* stators and *form wound* stators. Random wound stators are typically used for low power machines (few hundred KW) that usually operate at voltages less than 1000 volts. Such machines are not prone to partial discharge activity due to the low voltage.

Form wound stators are available in two forms i.e. coil type and roebel bar type. The roebel bar type stator has limited applications and is only used for very large generators (typically in the range of 50 MW or above) where inserting a coil type stator in a slot poses a significant risk of mechanical damage. The most commonly used stator structure in high voltage machines (>1000V) is the form wound coil type stator windings. Figure 3.7 shows the typical structure of a single form wound coil.

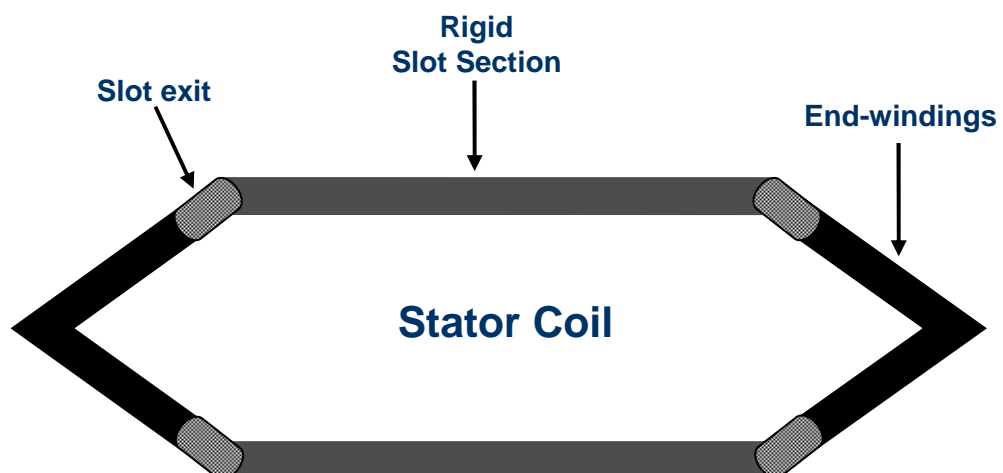


Figure 3.7 Form-wound stator coil

The coils are pre-formed, hot pressed to the correct profile and inserted into the stator slots. The part of the coil that is firmly supported by the stator core is called the slot section; whereas the overhang part of the coil (after slot exit) forms the end-windings. The slot section is usually wrapped with mica paper tapes bonded together with epoxy forming the 'ground-wall' insulation <sup>(70)</sup>. The ground-wall insulation separates the copper conductors from the grounded stator core. A semiconductive coating (carbon loaded tape or paint) is applied over the ground-wall insulation in the slot region. This coating, often referred to as the corona screen, prevents partial discharge that could occur in any air gap between the surface of ground-wall insulation and the side of the stator slot. A stress grading tape (silicon carbide powder) is applied at the slot exit overlapping the slot conductive coating and extending 10-15 cm into the end-winding region. The stress grading tape is designed to reduce the risk of partial discharge by reducing the electric stress along the surface of the coil from the line voltage in the end-winding region to nearly ground potential, where it joins the slot semi-conductive coating. After inserting all the coils in the stator, the stator slots are wedged to prevent any coil movement. Similarly the end-windings outside the stator slot are supported by a bracing ring, usually made of steel and insulated epoxy. Finally the stator windings are impregnated with resin and cured using a technique called 'Global VPI' <sup>(71)</sup>. This process helps in eliminating voids (except very small) in the insulation and to bond the main-wall and conductor together.

Depending on the various types of stress operating within a rotating machine and the condition of various insulation structures of the stator coils, the defect can either be located in the slot section or the end-winding region and are called 'slot discharges' and 'end-winding discharges' respectively.

### **3.3.3 Slot Discharges**

The slot section of a stator winding coil is usually covered with some form of conductive coating (corona screen) in order to prevent discharge between the insulation surface and stator slot walls. If the resin impregnation of the coil is complete and the corona screen is intact and adequately connected to the stator core, then there should be no discharge activity. In practice, most high voltage motors operating in the range of 6 KV and above have some degree of slot discharges like internal discharges due to small residual voids embedded within the insulation.

Surface discharge in the slot region is not normally possible unless the corona screen has sustained physical damage of some kind with the most likely cause being abrasion

against the slot wall either during manufacture or during service. When a machine is in service, the abrasion can occur if the coil sides have some freedom of movement. As stated in section 2.2.2, there are significant amount of electromagnetic forces exerted on the stator windings which can cause a loose coil to rub against the slot walls. Similar friction can take place if the slot wedges are loose and this can lead to the removal of small areas of semiconductive corona screen and possibly the main-wall insulation. This process may well be progressive and can result in a weak bonding between substantial areas of the corona screen and earth. This increases the surface resistivity resulting in a high surface potential that may eventually cause a discharge. Discharge to the slot walls will occur when the electric field in the gap is higher than the breakdown strength of the gas. This is dependant on the nature and the pressure of the gas and also on the width of the gap. However, it is known that the regions where the semiconducting surface coating becomes isolated from the earth (connected via stator walls), the discharge magnitudes will increase substantially. This is due to the high energy content caused by the relatively large effective value of capacitance involved.

The investigation undertaken by Jackson and Wilson <sup>(72)</sup> identified different forms of slot discharges in high voltage motors and generators and highlighted various factors that affect the slot discharge activity. The study reported that if there is a large air-gap between the insulation surface and slot wall (>0.2mm), discharge from the bare insulation to the earthed coating will erode the coating and extend the damaged area. The removal of the surface coating allows discharge between the insulation surface and the slot wall, reducing the service life of insulation.

Figure 3.8 shows the typical defects than can occur with the slot section of a rotating machine. The de-lamination of conductor insulation can cause an inter-turn fault. Internal voids are invariably present within the insulating material due to manufacturing tolerances. Such defects can cause internal type discharges. The thermal cycling can cause the de-lamination of insulation layers and promote discharge activity. The slot discharge activity caused due to the erosion of the corona screen can be accelerated due to coil vibrations. If progressive in nature, then this type of discharge can eventually cause the copper conductors to short with the stator slot resulting in an earth fault.

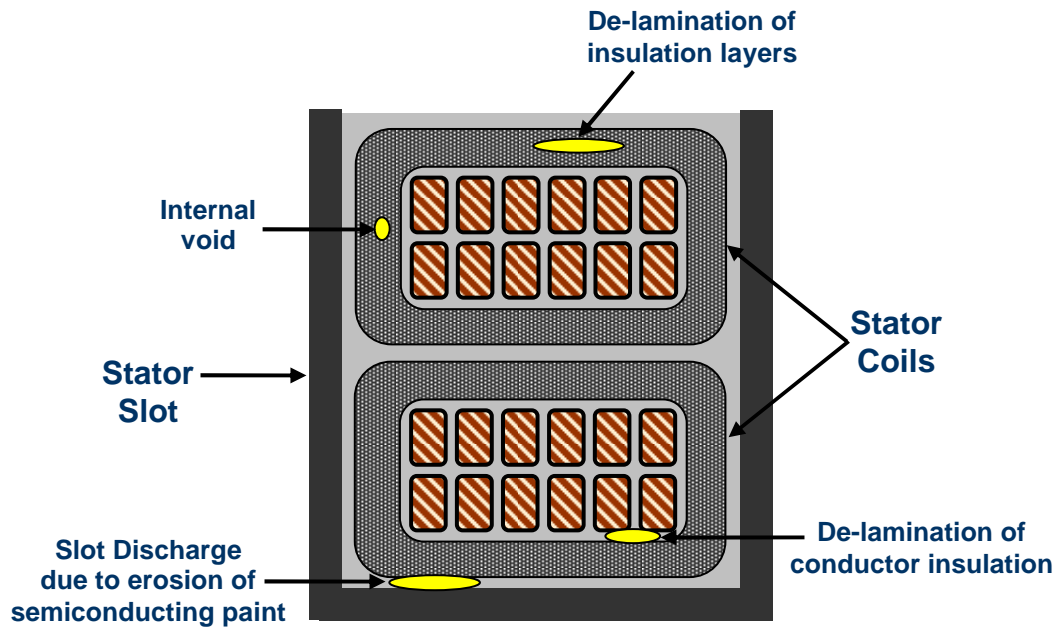


**Figure 3.8 Typical defects in slot section**

### 3.3.4 End-winding discharges

Rotating machines are often subjected to harsh environmental conditions where the stator windings can be exposed to contaminants like oil, grease, dust, dirt, salt, sand and moisture <sup>(73)</sup>. The source of contamination can be located inside the machine (oil and grease released from motor bearings) or outside (sand, dirt, insects, pollen etc.). Machines that operate in high humidity environments (hydro-generators) are also prone to attack from moisture that can enter a motor enclosure and condense onto the winding surfaces.

The effect of such contamination on the integrity of winding insulation depends on the type and level of contamination present in the environment in which it is located. Edwards <sup>(31)</sup> states that if the accumulation of contamination on high voltage stator endwinding reaches levels sufficient to significantly reduce the insulation surface resistivity, then at least three different degradation mechanisms are possible:

- a) Endwinding Internal discharge
- b) Phase-phase discharge
- c) Surface tracking

#### 3.3.4.1 Endwinding Internal Discharge

Most voids except very small ones are eliminated from the slot section of the stator coil as they are pre-formed and hot pressed to the correct profile creating robust and consolidated ground-wall insulation. However, that is not the case with the curved endwinding sections. This part of the stator coil needs to retain a degree of flexibility to allow the build of the stator winding. During the process of insertion of coils the endwinding sections are twisted and this leads to the displacement of ground-wall insulation immediately adjacent to the conductor insulation. This action tends to create voids between the ground-wall insulation and the insulated conductors. These voids in the endwinding region are not a cause of concern as long as the endwindings remain clean and free of debris. But the deposition of surface contamination, if conductive, can act as an extension of the earth structure of stator frame resulting in an increase of electric field intensity within the endwindings. This can initiate discharge activity and subsequent discharge erosion can lead to inter-turn insulation failure. Walker and Champion <sup>(74)</sup> have presented a practical investigation of inter-turn insulation failure caused by the contamination of voids between the conductors and ground-wall insulation in the endwinding region.

#### 3.3.4.2 Phase-to-phase discharge

Phase-phase discharges can occur if the stator coils of different phase groups have insufficient spacing between them. However, the spacing of the coils in the endwinding region is normally designed in such a way that during normal operation the discharges are unlikely to occur between coils of two different phase groups. But, it is difficult to ascertain that this will not happen as phase-phase discharges are found to occur from time-to-time, particularly on machines with high voltage ratings <sup>(31)</sup>. Again, this type of discharge activity is not a problem as long as the coil surfaces are clean and dry. This is because a clean insulating surface is a poor conductor of current and the discharges have relatively low energy and cannot cause a rapid erosion of insulation. However, the deposition of conductive surface contamination significantly reduces the surface resistivity and increases the effective surface area feeding current to the discharge, correspondingly increasing the discharge energy. It is commonly found that the solid contaminants have a tendency to be deposited on surfaces between phase groups due to electrostatic attraction to the high field region, instigating the occurrence of discharges between different phases.

### 3.3.4.3 Surface tracking

Acute surface contamination caused due to deposition of moisture / water on the insulation surface can cause a substantial amount of electric current to flow in the surface film. The current flow pattern is extremely complex. Local concentrations of high current density can lead to high energy surface discharge causing the carbonisation of the underlying insulation surface. The area of carbonisation continues to grow in a complex tree-like pattern and burns deeper into the surface. This can eventually lead to phase-phase failure or phase-ground failure.

Figure 3.9 shows the typical defects that can occur in the endwinding section of rotating machines.

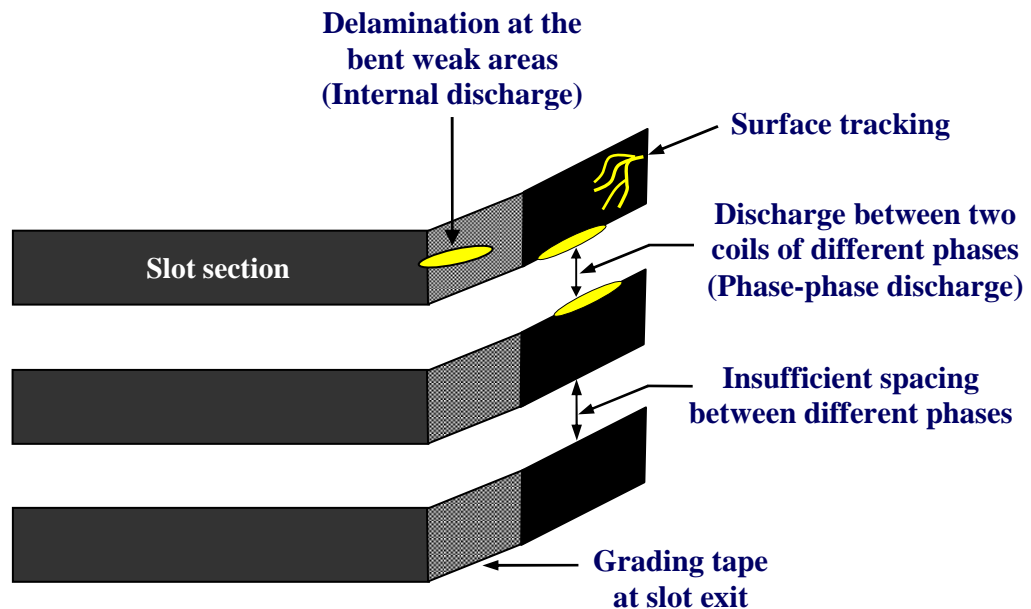


**Figure 3.9 Typical defects in endwinding section**

Another significant cause of discharges in the stator endwindings is the endwinding movement or vibration. The endwindings do not have the firm support of the stator core and are vulnerable to vibration. The endwindings are supported with an endwinding bracing that is designed to prevent excessive movement in the presence of electromagnetic forces. However, if the motor is subjected to a frequent starting duty then there is a tendency for some limited freedom of movement to develop. The resultant flexing of the coils can lead to fatigue failure of the insulation structure. The vibration can also have an effect of reduced spacing between coils and if coils from

different phase groups are involved then it can lead to phase-phase discharges. It can also cause abrasion of the anti-corona coating resulting in surface discharge.

### **3.4 Summary**

Partial discharges can be classified into three basic types i.e. internal discharge, surface discharge and corona discharge. In relation to stator windings, discharges can be classified based on their location i.e. slot discharges and endwinding discharges. Although extensive measures are taken during the manufacturing process of high voltage stator windings, a small magnitude of discharges will occur due to manufacturing tolerances. In-service degradation of stator winding insulation is accelerated by various factors like winding movement (vibration) and deposition of contamination on winding surface.

When a partial discharge occurs, irrespective of its type, a current pulse is generated and this pulse can be used for discharge detection. Having studied the different types of discharge mechanisms and the associated failure modes in stator windings, the next chapter details various techniques used for the detection of partial discharge.

# CHAPTER 4: PARTIAL DISCHARGE DETECTION

## 4.1 Introduction

Partial discharges (PD) were first observed in the gaseous inclusion of solids in 1878. A considerable amount of research has been undertaken since then to detect and measure very small discharges. A vast range of techniques are now available with each measuring certain specific quantities. Experience indicates that no one method can be applied to measure all quantities related to discharge. The relative use of each technique is largely dependant on the nature and type of equipment to be monitored due to vast differences in the actual physical structure.

When PDs occur, they are accompanied by various physical manifestations like light, heat, noise, chemical transformations, gas pressure, electromagnetic radiation, dielectric losses and electrical impulses. Hence, PDs can be detected and quantified by measuring any of these physical quantities using various methods. The PD detection can be grouped into two main categories:

1. Non-electrical detection techniques
2. Electrical detection techniques

The detection of electrical quantities like dielectric losses and electrical impulses are very popular techniques and are extensively used for the detection of PDs in rotating machines. The detection of electromagnetic radiation is most often used for detecting PDs occurring within high voltage switchgear and transformers. The non-electric detection methods are less popular as they tend to be less sensitive in many cases.

## 4.2 Non-Electrical detection techniques

The most common non-electrical PD detection techniques can be classified into three categories:

- a) Chemical detection
- b) Acoustic detection
- c) Optical detection

### 4.2.1 Chemical detection

PDs can be detected chemically because the current streamer across the void can breakdown the surrounding materials into different chemical components. Pressurised SF<sub>6</sub> gas is used as high voltage insulation in gas insulated switchgear (GIS) and GIS substations. Although SF<sub>6</sub> is non toxic and chemically very un-reactive, the decomposition of gas can take place under the presence of partial discharge generating bi-products like SOF<sub>2</sub>, SO<sub>2</sub>F<sub>2</sub>, SO<sub>2</sub>, SOF<sub>4</sub>, S<sub>2</sub>F<sub>2</sub>, S<sub>2</sub>F<sub>10</sub> <sup>(75, 76, 77)</sup>. As the concentration of these bi-products increase they can be detected by various gas detectors with sensitivities to a few ppm (parts per million). However, in GIS these gases may be greatly diluted due to the large volume of SF<sub>6</sub> and may take a longer time to be detected making this method less sensitive to detect gases in smaller concentrations.

In the case of power transformers, the PD activity generates gaseous compounds like hydrogen, methane, ethane, ethylene, acetylene and carbon monoxide in transformer oil and these gases can be detected by performing a chemical analysis <sup>(78)</sup>. Dissolved Gas Analysis (DGA) is the most popular technique used for on-line testing of power transformers to detect arcing and PD <sup>(78, 79, 80)</sup>. It is a simple on-line procedure causing minimal disruption and involves collecting an oil sample and performing a chemical analysis in a laboratory to detect the dissolved gases in oil. An assessment is made based on the gases present and their respective concentrations. The Duval triangle <sup>(151)</sup> is one such diagnostic method used for oil insulated high voltage equipment.

High Performance Liquid Chromatography (HPLC) is another technique that is used for detection of bi-products generated by degradation of paper insulation. The insulating paper used for the windings of power transformers contains cellulose as its main constituent. Cellulose is a natural polymer of glucose. Cellulose can degrade under the presence of heat, moisture and oxygen. Cellulose degradation reduces the degree of polymerisation, destroys interfibre bonding and causes loss of mechanical strength, leading to tearing and defibrillation <sup>(81)</sup>. Furans are major degradation products of cellulose insulation paper. The HPLC technique can be effectively used to monitor the formation of furan components during the ageing of the cellulose insulation paper as demonstrated by Unsworth and Mitchell <sup>(82)</sup>. However, chemical testing has limitations. It only provides an integrated measure of PD activity. It provides very little information about the nature, intensity, extent or location of PD <sup>(83, 84)</sup>.

## 4.2.2 Acoustic detection

The principle of acoustic PD detection is the detection and recording of the pressure waves generated by discharge within the insulation. A discharge results in the instantaneous release of energy resulting in the vaporising of material around the hot streamer. This vaporisation causes a small explosion, which excites a mechanical wave that propagates through the insulation <sup>(85)</sup>. The intensity of the emitted wave is proportional to the energy released in the discharge.

As the PD impulses are of short duration, the resulting wave signal has frequencies in the ultrasonic region that can range between 20 KHz and 300KHz <sup>(83)</sup>. Piezo ceramic transducers such as acoustic emission sensors and accelerometers are widely used for the detection of ultrasonic waves in an enclosure and provide the best sensitivity <sup>(86)</sup>. As the PD signals are not in the audible range, the airborne ultrasound instruments like 'ultrasound translators' use an electronic process called 'heterodyning' to accurately convert the ultrasound waves into an audible range. This enables the user to hear and recognise PD through an isolating headphone and can be effectively used to detect PD caused by corona, tracking and arcing <sup>(87)</sup>.

The advantage of using acoustic detection over chemical detection is that the location of discharge sources is possible using sensors at multiple locations. Another advantage of acoustic detection is that it is immune to electromagnetic interference (EMI). The immunity to EMI makes acoustic detection ideal for online PD detection because a better signal to noise ratio (SNR) will be obtained for the acoustic signal <sup>(88)</sup>. Acoustic detection is generally used for power transformers and switchgear due to the existence of excessive electrical noise at the measurement site.

Acoustic detection also has some disadvantages. The primary problem is the complex nature of acoustic wave propagation. The acoustic impedances between the PD source and detector can be extremely complex. The acoustic wave is distorted by a variety of factors like geometrical spreading of waves, frequency dependant velocity effects, transmission losses, reflections and absorption in materials. Due to these attenuation mechanisms the received acoustic signals have very low intensity. Hence, the sensor has to be very sensitive to detect small changes in signal amplitude in order to detect PD <sup>(84)</sup>. Secondly, it is very complex to quantify the relationship between the intensity of acoustic noise and the nature of the fault producing it <sup>(89)</sup>. Hence, acoustic detection is not generally used as the primary form of PD detection, but is rather used as a complementary technique in conjunction with other techniques (e.g. electrical methods) where PD location is essential.

### 4.2.3 Optical detection

The optical partial discharge detection is based on the detection of light produced as a result of various ionisation, excitation and recombination process during a discharge. Although all discharges emit radiation, the optical spectrum of different discharges is not the same. The amount of light emitted and its wavelength is dependant on the surrounding insulating medium (gaseous, liquid or solid) and different factors like temperature and pressure. The optical spectrum ranges from the visible ultraviolet range to the invisible infrared range<sup>(90)</sup>. For example faint corona in air emits radiation in 280nm – 410nm spectral range (~95% in UV region) making it invisible to the human eye. The wavelength of a strong flash discharge is between 400nm – 700nm. The spectrum of surface discharge along with solid dielectric is very complex and is dependant on various factors like type of electrode material, surface condition, etc.<sup>(91)</sup>. In gases with low pressure, energy in the range of 1% is emitted as discharge; this figure is even lower for liquids and solids<sup>(90)</sup>.

Two different measuring techniques are used for optical detection. The first technique comprises of using a UV corona imaging camera for the detection of discharges on the surface of electrical equipment. This technique is used for high voltage transmission lines and in power stations. The second technique involves the detection of an optical signal inside the equipment by using fibre optic cables as sensors and as transport medium for optical signal. This technique is suitable if the high voltage equipment is enclosed and light tight like transformers and GIS. An optical fibre samples light produced by PD inside the equipment and transmits the signal outside the equipment to a detection unit that converts light into electrical signal (photomultiplier). Detailed investigations of these techniques have been carried out by Cosgrave et al.<sup>(92)</sup> and Blackburn et al.<sup>(93)</sup>.

The optical detection method is immune to electromagnetic interference. However, this technique is not widely used in industry due to the cost of the equipment and invasive nature of the technology<sup>(84)</sup>. As air and SF<sub>6</sub> are 100% transparent, light can be detected from a large distance. However, in the case of liquid and solid insulation a section of emitted light will be absorbed and the detection may become difficult. Also, a relationship between the discharge magnitude and intensity of light is difficult to establish making it difficult to calibrate<sup>(90)</sup>.

### **4.3 Electrical detection techniques**

A vast range of electrical techniques have been developed over a period of years for the measurement of partial discharges. The main advantage of electrical detection is that they are perhaps more sensitive compared to other methods and hence are more popular and more frequently used. The currently used electrical detection technique lays emphasis on capturing the current pulse created by the electrical streamer within the void or the current due to surface discharge. A small amount of current flows every time a PD occurs creating a voltage pulse across the impedance of the insulation system. Measuring this pulse forms the primary means of detecting PD. A typical stator coil / bar may have numerous discharging sites and there may be hundreds of PD pulses generated each second. With the advancements in technology it is now possible to acquire an enormous amount of PD data on a pulse-by-pulse basis and analyse them using various signal processing techniques.

There are two basic approaches for electrical PD detection:

1. Power loss detection.
2. Detection of current pulses.

#### **4.3.1 Power loss detection methods**

A PD event is accompanied by emission of energy in various forms (i.e. acoustic, heat, light, RF, etc.). This implies that each PD event must absorb a certain amount of energy from the power frequency voltage to source the energy dissipated in a PD pulse. The measurement of this lost energy (expressed as loss tangent,  $\tan \delta$ ) provides an overall indication of dielectric losses and the general condition of the insulation <sup>(94, 95, 96)</sup>. This is a constant value for low voltages (below PD inception voltage), but will begin to rise at higher voltages (beyond PD inception voltage) resulting in higher dielectric losses as indicated in figure 4.1. A sudden increase of loss-tangent is attributed to internal discharges. Generally, many discharges are required to obtain an observable increase in  $\tan \delta$ .

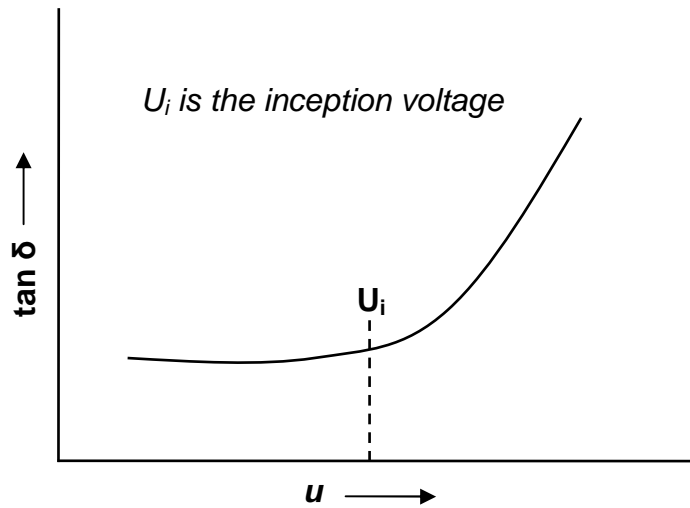


**Figure 4.1 Dielectric loss as function of voltage**

The dissipation factor  $\tan \delta$  is measured with a balanced bridge-type instrument like Schering bridge (or a derivative). Figure 4.2 shows a typical Schering bridge <sup>(97)</sup> used for measuring discharges. The impulse caused by a discharge is detected across resistor 'R<sub>4</sub>' in one arm of the bridge. When the bridge is balanced the value of  $\tan \delta$  can be found using the following equation:

$$\tan \delta = \omega R_4 C_4 \dots\dots\dots(4.1)$$

where R<sub>4</sub> and C<sub>4</sub> are the resistance and capacitance required to balance the bridge as shown in figure 4.2.

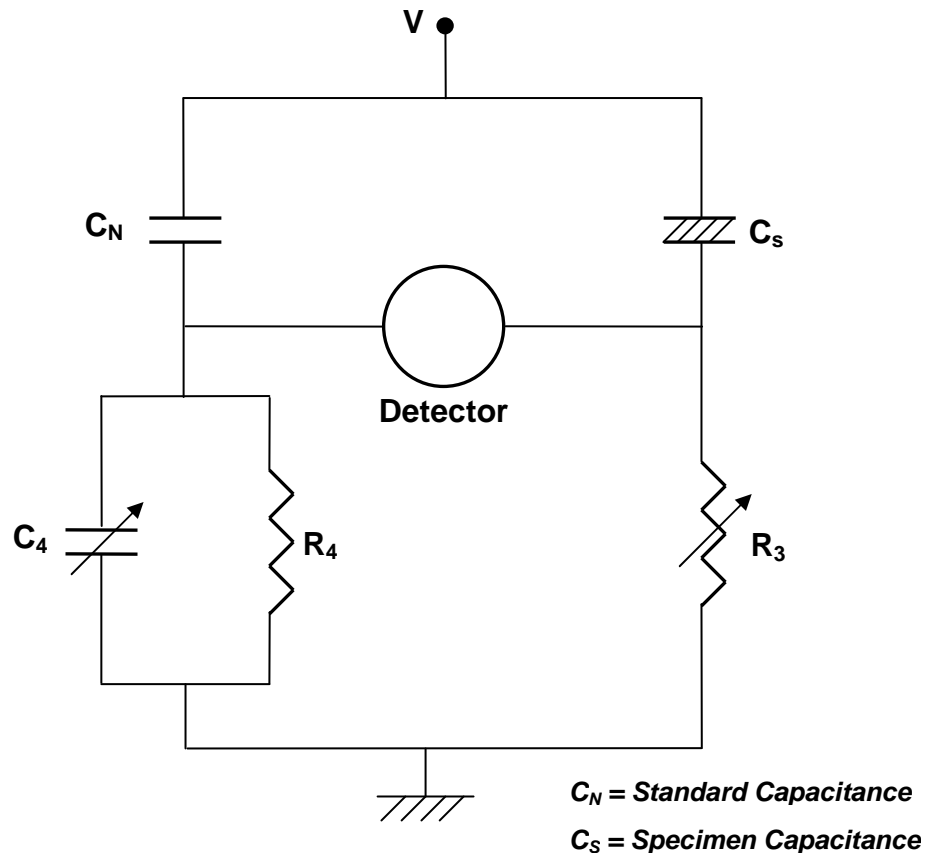


**Figure 4.2 The Schering Bridge Circuit <sup>(97)</sup>**

Another bridge-type instrument used for this application is the Transformer ratio arm bridge <sup>(98)</sup>. This bridge circuit operates by balancing the winding of a transformer by adjusting the number of turns to give a small response on the detector connected across the third winding of the transformer. The transformer bridge offers low impedance in balanced condition and has other advantages like higher sensitivity, stability of ratio accuracy and ease of matching null detector to bridge by simply varying the number of turns of the detector winding <sup>(99)</sup>.

Both of these bridge methods have some limitations. The Schering bridge is susceptible to the effects of stray capacitance and the transformer ratio-arm bridge may be affected by the strong magnetic field. Another method to overcome these problems is the Dielectric Loss Analyser (DLA). This is also a bridge method but uses an oscilloscope to balance the bridge. The bridge is balanced at low voltage (when no discharges are occurring) generating a horizontal line on the oscilloscope. As the voltage is increased, discharges can occur causing a vertical deflection of the trace on the screen. The combinations of horizontal and vertical deflections produce a parallelogram pattern (loop) on the screen and the area covered by the parallelogram

is directly proportional to the discharge energy <sup>(100)</sup>. Figure 4.3 shows the basic circuit of a DLA.

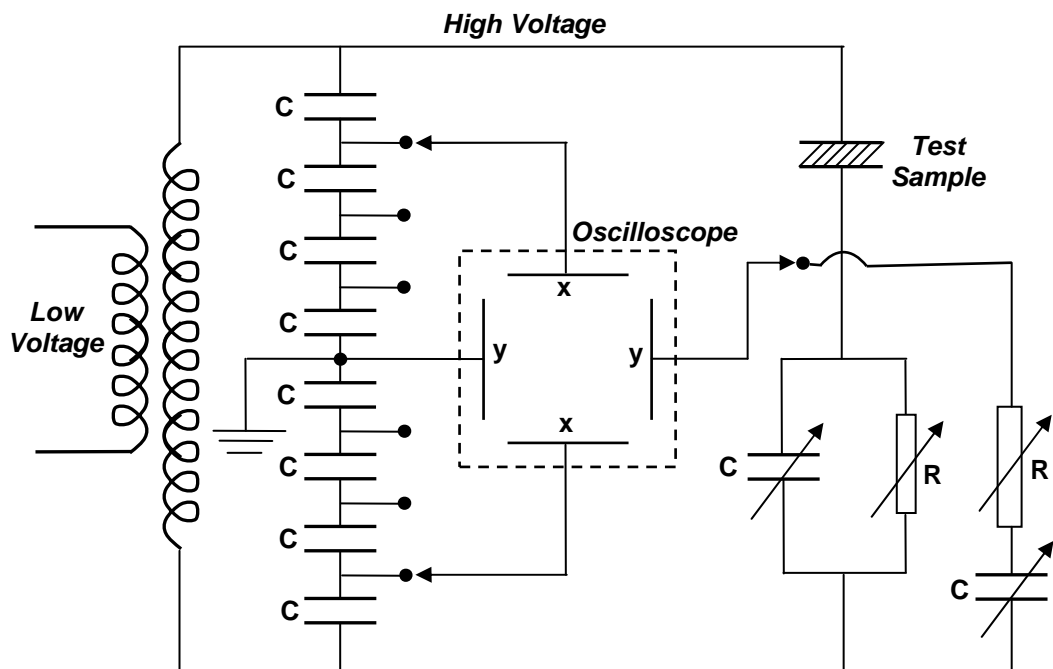


**Figure 4.3 – Basic circuit of Dielectric Loss Analyser <sup>(100)</sup>**

Although these techniques have been successfully applied in industry <sup>(101)</sup>, there are certain limitations. The major disadvantage is that they provide an integrated measure of PD activity making it difficult to detect the nature of PD activity. They cannot distinguish between the presence of a few large discharge sites (detrimental to insulation) and several small discharge sites (relatively innocuous). They are generally not very sensitive and can only be applied off-line. Hence they are often considered unsuitable as the primary means of insulation assessment.

### 4.3.2 Detection of current pulses

The current detection circuits operate by responding to the current pulses produced by discharges (section 3.2.1.1). The small amplitude current pulses are transformed into voltage pulses, which are amplified and then displayed on a suitable screen. These current detection circuits are classified in two different categories i.e. 'straight detection' and 'balanced detection' circuits.

#### 4.3.2.1 Straight detection method

A variety of circuits are used to detect the current pulses, but all these circuits will contain the following elements <sup>(102)</sup>:

- a) A discharge free high voltage source.
- b) A test sample ' $C_x$ ' that is affected by discharges.
- c) A high voltage coupling (blocking) capacitor ' $C_B$ ' connected across the test voltage source to facilitate the passage of current impulses.
- d) A detection impedance ' $Z$ ' across which the voltage impulses are induced caused by discharge current pulses in the sample.
- e) An amplifier ' $A$ ' to amplify these pulses.
- f) A display unit ' $O$ ' – usually a CRO for display.

Figure 4.4 shows the basic circuit for the straight detection method. The measuring impedance  $Z$  is either connected in series with  $C_B$  or  $C_x$ , depending on the value of  $C_x$ . If the value of  $C_x$  is large then the  $Z$  is placed in series with  $C_B$  so that the large charging current of  $C_x$  does not pass through the impedance  $Z$ .

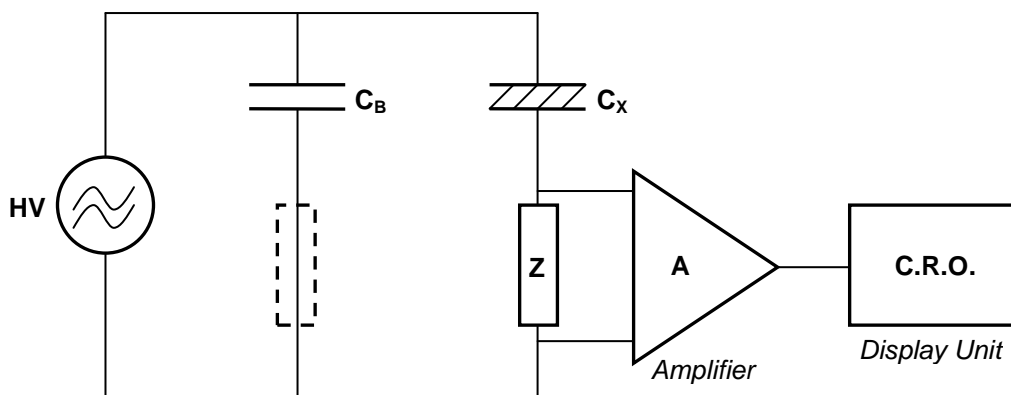


**Figure 4.4 Basic circuit for straight detection method <sup>(102)</sup>**

#### 4.3.2.2 Balanced detection method

The discharges that take place external to the sample (e.g. discharges in the high voltage source, the leads, bushings, terminals, etc.) cannot be easily distinguished from the discharges in the sample in the straight detection method. The balanced detection method essentially contains all the elements described in the straight detection method, but additional measures are taken to reject disturbances caused by discharges external to the sample. Figure 4.5 shows the basic circuit for balanced detection.

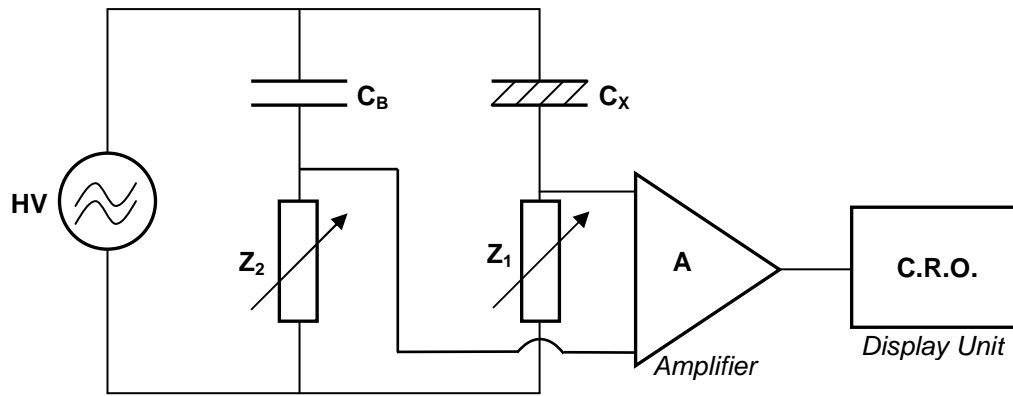


**Figure 4.5 Basic balanced detection method** <sup>(102)</sup>

As shown in figure 4.5, in addition to the series connection of test sample  $C_X$  and measuring impedance  $Z_1$ , a parallel branch of capacitor  $C_B$  (similar capacity as  $C_X$ ) and a series connected measuring impedance  $Z_2$  is inserted in the circuit. The differential amplifier A is connected between the two measuring impedances. If the two measuring impedances are adjusted in a way, that the voltage drops caused by external disturbances are equal for both measuring impedances  $Z_1$  and  $Z_2$ , then these disturbances coming from outside the two parallel branches are eliminated.

### 4.3.3 On-line electrical detection systems

On-line electrical detection systems are usually designed for either narrow band or wide band operation and are capable of providing data on each individual discharge event. PD pulses have rise times in the range of 10 to 100 ns. This corresponds to a frequency spectrum extending in the region of 100 MHz. Therefore, there is wide band of frequencies to be selected for detection. In practice there is a limit on the lower end of the frequency range so that the main frequency voltage and its harmonics are below the noise level of the detector, discouraging the operation below 10 KHz or so. The upper frequency is restricted due to the attenuation effects of the high frequency signal while propagating through the stator windings. Wilson et al. <sup>(112)</sup> showed that the detection of signals with bandwidth in excess of 1 MHz may produce up to 50 fold attenuation when travelling from remote sites to the terminals of stator windings. They stated that a frequency range of 20 – 300 KHz is most suitable for rotating machines as the attenuation errors are restricted to within a factor of two to three. In general, therefore most narrow and wideband detectors select their pass-bands between 20 KHz and 300 KHz. In fact harmful discharges tend to have longer decay times (tails), thus containing a lower range of frequencies.

It is well established that the individual discharge magnitudes can be indicative of the relative size of the individual degradation site and the magnitude-phase relationship (in relation to mains frequency) can provide information regarding the nature and form of discharges <sup>(103 – 105)</sup>. The two most popular PD pulse measuring techniques are use capacitive sensors for measuring the voltage or use inductive sensor for measuring current. Both these methods require a time domain recording device to capture the PD signal. The capacitive technique, often referred to as ‘direct probing’ technique, is not completely non-invasive as it requires connecting capacitive sensors like capacitive couplers to high voltage phase terminals. However, the development of permanently installed couplers connected to the machine terminals has proven to be a well-known approach for discharge detection in rotating machines <sup>(106-108)</sup>. Sedding et al. <sup>(111)</sup> developed a PD coupler called a ‘Stator Slot Coupler’ that can be used with an ultra wideband system for reliable discrimination of PD signals from noise in turbine generators.

The inductive techniques are typically of narrow-band types and use inductive sensors like radio frequency current transformers or Rogowski coils. They are clipped round the line-end of the winding at the terminal box of the motor and are electrically isolated making it a completely non-invasive technique. However, the ringing output can severely limit the pulse resolution. Kouadria & Watt <sup>(109, 110)</sup> have described the application of a PD detection system that uses Rogowski coils as sensors for detection of discharge activity in rotating machines and presented various case studies.

The RF emission from PD activity can be detected by aerial techniques <sup>(113)</sup>. Stone and Sedding <sup>(114)</sup> have reported the use of a TVA (Tennessee Valley Authority) probe to locate discharge sites in rotating machines by detecting RF energy. Although measurements made by the TVA probe is an effective means to get a detailed evaluation of the condition of a winding, it is an off-line technique that requires long measurement and disassembly time <sup>(115)</sup>.

Electrical detection also has limitations. The primary limitation of electrical testing is its susceptibility to extraneous interference when compared to other techniques. The PD signals that are acquired on-site can contain significant amounts of interference arising from various sources making the measurement process more intricate. In some cases it becomes extremely difficult or even impossible to distinguish between noise and PD because of short PD pulse width. This problem may lead to false detection of partial discharges. Another problem with electrical detection is that the received pulse characteristics are highly dependant on the geometry of the HV machine. Different

components in the machine can distort the pulse shape needed to characterise the PD fault and can lead to erroneous detection <sup>(112, 116)</sup>. In order to overcome all these limitations, intensive signal processing techniques are deployed on the acquired PD signal to separate the PD signals from noise and extract maximum information from it. Despite these limitations, electrical detection techniques are by far the most popular and extensively used around the world.

## **4.4 Sensors used for electrical PD detection**

Various types of sensors are used to detect PD on different types of high voltage equipment. The choice of sensor is influenced by factors like suitability of the sensor for detection, the costs involved and the type of application. A suitable PD sensor should cover the following characteristics <sup>(117)</sup>:

- a) Should not influence the service condition of the equipment
- b) Should have at least the same life performance as the equipment on which it is installed
- c) Easy installation of sensors
- d) Inherent against ambient on-site conditions

### **4.4.1 Classification of sensors**

The sensors used for electrical PD detection can be classified into two different types:

- a) Inductive type sensors (magnetic field sensors)
- b) Capacitive type sensors (electric field sensors)

#### **4.4.1.1 Inductive type sensors**

The inductive type sensors are designed to detect the magnetic field of the transient PD current. The inductive field coupling is usually done with a magnetic field antenna, a Rogowski coil or an RF current transformer. Some of the characteristics of inductive type sensors are as follows:

- Well suited for on-line measurements with compact portable equipment
- Provide galvanic isolation
- Can be installed around cables easily due to simple construction
- Installation does not require machine to be shutdown
- Sensitivity is reduced compared to the capacitive probes

#### 4.4.1.2 Capacitive type sensors

The capacitive type sensor is designed to detect the electric field energy of PD pulses with a metallic electrode structure or additional metallic foil layers placed into the electric field. Some of the characteristics of capacitive type sensors are as follows:

- Well suited for on-line measurements with compact portable equipment
- Don't provide galvanic isolation and the sensor is subject to HV
- Pre-installation is recommended
- Machine needs to be shutdown for installation (if machine is on-line)
- Sensitivity is better than the inductive type sensors

Some of the most popularly used inductive and capacitive type sensors used for PD detection in rotating machines are described in the following section.

#### 4.4.2 Rogowski Coil

Invented in 1912 by Walter Rogowski, the Rogowski coil is essentially an air-cored current transformer and is very well suited for measuring PD like transients. It is designed to detect the magnetic field caused by flow of current without the requirement to make an electrical contact with the conductor. It operates on a simple principle and can be considered as a flux to voltage transducer. A non-ferrous core or an 'air cored' coil is placed round the conductor in a toroidal manner such that the alternating magnetic field produced by the current induces a voltage in the coil. The voltage output is proportional to the rate of change of current. If this output voltage is integrated, then an output proportional to current can be obtained.

The voltage induced in the coil wound around the torroid is proportional to the time derivative of the current flowing through the conductor passing through the torroid. The relationship is given by the following equation <sup>(118)</sup>:

$$v_{coil} = \mu_0 A n \frac{di}{dt} \dots\dots\dots(4.2)$$

where,

' $\mu_0$ ' = permeability of air

'A' = turn area

'n' = number of turns per unit length

The product of ' $\mu_0 * A * n$ ' is called the mutual inductance 'M' of the coil.

Hence, in order to obtain a voltage signal that is proportional to the current waveform it is necessary to integrate the coil output ' $V_{coil}$ '. Electronic integrators consisting of passive integration networks are used for this purpose. It is also possible to design a 'self-integrating' Rogowski coil by using a low resistance as terminating impedance <sup>(118)</sup>.

There are two popular forms of Rogowski coil designs. One is a coil wound on a rigid toroidal core intended for permanent installation and high precision measurements. A clip-on version of the rigid toroid is also available and can facilitate ease of installation. The second design is the coil wound on a flexible core. They are compact in design and versatile. However, the rigid core coil provides better accuracy as the flexible coil is prone to change in characteristics due to turn displacement <sup>(119)</sup>. The geometry of the coil plays an important role in the electrical performance. The sensitivity of the Rogowski coil can be increased by having multi-layered coils. But this increases the inductance, which has a detrimental effect on the bandwidth <sup>(118)</sup>.

The application of Rogowski coils for detecting PD is popular in the UK North Sea oil & gas industry <sup>(109, 110)</sup>. A general arrangement of a Rogowski coil PD detection circuit for rotating machines is shown in figure 4.6. Figure 4.7 shows a photograph of typical installation of Rogowski coils within a motor terminal box.

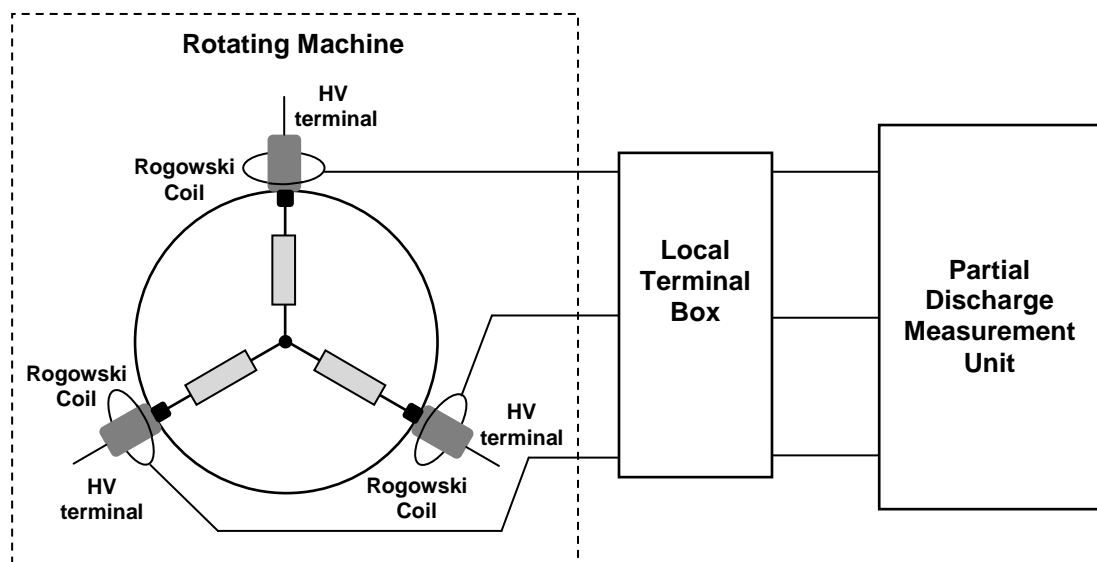


**Figure 4.6 Rogowski coil PD measurement circuit for rotating machines**



**Figure 4.7 Photograph of Rogowski coil installation inside a motor terminal box (Courtesy Dowding & Mills)**

Given below are some advantages and disadvantages of using Rogowski coils for PD detection:

Advantages:

- It does not need a magnetic core, so the output signal is not affected by saturation effects. Hence it is highly linear even when subjected to large primary currents.
- It has a low inductance and hence can respond to fast changing currents enabling a high bandwidth measurement.
- It can be made open-ended and flexible, allowing it to be wrapped around a live conductor without disturbing it making it completely non-intrusive.
- A correctly formed coil, with equally spaced windings, is largely immune to electromagnetic interference.
- Reduced size compared to an equivalent current transformer

Disadvantages:

- The sensitivity of the Rogowski coils is lower when compared to the radio frequency CT and the capacitive coupler <sup>(120)</sup>.
- If not designed properly, it is susceptible to external magnetic interference.

### 4.4.3 Radio frequency current transformer

The Radio Frequency Current Transformers (RFCT) has been used for on-line PD monitoring of machines <sup>(121)</sup>. The Rogowski coil and the RFCT are both inductive type sensors and are closely related to each other, but there exists a functional difference. The RFCT produces an output current that is proportional to the primary current whereas a Rogowski coil produces an output voltage that is proportional to the rate of change of primary current.

The relationship between the induced secondary current and the primary current is given by the following equation:

$$I_s = \frac{n_p}{n_s} \cdot I_p \dots\dots\dots (4.3)$$

where

$n_p$  = number of turns in primary winding

$n_s$  = number of turns in secondary winding

The high frequency signal generated by PD propagates through the stator winding and supply cables and is detected by the RFCT as high frequency transients. The output from the RFCT can be connected to a CRO or any commercially available equipment.

By construction the RFCT is again very similar to the Rogowski coil, apart from the fact that the RFCT has a core that is made of magnetic material like ferrite. The RFCT can be designed to work with a frequency of about 100 KHz up to 100MHz. The core material determines the low frequency operating limit whereas the upper frequency is limited by the inductance of the circuit. Although the magnetic material in the core increases the sensitivity of the output, it adversely affects the operating bandwidth. It also reduces the dynamic range and linearity. The magnetic materials tend to saturate at high flux densities. So the RFCT tends to saturate when used with high current machines. The linearity also deteriorates as the flux densities approaches the saturation points. Hence it is not suitable for use with machines having a high current rating. Physically, the RFCT tends to be more bulky when compared with an equivalent Rogowski coil.

The RFCT is also available in two forms i.e. the solid core RFCT and the split core RFCT. The solid core RFCTs are available in a range of sizes and sensitivities. The

split core RFCTs are more expensive and are better for general-purpose use than the solid type as they can be applied without interrupting the circuit. Traditionally, the RFCT was placed around the neutral-to-earth connection as it has a lower level of power frequency avoiding the saturation problem. More recently attempts have been made to connect the RFCT around screened supply cables. However, the success has been limited due to power frequency saturation problem, particularly with high power machines with currents above 250 Amperes <sup>(122)</sup>.

#### 4.4.4 Capacitive coupler

The transients generated by PD travel through the stator windings towards the machine terminals. If a sensing circuit is coupled in this path, then some part of the transient would flow through this circuit. A high voltage capacitor can be used as a sensor to detect these partial discharge transients. The detection unit consists of the coupling capacitor and the measuring impedance. The circuit is characterised by a high-pass filter performance and is designed to block the mains frequency. A typical arrangement of a capacitive coupler detection circuit is shown in figure 4.8. The termination circuit converts the PD current pulses to voltage pulses which can be recorded by a PD measuring instrument for a detailed analysis.

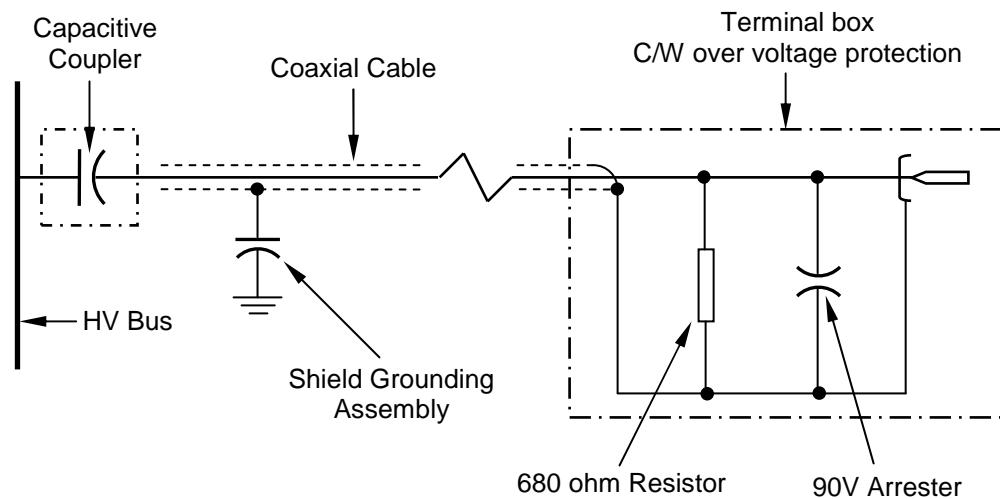


**Figure 4.8 Capacitive coupler detection circuit** <sup>(123)</sup>

There are two types of capacitive couplers available and the choice of each depends on the type of application.

- a) Cable type
- b) Epoxy mica encapsulated type

The cable type couplers are the most commonly used as they have a higher voltage rating compared to the epoxy mica type. But they are also comparatively larger in size and have a lower temperature rating. The epoxy mica type has a lower voltage rating but benefits from a high temperature rating. It is also comparatively smaller in size. The cable type couplers are available in a standard 80 pF value and are generally terminated with a 50 Ohm resistor as measuring impedance. The epoxy mica types are also available in a standard value of 80 pF, but more recently they have been manufactured with higher values of 500 pF and 1000 pF leading to wideband PD detection with better sensitivity <sup>(124)</sup>. Zhu & Halliburton <sup>(123)</sup> carried out laboratory tests and field testing of 80 pF and 500 pF coupling capacitors and concluded that the 500 pF couplers have better detection sensitivity than the 80 pF couplers and were still capable of avoiding noise.

A minimum of one coupling capacitor per phase (i.e. three per machine) is installed at the machine terminals. In the case of large motors and turbo generators two capacitive couplers per phase (i.e. six per machine) are installed. Using two couplers help to reject external PD like noise pulses. Both couplers are placed at least 2 meters apart and a 'time of flight' technique is adopted to distinguish between external PD like pulses and PD pulses from the machine. However, only one coupler per phase is sufficient for most motors. This is because most motors have long connecting power cables (usually >100 metres) and this heavily attenuates and filters out any high frequency PD like disturbances and effectively blocks it from entering into the measuring circuitry <sup>(107)</sup>.

As the capacitive couplers are connected in the motor terminal box and connected to the main terminals of the machine the installation usually requires a short outage. Care should be taken during installation to maintain the creepage distances depending on the operating voltage. One of the main advantages of capacitive coupler is that it has higher sensitivity compared to the Rogowski coil and the RFCT. However, it is not completely non-intrusive as the capacitor is directly connected to the HV terminals of the stator windings and the electrical integrity of the capacitor is crucial. Also, the capacitive coupler itself should be discharge free <sup>(122)</sup>.

#### **4.4.5 Stator slot coupler**

Stator slot coupler (SSC) developed by Sedding et al. <sup>(125)</sup> is a relatively new type of PD detection sensor and is mostly used in large turbine generators. A SSC is an ultra wideband directional electromagnetic coupler. It cannot be classed as a purely

capacitive or inductive coupler. It is rather a stripline antenna built on a ground plane having coaxial outputs at each end. It is installed on top of the stator winding bars, under the wedges, at the ends of the core slots. This position provides the optimum location for reliable detection of PD in the machine since the detector is as close as practically possible to the PD sources of interest. A minimum of six SSCs are fitted to cover the entire stator windings. It detects any electrical signal in the frequency range of 10 MHz to 1000 MHz and is highly sensitive to PD signals originating from sources close to the SSC. The dual output of the SSC helps in distinguishing PD from the slot and PD from the adjacent endwinding by calculating the pulse arrival times at both ends <sup>(125)</sup>.

One of the main advantages of SSC is that it has a wide bandwidth and is located close to the discharge source making it easy to eliminate external sources of interference. Furthermore, these couplers are directional and help in locating the source of discharge. The disadvantage of using SSC is that they have to be fitted during the manufacturing stage or a major outage is required for the installation. Also, the SSC must be sufficiently robust to endure the demanding conditions imposed during the installation of the device. It also demands specialised materials for its construction, as it has to withstand the thermal and mechanical stresses in the rotating machine <sup>(125)</sup>. Although this technique has good potential to eliminate electrical interference, its application has been restricted to a few large machines like turbine generators or critical motors, possibly due to the intrusive installation procedure.

Rogowski coil, RFCT and capacitive coupler remain the most widely used electrical PD detection sensors. The Rogowski coil is extensively used in the UK North Sea Oil Industry and is used in a number of mainland applications. The capacitive coupler technique was developed by Ontario Hydro (Canada) and has found widespread use in North America. Many installations also exist in UK and the rest of the world. Each of these sensors has some advantages over the others. A comparison of these sensors is shown in Table 4.1.

Parameter	Capacitive Coupler	RFCT	Rogowski Coil
<b>Types</b>	1) Cable type 2) Epoxy Mica insulated type	1) Solid core ferrite 2) Split core ferrite type	1) Solid core 2) Split core type
<b>Sensitivity</b>	Has the best sensitivity	Better than Rogowski coil	Has the least sensitivity
<b>Performance</b>	Sensitivity depends on the value of the capacitance and has a directly proportional relationship	Sensitivity depends on the type and grade of the ferrite material used.	Sensitivity depends on the number of windings and has a directly proportional relationship.
<b>Installation</b>	Requires direct connection to the HV terminals. Shut down required for installation.	Installed around the cables and require no direct connection to the HV terminals. No shut down required for installation.	Installed around the cables and require no direct connection to the HV terminals. No shut down required for installation.
<b>Size</b>	Smallest compared to the other two types	Comparatively bigger for the similar specification of Rogowski coil	Comparatively small for a similar specification of RFCT
<b>Linearity</b>	N/A	Less linear compared to Rogowski coils	Output is very much linear
<b>Saturation Limits</b>	N/A	Saturates at high currents; thus not suitable for machines with high current rating.	Being air-cored, it does not saturate at high currents making it suitable for machines with high current rating.
<b>System Capacitance</b>	The larger the system and plant capacitance's, relative to the coupler capacitance, the lower the sensitivity of the coupler technique.	The higher the system capacitance, the higher the sensitivity.	Same as RFCT
<b>Application</b>	They are best suited for plants that are connected to system by bus bars.	Best on system that uses cables as the means of connection.	Same as RFCT

**Table 4.1 Comparison of various electrical PD detection Sensors**

## 4.5 Review of commercial available PD detectors

As a part of new product development, it was thought necessary to study the existing market available products used for PD detection and analysis. A detailed comparative study of these products in terms of its features and capabilities would help in knowing the latest trends in the technology and would provide some inputs for the new design, thus helping in the development of a competitive product. Research was carried out through different means, mainly through the internet, to identify the various companies that manufactured PD detectors. Given below is the list of manufacturers of PD detection equipment:

1. IRIS Power Engineering (North America)
2. ADWEL International Limited (Canada)
3. PD Diagnostix Systems (Germany)
4. M&B Systems Power Test Equipment (UK)
5. TECHIMP (Italy)
6. Tettex Instruments (Switzerland)
7. HIPOTRONICS (USA)
8. ROBINSON Instruments (UK)

The above list is not exhaustive but covers some of the leading manufacturers across the globe. A variety of products exists in the market and choice of equipment can be influenced by many factors depending on the type of application and monitoring requirements. Some of the main factors are:

- Periodic or continuous monitoring
- Permanent installation or portable system
- Type of sensor interface (capacitive coupler / HFCT / Rogowski coil)
- Type of electrical machine (motor / generator / cable / switchgear)
- Monitoring only function or Monitoring & analysis
- Connectivity options (for alarm systems and remote monitoring)

A detailed study of various market available PD monitoring products was carried out but the data on individual products is not presented here as it is beyond the scope of this thesis. The comparative study has been included in Appendix A-1. However, a general discussion regarding various features and its significance to new system design is presented here.

- It was generally observed that most PD detector systems were designed to be a multi-function system capable of detecting PD from various electrical equipment (rotating machines / cables / switchgear). This will have an impinging effect on the cost and complexity of the system. The aim of the new system design is not to build a general purpose PD detector, but is specifically meant for PD monitoring in rotating machines only.
- The system design varies depending on the type of PD sensor being used as different sensors tend to have different characteristics (bandwidth, sensitivity, etc.). Making the system suitable for all types of sensors would unnecessarily raise the cost of the system development and that of the system. The project requirement dictates that the new system should be suitable for PD monitoring with Rogowski coils (PDC-85 Model, manufactured by Dowding & Mills).
- Many PD detectors have analogue input functions accepting inputs from temperature sensor and humidity sensor. As discussed in chapter 2, temperature and humidity influences PD activity, but the effect of this change in PD activity on the actual insulation degradation is a relatively slow process. While this feature can prove useful in continuous PD monitoring systems, it is not of any relevance for a periodic monitoring PD detector system as the data is acquired over a very short period of time (few minutes) and the monitoring intervals are fairly large (few months). The new system falls under the 'periodic monitoring' category.
- It was observed that a variation of bandwidths exist for different systems ranging from a few KHz to a few GHz range depending on the application of the system. This parameter is important because the higher the bandwidth, the higher would be the burden on the data acquisition hardware. This directly influences the hardware cost of the equipment. Bandwidth requirement is dictated by the characteristics of the detecting sensor (Rogowski coil in this case) and the equipment to be monitored (rotating machines in this case). Considering both these factors, the bandwidth requirement of the new system is chosen to be less than 500 KHz.
- Some systems provide alarm features and connectivity options for incorporating the system within the plant SCADA (Supervisory Control and Data Acquisition). The system can send an alarm to the control room if the PD activity exceeds a user set threshold. Although this feature looks very attractive, it has experienced very limited success in the industry due to spurious alarms caused by external interference.

Also, such an alarm feature is applicable only for a continuous monitoring system and is not considered relevant for the new design.

- Relatively new systems have now started to offer connectivity options like USB and Ethernet that could be used for remote monitoring. This feature definitely has its advantages and can lead to efficient maintenance. Although this is a useful feature it will not be included in the new design at this stage. This is due to the practical difficulties of implementing such a system. Remote monitoring demands either individual data acquisition (DAQ) equipment per machine (very expensive option) or a centralised DAQ unit with multiplexed inputs from various machines. A centralised DAQ unit with multiplexed input means longer cable runs (Ethernet or fibre optic) which can affect data quality. Also, remote monitoring requires secured intranet access to a client's server and this could pose certain issues for implementation.

## **4.6 Summary**

A variety of techniques exist for the detection of PD. Electrical detection techniques are most popularly used for rotating machines. On-line techniques are preferred over off-line techniques for reasons well established. Different sensors are available for electrical detection of PD (i.e. Rogowski coil, RFCT, capacitive coupler, stator slot coupler); each having some advantages over the other. The study of various commercially available PD detectors was essential and proved useful to get familiarised with the latest trends in PD detection techniques and provided inputs for new system design. The next chapter details the hardware development of the new system.

# CHAPTER 5: SINGLE PHASE DISCHARGE MONITORING HARDWARE

## 5.1 Introduction

The concept of computer based PD measurement has been in existence since the 1970s; however the performance of the system was limited by the available technology. Over a period of years the advancement and application of digital technology and electronics has significantly improved the process of acquiring, storing and processing vast amounts of PD data. Austin & James <sup>(126)</sup> presented a paper in 1976 describing the use of a mini-computer for detecting PD. Several authors since then have developed a variety of systems in an attempt to provide more power and data processing capacity for digital analysis of PD. A brief historical perspective of this development was published by James & Phung <sup>(127)</sup>.

One of the major advantages of computer-based measurement is that the PD data can be acquired and stored on a pulse-by-pulse basis making it possible to post-process the data and calculate various statistical moments that can provide information for the characterisation of PD data. Figure 5.1 shows a basic representation of a computer based PD detection system.

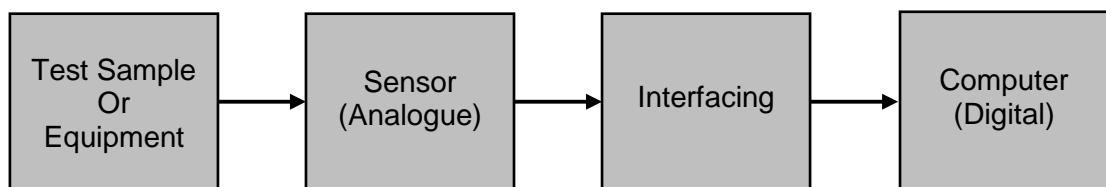


**Figure 5.1 General block diagram for computer based PD detection system** <sup>(127)</sup>

There are three main components of the measurement system. The sensor detects the analogue PD signals. The interfacing circuit provides any signal conditioning requirements and converts the information to digital format using an A/D converter. The raw digital data is then transferred to a computer which displays the PD data in desirable formats and allows post-processing and storage of PD signals.

## 5.2 Hardware Specifications

Prior to the design process it is necessary to establish the hardware specifications of the data acquisition system. Table 5.1 details the hardware specifications of the signal conditioning unit along with the specifications of the digitiser, determined as discussed below.

**Table 5.1 Data acquisition hardware specifications**

<b>Signal conditioning hardware specifications</b>	
<i>Filter lower cut-off frequency</i>	30 KHz
<i>Filter upper cut-off frequency</i>	300 KHz
<i>Filter stop-band attenuation</i>	48 dB (min)
<i>Amplifier bandwidth</i>	300 KHz
<i>Minimum amplifier gain</i>	x40
<i>Maximum amplifier gain</i>	x2700
<i>Gain steps</i>	x40, x90, x120, x180, x300, x450, x600, x900, x1200, x1800, x2700
<b>Digitiser unit specifications (Data acquisition card)</b>	
<i>No. of data acquisition channels</i>	4 channels (with simultaneous sampling)
<i>DAQ resolution</i>	8 bits (min)
<i>Minimum sampling frequency</i>	3Ms/S

The gain steps highlighted in blue are currently available in the existing StatorMONITOR unit. However, these settings are too far apart to efficiently accommodate discharge signals of various amplitudes. Based on the past experience of Dowding & Mills in measuring PD from rotating machines, it was decided to have some intermediate gain steps as shown in Table 5.1. The initial implementation of the project will be done using a DAQ card with a resolution of 8 bits with a possibility of expanding to 12 bits in future. A resolution of 12 bits will place more stringent requirements on the filtering stage. An 8-bit DAQ card will need a stop band attenuation of 48 dB, whereas a 12-bit DAQ card will demand a stop band attenuation of 72 dB. Hence, the hardware will be designed to accommodate a 12-bit system.

With the establishment of the hardware specifications, the next section deals with the system block diagram and the actual design aspects of individual sections of the signal conditioning unit.

### 5.3 System Hardware Overview

The final objective of this project was to develop a hardware system that was capable of acquiring PD data from all three phases of the machine in a simultaneous fashion. However it was first thought to design a single phase prototype system and evaluate its performance and feasibility. If the performance is found to be satisfactory, then the design can be adapted for a complete three phase system. The block diagram of the initial partial discharge monitoring system can be seen in Figure 5.2.

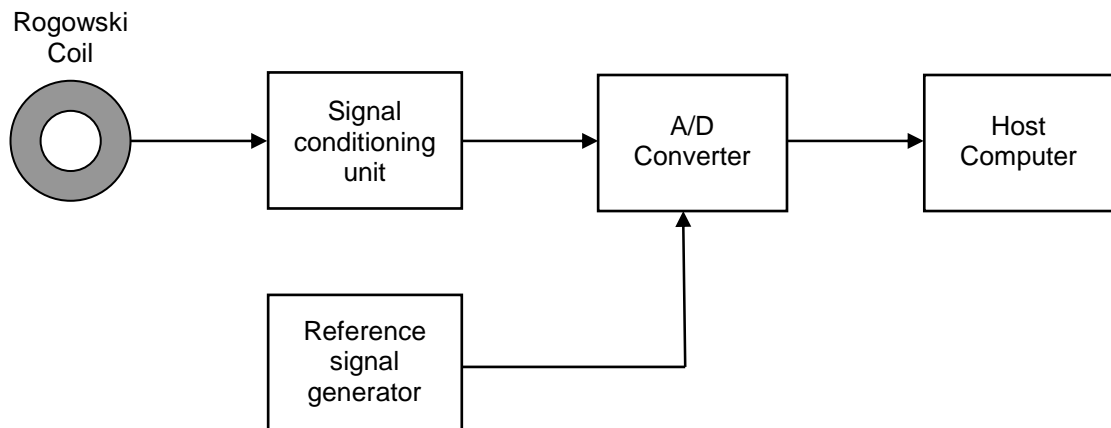


**Figure 5.2 – Basic Block diagram of single phase monitoring system**

The brief description of this system is as follows:

The Rogowski coil acts as the PD detection sensor and is clamped around one of the phases of the mains supply cable connected to a rotating machine. The Rogowski coil is designed to pick up the high frequency current pulses caused by PD that propagate through the stator windings towards the supply terminals. The signals then pass through the signal conditioning unit which is essentially a band-pass filter and a high gain (variable) amplifier. The lower cut-off frequency of the band-pass filter is selected such that the unwanted high amplitude mains frequency signal is blocked and does not interfere with the measurement circuitry. The upper cut-off frequency of the filter is dictated by the anti-aliasing requirements that are necessary to prevent any sampling errors. The high gain amplifier is necessary to measure the inherently low amplitude PD signals. However, the gain needs to be variable in order to accommodate small as well as large amplitudes of PD.

After filtering and amplification, the signal is then digitised using an A/D converter. The A/D converter was implemented by using a readily available data acquisition card that

supports high a sampling rate sufficient for acquiring the high frequency PD signals. A reference signal is generated using one of the phases from the three phase mains supply by means of a step down transformer. The reference signal is necessary to trigger the acquisition and also provides phase related information regarding discharges. The reference signal is also digitised simultaneously along with the signal from the Rogowski coil. The digitised data is then displayed and stored within the host computer.

An attempt was made at all stages of development for the design to be as flexible as possible in order to facilitate any design changes or further expansion.

The following section provides a detailed description of individual components of the system.

## **5.4 The Rogowski Coil**

The operating principle and the advantages of using a Rogowski coil as a PD sensor has already been discussed in chapter 4. The design of the coil has a significant effect on its performance, particularly in relation to its bandwidth and sensitivity. Usually a trade-off is made between bandwidth and sensitivity to achieve an optimal performance. This directly has an influence on the design of the measurement system.

It was not within the scope of this project to design a new Rogowski coil. The new system design was specifically targeted for use with PDC-85 Rogowski coils designed by Dowding & Mills that have been already installed on a substantial number of machines in the North Sea Oil Industry. The upper frequency limit of this coil is approximately 300 KHz. The sensitivity of the coil to the mains frequency current is 0.1mV/A. A brief description of the PDC-85 coil is provided here. The PDC-85 coils are BAS00ATEX2051 certified (EX II 2 G EExe II T6 @ 1000Amps, Ambient temperature from -20 to 60 degrees) to satisfy the safety regulation. This allows the transducers to be fitted as close to the winding as possible (machine terminals) even on machines located in hazardous environments. In order to simplify the installation, the coils have been designed to be split into two halves, eliminating the need to disconnect the supply cables from the machine terminals. A standard PDC-85 coil is shown in figure 5.3 (a)

The inner diameter of the coil is 85 mm and is best suited for installation on the standard Elastimold connectors. However it can also be installed on various sizes of HV cables with diameter of less than 85 mm or on HV bus bars with less than 85 mm

width. Figure 5.3 (b) & (c) show the installation of PDC-85 coil on cable and bus-bar. The datasheet of PDC-85 is provided in Appendix A-2.

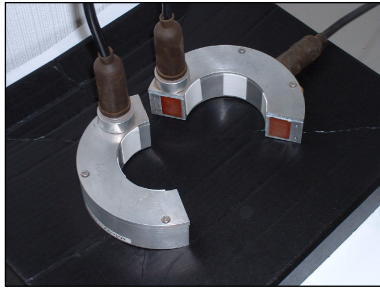


Figure 5.3 (a) Standard PDC-85 coil



Figure 5.3 (b) PDC-85 installed on HV cable



Figure 5.3 (c) PDC-85 installed on bus bar

**Figure 5.3 Rogowski Coil & Installation (Courtesy Dowding & Mills)**

### 5.4.1 Impulse response of Rogowski Coil

It is important that the PDC-85 Rogowski coils are sensitive enough and able to pick up high frequency current signals and output them in a measurable range. A discharge pulse is made of two components. These are:

1. Rise time known as the front of the pulse
2. Fall time, tail of the pulse

In order to generate the pulses, first a signal generator is used to produce a square wave. An RC circuit allows the generation of pulses. The frequency of the pulse can be controlled with the values of R and C, while their magnitude can be controlled with the signal generator, thus allowing pulses to be in desired range. The RC circuit used for generating pulses is shown in figure 5.4.

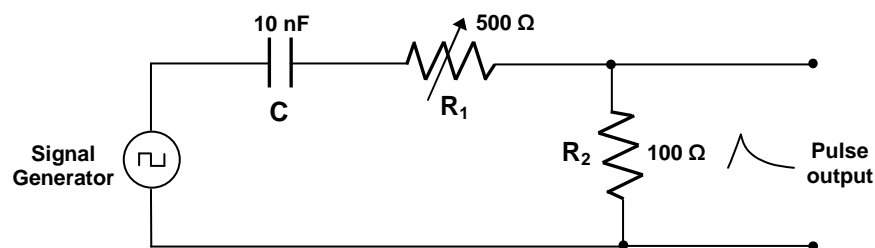


**Figure 5.4 RC circuit for generating pulses**

The circuit shown in figure 5.4 is made of a 10nF capacitor in series with 100 Ohm and 500 Ohm variable resistor. These values of components give a practical pulse with frequencies in the range of 40-200 KHz (i.e.25μS to 5μS).

A test set-up was made to measure the response of the PDC-85 Rogowski coil. The set-up was in accordance to the procedure stated by Dowding & Mills (manufacturer) and the block diagram of the test set-up is shown in figure 5.5.

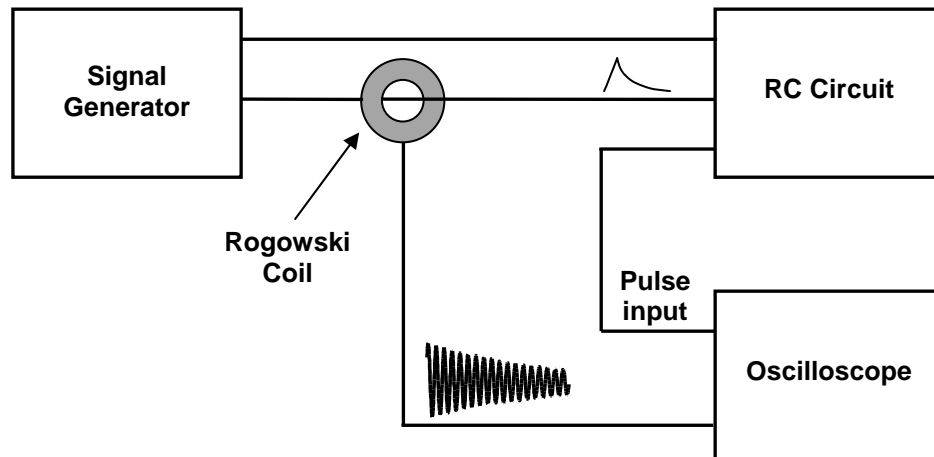


Figure 5.5 Set-up for testing the response of PDC-85 Rogowski coil

The response of the Rogowski coil (yellow graph) to a 1V, 200 KHz pulse is shown in figure 5.6

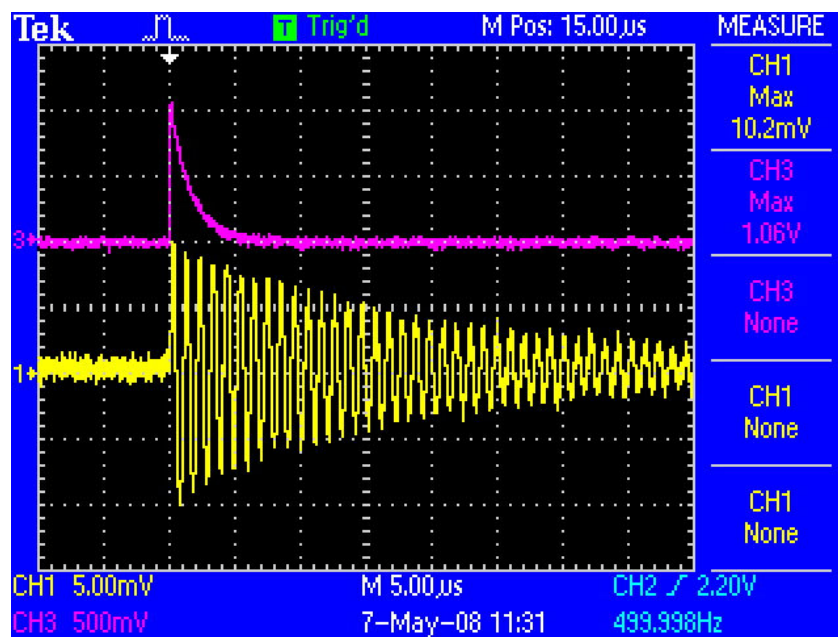


Figure 5.6 Pulse response of PDC-85 Rogowski coil

It can be seen from figure 5.6 the width of the pulse is about  $5\mu\text{S}$  (i.e. 200 KHz). The pulse voltage is measured across resistor  $R_2$  (100 Ohms) shown in figure 5.4. The measured pulse voltage is 1V implying a pulse current of 0.1A. The response of the Rogowski coil is a damped oscillatory signal with a peak value of 10.2 mV. It is important that the ripples in the damping signal are attenuated to an acceptable level within a set time. As per the manufacturer's specifications a 60% attenuation in  $20\mu\text{S}$  is considered satisfactory for this test. As seen in figure 5.6, the amplitude of the damping signal has reduced from 10.2mV to 4mV in  $20\mu\text{S}$  (60.8%).

## 5.5 Signal conditioning unit

The signal conditioning unit has two main functions:

- a) Filter out signals that are not within the band of interest
- b) Amplify the small amplitude PD signals to a sufficient level to make it suitable for the digitisation process.

Prior to the actual design process it is first necessary to establish the signal conditioning requirements of the system.

### 5.5.1 Signal conditioning requirements

Filtering and amplification are an integral process of any Data Acquisition (DAQ) system. Generally, in relation to DAQ systems, filtering is mainly used to prevent the aliasing of signals that are out of band of interest. It is a common practice to have an anti-aliasing filter (AAF) prior to the A/D conversion to remove the frequency components that are beyond the ADC's range. The AAF is actually a low-pass filter that is designed to provide a cut-off frequency to remove the unwanted signal from the ADC input or at least attenuate them to a point where they will not adversely affect the sampled performance.

A measured signal can contain noise from various sources i.e. electronic current and voltage noise, radio interference noise, mains coupling or aliasing. Filtering the noise from the signal of interest is a critical to signal measurement. Generally speaking, signal filtering function can be provided in analogue domain and/or digital domain. Analogue filters are typically implemented prior to analogue-to-digital conversion. In contrast digital filtering is implemented after analogue-to-digital conversion. Each type of filtering has its own applications. Digital filtering can minimise noise injected during

the conversion process <sup>(128)</sup>. Analogue filtering is not capable of doing this. However, if the measured signal is coupled with any external high frequency signals then they have to be filtered prior to analogue-to-digital conversion in order to prevent aliasing. An analogue filter can be used for this purpose. Hence it was decided to implement an analogue AAF filter as a part of signal conditioning unit.

The system also needs a low noise, high gain amplifier with a wide range of variable gains. The combined process of filtering and amplification can be realised with different configurations as shown in figure 5.7 (a), (b) & (c).

In figure 5.7 (a) (configuration 1); the filtering process is performed before amplification. This configuration may not be very suitable as the incoming signals have extremely small amplitude and cannot be directly subjected to filtering without any amplification. It would also affect the signal-to-noise (SNR) adversely as all the electronic noise introduced in the filter stages would be amplified to a greater extent in the gain stages. It would be suitable to amplify the signals first and then perform any filtering on them. This is implemented in figure 5.7 (b) (configuration 2). The incoming signals are amplified first to a suitable value and then subjected to filtering. This may be a suitable solution, but the drawback is that it could lead to saturation problems if the mains frequency component is present in the signal. The amplitude of the mains frequency signals is comparatively higher than the PD signals. Amplifying the entire signal spectrum in one stage may lead to saturation problems (due to the high amplitude of mains frequency).

Another possible way of performing the process is by splitting the amplification stage in two stages. The signals from the coils can be amplified to a certain extent and then passed through high-pass filter to remove the mains frequency content. The signals can then be subject to low-pass filtering to filter the high frequency content. Further amplification can be provided after filtering. Hence it would be desirable to have some initial amplification followed by band-pass filtering and then provide further amplification. Such an arrangement is shown in figure 5.7 (c) (configuration 3).

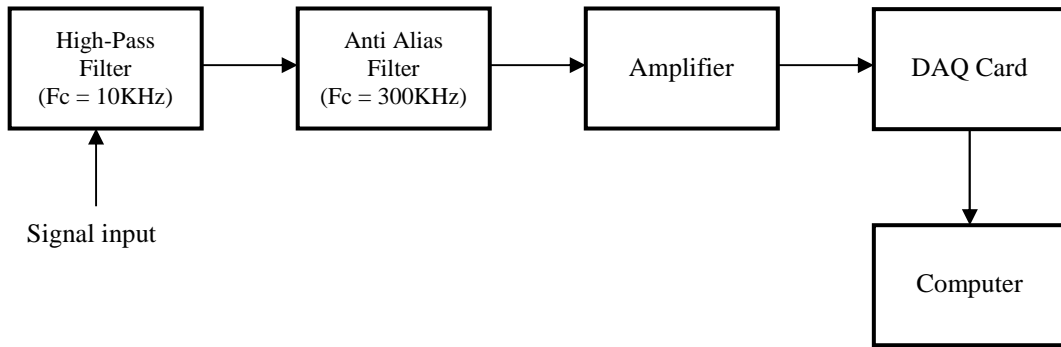


Figure 5.7 (a) – DAQ configuration 1

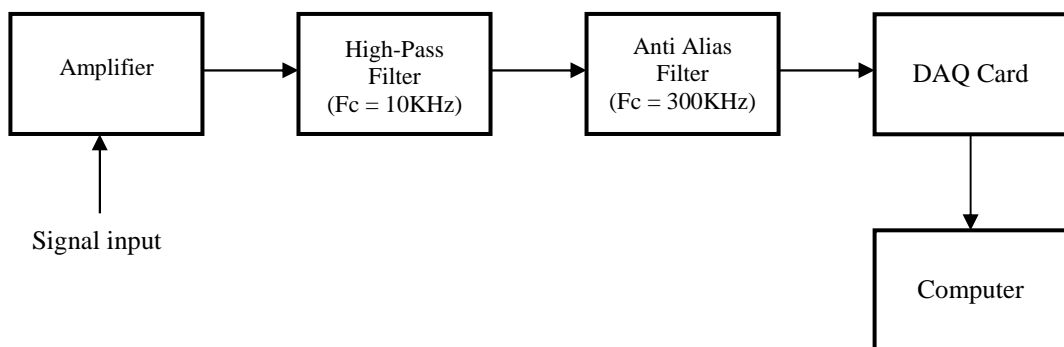


Figure 5.7 (b) – DAQ configuration 2

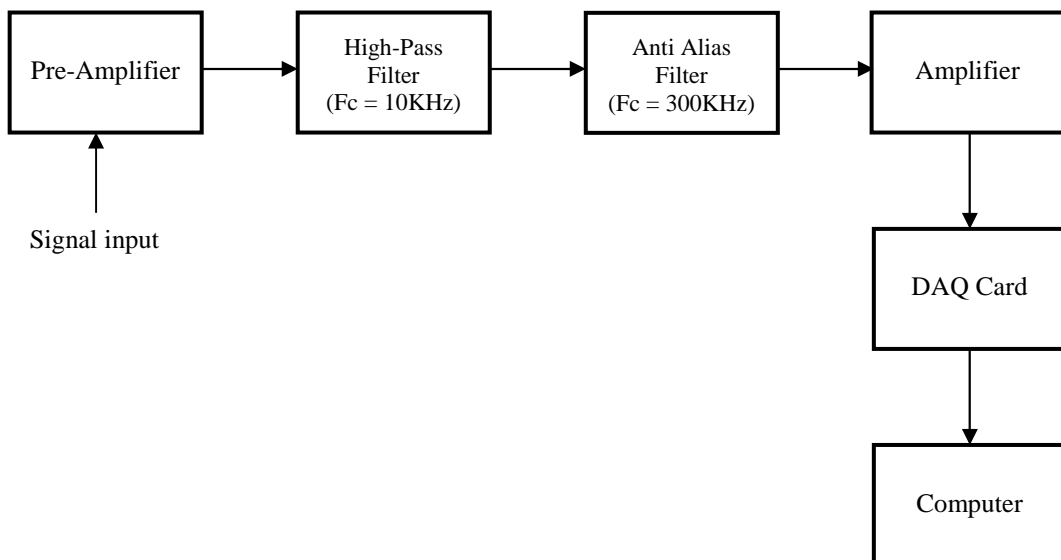


Figure 5.7 (c) – DAQ configuration 3

**Figure 5.7 Different configurations of DAQ system**

With the establishment of the signal conditioning requirements the next section deals with the design aspects of individual sections of the signal conditioning unit.

### 5.5.2 The Anti-Aliasing Filter (AAF)

The A/D converters are usually operated with a constant sampling frequency when digitising the analogue signals. The sampling frequency is governed by the Nyquist criteria, which states that the sampling frequency  $f_s$  should be at least twice the maximum input frequency. In other words only the input signals with a frequency below  $f_s/2$  are reliably digitised. If the input signal contains frequencies greater than  $f_s/2$ , then a portion of the signal can 'fold back' and get mixed with the signals present within the frequency range of interest. This makes it impossible to distinguish between signals below  $f_s/2$  and signals above  $f_s/2$  causing an error in measurement. This error is called 'aliasing'. The process of aliasing can be eliminated by using a suitable analogue low pass filter prior to the digitisation process.

The anti-alias filters can be implemented either using a passive filter network or by an active filter network. The passive filter network is realised by using passive devices such as resistors and capacitors. The output impedance of a passive filter is relatively high when compared to an active filter. Since the resistor value is typically large to keep the capacitors at a reasonable value, the next stage device can see significant load impedance. For example, a 1 KHz low pass filter which uses a  $0.1\mu\text{F}$  capacitor would need a  $1.59\text{K}\Omega$  resistor for implementation as shown in figure 5.8. This value of resistor could create an undesirable voltage drop or make impedance matching difficult. This will be particularly important where the passive filter contains multiple stages and the loss of signal can become quite severe. This is called insertion loss. Consequently, passive filters are typically used to implement a single pole filter. This application however will need a higher order filter thus calling for an active filter design.

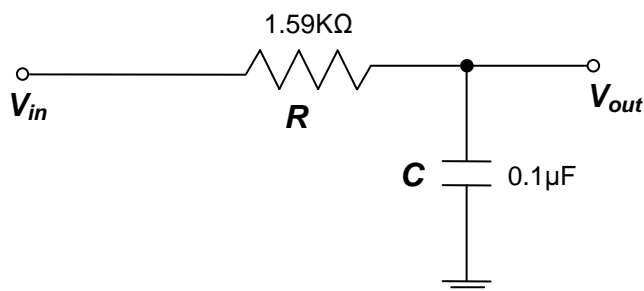


Figure 5.8 Passive single pole low-pass filter ( $f_c = 1\text{ KHz}$ )

The active filter is implemented using op-amps, resistors and capacitors. One of the main advantages of using an op-amp is that it has high input impedance and low output impedance reducing the insertion loss. In fact, active filters can also be designed to provide some gain. Depending on the response required, many stages of op-amps can be cascaded together to achieve a sharp 'knee' and steep roll-off characteristics. However, the disadvantage of cascaded filters is that they can limit the available bandwidth and may be affected by drift.

The active filters can be classed into different families i.e. Butterworth, Chebyshev Bessel and Elliptic. Each of these families has some advantages and disadvantages over others. The Butterworth filters have the flattest pass-band region i.e. least attenuation over the desired frequency range. However, the phase change with frequency is not very linear and the stop-band roll-off rate is not the best amongst all families. The Chebyshev filter has one of the best stop-band roll-off rates making it possible to use less number of sections for a given design. However, this type of filter contains a ripple in the pass-band region (i.e. gain is not constant gain in pass-band) and is not desirable. Also, it has the poorest phase linearity in all three families. The Bessel filter has linear phase characteristics, but the stop-band roll-off rate is worse than the Butterworth family. Compared to Butterworth and Chebyshev, elliptic filters have the most rapid transition band. However, the elliptic filters have ripple, both in pass-band and in stop-band. Due to maximal flat-band response the Butterworth and Bessel types are considered most suitable for AAF.

One of the important design factors to be considered while building an AAF is that the minimum gain of the filter in stop-band should be less than the Signal-to-Noise Ratio (SNR) of the sampling system. This is illustrated in figure 5.9.

The  $f_s/2$  is the 'fold-over' frequency;  $f_a$  is the frequency at which the magnitude goes below the resolution of the converter. Any signal up to frequency  $f_a$  (e.g. at X) would not produce an image frequency in the required band, but if there was a component (Y) outside  $f_a$  then that would give an alias component. Now the frequency  $f_a$  is the stop-band frequency that is governed by the SNR of the sampling system.

For instance, if a 12-bit A/D converter is used, the ideal SNR is ~72 dB. The filter should be designed so that its gain in stop-band is at least 72dB less than the pass band gain. An increase in the A/D converter's resolution by 1 bit would lead to an improvement of SNR by approximately 6dB. Similarly an 8-bit system would have an SNR of ~ 48 dB.

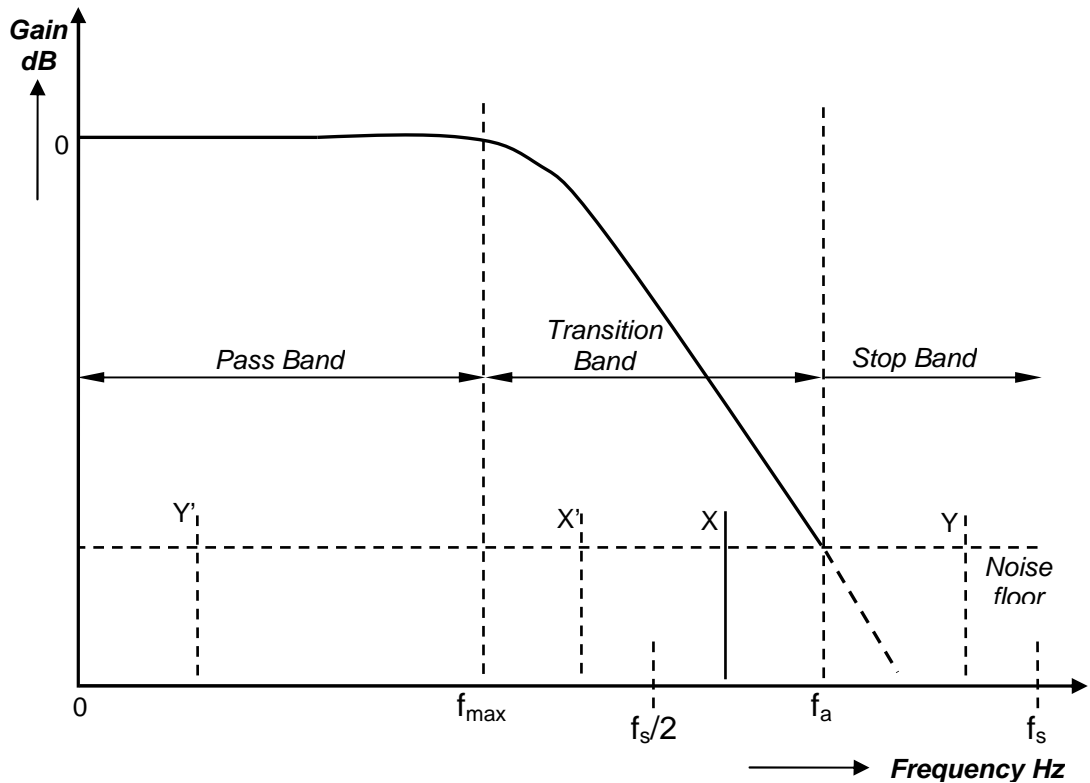


**Figure 5.9 Anti-aliasing filter characteristics**

The stop band frequency  $f_a$  can be calculated with the following relationship:

$$f_a = f_s - f_c \dots \dots \dots (5.1)$$

where,

$f_s$  = sampling frequency

$f_c$  = cut-off frequency

The required AAF will be designed based on the specifications given below:

- The maximum frequency of interest  $f_{max}$  is 300 KHz. In order to achieve a completely flat response in the desired frequency range; a higher cut-off frequency  $f_c$  of 500 KHz is selected.
- The minimum sampling frequency  $f_s$  is 3MHz. Hence, the calculated stop band frequency  $f_a$  is 2.5 MHz (as per equation 5.1). A higher sampling frequency (>3 MHz) will only better the attenuation at the stop-frequency.
- Though the initial experimentation would be carried out using 8-bit DAQ cards, the hardware will be designed to accommodate a 12-bit system which has more

stringent demands on the filter. Hence, the attenuation of stop-band frequencies should be at least 72 dB.

Based on these given specifications, the desired frequency response from the AAF is shown in figure 5.10.

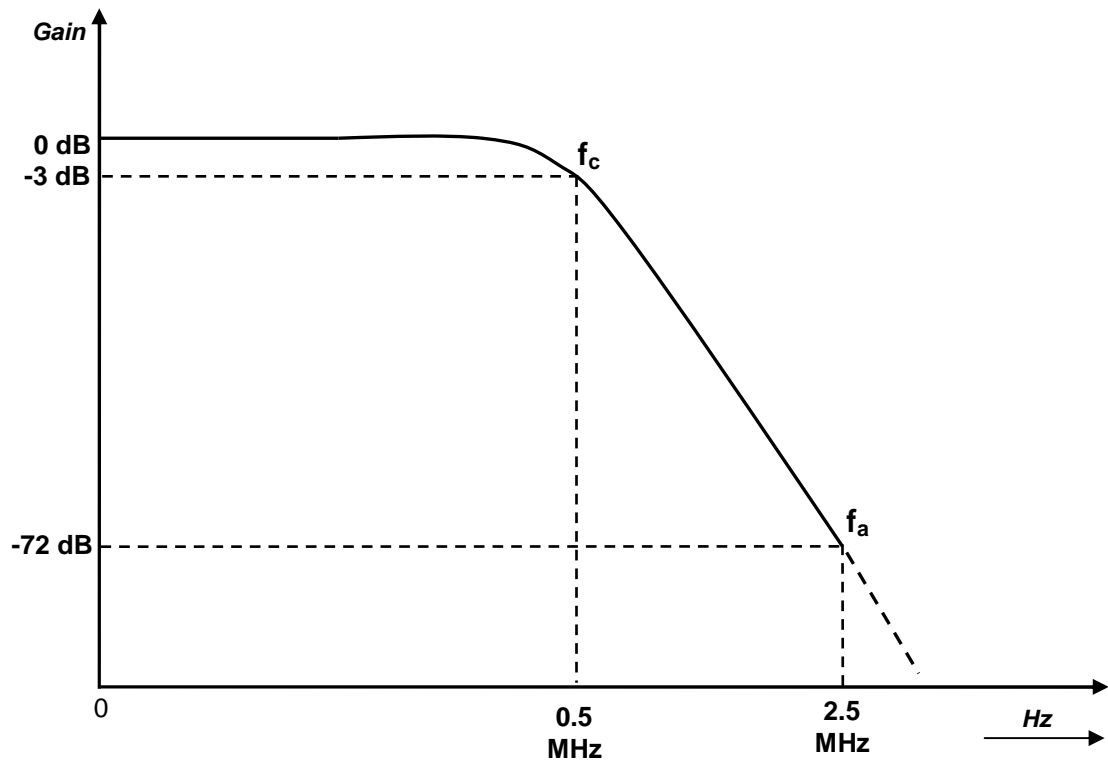


**Figure 5.10 Desired response of AAF filter**

The design of higher order cascaded filters are usually implemented using pre-determined active filter polynomials for design. The Butterworth polynomials have good amplitude characteristics whereas the Bessel polynomials are optimised by linear phase characteristics. But the Bessel filters do not have adequate roll-off characteristics and are considered unsuitable for this application. Amongst the Butterworth and Chebyshev filters, Butterworth has a flat amplitude response in the pass-band and has a better phase linearity. Hence it was decided to implement a Butterworth filter design with a standard Sallen-Key configuration.

It is first necessary to establish the order of filter required to achieve the required attenuation. The next stage would be to calculate the resistor and capacitor values to the desired cut-off frequency. If required, gain can be added in each stage. The gain varies the 'Q' of the filter and has an effect on the sharpness of the 'knee' of the filter. Figure 5.11 shows a standard second order Sallen-Key low pass filter design.

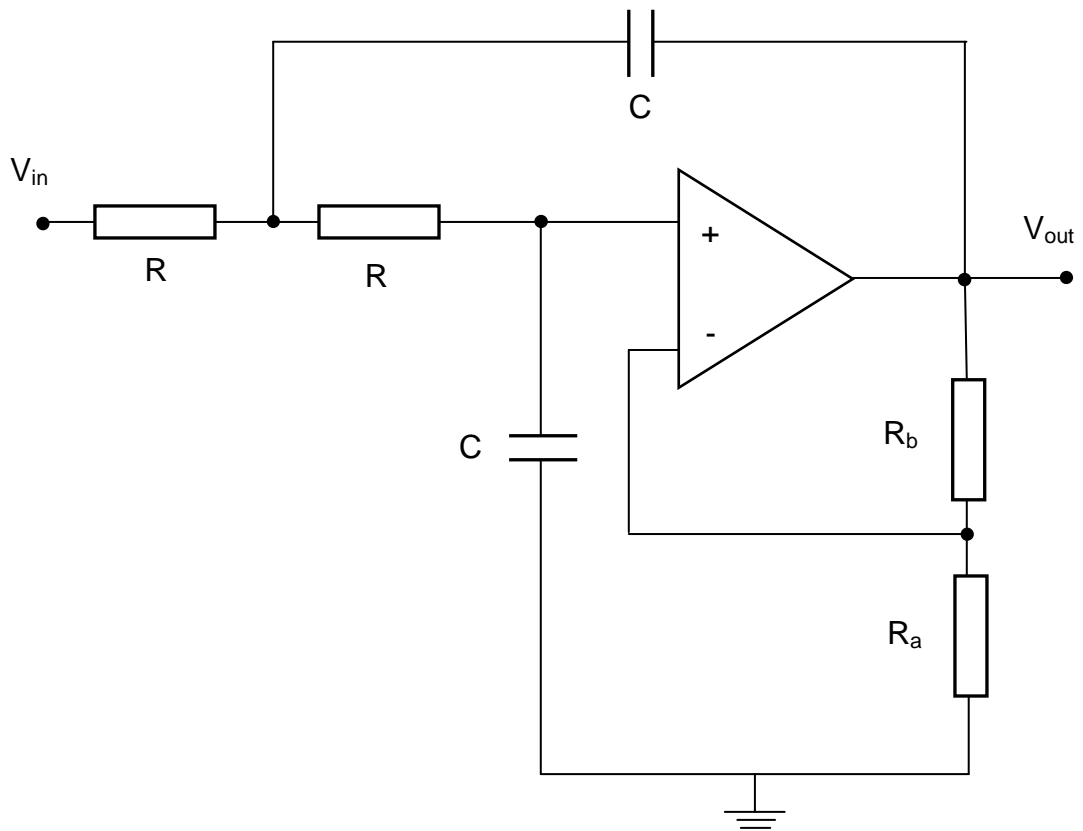


**Figure 5.11 Sallen-Key second order low-pass filter circuit**

5.5.2.1 Filter Calculations

The Butterworth response is given by the following formula:

$$|H(j\omega)| = \frac{1}{\left[1 + \left(\frac{\omega}{\omega_c}\right)^{2n}\right]^{1/2}} \dots\dots\dots (5.2)$$

$$\therefore 72.25dB = \frac{1}{2} \times 20 \log \left[1 + \left(\frac{2.5}{0.5}\right)^{2n}\right]$$

$$\therefore 72.25dB = 10 \log [1 + (5)^{2n}]$$

$$\therefore n = 5.1$$

$$\therefore n = 6 \text{ (nearest practical value)}$$

where  $H(j\omega)$  = filter gain;  $\omega$  = frequency;  $\omega_c$  = cut-off frequency;  $n$  = order of filter

The calculated order of filter required is 5.1. The nearest practicable value would be a 6<sup>th</sup> order filter. The cut-off frequency of the filter can be calculated using the following formula:

$$f_c = \frac{1}{2 \times \pi \times R \times C} \dots\dots\dots(5.3)$$

where R = value of resistance; C = value of capacitance.

The value of  $f_c$  is 500 KHz. The filter will be implemented using standard values of capacitor and resistor. A standard value capacitor C = 470 pF is chosen and the resistor value is calculated.

$$500\text{KHz} = \frac{1}{2 \times \pi \times R \times 470\text{pF}}$$

$$\therefore R = 677.6\Omega$$

$$\therefore R \approx 680\Omega \text{ (nearest practical value)}$$

Substituting the values for R and C in equation 5.3 gives a cut-off frequency value of **498.23 KHz** which is acceptable for the application.

Referring to figure 5.11, the gain A of the filters is dependent on resistors  $R_a$  and  $R_b$  and is given by the following formula:

$$\text{Gain}(A) = 1 + \left( \frac{R_b}{R_a} \right) \dots\dots\dots(5.4)$$

Similarly, the relationship between 'Q' of the circuit and gain A is given by:

$$A = 1 + \left( \frac{1}{Q} \right) \dots\dots\dots(5.5)$$

The gain for each stage is calculated based on the optimal 'Q' values stated in the Butterworth filter table <sup>(129)</sup>. The 'Q' values for a 6<sup>th</sup> order Butterworth filter are given below:

$$1^{\text{st}} \text{ section } (Q_1) = 0.518$$

$$2^{\text{nd}} \text{ section } (Q_2) = 0.717$$

$$3^{\text{rd}} \text{ section } (Q_3) = 1.932$$

The above 'Q' values can be substituted into equation 5.5 to calculate the gain for each stage. The gain value can then be used to calculate the resistor values  $R_a$  and  $R_b$ .

### 1<sup>st</sup> Section:

$$A_1 = 3 - \left( \frac{1}{0.518} \right) = 1.07$$

Assuming ' $R_{a1}$ ' = 12K $\Omega$ ;

$$1.07 = 1 + \frac{R_{b1}}{12K\Omega}$$

$$\therefore R_{b1} = 840\Omega \approx 820\Omega \text{ (nearest preferred value)}$$

Worst case gain values for  $A_1$  (assuming a tolerance value of 1% for resistors)

$$A_{1L} = 1 + \frac{811.8\Omega}{12.12K\Omega} = 1.067 \text{ (Lowest value)}$$

$$A_{1H} = 1 + \frac{828.2\Omega}{11.88K\Omega} = 1.07 \text{ (Highest value)}$$

### 2<sup>nd</sup> Section:

$$A_2 = 3 - \left( \frac{1}{0.707} \right) = 1.586$$

Assuming ' $R_{a2}$ ' = 1K $\Omega$ ;

$$1.586 = 1 + \frac{R_{b2}}{1K\Omega}$$

$$\therefore R_{b2} = 586\Omega \approx 560\Omega \text{ (nearest preferred value)}$$

Worst case gain values for  $A_2$  (assuming a tolerance value of 1% for resistors)

$$A_{2L} = 1 + \frac{554.4\Omega}{1010K\Omega} = 1.549 \text{ (Lowest value)}$$

$$A_{2H} = 1 + \frac{565.6\Omega}{0.99K\Omega} = 1.571 \text{ (Highest value)}$$

### 3<sup>rd</sup> Section:

$$A_3 = 3 - \left( \frac{1}{1.932} \right) = 2.482$$

Assuming 'R<sub>a3</sub>' = 680Ω;

$$2.482 = 1 + \frac{R_{b3}}{680\Omega}$$

$$\therefore R_{b3} = 1.008K\Omega \approx 1K\Omega \text{ (nearest preferred value)}$$

Worst case gain values for A<sub>3</sub> (assuming a tolerance value of 1% for resistors)

$$A_{3L} = 1 + \frac{990\Omega}{686.8\Omega} = 2.442 \text{ (Lowest value)}$$

$$A_{3H} = 1 + \frac{1010\Omega}{673.2\Omega} = 2.5 \text{ (Highest value)}$$

The total calculated theoretical gain (A) of the 6<sup>th</sup> order AAF filter would be

$$A = A_1 \times A_2 \times A_3$$

$$\therefore A = 1.068 \times 1.56 \times 2.471$$

$$\therefore A = 4.12$$

$$\therefore A = 12.29dB$$

Lowest worst case gain value (A<sub>L</sub>):

$$\therefore A_L = 1.067 \times 1.549 \times 2.442$$

$$\therefore A_L = 4.036$$

$$\therefore A_L = 12.12dB$$

Highest worst case gain value (A<sub>H</sub>):

$$\therefore A_H = 1.07 \times 1.571 \times 2.5$$

$$\therefore A_H = 4.202$$

$$\therefore A_H = 12.47dB$$

The prototype circuit was built to evaluate its performance. The complete circuit diagram is given in Appendix A-3.2. The frequency response of the filter is shown in figure 5.12. It can be seen from figure 5.12 that the actual cut-off frequency (-3dB point) occurs at approx. 450KHz. These errors could be attributed to Vero-board prototyping and component tolerances. The filter however has a flat-band characteristic in the desired frequency range. The pass-band gain is about 12.26dB which is fairly close to the calculated value. The attenuation should be about 72 dB at 2.5MHz; however this could not be tested due to limitations on the frequency generator. The filter is initially

intended to be used for an 8-bit DAQ. Hence the above filter is considered sufficient for the application.

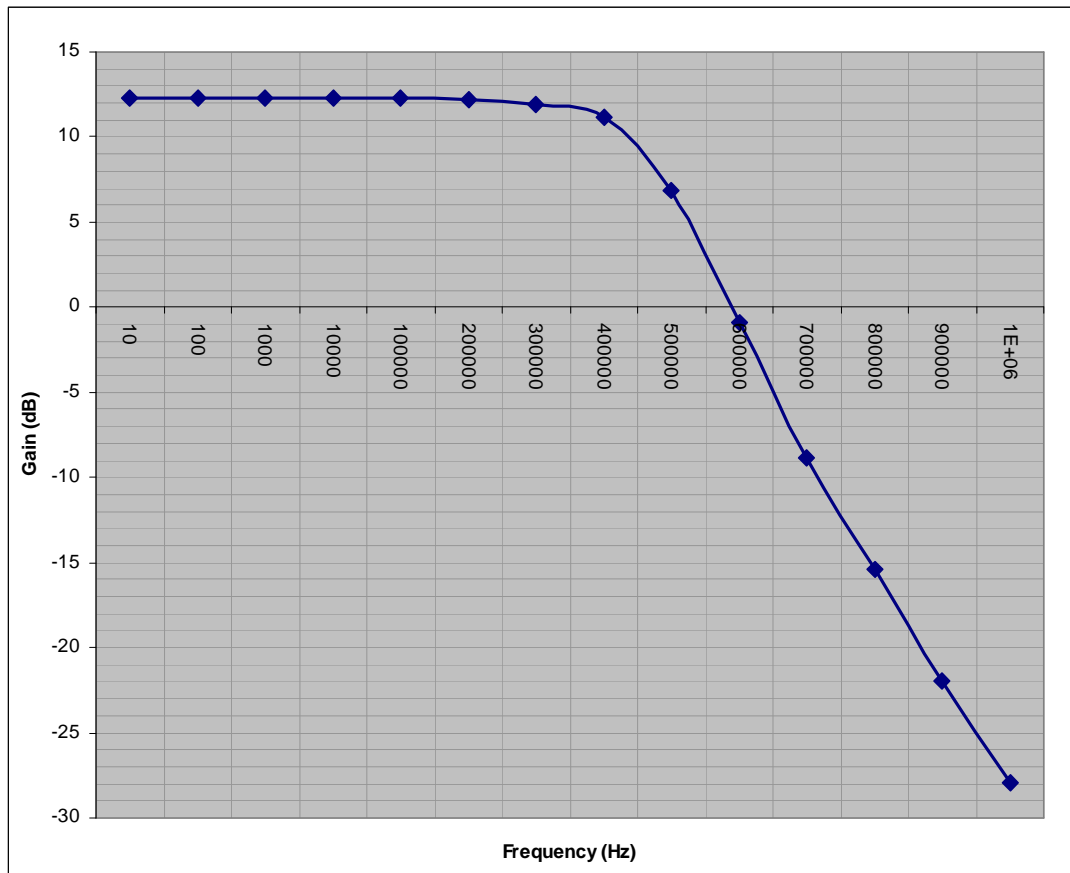


**Figure 5.12 Practical frequency response of the AAF**

### 5.5.3 The High pass filter

The Rogowski coils are designed for high frequency and are relatively insensitive to the mains frequency. But the amplitude of the mains frequency signal is very high compared to the partial discharge signal. The presence of even a fraction of the mains frequency signal could lead to inefficient utilisation of the dynamic range of the A/D converter. The main intention is to dedicate the entire dynamic range of the A/D converter only for digitising PD signals. This will help in better discrimination of PD pulses. A high pass filter with a cut-off frequency of 10KHz was designed to eliminate any 50Hz signal along with its harmonics. Similar to the AAF design, a Sallen-key Butterworth filter configuration was adopted to obtain a flat frequency response in the pass band. A lower cut-off frequency of 10KHz was chosen instead of 30KHz to ensure a flat frequency response in the desired range. A 4<sup>th</sup> order filter was constructed which had a gain of '8.13 dB'. When cascaded with the AAF, the resultant band-pass filter gave a theoretical combined gain of 20.6 dB in the passband. The complete circuit

diagram for the high pass filter is given in Appendix A-3.1. The frequency response of the combined band-pass filter is shown in figure 5.13.

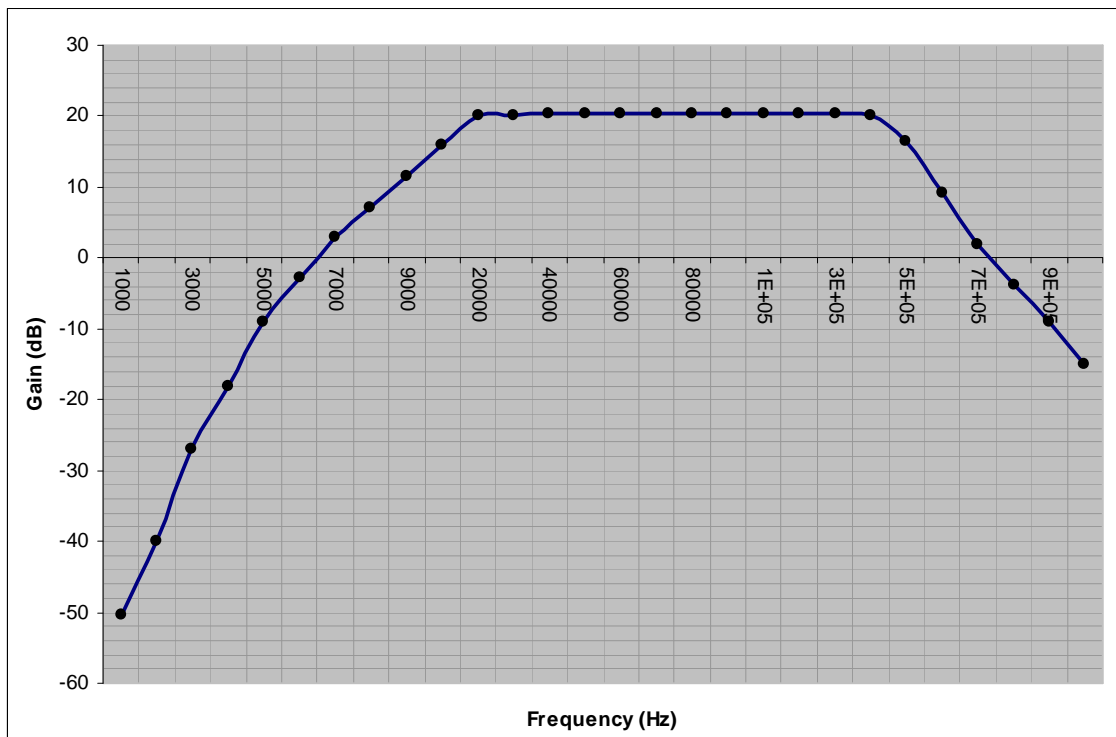


**Figure 5.13 Frequency response of the combined band-pass filter**

### 5.5.4 High-Gain Amplifier

A high gain-bandwidth product (bandwidth of 300KHz and gain of 2700) requirement as stated in table 5.1 impose a significant demand on the amplifier. Also, due to the noise sensitive application, the susceptibility of the amplifier to small noise and pick-ups is of paramount importance. It is an acknowledged fact that the amplifiers themselves can be a source of noise, and a poor design can compound this problem to a greater extent.

Some of the factors, which would play a major role in the design of the amplifier, are as follows:

- Gain Bandwidth Product
- Slew-rate
- Input / Output impedance
- Frequency / Phase response
- Noise susceptibility
- PCB layout

Simulation of amplifier circuits is a good starting point, but it is more practical to build a prototype amplifier and carry out a detailed performance testing of the same. Areas such as stability and phase response need careful consideration. The current bandwidth requirement of the amplifier is 300 KHz. However, the amplifier will be designed with a bandwidth of 1MHz, bearing in mind the options for any future development. The total amplification required would be in the range of 2500 to 3000. The active low-pass filter and the high-pass filter provide a combined passband gain of '10'. The amplifier still shares the burden of providing a gain in the range of 250-300 with a bandwidth of 1MHz. As discussed in section 5.5.1, the gain will be split in two stages i.e. first stage prior to filtering and the second post-filtering. The splitting of the gains in various stages should be such that the gain values stated in table 5.2 are achievable. The initial amplifier stage connected to the coils would play a major role in the noise performance of the complete amplification process.

It is necessary to make the amplifier gains variable in order to accommodate PD signals with a wide range of amplitudes. The variable gain values were carefully planned to provide a wide range of gains with desired gain intervals. The first stage amplifier was designed to provide a variable gain of 2, 3, 6, 15 and 20. The second stage amplifier was designed to provide a variable gain 2, 3, 6, 12 and 18. A combination of these values will effectively provide a wide range of gain values including the gain steps stated in table 5.1. There was a reason for splitting the gain values in such a manner. The system currently being used by Dowding & Mills have certain defined gain values. This system, known as StatorMonitor®, has been successfully used in the industry, but is now becoming outdated. Implementing the gain values similar to the StatorMonitor system will provide an opportunity to benchmark the performance of the new system against a proven system.

Building the amplifier on the prototyping boards (bread-boards) is not considered suitable as the signal frequency is relatively high. At these frequencies, the capacitances of the prototyping board are prominent and may become coupled with the circuitry to add undesirable effects. For example, it could add a positive feedback path through its capacitance making it unstable at high frequencies. A printed circuit board, if designed properly (layout design affects performance) would avoid such effects. However, the initial single-channel prototype was built on a Vero board.

Both amplifiers were implemented using op-amp MAX437 in a non-inverting configuration. The op-amp has a gain-bandwidth product of 60 MHz with a low input noise of  $4.5\text{nV}/\sqrt{\text{Hz}}$ . The gain of the amplifier is varied by switching the feed-back

resistors using a rotary switch. The circuit diagram for both the amplifiers is given in Appendix A-3.1 and A-3.3.

During testing, it was observed that the amplifier had a tendency to become unstable causing oscillations and jittery waveforms. Initial thoughts hinted towards a noise pick-up from some source. On investigation, it was found that the source of noise was the rotary switch. In fact the noise was being picked-up by the wires connecting the rotary switch and the feed-back resistors of the amplifier. All the wires connecting the rotary switch to the amplifier were covered in a metallic braid and the braid was connected to ground. The metallic braid provided good shielding to connecting wires and effectively helped in minimising the noise pick-up. The frequency response of the amplifier was tested for different gains. The results for the input variable gain amplifier are shown in figure 5.14.

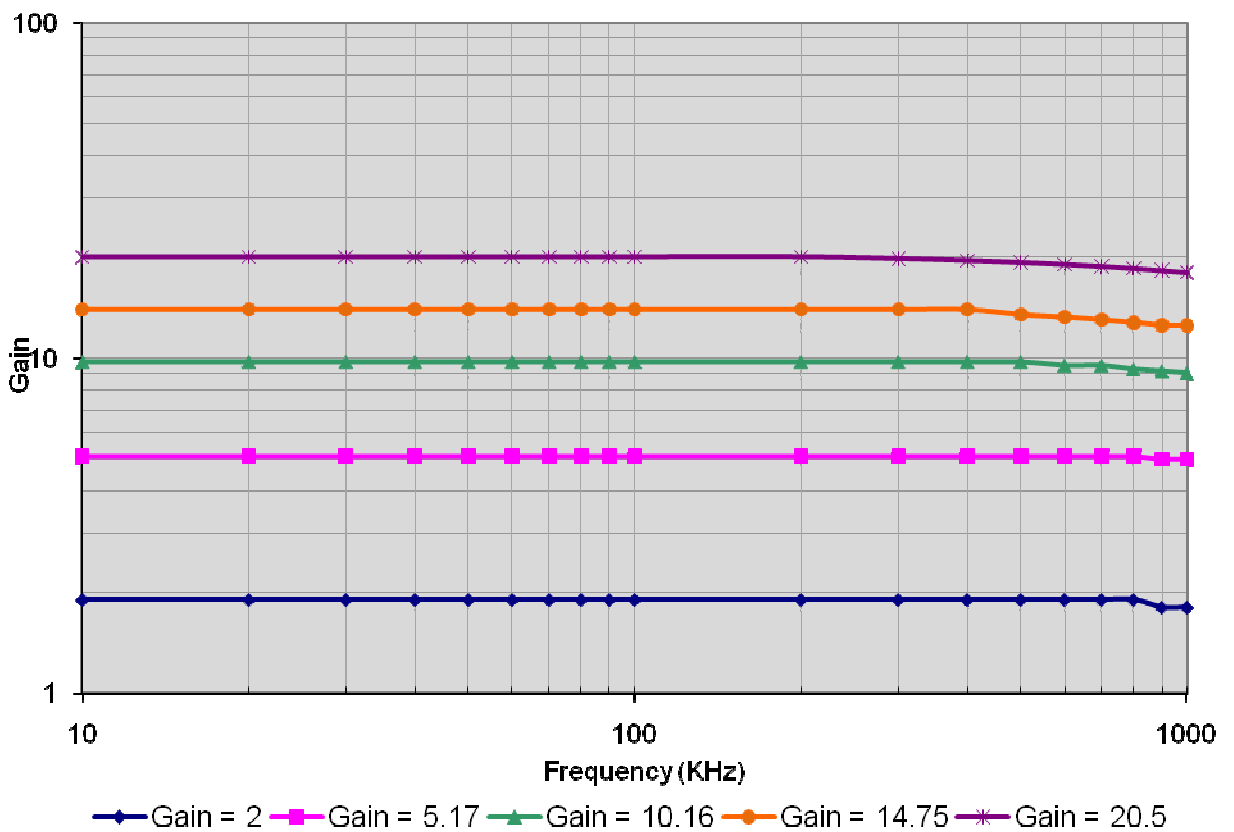


**Figure 5.14 Frequency response of input variable gain amplifier**

The frequency response of the amplifier is linear in the lower gain ranges. At higher gains (i.e. 15 & 20), it was observed that the gain does drop slightly as frequency increases. This is due to the gain-bandwidth limitation of the op-amp. Even with the deteriorated performance, the frequency response is still considered sufficient for the current bandwidth (i.e. 300 KHz). The output amplifier was also constructed and tested

in a similar fashion and was found to have a similar performance. The frequency response is not shown here for brevity. The circuit diagram is given in Appendix A-3.3.

The variety of gains achievable using the combination of both amplifiers is shown in the gain matrix in table 5.2. The gain values given in the gain matrix are a product of input and output amplifier gains multiplied with a factor of 10 (gain added by the band-pass filter) to give the effective gain of the system. The values stated in brackets (highlighted) are the gain values of the existing StatorMonitor system. In the complete scheme of cascading various stages, the input amplifiers was cascaded to the band-pass filtering circuit and then followed by the output amplifier as shown in figure 5.7 (c)

		First Amplifier				
		Gain	2	3	6	15
Second amplifier	2	40 (37)	60	120 (128)	300 (270)	400
	3	60	90	180	450	600 (641)
	6	120 (128)	180	360	900	1200 (1280)
	12	240	360	720	1800	2400
	18	360	540	1080	2700 (2706)	3600

**Table 5.2 Numerical Gain Matrix for combination of input and output amplifier**

### 5.5.5 Isolation transformer

The output of Rogowski coils are connected to the signal conditioning unit through BNC cables. One end of the Rogowski coil is connected to the machine ground. This can introduce ground-loop circulating currents in the measuring circuit and can have an undesirable effect. In order to break the ground-loop and prevent the flow of circulating currents it was decided to isolate the incoming signals from the Rogowski coils by means of an isolation transformer.

The isolation transformer should be suitable for high frequency signals. Several attempts were made with varying configurations to wind a suitable 1:1 high frequency transformer. The number of turns was varied (35:35, 70:70, 100:100) to alter the

bandwidth performance. However, the capacitive coupling between the primary and secondary windings posed a problem at high frequencies. In order to overcome the capacitive coupling problem, the following methods were adopted:

- Primary winding on bottom half and secondary winding on the top half of the bobbin (and vice versa).
- Metal plate shielding connected to ground separating the primary and secondary windings.
- A tertiary winding connected to ground between the primary and secondary windings.

The metal plate shielding and the tertiary winding method did show an improvement in the bandwidth performance, but it was still not considered to be satisfactory. After several attempts a 1:10 ratio (instead of 1:1) transformer was wound with 18 turns in the primary and 180 turns in the secondary. The primary winding was on the bottom half followed by the secondary winding on top. The transformer was completed using an 'RM-8' core and provided a bandwidth of about 300 KHz. The improvement in the bandwidth can be attributed to better construction and the core material used.

However, a bandwidth of 300 KHz will not be sufficient due to the effect of cascading multiple stages resulting in a reduction of the overall bandwidth. This will have to be addressed when designing the three phase system.

Using this isolation transformer provided an additional gain of '10' which was not considered suitable for the prototype already built. Hence an attenuator had to be inserted in the circuit to compensate for the additional gain. It would not be practical to have an attenuator prior to the isolation transformer. Hence it was decided to have an attenuation of '10' after the first input amplifier. This was implemented by using a voltage divider circuit at the output of the amplifier (4.2K $\Omega$  & 470 $\Omega$ ). When cascaded with the filtering circuit, attenuation in the output of filter was observed. Probing the individual sections of the circuit (without cascading) seemed to be working as designed. On investigation the problem was found to be the voltage divider circuit used for attenuation. The resistance values used were quite high compared to the output impedance of the amplifier. The values of the resistors in the divider circuit were reduced by a decade and this resolved the problem.

## **5.5.6 Reference signal generator**

A reference signal (50 or 60 Hz sine wave) is used to trigger the acquisition of PD signals. This signal is generated by connecting the supply voltage to a simple step down transformer i.e. 230 volts primary to 9 volt secondary. The actual transformer used had a 9 volt centre tapped secondary. One of the outputs of the transformer is connected to a passive network of resistor and capacitor that act as a low pass filter with a cut off frequency of 160 Hz. This is followed by a potential divider circuit with a potentiometer to adjust the amplitude of the reference signal. The second output of the transformer (out of phase by 180°) was also connected to an identical filter network and potential divider circuit. A switch was provided to select between the two taps. Although two taps are not necessary, it was wired just to provide some added redundancy.

The circuits are powered using a standard, market available power supply with an output of +/- 5 V (100mA). The main circuit ground is connected to the chassis. The chassis is grounded via a switch that can connect the chassis either to the mains supply ground or to an external earth point (machine earth). When testing on-site, it was found that the main power-supply ground can be noisy and this can get coupled in the measurement. Under such circumstances it becomes necessary to provide a clean earth connection (shortest ground path) to make any measurement. Hence, an option was provided by means of a switch to connect the circuit ground (chassis) to the main power supply ground or an external clean ground point as shown in Appendix A-3.3. Figure 5.15 (a) and (b) shows the front panel and the internal assembly of the unit.



**Figure 5.15 (a) Front panel of single channel hardware system**

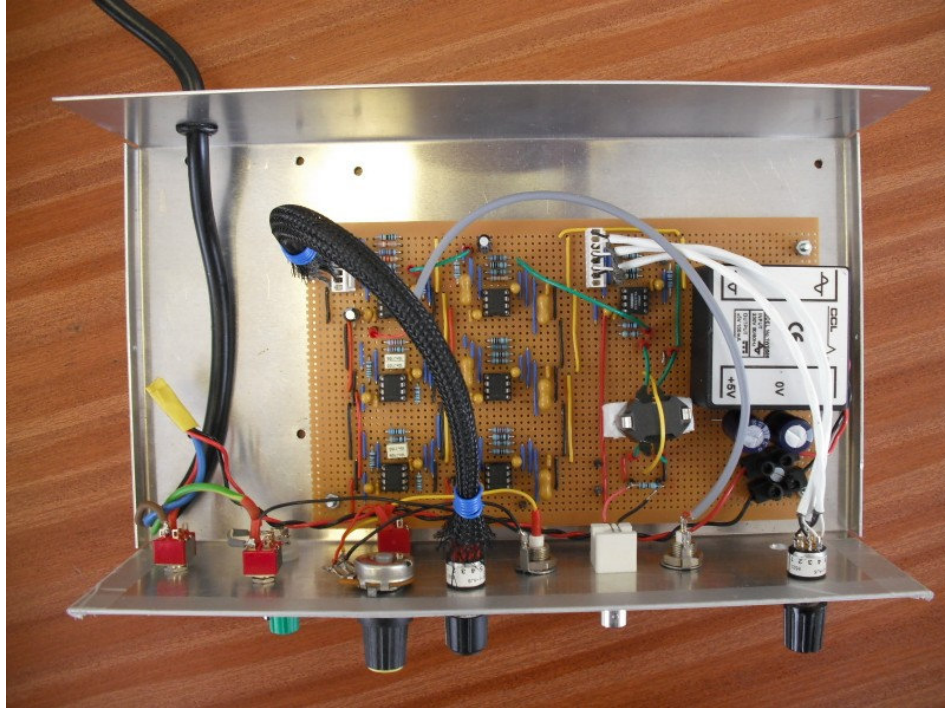


**Figure 5.15 (b) Internal assembly of single hardware channel system**

## **5.6 Analogue to digital converter**

The A/D converter is one of the most significant components of the system as the digitizing speed has a direct influence on the amplifier and filter design. It can be the most expensive component and is instrumental in determining the overall performance of the prototype system. Instead of designing the A/D converter circuit discretely, it was decided to use a market available data DAQ card that would be suitable for the application. For the development of a single channel system, it was sufficient to use a two channel DAQ card i.e. 1 channel for the reference signal and 1 channel for the phase signal. The sampling speed should be a minimum of 3Ms/s and the card should be capable of simultaneous sampling. Eventually a complete three phase unit will require 4 input channels i.e. 1 channel for the reference and 3 channels for the phase signals. Hence, the choice of DAQ card must allow such expansion.

The sampled data is initially stored in the on-board memory available on the DAQ card before it is transferred onto the host computer. It goes without saying that a higher sampling rate will require a greater amount of memory to store the sampled data. The memory requirement also depends on the resolution of the sampled data. For example, if a signal is sampled at 1KHz with an 8-bit resolution, 1KB of memory is required to

store the data captured in 1 second. But if the resolution was 12-bit and the data was sampled at the same rate for the same amount of time, the required memory would be 2KB (1K word). Thus the sampling frequency and the resolution are the key factors dominating the memory requirements.

The signal bandwidth of the required system is about 300KHz and the minimum sampling frequency is 3Ms/s. The signal is to be continuously and simultaneously sampled on all channels for a minimum period of 20ms (1 cycle of 50 Hz signal). With these given conditions, the memory requirements for 8-bit DAQ card can be calculated as follows:

Memory Requirements:

- Sampling Frequency = 3Ms/S
- Number of samples captured in 20 ms = 60,000
- Total number of samples for 2 channels in 20 ms = 1,20,000
- Total number of samples for 4 channel in 20 ms = 2,40,000
- Minimum Memory required for 2 channels (8-bit system) = **120 KB**
- Minimum Memory required for 4 channels (8-bit system) = **240 KB**

Hence the minimum memory requirement for a 2 channel DAQ would be 128KB (standard value) or 256 KB for a 4 channel DAQ. The DAQ card chosen was NI-5102 manufactured by National Instruments. The DAQ card has a resolution of 8 bits with 2 simultaneously sampled input channels. It has a total onboard memory of 663,000 samples which exceeds the requirement for this application and is capable of sampling speeds of 20Ms/s in real time mode. Additionally there is a provision to synchronise two DAQ cards which can later be used for the complete 3 phase system. Also, the DAQ card is provided with NI-LabVIEW software drivers making it easier to develop the DAQ software. The card interfaces the computer through a PCMCIA interface. This interface was specifically chosen to enable a laptop computer interface. This is because the end product needs to be a portable system making other interfaces like PCI not suitable for this application. A PXI system is a possibility, but the current cost of a PXI system is considered prohibitive due to the budgetary constraints of the project.

All the individual sections of the signal condition hardware were developed and tested. The detailed block diagram of the complete single channel system is given in figure 5.16.

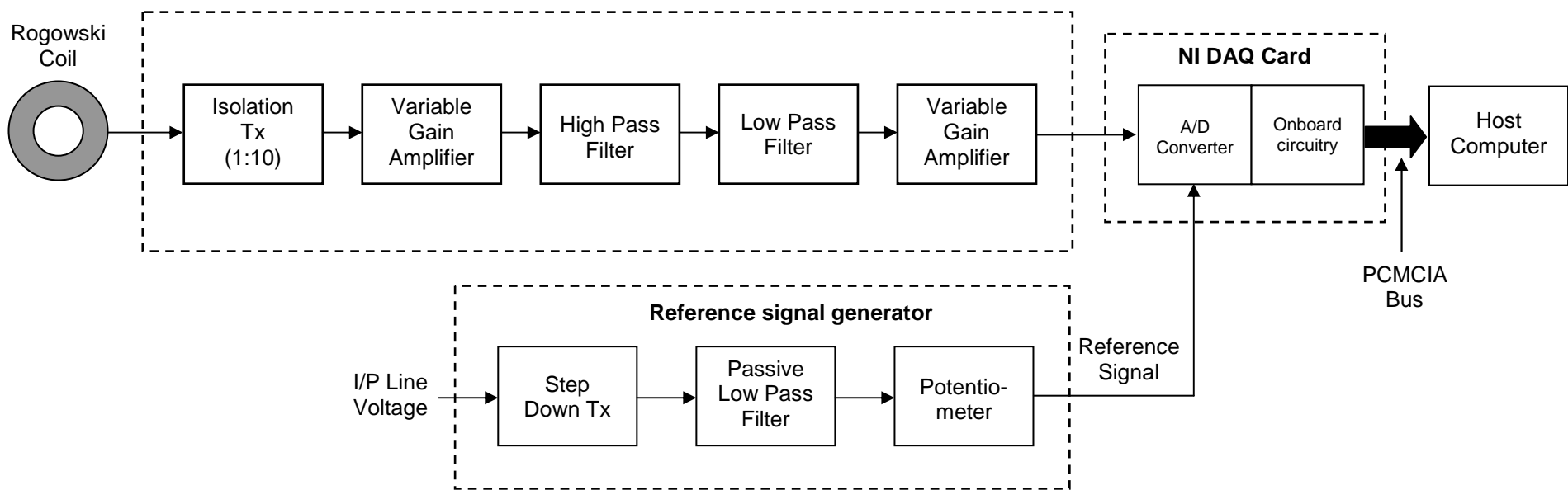


**Figure 5.16 Complete block diagram of a single phase system**

## **5.7 Summary**

Investigations were carried out into various signal conditioning aspects of the PD signals. Filtering and amplification forms the heart of signal conditioning and the choice of A/D converter has a dominant influence in designing these circuits. Prototype hardware of a single channel data acquisition unit encompassing a band-pass filter (10KHz-500KHz) and a high gain amplifier was developed and tested under laboratory conditions. The test results are presented and performance of the hardware is deemed to be satisfactory.

The next stage of prototype design would be the development of DAQ software that is capable of acquiring and storing the discharge data in desired format.

# CHAPTER 6: SINGLE PHASE DATA ACQUISITION SOFTWARE

## 6.1 Introduction

Any PD instrumentation system must have a facility to view the live PD data and record the raw PD data in order to allow post-processing of signals. Permanently stored PD data can be used for comparison and trending of PD activity when subsequent measurements are made over a period of time. The main objective of the data acquisition software was to provide a user friendly interface that can be used to acquire the raw PD data from Rogowski coils and store them in an appropriate format. The main functions of the software are summarised below:

### *a) Hardware Control*

The DAQ card NI-5102 is interfaced to the host computer via a PCMCIA interface. The software must be capable of configuring the DAQ card with appropriate acquisition setting and initiate the acquisition process when prompted.

### *b) Acquiring and displaying PD data*

The software should be capable of acquiring and displaying live PD data in a continuous manner. This allows the user to observe the PD signals on the computer screen (like an oscilloscope) and make the appropriate changes to the gain settings. Optimum gain setting is necessary to accommodate large as well as small PD signals without compromising the dynamic range of the A/D converter.

### *c) Storage of PD data*

The software must have a facility to allow the user to permanently store the acquired raw PD data on a computer hard drive or any form of permanent memory storage. This enables the user to undertake the post-processing of signals and carry out a detailed analysis.

### *d) Retrieval of PD data*

In order to get the maximum information from the PD data, it is a normal practice to acquire data over a large number of cycles. The provision of retrieval of PD data allows the user to check if the entire data set was acquired correctly. It can also be used to

make comparisons of the acquired data sets over a period of time enabling a PD trend analysis, which is considered a vital tool in insulation diagnosis.

## 6.2 Software specifications

Based on the description above, the software specifications for a single channel system were established as shown in Table 6.1.

**Table 6.1 Software specifications for single channel PD system**

<i>Purpose</i>	Software to acquire, display and store PD data acquired from a single phase of rotating machine.
<i>Programming Software</i>	LabVIEW (Version 8.2)
<i>Hardware control requirements</i>	Configure and control NI-5102 data acquisition card via PCMCIA interface.
<i>Acquisition Requirements</i>	<ul style="list-style-type: none"> <li>• Data to be acquired from 2 channels (Ch0 = reference signal; Ch1: PD data).</li> <li>• Sampling Frequency = 5 Ms/s</li> <li>• Voltage Range = +/-2V</li> <li>• Acquisition period = 20ms (one cycle)</li> </ul>
<i>User Interface (Front Panel)</i>	<ul style="list-style-type: none"> <li>• 4 push buttons for 'Acquire', 'Write', 'Read' and 'Stop' functions.</li> <li>• 2 display graphs i.e. one for displaying the acquired data and the other for displaying the retrieved data from disk.</li> </ul>
<i>Storage requirements</i>	<ul style="list-style-type: none"> <li>• Storage format: NI-HWS</li> <li>• Reference signal &amp; PD data to be stored in 2 individual files.</li> <li>• Data retrieval using 'Read' function – data to be displayed on graph.</li> </ul>

### **6.3 Introduction to LabVIEW software**

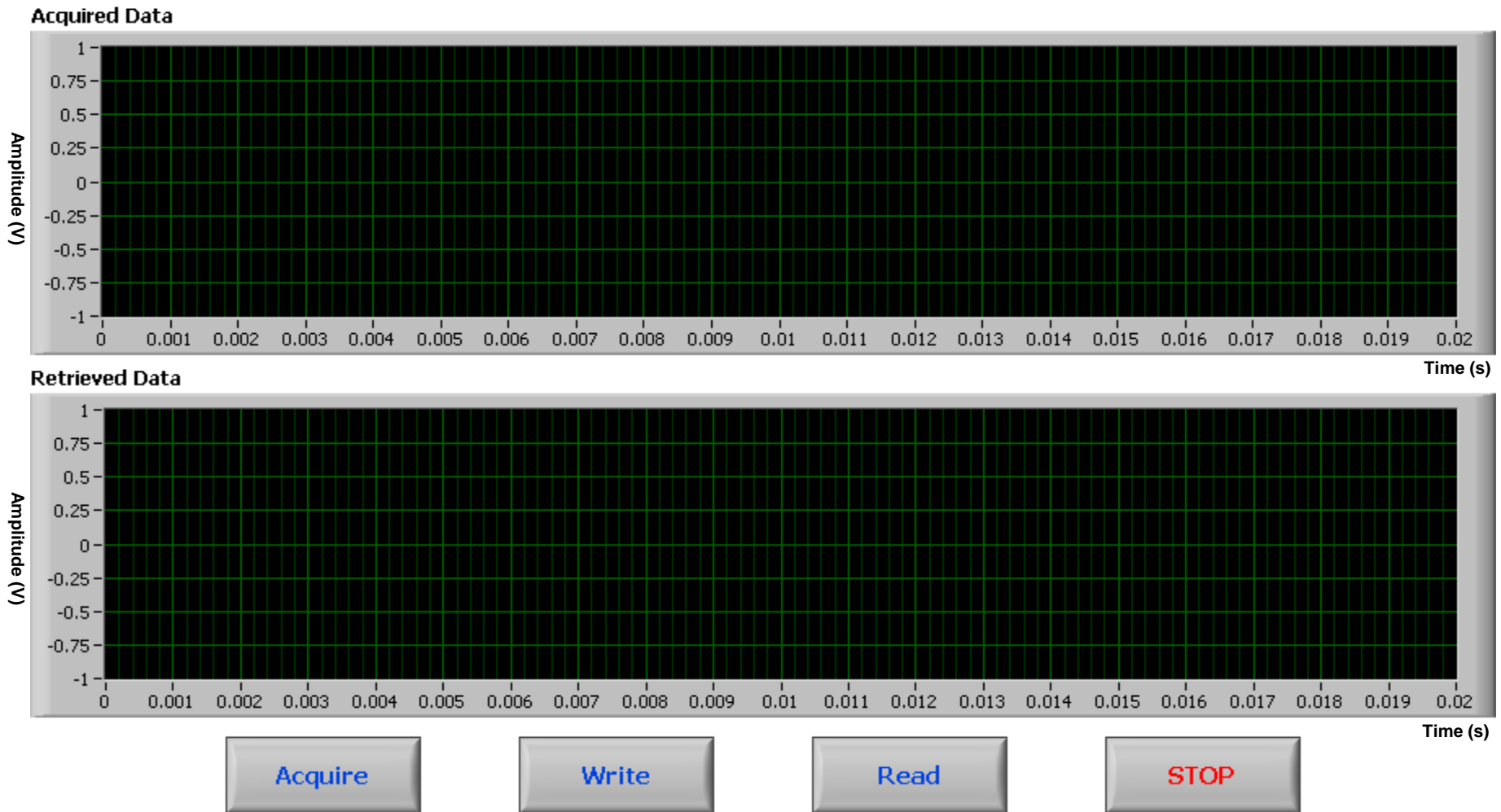
The LabVIEW software by National Instruments is a powerful graphical programming environment that is well known in the field of virtual instrumentation. The programming is carried out in the form of a block diagram using intuitive drag-and-drop type graphical icons and wires that resemble a flowchart. The software is provided with built-in libraries for data acquisition, visualisation and analysis helping to reduce the development time. The software provides various execution loops such as 'IF' loop, 'WHILE' loop or 'FOR' loop and is similar in many aspects to text based programming languages like 'C'. In text based languages the program flow is determined by the sequence of lines of code, whereas the data flow in LabVIEW is determined by wiring of data elements. This brief introduction is provided here for ease of understanding. More details about programming in LabVIEW can be found in the user manual <sup>(130)</sup> provided by National Instruments.

A program written using LabVIEW (version 8.2) is called a Virtual Instrument (VI). Each program essentially has two parts – a front panel and a connector pane (block diagram). The front panel provides an interactive user interface with all the required controls whereas the block diagram is the back-end that actually contains the program code. The programmes generated using LabVIEW have file names with extension '\*.vi'

### **6.4 Data Acquisition Software**

Figure 6.1 shows the front panel of a single channel data acquisition system for this work. Various controls are provided to the user for controlling the acquisition process.

# Single Channel StatorMonitor System



101

Figure 6.1 Front Panel of Single Phase acquisition program

The two graphs on the front panel show the acquired data and retrieved data. The program is capable of acquiring 2 signals simultaneously i.e. 50 Hz sine wave used as a reference signal and PD data from one phase. The 'Acquire' function configures the DAQ card with appropriate settings and acquires data over a 20 ms period with a sampling frequency of 5Ms/s. The minimum sampling requirement for the application was 3Ms/s. However, acquiring data at a higher sampling frequency will reduce the burden on AAF filter. The memory requirement for acquiring data with 5Ms/s will be 200,000 samples/cycle for two channels. The NI-5102 DAQ card has an onboard memory of 663,000 samples which is more than sufficient for the application. This data is displayed in the top graph. If the acquired data is too small or too big, then the gain settings on the signal conditioning unit can be altered and another data set can be obtained.

The 'Write' function stores the acquired data in a file at a desired location set by the user. The data is split and stored in 2 separate files – one file stores the reference signal and the other stores the PD data. The 'Read' function is used to retrieve the data from a stored file and display the data on the bottom graph. The program prompts the user to select the path of the desired file. Finally, the 'Stop' function allows the user to exit from the program. The LabVIEW code for this program is given Appendix A-5.1.

The software was interfaced with the hardware and tested under laboratory conditions with simulated signals. The performance was found to be satisfactory. The next stage was to carry out testing with real PD signals in an industrial environment.

## **6.5 On-site testing of the single channel system**

It was necessary to study the behaviour of the system in an industrial environment with real PD signals. Unfortunately, high voltage test facilities were not available within Dowding & Mills (Aberdeen) or at Robert Gordon University. Hence it was difficult to get access to real PD data.

However, with the co-operation of Dowding & Mills a field-trip was arranged to a petroleum refinery plant in the UK. This provided an opportunity to test an 11KV machine on-site. The main purpose of this field-trip was to gather some real PD data and save it.

### 6.5.1 The test set-up

The 11KV machine was already installed with permanently fitted Rogowski coils manufactured by Dowding & Mills. The coils were located very close to the machine terminals in the high voltage terminal box. Due to the presence of high voltage in the machine terminal box, it was necessary to terminate the output connections of the coil externally (out-with the main HV terminal box). This eliminates the need of HV access during every test and makes the testing process safer. The output from the three coils (one per phase) was terminated in a local terminal box with screw terminals. The complete test set-up is shown in figure 6.2.

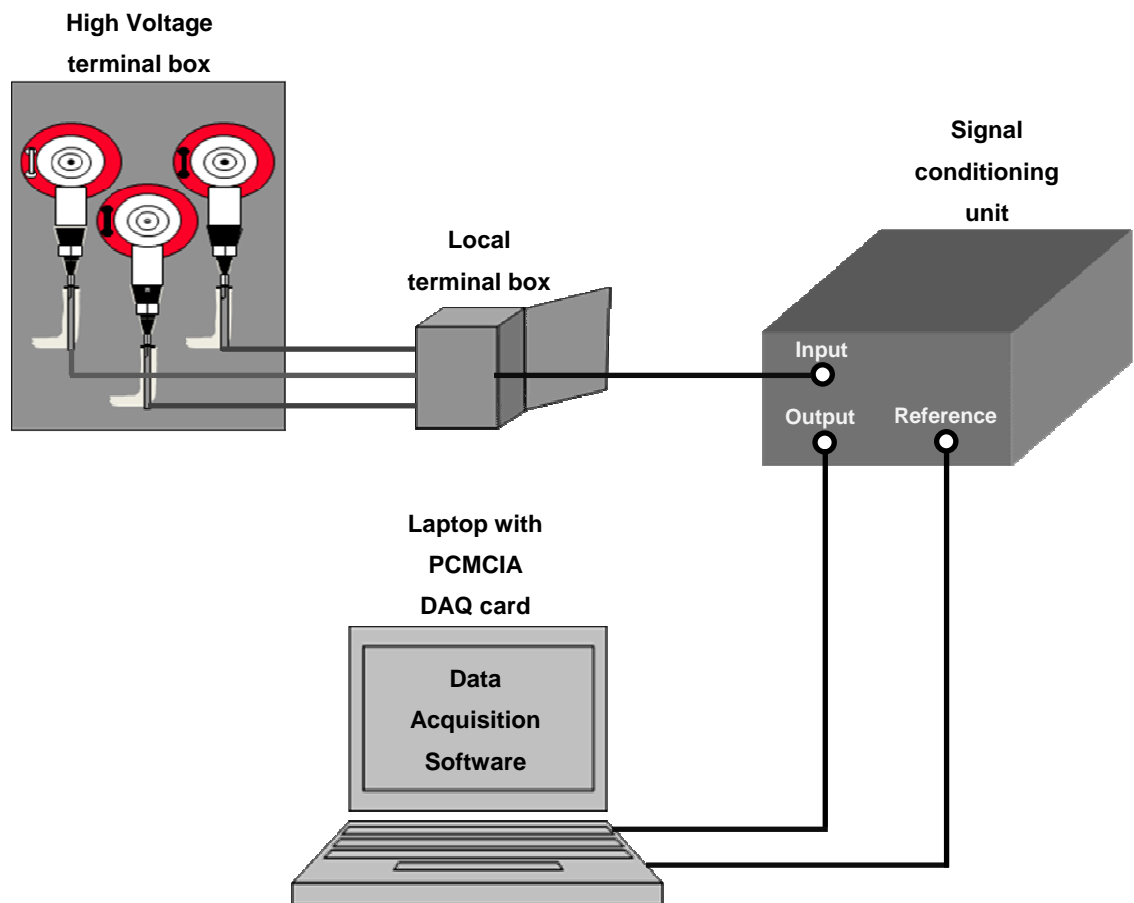
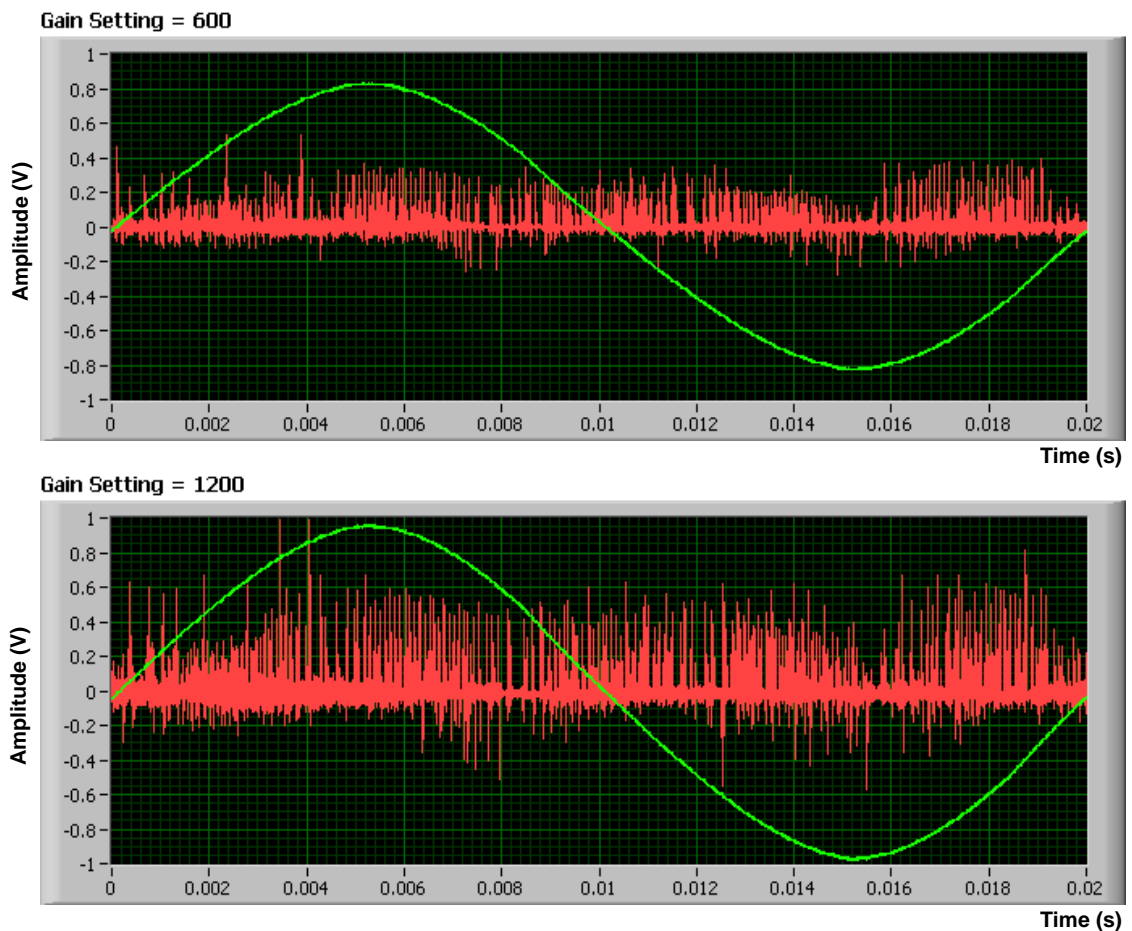


Figure 6.2 Test set-up for single phase data acquisition

## 6.5.2 The waveform display

The testing was carried out using various gain settings and the data was acquired with a sampling rate of 5 Ms/s. In this case the most suitable gain settings were found to be '600' and '1200'. Figure 6.3 shows the graphs for a single phase data along with the reference signal (green) for both the gain settings.



**Figure 6.3 PD data acquired with different gain settings**

It can be observed from the graph above that some pulses are clipped with a gain setting of '1200' whereas all the data acquired with a gain setting of '600' is within range. Another data set was acquired with the maximum sampling rate possible with the DAQ card i.e. 10 Ms/s per channel. However the file size with the higher sampling rate was considered too large. Only after further signal processing can it be commented if sampling with such high frequency will provide any substantial benefits. Theoretically a sampling rate of 5Ms/s is more than 15 times the maximum frequency of interest (i.e. 300KHz) and should be sufficient.

### 6.5.3 Data Analysis

It can be seen from figure 6.3, that the acquired PD data did not resemble a typical PD pattern. A typical PD pattern commonly found in most machines occurs in well defined bands in the first and third quadrant of the sine wave. This is shown in figure 6.4 (data provided by Dowding & Mills from their PD database).

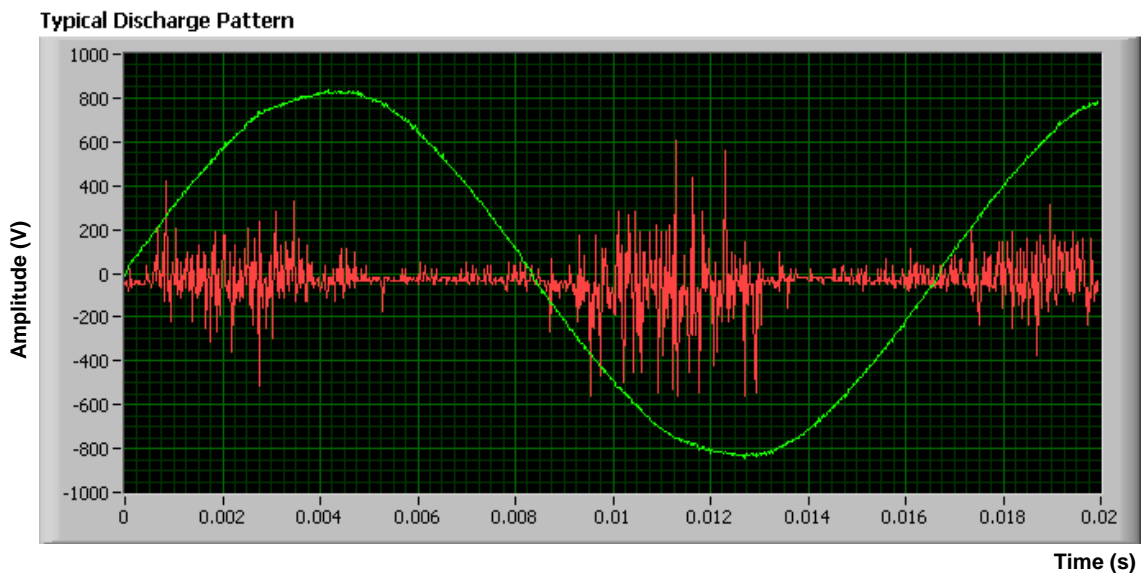


**Figure 6.4 Typical banded discharge activity**

Comparing the acquired PD data to typical PD pattern indicates that the acquired data is not of a very good quality and has some form of external interference. There is a strong possibility that external interference has a similar frequency spectrum to that of PD data. This is because any external interference beyond the bandwidth of 30-300KHz will be filtered by the signal conditioning unit.

A Fast Fourier Transform (FFT) analysis on the acquired signal can highlight the frequency components present in the signal spectrum and may help to identify the source of noise. The results of the FFT analysis are shown in figure 6.5. It can be seen from the FFT spectrum graph that the main fundamental noise frequency is present at 40KHz. This noise also appears at the harmonic frequencies of the fundamental (i.e. 80KHz, 120KHz, 160KHz and so on). It is inferred from the FFT spectrum that the noise is possibly being caused due to multi-speed motor drives or some form of switching device connected on the same power line. The multi-speed drives use a high frequency carrier signal for achieving speed control and this carrier frequency may be the source.

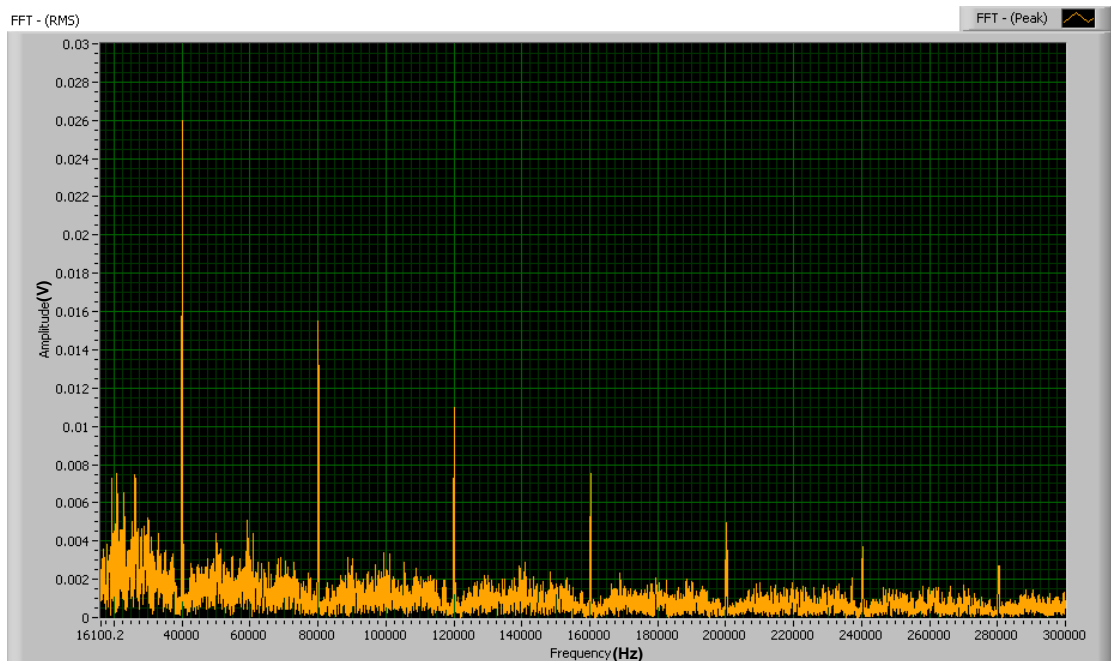


**Figure 6.5 FFT spectrum of the acquired PD signal**

Attempts were made to filter out the interference present within the frequency band of interest using two different techniques and are presented below.

#### 6.5.3.1 Filtering Noise – Method 1

The acquired data was first subjected to an ‘Amplitude’ base filtering technique. Minimum and maximum threshold limits were set and the waveform was analysed on a sample by sample basis. Any waveform value beyond the set threshold value is assumed to be noise and the value is set to zero.

In this case, a threshold limit of +/- 0.25 volts was set at the output of the acquired signal and the results were evaluated. The threshold value was chosen by comparing the acquired signal to the typical PD cycle shown in figure 6.4. It was assumed that the pulses out with the typical PD occurring region are possibly caused due to noise and the amplitude of these pulses was taken into consideration for deciding the threshold value. The program description and LabVIEW code for this filtering method is given in Appendix A-5.2. Figure 6.6 shows the original PD waveform along with the filtered one (in time domain) for comparison. Visual observation of the graphs indicates that the noise level has reduced, but not eliminated completely. As the data on the graph is very dense (100K points plotted per 20ms), not much can be commented on the effectiveness of filtering by visual observation. Performing an FFT analysis on the filtered signal may provide better insights. The FFT graphs are shown in figure 6.7.

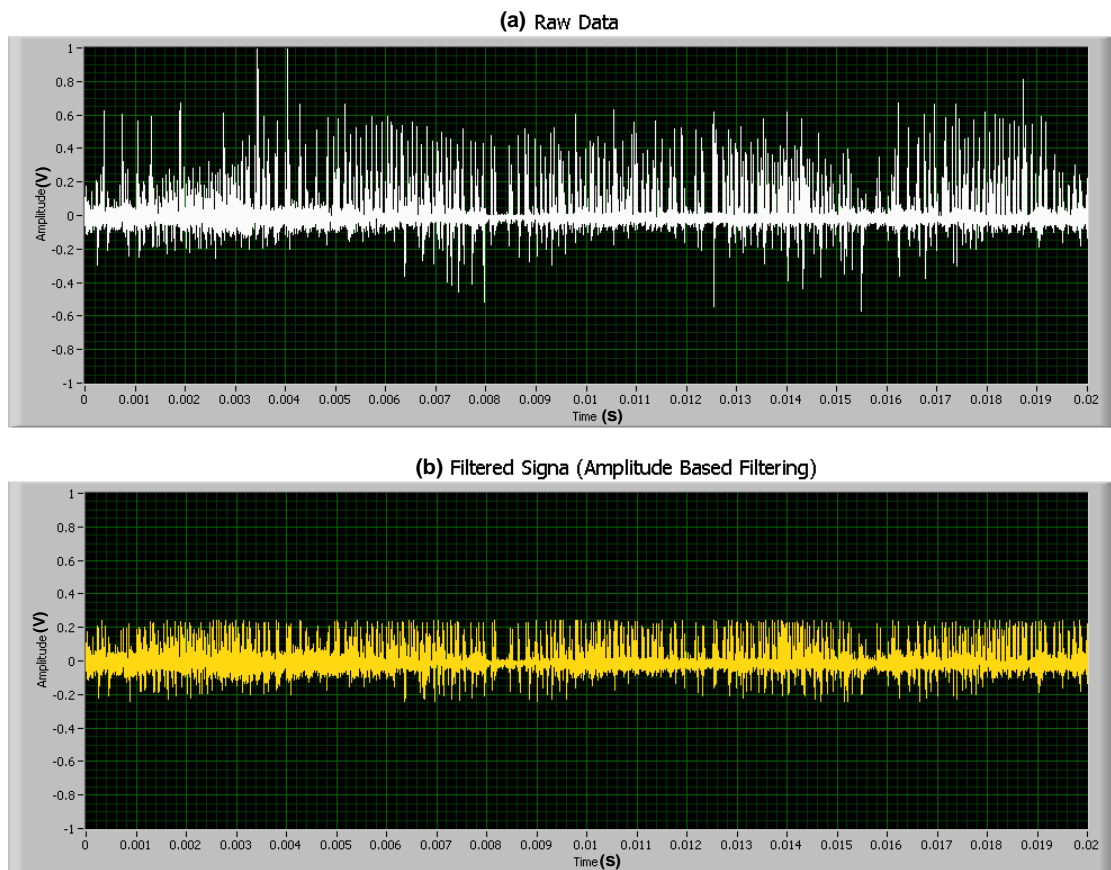


**Figure 6.6 Amplitude based filtering – time domain waveforms**

The FFT waveforms in figure 6.7 indicate that the 40KHz noise and its harmonic frequencies have a reduction in amplitude due to the filtering process, but have not been completely eliminated. The fallacy lies with the method of filtering adopted. For example, if a noise pulse has a frequency of 40KHz (or its harmonic frequency) and an amplitude of less than  $\pm 0.25V$  then it will still be retained in the original waveform. Hence there is only a reduction in the overall amplitude of noise pulses.

There is another disadvantage associated with this method of filtering. For, example, if a PD pulse has amplitude greater than the set threshold, it will be set to zero value and the pulse would be lost. The PD pulses with higher amplitudes are of paramount importance as they contain higher energy to cause insulation damage and should not go undetected. Additionally, a skilled user would be required to set the appropriate threshold limits. Even then this might seem an impossible task where the amplitude of PD pulses and noise pulses are in a similar range. Hence, 'amplitude based filtering' method is not considered to be a preferred method for filtering noise.

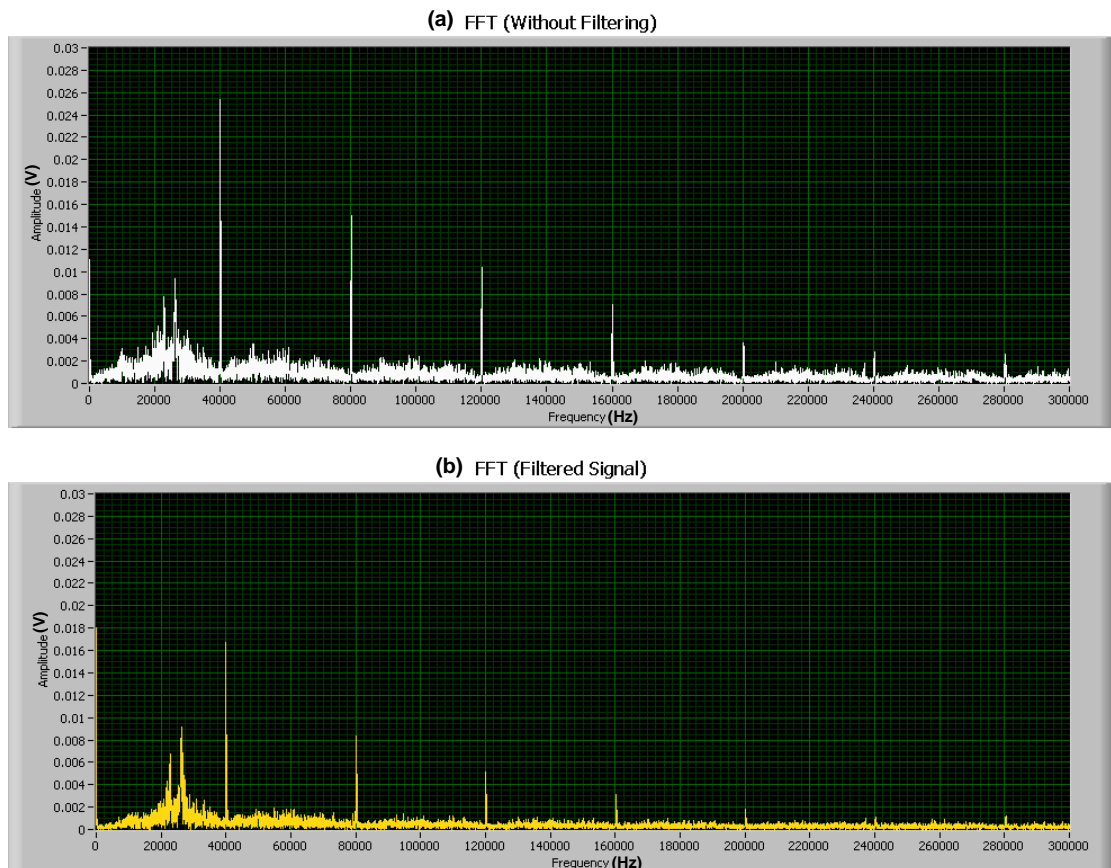


**Figure 6.7 Amplitude based filtering – frequency domain waveforms**

### 6.5.3.2 Filtering Noise – Method 2

The system has been designed to acquire and analyse signals only in a frequency range of 30-300 KHz. Any frequencies acquired beyond these values will not have true amplitude as they would be attenuated in varying proportions by the hardware filters present in the external signal conditioning unit. But, the external filters do not have a brick-wall response. The frequencies present in the transition band (due to the finite roll-off of filters) will still be present in the acquired spectrum. There is also a possibility of certain frequencies being present (within the frequency band of interest) due to electromagnetic pick-up.

This can be verified by observing the complete frequency spectrum of the signal as shown in figure 6.8. It is evident that the frequencies beyond 300KHz are still present in the signal spectrum. These unwanted frequencies would affect the quality of the acquired signal. Hence it was decided to implement a software band-pass filter to eliminate the unwanted frequencies.

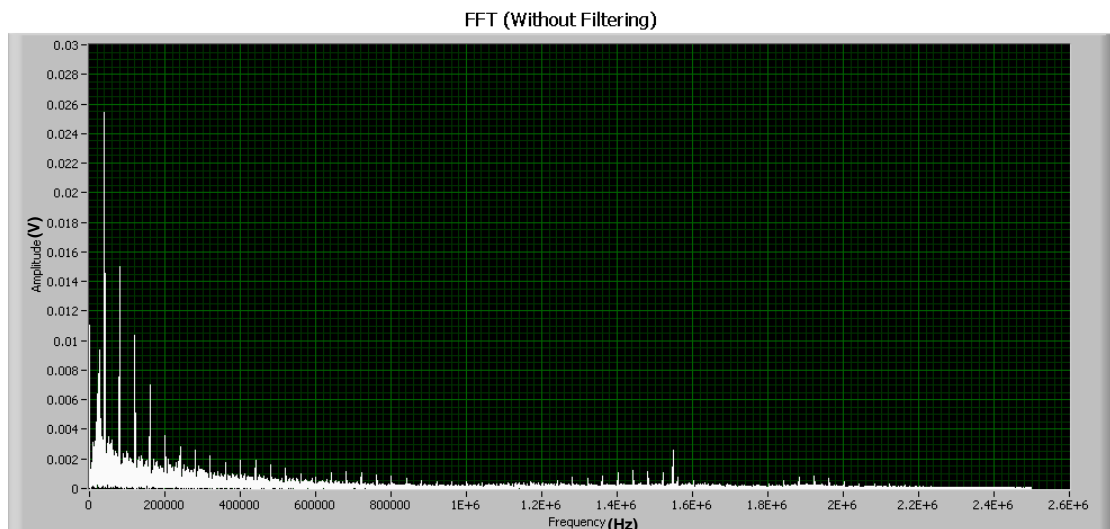


**Figure 6.8 Complete frequency spectrum of the acquired signal**

A software band-pass filter (6<sup>th</sup> order Butterworth IIR Filter) with a lower cut-off frequency of 30KHz and upper cut-off frequency of 300KHz was implemented. The lower cut-off frequency was changed from 10KHz to 30KHz and the upper cut-off was changed from 500KHz to 300KHz in order to eliminate all frequencies beyond range of interest i.e. 30KHz – 300KHz (During the hardware design stage the cut-off frequencies were altered to 10KHz and 500KHz only to achieve a complete flat response in the desired frequency range).

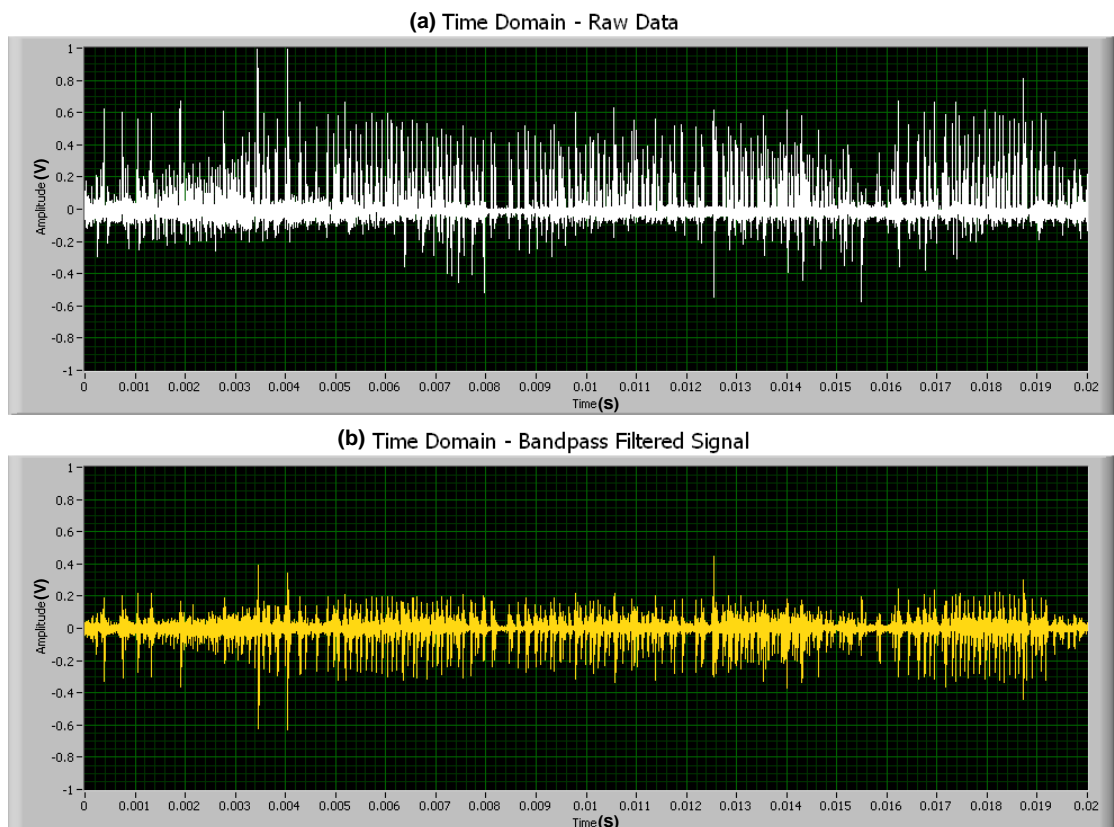


**Figure 6.9 Band-pass filtering – time domain signal**

After filtering the signal in the time domain appears to have improved, as the high frequency noise was suppressed. This can be seen in figure 6.9. The FFT waveform of the band-pass filtered signal is shown in figure 6.10. The highlighted area shows that high frequency signals beyond 300 KHz have been effectively suppressed.

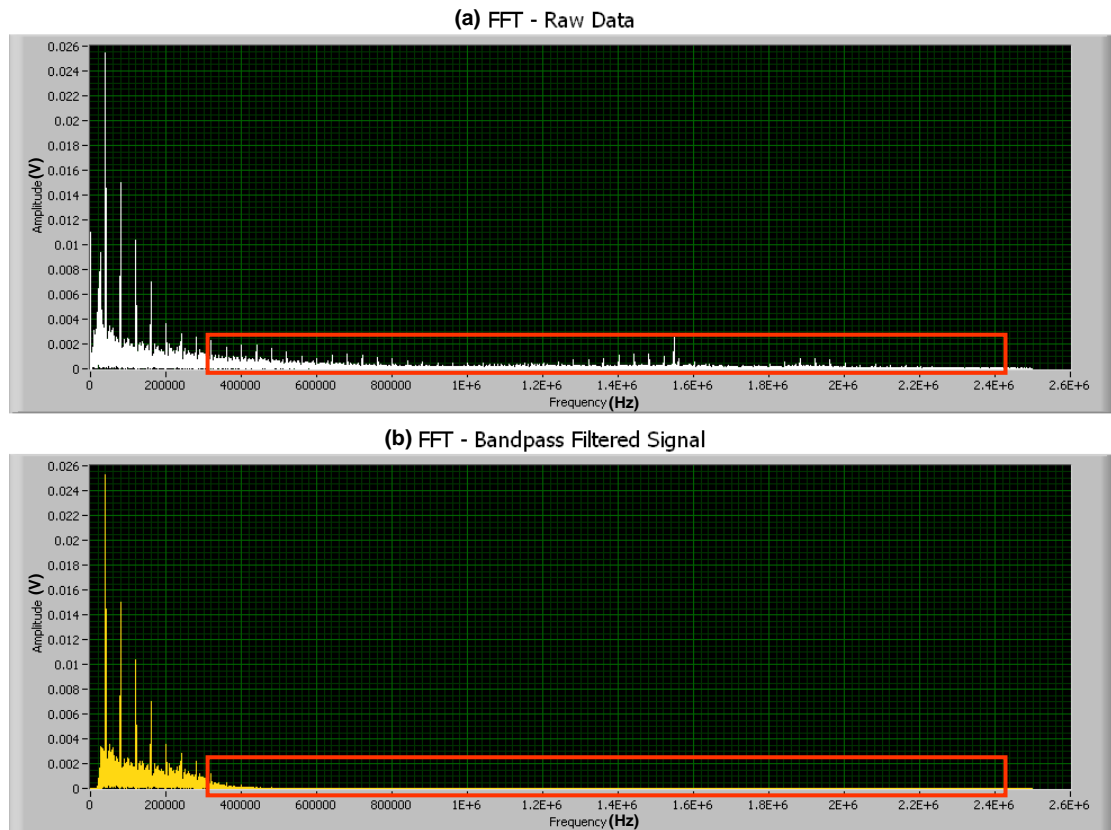
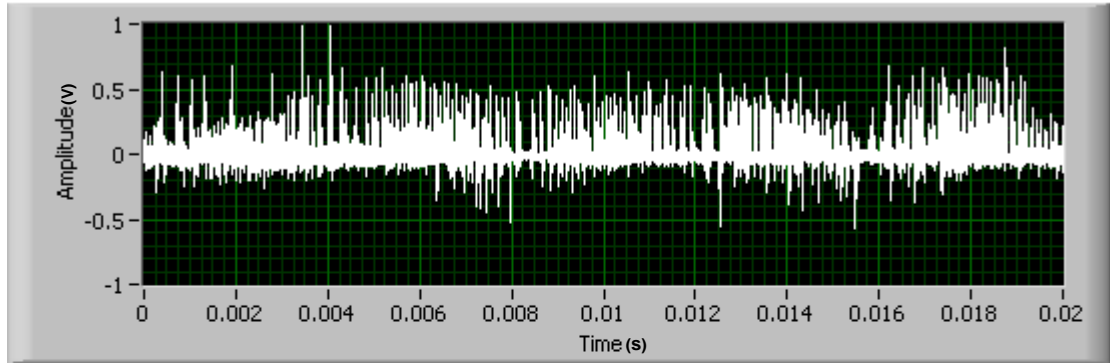


**Figure 6.10 Band-pass filtering – frequency domain signal**

Though all the frequencies beyond 300KHz and below 30KHz have been filtered, it is still necessary to filter the 40KHz switching noise and its harmonic elements. One way of doing it would be to have band-reject filters with their cut-offs set to the harmonic frequencies. This was implemented using software filters. 6<sup>th</sup> order band-reject Butterworth IIR filter with lower cut-off frequency of 39KHz and upper cut-off frequency of 41KHz was implemented to eliminate the 40KHz switching noise. Similar filters (with 2KHz band-reject window) were configured to eliminate up to 7<sup>th</sup> harmonic of 40KHz i.e. 280KHz. The results can be seen in figure 6.11 and figure 6.12. The LabVIEW code can be found in Appendix A-5.3. The time domain waveform in figure 6.11 visually indicates that the filtered waveform appears to have reduced noise level when compared to the raw data. The results of the effectiveness of filtering are better viewed in the frequency domain waveforms shown in figure 6.12. It can be seen from the FFT waveforms that the 40KHz noise and its harmonics have been successfully filtered out from the signal spectrum.

Time Domain - Raw Data



Time Domain - Filtered Signal (Bandpass + Bandreject)

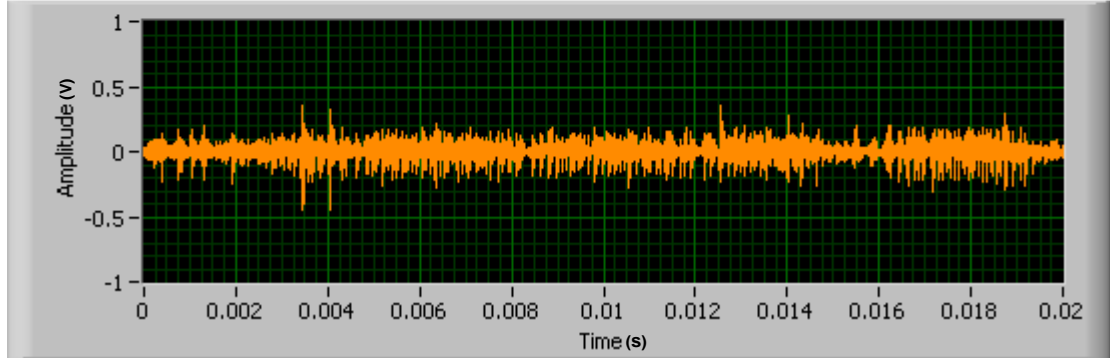
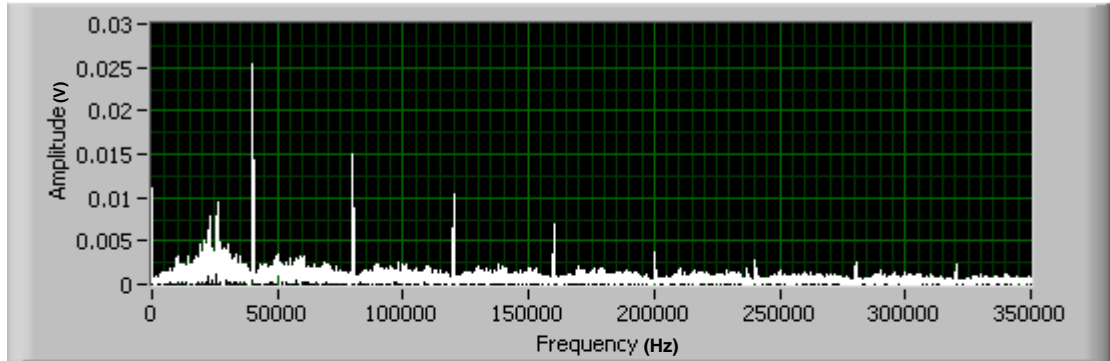


**Figure 6.11 Band-reject filtering – time domain signal**

FFT - Raw Data



FFT - Filtered Signal (Bandpass + Bandreject)

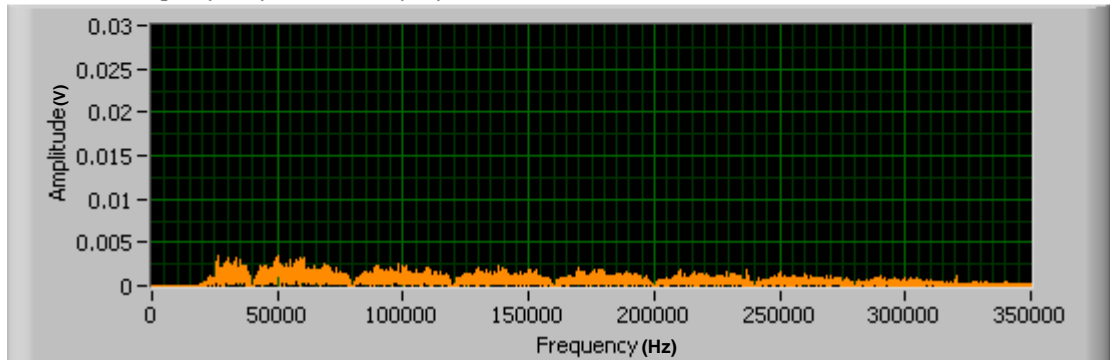


**Figure 6.12 Band-reject filtering – frequency domain signal**

The disadvantage of this method of filtering is that a certain amount of partial discharge data may be lost in the filtering process. This can happen if PD pulses are present in the frequency bands that are set to be rejected by the band-reject filters. Also, this filtering technique is only suitable to filter out the switching noise generated by devices like variable speed drives. Other forms of noise may be present in the PD spectrum. Further investigation is required to detect and filter these other forms of noise.

During the course of this project emphasis was laid on developing a data acquisition system for the detection of PD signals. Noise filtering techniques and PD data analysis will be a part of a future project and beyond the scope of this thesis.

## **6.6 Summary**

DAQ software was developed to acquire PD signals from a single phase of a rotating machine. The software is capable of acquiring, displaying, storing and retrieving PD data. On-site testing was carried out on an 11KV machine to acquire some real PD data and assess the system performance. The acquired PD data had external interference signals present in its spectrum. Two different noise-filtering techniques were evaluated for filtering the noise and the results for each of the techniques have been presented.

The next section describes the design and development of a complete three channel PD detection system.

# CHAPTER 7: THREE PHASE PARTIAL DISCHARGE MONITORING HARDWARE

## 7.1 Introduction

Having tested the single channel prototype system on an industrial site, the next step forward was to design a complete 3-channel system that was capable of acquiring data from all three phases of the machine in a simultaneous manner. Detecting discharges from all three phases simultaneously has advantages over the single-channel approach. For example, a phase-phase discharge can be effectively detected by a three channel system as the discharge pulse occurs simultaneously in the phases involved. A single phase system will not be capable of making such measurements. It also provides greater possibilities for signal processing associated with noise rejection and data analysis.

## 7.2 Some design considerations

The design of the new 3-channel system hardware is similar to its single-phase counterpart in most aspects. However, certain design modifications were made that emerged during the testing of the single-channel prototype system. Some of the major highlights are mentioned below:

- The PD detector unit is mainly intended to be used on the offshore platforms in the North Sea with limited mainland application. Most offshore sites have a mains supply voltage of 110 volts, whereas on-shore sites have a supply voltage of 220 volts. Hence, the power supply for the signal conditioning needs to be a universal input type (i.e. 110V & 220V). The standard available switch-mode universal power supplies were not used to avoid any interference caused by the switching elements within the power supply itself. Instead, a linear power supply has been used with an option of supply voltage selection (i.e. 110V or 220V).
- The single channel prototype had two rotary switches for the individual control of the input and output amplifier. However it was found to be inconvenient to change the individual gain setting during the actual testing. The new design implements a common shaft arrangement to change the gain of both the amplifiers using a single knob. The number of available gain settings has also been modified to amplify partial discharge signals of various amplitudes.

- The single channel prototype was built on a strip-board commonly used for prototyping electronic circuits. However, this is not ideal for high frequency applications. The parasitic capacitance of the board can have an undesirable effect and deteriorate the performance. Hence the new hardware was designed and built on Printed Circuit Boards (PCB). Efforts were taken to reduce noise during the PCB design by providing a sufficient area of ground plane.
- The signal input / output BNC connectors and the gain selecting switches located on the front panel have been mounted directly onto the PCB to avoid additional wires and connections; thus helping to reduce unwanted noise pick-up.

### **7.3 System block diagram**

Figure 7.1 shows the complete detailed block diagram of the three phase PD detection unit. The block diagram is very similar to the single phase system. Any minor modifications in the individual blocks have been described in the next section.

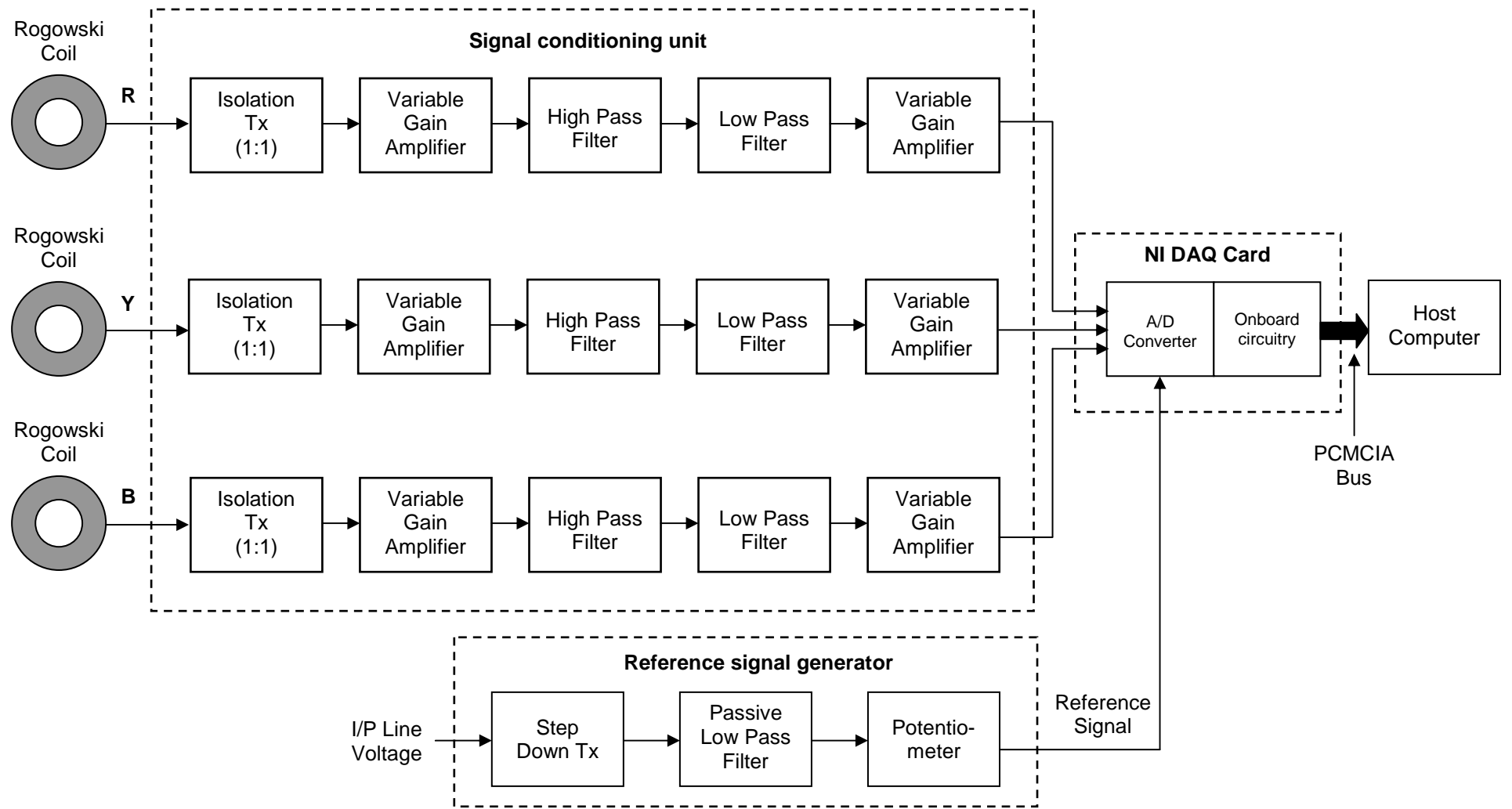


Figure 7.1 Complete Block diagram of three phase PD detection system

The description of the individual blocks of the three phase system is given below.

## **7.4 The Rogowski coil**

No changes were made to the design of the Rogowski coil due to the associated commercial implication of changing the existing Rogowski coils already installed on a world-wide basis.

## **7.5 Signal conditioning unit**

### **7.5.1 Isolation transformer**

The single channel system used a hand-wound transformer with a turns ratio of 1:10 (i.e. 18 turns primary and 180 turns secondary) build on a RM-8 core. The frequency response of this transformer was fairly linear in the desired frequency range of 30KHz to 300KHz. However, there was a small voltage drop in gain at frequencies higher than 250KHz. This will affect the accuracy of the system in its higher frequency range. A standard market available 1:1 isolation transformer with a frequency bandwidth of 1MHz was identified and used in the new design. This transformer has a linear frequency response in the desired range. The additional gain of 10 provided by the previous transformer design has been compensated for in the amplifier stage.

### **7.5.2 Input variable gain amplifier**

The design and configuration of the input variable gain amplifier was similar to that used in the single channel system. (The op-amp MAX-437 used in the single channel prototype was an obsolete component and not recommended for new designs.) Hence, another op-amp AD8055A was selected for the new design. AD-8055A has a gain bandwidth product of 300MHz with a input noise of  $6\text{nv}/\sqrt{\text{Hz}}$ . The amplifier is implemented in a non-inverting configuration and the gain of the amplifier is varied by switching the feedback resistors using a rotary switch. Based on the testing of a single channel system, minor changes were made in the feedback resistor values to achieve more accurate gains. In the single channel system a voltage divider circuit was connected at the output of this amplifier to reduce the signal by a ratio of 10. This was done to compensate for the additional gain provided by the isolation transformer. In the new design the isolation transformer has a ratio of 1:1; hence the voltage divider circuit was eliminated. This amplifier provides a variable gain of 2, 3, 6, 15 & 20. Figure 7.2

shows the performance of the amplifier with different gain settings. The amplifier has an improved frequency response compared to the single phase system. The circuit diagram is provided in Appendix A-4.1.

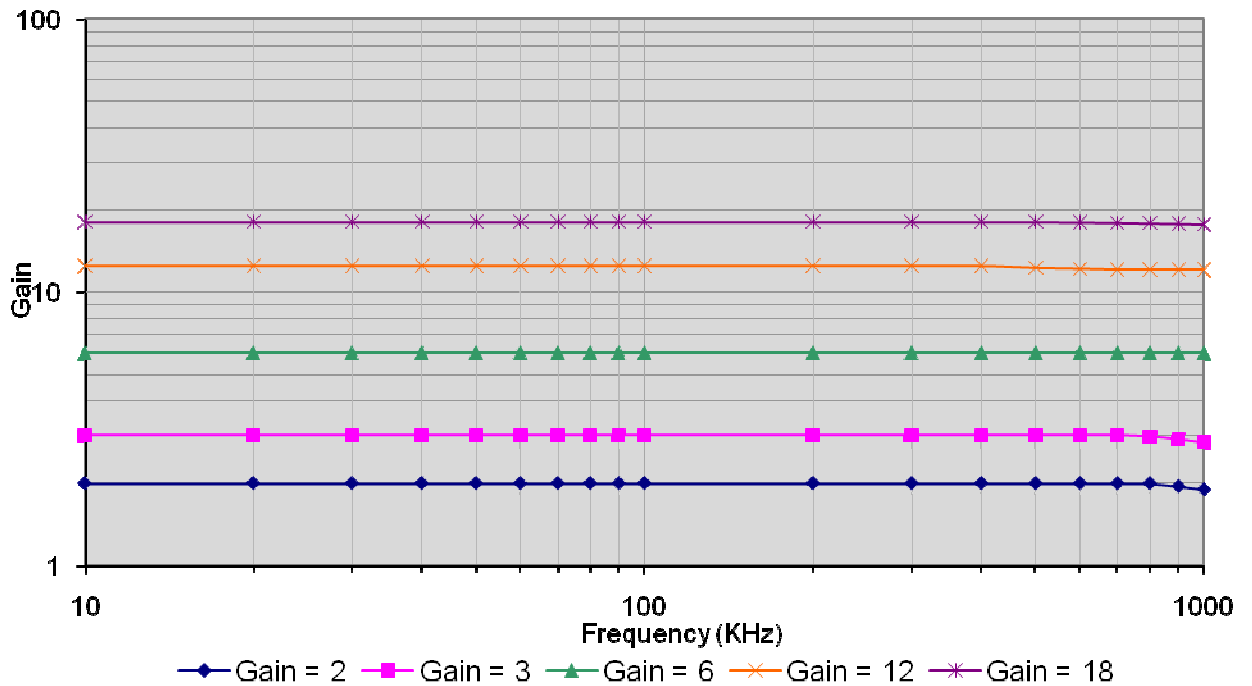


**Figure 7.2 Frequency response of input amplifier (3-phase system)**

### 7.5.3 High pass filter

The design of the high pass filter has essentially remained unaltered. The filter was implemented using the op-amp AD8055A instead of MAX-437 for reasons already stated. Polypropylene film capacitors were used as they have close tolerances and low losses and are specifically used in filter networks. The filter has a cut-off frequency of 10KHz and provides a fixed gain of '2.55' (8.13dB).

### 7.5.4 Low-pass (AAF) filter

This 6<sup>th</sup> order Sallen-key Butterworth low-pass (AAF) filter was also built using AD8055 op-amps. The design and the configuration remain the same as the single channel system. The filter has a cut-off frequency of 500KHz and provides a fixed gain of '4.12' (12.3dB). This filter is cascaded with the high-pass filter to provide a bandwidth of 10-500KHz and a signal gain of '10' (20dB). The frequency response of the combined band-pass filter is shown in figure 7.3.

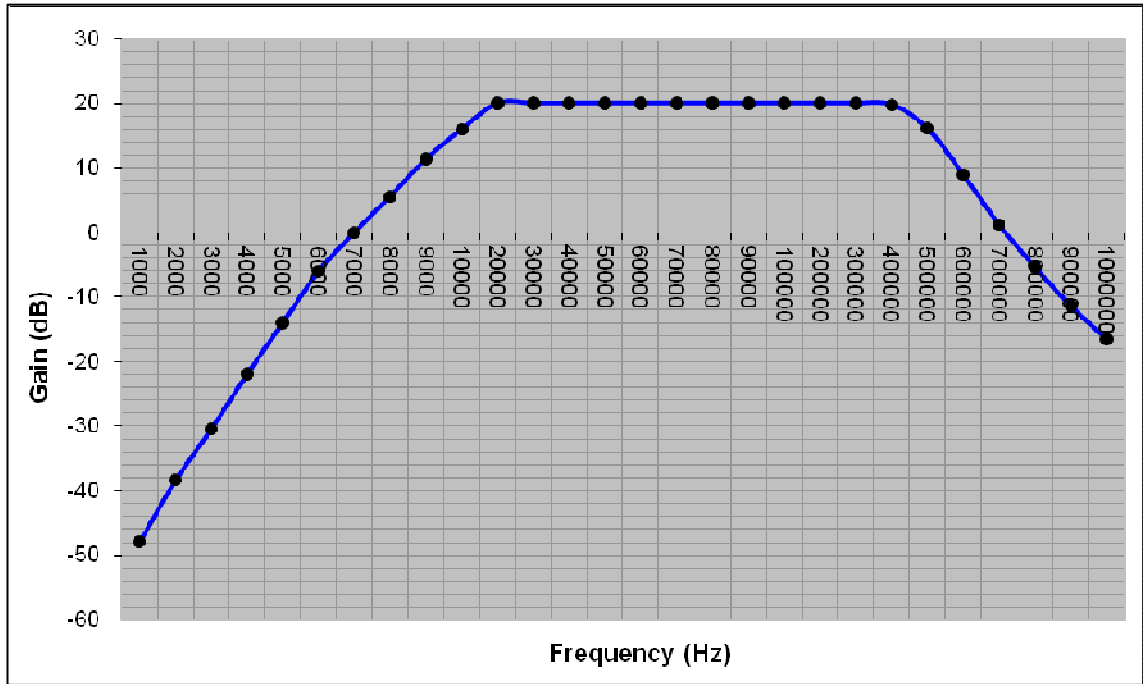


**Figure 7.3 Frequency response of band-pass filter (3-phase system)**

### 7.5.5 Output variable gain amplifier

The design and construction of the output variable gain amplifier is almost identical to the input amplifier, apart from a few gain settings. The gain settings for the output amplifier are 2, 3, 6, 12 and 18. The circuit diagram is provided in Appendix A-4.4. As stated earlier, a common shaft connects the gain switching mechanism of both the amplifiers. Each rotary switch wafer has a single pole 12-way switch mechanism. Thus a maximum of 12 different gain combinations can be obtained.

The complete details of the gain settings along with the overall system gain are given in table 7.1. The designed gain settings were practically verified in the laboratory. All gain settings were tested with a 100KHz sine wave signal with varying amplitudes to prevent gain saturation.

**Table 7.1 Gain setting details of 3-phase system**

Switch Position	Theoretical				Overall Gain (Practical)	Gain Error (%)
	Input Amplifier Gain	Band-Pass Filter Gain	Output Amplifier Gain	Overall Gain (Theoretical)		
1	2	10.25	2	41	40	2.4
2	3	10.25	3	92	90	2.2
3	6	10.25	2	123	122	0.8
4	6	10.25	3	185	180	2.7
5	15	10.25	2	308	310	-0.6
6	6	10.25	6	369	360	2.4
7	15	10.25	3	461	450	2.4
8	20	10.25	3	615	600	2.4
9	15	10.25	6	923	900	2.5
10	20	10.25	6	1230	1200	2.4
11	15	10.25	12	1845	1750	5.1
12	15	10.25	18	2768	2600	6.1

It can be seen from the table 7.1 that the gain error in most settings is less than 2.5%. Only the high gain settings (1750 & 2600) have a slightly higher gain error (5-6%). There is a possibility that this error may have occurred due to component tolerances and/or due to the limitation of the signal generator. The minimum voltage that could be generated by the signal generator was 1mV. Even a very small error in the amplitude of the generated signal may have a significant impact on the gain calculation due to the high gains involved. However, a gain error of 6% at the highest gain setting is still acceptable and considered satisfactory for this application. This is because the highest gain setting will only be used when the amplitude of PD signal is very low. The low amplitude PD signals are not considered critical as they do not affect the winding insulation significantly. Thus, a small measurement error at high gain setting will not have any substantial influence on the overall analysis.

The design of the reference signal generator was not changed. Some changes had to be made in the power-supply design. The minimum power requirements were first established by connecting all the electronic circuitry to a +/- 5V DC power source. The total current drawn was measured to be approximately 175mA in each rail. A market available power supply was selected that could supply +/- 5V DC with 250 mA current in each rail. The power supply also had a provision of 110V or 220V input which was a mandatory requirement of the project. A toggle switch was provided to the user for selecting the mains supply voltage. Figure 7.4 (a) and (b) shows the front panel and the internal assembly of the complete three phase unit.



**Figure 7.4 (a) Front panel of the 3-channel hardware system**

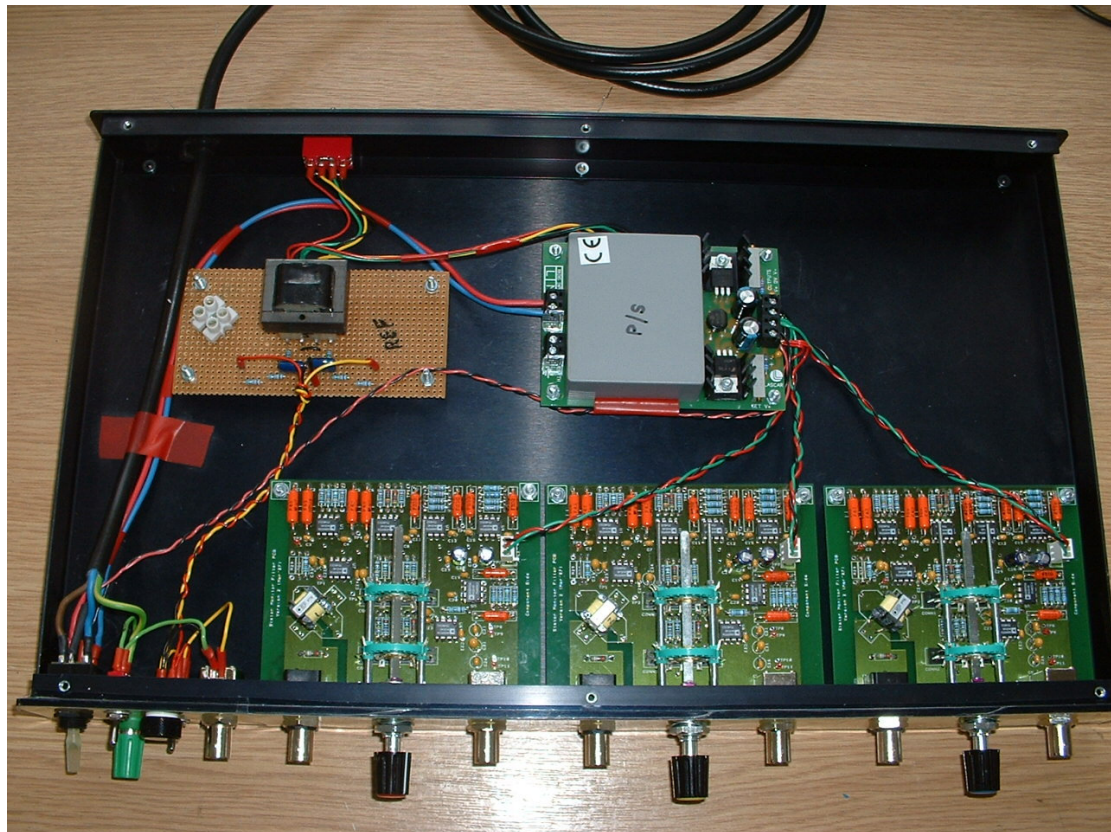


**Figure 7.4 (b) Internal assembly of 3-channel hardware system**

Like the single-channel system, the provision of connecting the main circuit ground to supply earth point or to an external earth point was also provided in the system.

## **7.6 Analogue to digital converter**

The NI-5102 DAQ card that was used for the single channel system has two simultaneously sampled input channels. However, for implementing a 3-phase system, four simultaneously sampled channels are required (1 reference signal and 3 phase signals), necessitating the use of two DAQ cards. The NI-5102 DAQ cards have a provision to synchronise more than one DAQ card through the synchronising input

called 'PFI0'. This makes it possible to initiate an acquisition simultaneously on both cards. A connector-box was made that was suitable for BNC inputs from the signal conditioning unit and interfaced the DAQ cards to the laptop through PCMCIA interface as shown in figure 7.5.



**Figure 7.5 DAQ card interface box**

## **7.7 Summary**

A three channel prototype hardware for detecting PD has been developed on the basis of a single channel system. Some of the issues that were highlighted during the testing of the single channel system have been taken into consideration while designing the new system. The hardware was developed on printed circuit boards and measures were taken to minimise the system noise. The completed apparatus was tested in laboratory conditions with the results indicating an improvement in the performance, particularly the frequency response of the amplifiers under high gain conditions.

The next chapter deals with the designing of DAQ software for the three phase system. It also details the testing of the system in an industrial environment.

# CHAPTER 8: THREE PHASE DATA ACQUISITION SOFTWARE

## 8.1 Introduction

The three phase data acquisition software was based on a similar architecture to that of the single phase system, but was different in certain aspects. Firstly, the amount of data handled by the software was significantly larger compared to the previous application. A high sampling rate of 5 Ms/S would generate 400,000 samples (4x10000 samples) for each cycle of data (20ms). This has an implication on designing the software and recording the signals into a file and the associated file sizes. Secondly, the user interface had to be modified to accommodate the display of all three channels. Also, the acquisition on all 4 channels had to be initiated simultaneously with the live PD data displayed in the screen.

The software was developed on a modular basis from the early stages of the project development making it easier for any continual development or expansion. The basic architecture of the software remained fairly similar.

## 8.2 Data acquisition software

Figure 8.1 shows the front panel of the three phase DAQ system. The display section has been modified to a greater extent. There are three graphs on the front-panel. The top graph displays the reference sine wave signal along with the red phase PD data. The middle and bottom graphs display the yellow and blue phase PD data respectively.

The various controls provided to the user for controlling the acquisition process remains the same as the single channel system with some minor behavioural changes. The 'Acquire' function initiates the data acquisition process and acquires data over a period of 20ms and displays it on the screen.



Figure 8.1 Front panel of three phase data acquisition program

However, there is a modification in the behaviour of the 'Write' and 'Read' function. The 'Write' function is used to permanently record the data onto a disk. The data is stored in 4 separate files – one stores the reference signal and the remaining 3 store the respective PD data. Hence when the 'Write' function is initiated, the user is prompted for a file name 4 times in a consecutive manner. The data is stored in different files in order to study the PD signals on an individual basis. The software will eventually be modified to store all the data in one single file. Similarly, when the 'Read' function is initiated, the program prompts the user to select the path of 4 different files in a consecutive manner.

Another difference in this program is that the data retrieved is displayed on the same graphs as the data acquired. This is because a large amount of data is viewed on a small laptop screen. The user, at no point of time would need to use the 'Acquire' and 'Read' function simultaneously. Hence the provision of individual graphs provides no real advantage. A separate display was used in the single channel system only to verify if the data was being written and read in a correct format and is no longer needed.

It was necessary for the application to start the data acquisition process on all 4 channels at the same time. It was initially thought to provide a 'trigger' signal from the software to the 'PFI0' line on the DAQ cards to synchronise the acquisition. However, a simple hardware solution worked effectively. The NI-5102 DAQ card have an analogue trigger input called TRIG. The incoming reference signal (50 Hz sine wave) was connected to the TRIG input of both DAQ cards. The trigger source for both DAQ cards was set to TRIG input and the triggering was configured to 'high-hysteresis' triggering mode. In this mode a trigger is generated when a signal is greater than a set 'high value' with the hysteresis specified by a set 'low value'. The high value was set to 0 volts and the low value was set to -0.5 volts. Thus a trigger is generated, initiating the data acquisition every time the reference sine wave made a positive going zero cross. On completing the data acquisition of one complete cycle (20mS) it is transferred from the DAQ board memory to the host computer and displayed on the screen. The user can then review the data and store it.

The data is stored in the NI-HWS (Hardware Waveform Storage) format. It is a flexible file format that offers data compression, making it suitable to store large amounts of scientific data. Hence it is the recommended file format by National Instruments for storing multiple channels of waveform data.

### 8.3 On-site testing of 3-channel system

Due to the lack of high voltage facilities, most of the hardware testing was heavily dependent on testing the machines available at industrial sites. This had an adverse effect on the time required for prototype testing. It was operationally difficult and time consuming to acquire suitable permission for testing the high voltage machines on industrial sites. Again, with the co-operation of Dowding & Mills, a site-visit was arranged to another petroleum refinery plant in UK. The main purpose of this site-visit was to acquire data and test the performance of the three channel system. In the absence of high voltage test facilities it was thought that the best way of testing the new system would be to benchmark its performance against the existing proven StatorMonitor system. Hence the testing was carried out with both the systems. The data collected from both systems was stored and compared at a later stage. The complete test set-up for the three phase system is shown below in figure 8.2.

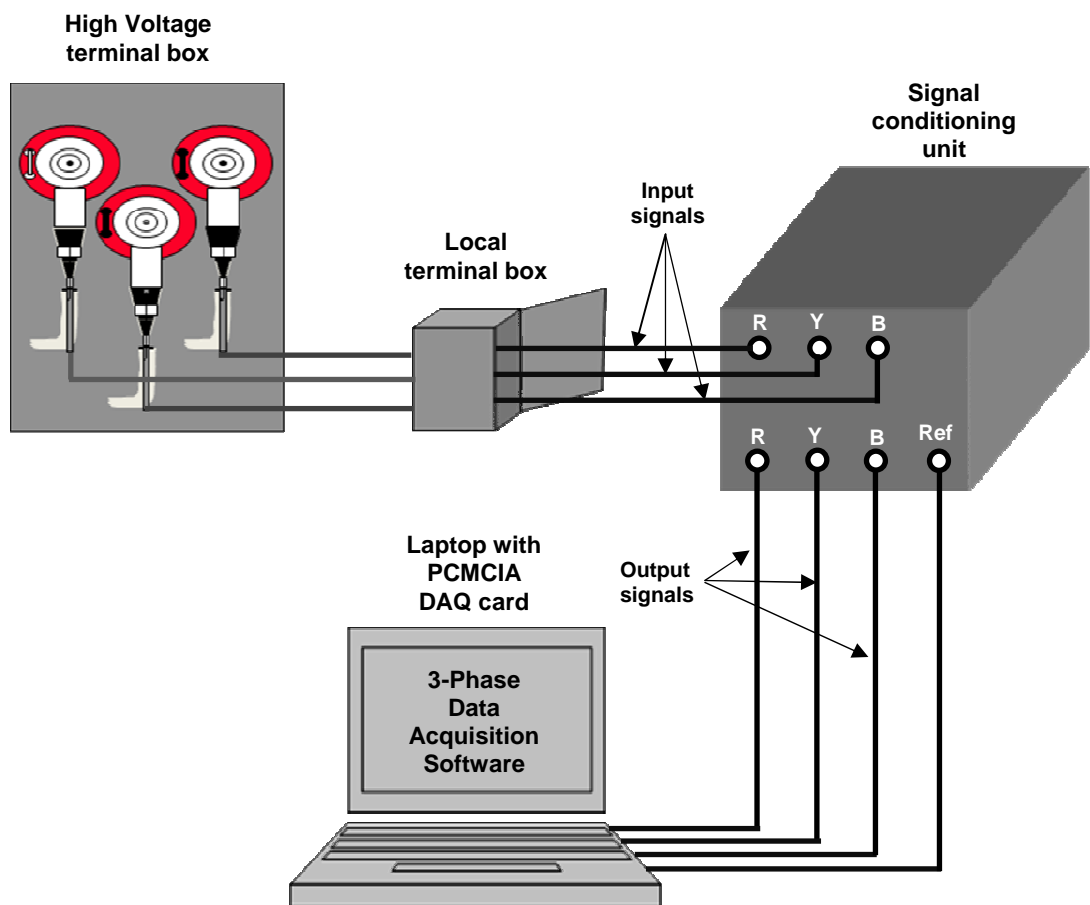


Figure 8.2 Test set-up for three phase data acquisition

### 8.3.1 Comparison of system performance

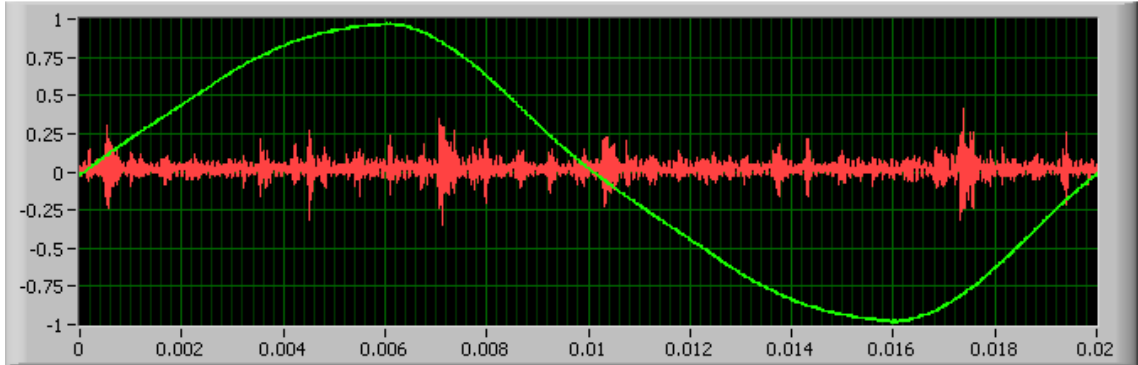
The site-visit provided an opportunity to acquire PD data from 3 different machines. A snapshot of three phases PD data acquired from one of the machines is shown in figure 8.1. In order to facilitate a comparison of the existing StatorMonitor system with the new three phase system data was acquired using both systems with the new software. Various sets of data were acquired with different gain settings and the acquisition was carried out simultaneously on all three phases with a sampling frequency of 5 Ms/S. Comparisons were made with data acquired from all three phases. However, for the sake of discussion only a single phase data has been presented here. The data on the remaining two phases show a similar performance.

Figure 8.3 (a) shows the data acquired from an 11KV generator unit 'M1'. The top graph shows the data acquired with the new three phase system with a gain setting of '1200'. The second graph shows the data acquired with the existing StatorMonitor system with the same gain setting for comparison. Although the signal in itself has some noise present in it, visual examination of the waveforms indicates that both signals look similar and have similar amplitudes. The gain settings were varied and various data sets were acquired. Figure 8.3 (b) shows the data gathered from the same machine with a gain setting of '2700'. Again, the data acquired from both systems show a good correlation.

Data was also acquired from another machine 'M2' which was an 11KV pump motor. Figure 8.4 (a) shows the data acquired with a gain setting of '310' and figure 8.4 (b) shows the data acquired with gain setting of '600'. The PD data acquired from this machine had a significant resemblance to the typical discharge pattern found in most rotating machines.

There are minor differences in waveforms acquired from both machines. The primary reason for this difference is that both hardware signal conditioning units have different amplifier and filter designs, hence the performance may differ slightly. Secondly, the data shown in the graphs belong to different cycles. During the process of data acquisition, data was first acquired using the new system followed by the StatorMonitor system.

New Three Phase System - M1 (Gain = 1200)



StatorMonitor System - M1 (Gain = 1200)

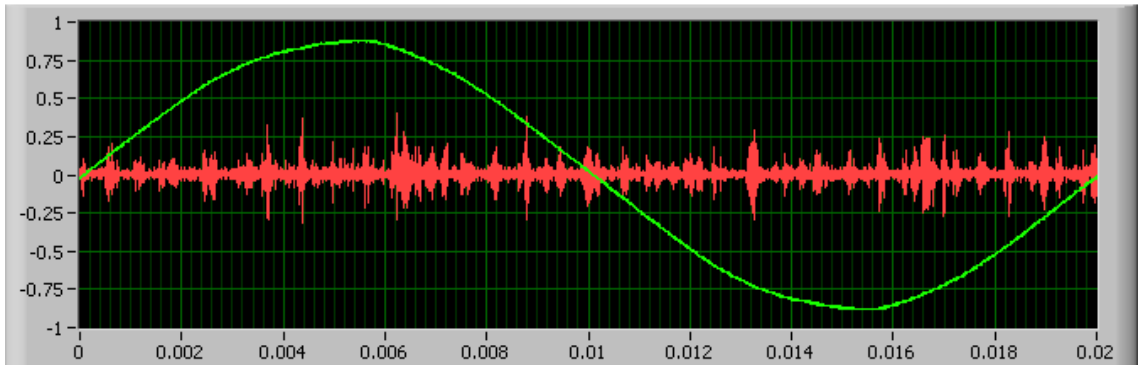
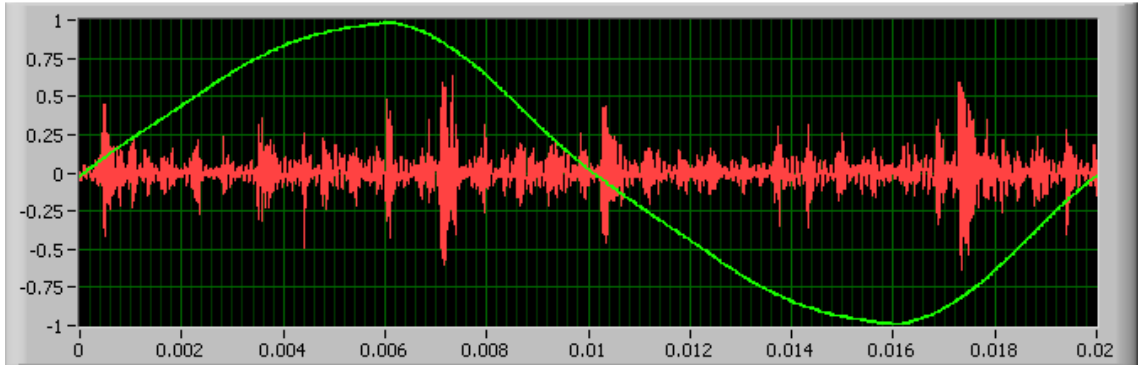


Figure 8.3 (a) PD data for machine M1 with gain of 1200

New Three Phase System - M1 (Gain = 2700)



StatorMonitor System - M1 (Gain = 2700)

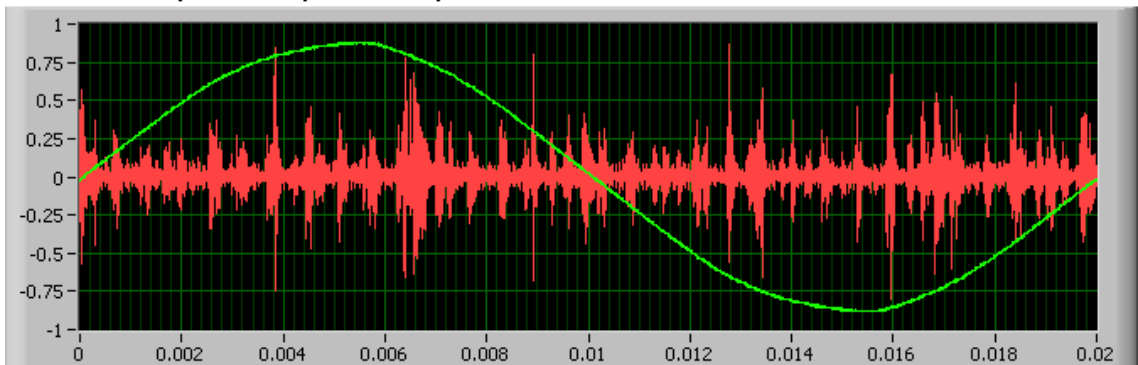
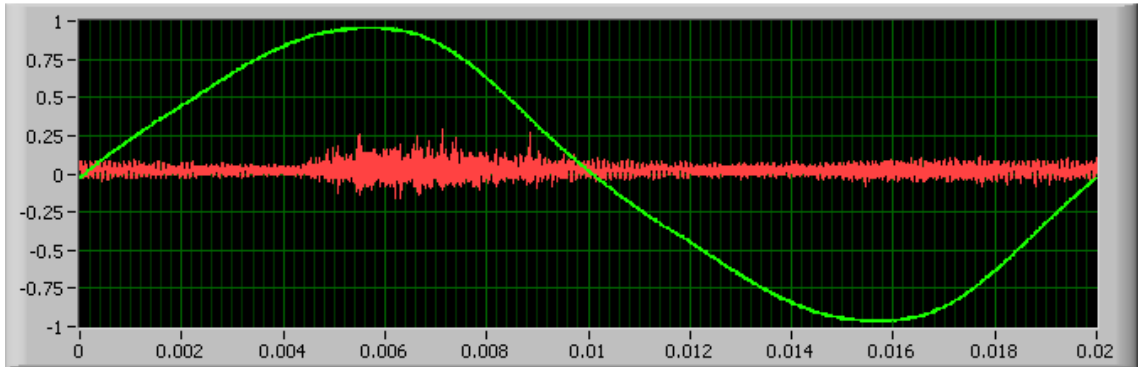


Figure 8.3 (b) PD data for machine M1 with gain of 2700

New Three Phase System - M2 (Gain = 310)



StatorMonitor System - M2 (Gain = 310)

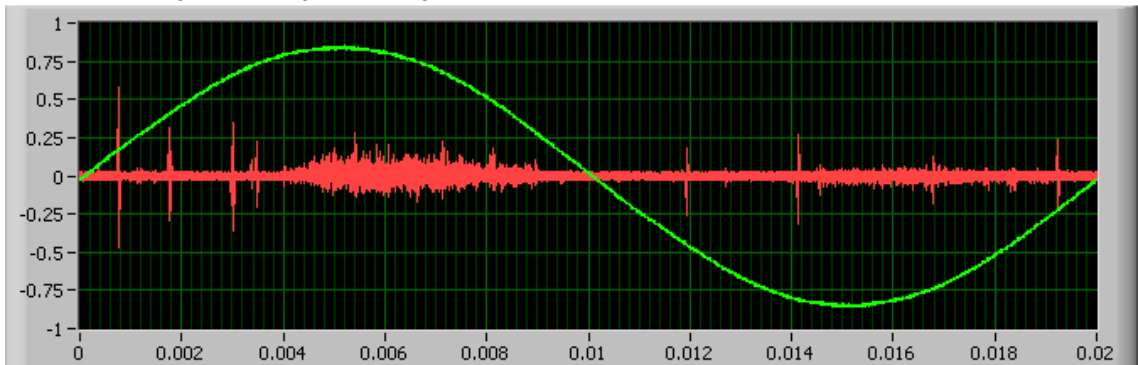
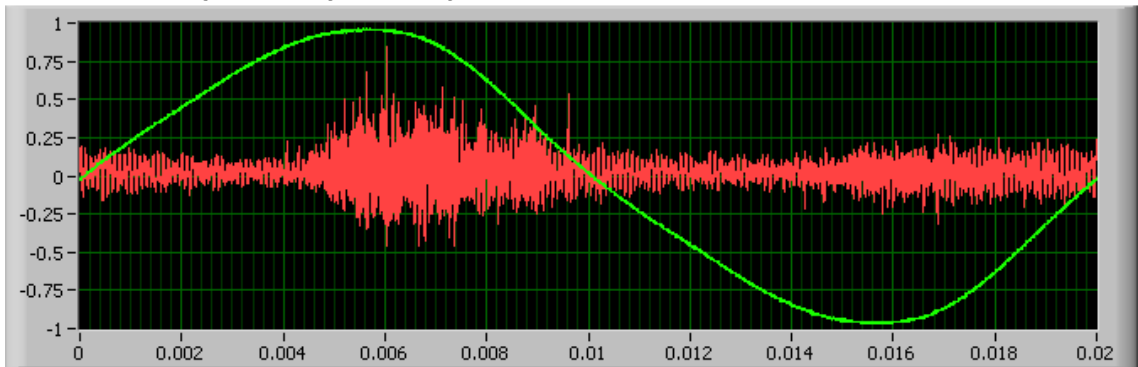


Figure 8.4 (a) PD data for machine M2 with gain of 310

New Three Phase System - M2 (Gain = 600)



StatorMonitor System - M2 (Gain = 600)

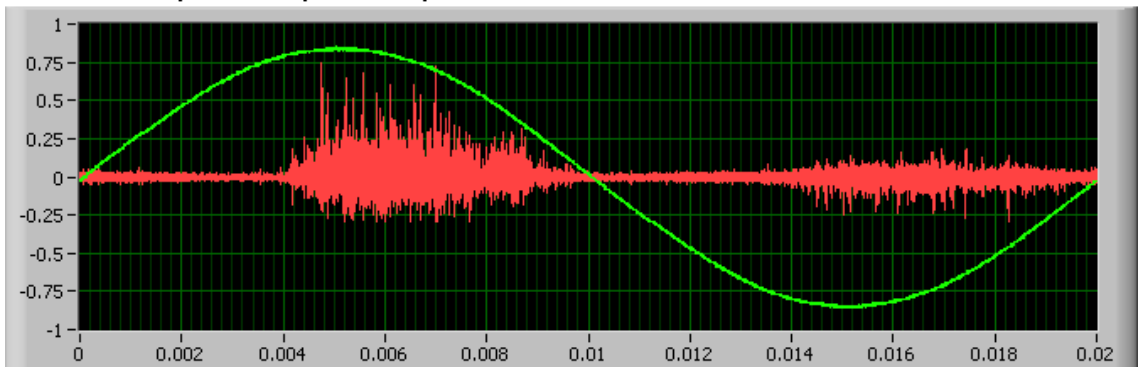


Figure 8.4 (b) PD data for machine M2 with gain of 600

Another method of comparing the performance was to analyse the data through the StatorMonitor analysis software. The analysis software was designed and developed by Dowding & Mills and is specifically intended for use with PD analysis of rotating machines. However, in order to analyse the data through this software, the raw PD data had to be provided in a certain format. The data acquired was stored in NI-HWS format and was not compatible with the existing software.

### **8.3.2 Continuous data acquisition**

The three-phase DAQ software described in the previous section was capable of acquiring three phase PD data only for 1 single cycle at a time. A single cycle of PD data does provide a brief snapshot of the PD activity, but it is not considered sufficient to carry out a detailed analysis. This is because PD is inherently random in nature. A PD pulse that appears in one cycle may not appear in another. Hence, in order to provide statistical robustness, the PD data is always acquired over a larger number of cycles. It also helps in the implementation of various noise-detection and elimination algorithms for a reliable analysis of PD.

The software was further modified to be able to acquire data from all three phases of the machine over a period of 50 cycles. The LabVIEW code for this program is given in Appendix A-5.4. The behaviour of 'Acquire' function remains the same as in previous program. Modifications were made to the 'Write' and 'Read' functions. On initiating the 'Write' function, the user is prompted to enter a file name 4 times in a consecutive manner i.e. first file prompt for reference signal followed by 3 prompts to store the PD data of each phase. The program then acquires and stores the PD data for 50 cycles (not necessarily consecutive) in an automatic manner, appending the data to the respective files every cycle. Similar changes were made to the 'Read' function to read the data for complete 50 cycles in a continuous manner. The number of cycles to 'Write' and 'Read' could be changed to '100' cycles or even more; but this will have a severe implication on the file size and will need to be addressed carefully.

Another site-visit was arranged to a steel manufacturing plant in the UK providing another opportunity to test the system. The modified software for continuous acquisition of 50 cycles was tested there on 2 different generators. A one cycle snapshot of three phase PD data acquired from one of the generators tested is shown in figure 8.5. The data was acquired with a gain setting of '600' with a sampling frequency of 5Ms/s.

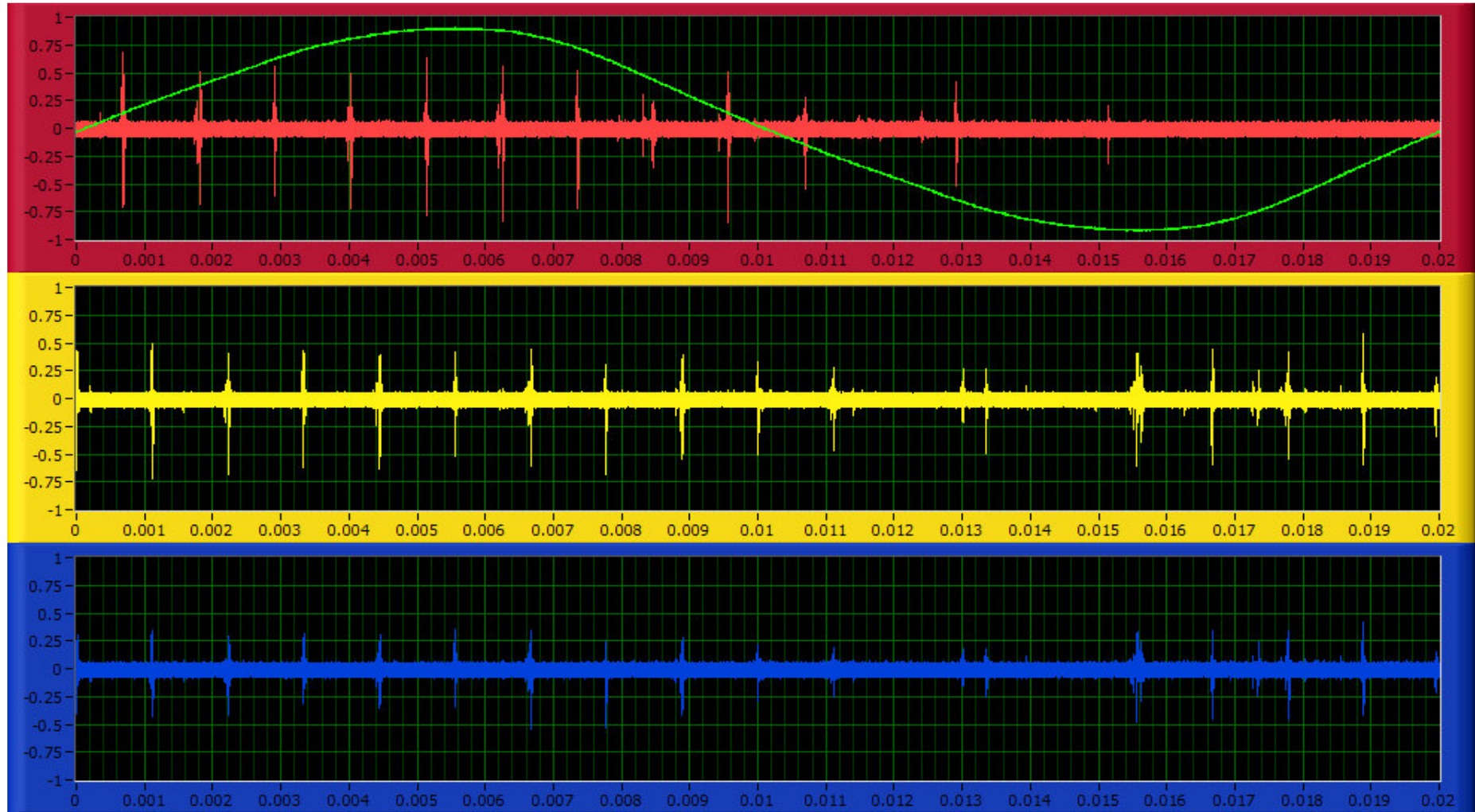


Figure 8.5 Single cycle PD data from a generator (Gain = 600)

### 8.3.3 PD and noise

The data acquired from the generator shown in figure 8.5 has a significant amount of noise superimposed over it. Such a classic pattern of noise is usually generated by some form of converter equipment. A converter contains switching elements like thyristors that switch on and off at regular intervals. This switching process generates high frequency pulses that propagate through the supply lines in the power system and can cause interference. The amplitude of such interference pulses is relatively higher compared to PD and tends to mask all PD data, making the PD detection process more intricate.

The interference pulses generated by converters are periodic in nature and usually occur in numbers like 12, 18, or 24 pulses per cycle. These pulses being high frequency in nature do not usually cause any interference in most of the equipment connected to the supply. But it can interfere to a great extent when measuring PD as shown in figure 8.5. The high frequency noise generated by convertor equipment has a similar frequency bandwidth to that of PD pulses. Hence these noise pulses cannot be eliminated by external hardware filters.

If these noise pulses are not detected and eliminated, then it can have a profound effect on the data analysis and a healthy machine could be misdiagnosed as a faulty one. Hence, PD analysis software should be able to overcome this problem by identifying the periodic noise pulses and omit them from analysis. The very fact that these noise pulses occur at regular intervals opens up many avenues for detecting and eliminating them. Statistical techniques can be used to locate these pulses in the acquired data. These pulses can then be 'windowed' out by deciding an appropriate width for the window. It is obvious that any PD data present within that window will be lost. However, this is not a cause of concern as the PD data located within that window was already masked due to high noise pulse. Such techniques for noise elimination and data analysis will be investigated at a later stage of this project and will not be presented here.

### 8.3.4 Data Compression

Acquiring and storing raw PD data requires a significant amount of memory. The file sizes of PD data acquired using the single channel system and the three- channel monitoring system were studied to check the memory requirements for file storage. The single channel system stores the reference signal and one phase data for one cycle in two individual files in the NI-HWS file format. The data sampling rate was 5 Ms/s. The combined memory required to store both these files was approximately '1.6 MB' which is considered large enough for just one cycle of PD data.

The three-channel monitoring system acquires the data with the same sampling frequency of 5 Ms/s, but the data was acquired on 4 channels (i.e. 1 reference + 3 PD phase data) over a period of 50 cycles. The data acquired from each channel for 50 cycles was stored in individual files and each of these files required a memory of approximately '20MB'. This means a combined memory of approximately '80 MB' will be required to store the raw PD data for just 1 test on 1 machine. This memory requirement is considered too large for a practical PD measuring system. A lot of PD analysis is dependant on the trending of PD activity requiring storing historical PD data for over a period of a few years impinging an enormous demand on memory required to store this data. Hence, there is a need for some method of data compression for storing PD data.

Another factor to be considered for data compression was to store the PD data in a format that could be used with the existing StatorMonitor analysis software. This would be useful to benchmark the system performance. The existing data storage format used by the analysis software had to be studied in order to establish the compression requirements and data formatting.

The existing analysis software reads the data that is stored in a binary format. One of the most common methods of data storage in LabVIEW is the .lvm format. The .lvm file format is a tab separated text file format which stores the ASCII values. This makes it easy to parse, and easy to read in a spreadsheet program like Microsoft Excel or a text editor like Notepad. However, the file format is not designed for high performance or very large data sets. A binary file format such as HDF5 is used for very large data sets as their disc footprint is smaller compared to ASCII format. The NI-HWS file format is based on HDF5 file format and specifically designed for use with modular instruments developed by National Instruments. Hence the NI-HWS format was used to store the site testing data. But, the NI-HWS file format was also considered incompatible as the existing software reads the data in a particular order in binary format.

The analysis software reads data values from a 2D array and the stored data has to be in a binary format. The array format is shown in table 8.1. The resolution of data is '1024' points per cycle and 100 cycles of data are required to run the analysis routine.

As the software reads '1024' points per cycle, the existing data resolution of 100,000 points per cycle will have to be reduced to 1024 points by means of a data compression technique without losing any important information. This meant a reduction of data resolution by a factor of 98. An algorithm was developed for performing the data compression. The raw PD data was divided into small windows of 98 elements and the highest value in the data set preserved. The LabVIEW code from this program is given in Appendix A-5.5.

**Table 8.1 Data storage format for StatorMonitor PD analysis software**

	Reference (sine wave)	PD Data (Red phase)	PD Data (Yellow phase)	PD Data (Blue phase)
<b>Cycle 1</b>	1	1	1	1
	2	2	2	2
	1024	1024	1024	1024
<b>Cycle 2</b>	1	1	1	1
	2	2	2	2
	1024	1024	1024	1024
<b>Cycle 100</b>	1	1	1	1
	2	2	2	2
	1024	1024	1024	1024

The effect of data compression is shown in figure 8.6. The top graph shows the data with full resolution and the bottom graph shows the reduced resolution graph. The

reduction in resolution of course meant significant loss of PD data. However, the highest peaks are the most important and have been preserved. Although, a frequency domain analysis would be impossible after such a compression, it can be seen that the overall discharge envelope has been reasonably preserved. There was a significant reduction in the file size requirements. The overall file size was reduced from '80 MB' to '0.8 MB for 50 cycles of PD data. This means the file size for 100 cycles would be around '1.6 MB' and is considered to be reasonably practicable.

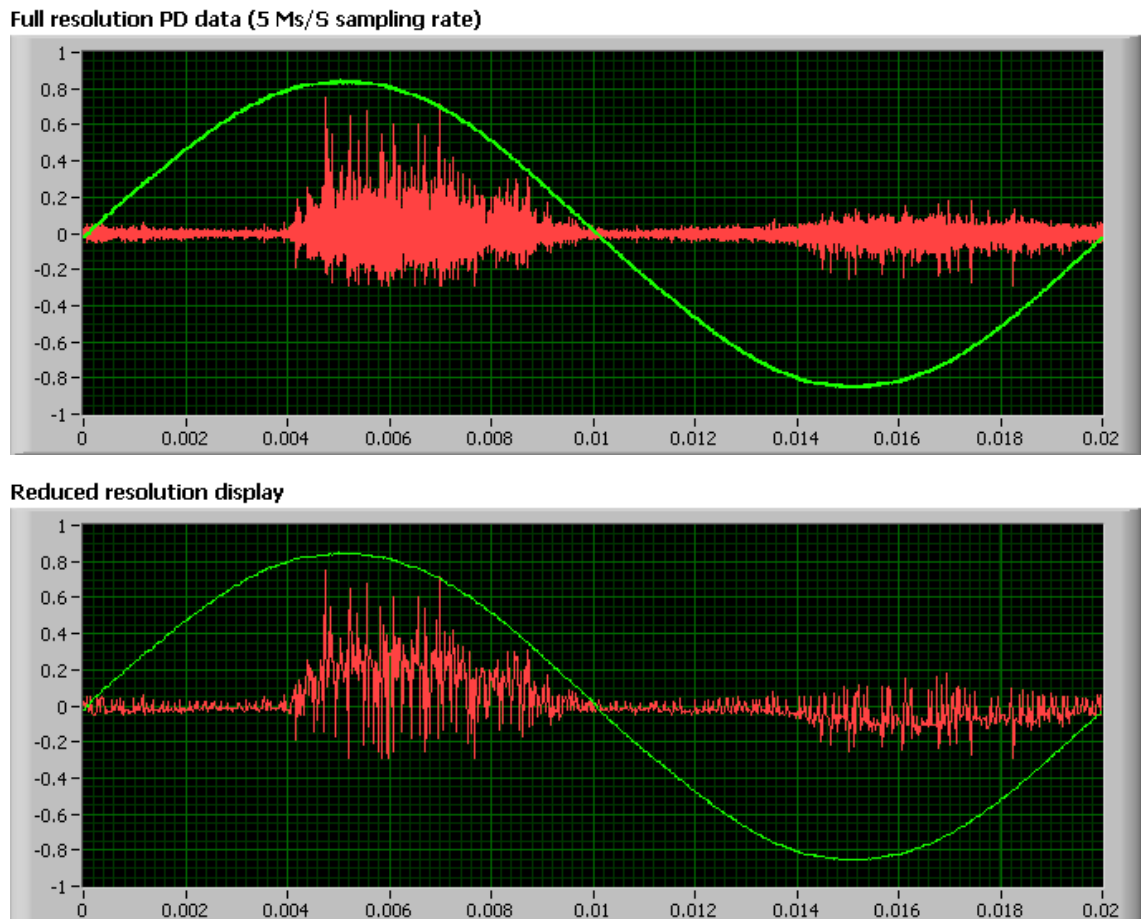


**Figure 8.6 Effect of data compression of raw PD data**

## **8.4 USB data acquisition system**

The use of 2 DAQ cards with a PCMCIA bus interface was not considered to be the best option for future development as the PCMCIA format is becoming outdated. The availability of laptop computers with 2 PCMCIA slots is sparse. Hence, various market available DAQ cards were researched with alternative interface options. A USB interface was thought to be the most suitable option as laptops with three to four USB ports are readily available in the market.

'Handyscope-HS4' by Tie-pie' engineering is a four channel simultaneous sampling USB DAQ card with a maximum sampling frequency up to 5 Ms/S and has an on-board memory of 512 MB. It is relatively inexpensive compared to some of the competitor's products and was thought to be a viable option. The device was equipped with suitable drivers for LabVIEW software interface. An attempt was made to develop another DAQ program using the new USB DAQ card. However, the development proved to be time consuming due to certain issues with the way the device drivers interfaced with LabVIEW software. The device drivers also did not provide sufficient options and control for triggering signals. Hence, the Handyscope-HS4 was not considered to be the preferred option.

It was best considered to avoid 3<sup>rd</sup> party drivers for LabVIEW interface. It was decided to choose a DAQ card provided by National Instruments for its excellent device driver interface and ease of programming. The 'NI –USB 5132' DAQ was chosen for the application. The DAQ card has 2 simultaneously sampled channels with a resolution of 8-bits and is capable of sampling speeds up to 50 Ms/S. This means two DAQ cards will have to be used for the complete three channel system and will need 2 USB ports on the laptop computer. This is not considered as an issue as most laptops have three four USB ports. The DAQ cards also provide an option for synchronisation through the 'PFI1' connection.

The three phase DAQ software was modified for using the USB DAQ devices. Due to the types of synchronisation options available with this DAQ card, a software based synchronising technique was adopted. Data compression was also incorporated in the program and changes were made to the data storage format. This change was necessary in order to use the StatorMonitor software for analysis and will help to assess the performance of the system. The front panel of the new USB DAQ software is shown in figure 8.7. The program description and LabVIEW code is given in Appendix A-5.6.

The three channel hardware along with the newly developed USB DAQ software is now awaiting field trials for performance assessment.

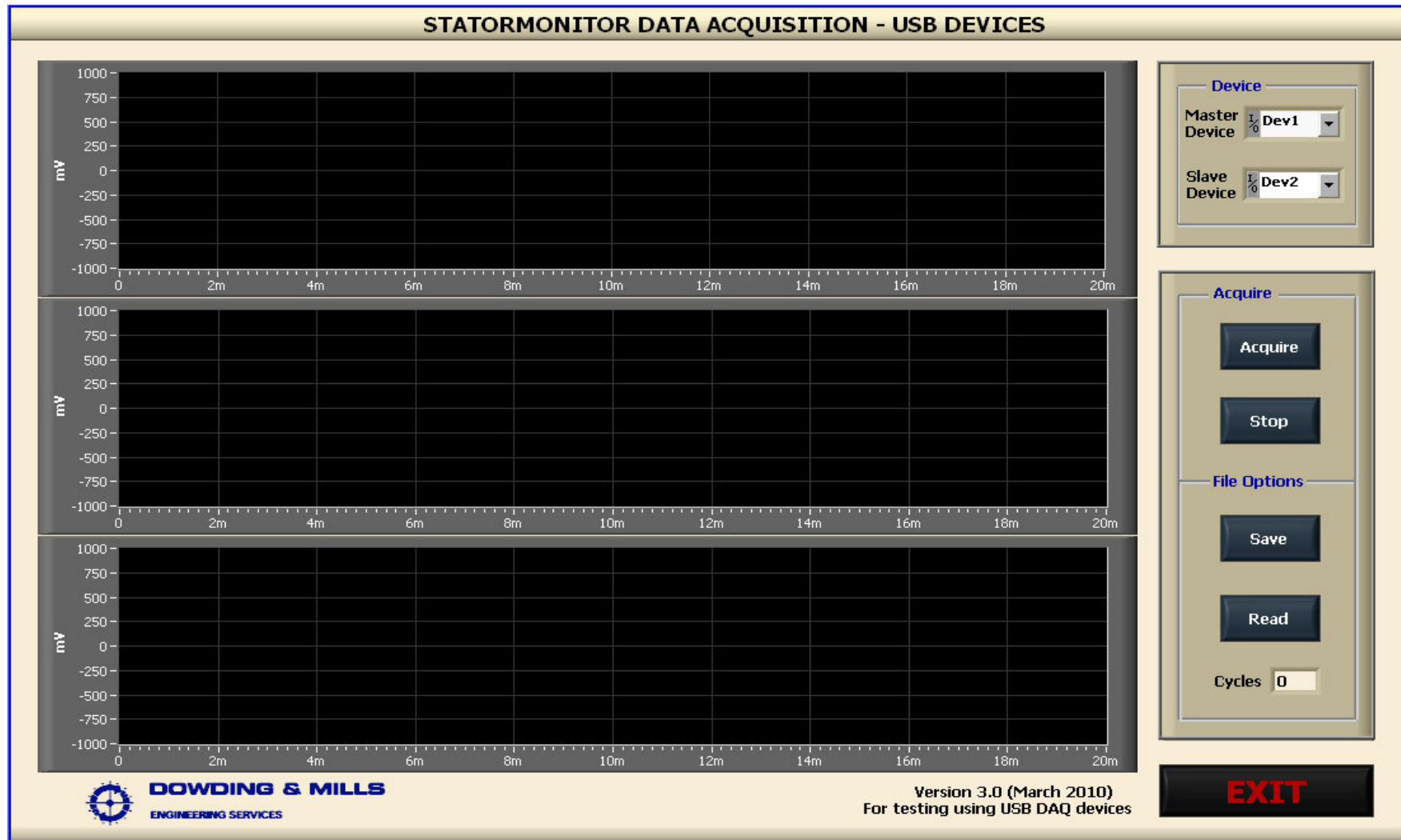


Figure 8.7 Front panel of three phase USB DAQ system

## **8.5 Summary**

DAQ software developed for a three channel prototype system was capable of simultaneous acquisition of three phase PD data. The software along with the associated hardware was tested in an industrial environment. Modifications were made to accommodate continuous acquisition of PD data over a period of 50 cycles. The performance of the system was compared with the existing StatorMonitor system with various gain setting and was found to be satisfactory. The PCMCIA interface for DAQ systems is rapidly becoming obsolete. Hence a new DAQ system with a USB interface was developed. The program was also modified to maintain its compatibility with the StatorMonitor software.

The new system will need to be tested on actual machines to assess the performance.

## CHAPTER 9: DISCUSSION

The data acquisition hardware for acquiring and storing PD pulses form an important part of any PD instrumentation system. Equally important is software that is capable of filtering noise, provides tools to view the PD data in different forms and allows statistical signal processing to aid the analysis process. Another important feature of PD analysis software is the capability to display and analyse historical PD data which helps in trending the PD activity over time. Some of these features that are desired from PD instrumentation software are discussed here. These features will be considered in future during software development.

### 9.1 Software Development

The software developed during the course of this project is capable of acquiring real PD data and storing it onto disk with limited options for displaying data. However, this area of software development will need a significant amount of work and research to be carried out for developing a complete PD detection and analysis system. The work needs to be considered with three different areas:

- a) Noise detection and filtering
- b) PD Data display methods
- c) PD Analysis techniques

#### 9.1.1 Noise detection and filtering

The PD data is often blurred with noise and external interference making it difficult to discriminate between noise pulses and the PD pulses. Measures can be taken reduce the voltage and current noise by selecting low-noise op-amps and by hardware design. However, in some cases where the external noise level is high compared to the PD, the entire PD signal can be lost. This is because the A/D converter has a fixed resolution and the extremely small PD pulses may be quantised into the lowest level. The noise could be arising from two sources i.e. thermal or external. The thermal noise that arises due to the amplifiers and the detection impedances are relatively insignificant compared to the noise from external sources <sup>(132)</sup>.

The external noise characteristics can be categorised into three types <sup>(133)</sup>:

- Continuous noise signals caused by communication networks
- Pulse-shaped signals occurring at a nearly constant phase angle caused by phase angle controls (thyristor switching)
- Non-continuous pulse shaped signals caused by corona or switching in the high voltage system.

The repetitive type pulses that occur due to thyristor switching are relatively easier to be detected and filtered. A rudimentary scheme was described in section 8.3.3. A noise gating technique can be used for detecting such repetitive pulses. However the other types of interference can be difficult to identify. The application of adaptive digital signal filtering <sup>(134)</sup> and neural networks <sup>(133, 135)</sup> is becoming increasingly popular in this area. Kopf and Feser <sup>(136)</sup> have proposed some digital methods for off-line and on-line filtering of noise from PD. Various authors have also proposed the use of 'Wavelet Analysis' for de-noising of PD signals <sup>(137, 138)</sup> and have shown promising results. These various digital techniques can be evaluated and a suitable technique can be developed for eliminating / reducing noise from the PD signal.

### **9.1.2 PD data display methods**

The visualisation of PD data is one of the important aspects of the PD analysis process as it can help to detect noise and to estimate the severity of the discharges. The fact that the data has been recorded in the digital domain provides the opportunity to process the data and display it using various methods that can provide more information and aid the analysis process. Several graphical representations of PD have been established within the industry.

A 'pulse height distribution' display can be used to determine the repetition rates of various discharge amplitudes as shown in figure 9.1. The 'x' axis of the graph shown in figure 9.1 represents the increasing amplitude of PD pulses. The 'y' axis represents the number of pulses occurring in a specified time or data set (e.g. 100 cycles). This graph is useful to visualise the repetition rates of various discharge amplitudes. It goes without saying that the high amplitude discharges with high repetition rates will be detrimental to the insulation. However, one of the major disadvantages of this technique is that the phase information of discharge pulses is completely lost.

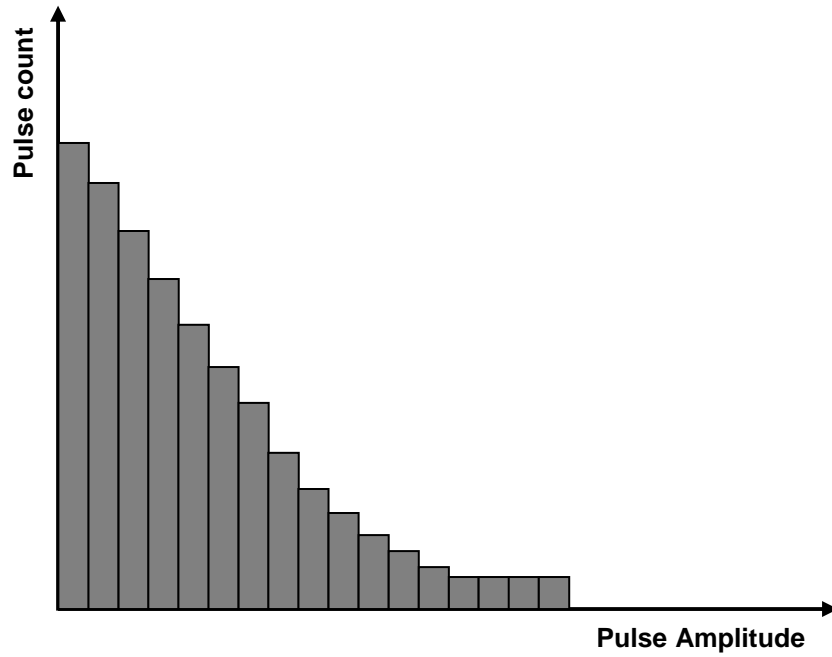


**Figure 9.1 Pulse height distribution graph**

Another popular method to display PD is the phase resolved PD pattern. Such a phase resolved PD pattern (also called ' $\phi$ -q-n' pattern) is shown in figure 9.2.

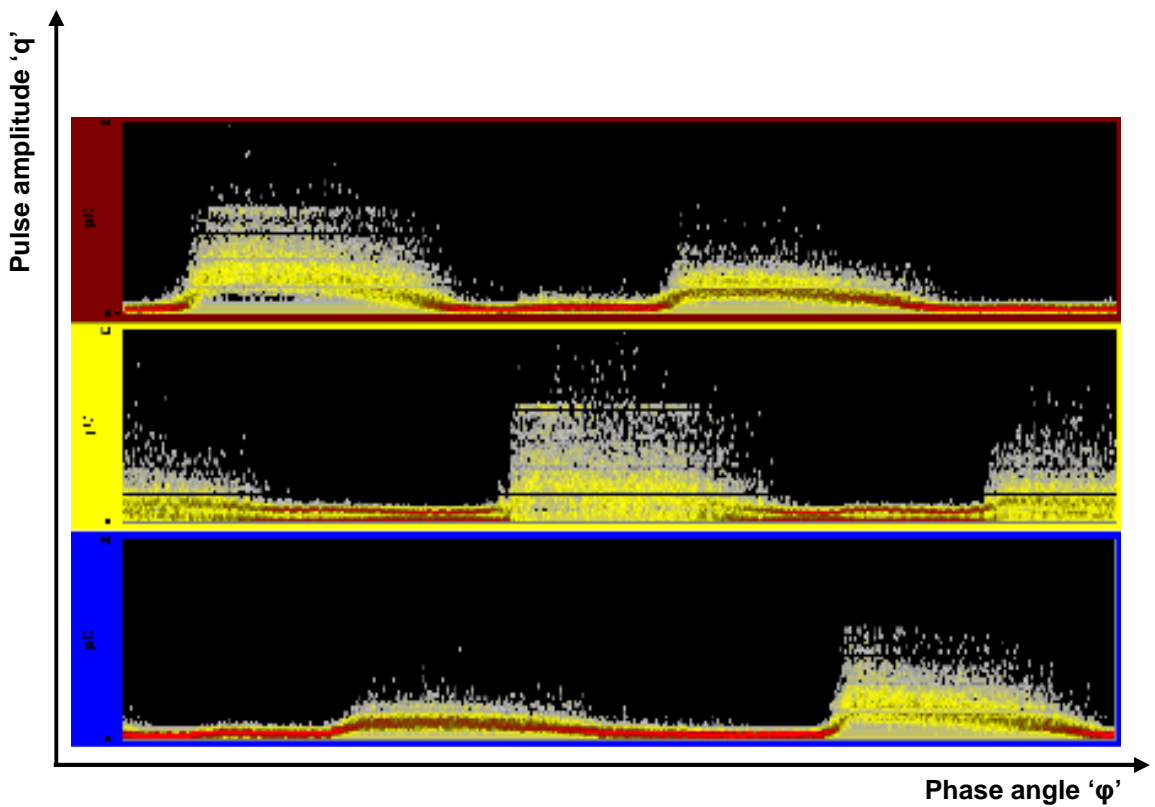


**Figure 9.2 ' $\phi$ -q-n' pattern display of PD data**

The phase voltage is divided into a small number of windows. Discharge parameters like the apparent discharge magnitude 'q' and the phase angle 'φ' of individual pulses within that window can be calculated and stored using a software program. The computation can be performed on the complete data (e.g. 100 cycles) and the corresponding repetition rate 'n' for each phase window can be calculated and stored<sup>(139)</sup>. Now these three parameters can be viewed on a 3-D plot and is often referred as the 'φ-q-n' pattern. Alternatively, it can also be plotted on a 2-D with colour-coding of PD pulses as the 3<sup>rd</sup> axis.

Referring figure 9.2, each individual PD pulse is represented by a dot at its corresponding amplitude on 'y' axis and its corresponding phase position on 'x' axis. The repetition rate 'n' of pulse is coded with different colours with red being a high repetition rate and grey being a low repetition rate. The 'φ-q-n' pattern indicates the predominance of PD pulses in '+ve' and '-ve' cycle and this can be used for detecting various sources of discharge activity<sup>(139)</sup>. Statistical parameters like 'Skewness' and 'Kurtosis' can be calculated which is useful for determining the characteristics of PD activity<sup>(140)</sup>. Hence, as this type of PD display gives vast amounts of information for analysis it is popularly used for PD analysis of rotating machines<sup>(141, 142)</sup>. The development of a software program capable of displaying phase resolved PD patterns will prove useful for data analysis.

### 9.1.3 PD Analysis techniques

Visual analysis of PD data still remains the most widely used method in the field of PD monitoring. Unfortunately, it needs a considerable amount of experience and expertise in order to draw a meaningful interpretation from the PD signals. It is also well known that the absolute analysis of PD cannot be considered as a reliable indicator of insulation condition due to the following factors<sup>(143)</sup>:

- *PD calibration problems*

The conventional PD calibration technique is not applicable to rotating machines as the PD is not measured at the actual PD site, but at the terminals of the winding. The stator winding of every machine is different and can have a different effect on PD pulse as they travel through the winding. Hence every machine will need individual calibration where a pulse of known amplitude is injected and the response is measured. This is impracticable in most conditions where on-line measurement is a requirement.

- *PD location*

The location of PD has a direct effect on the magnitude detected at the machine terminals. It is known that the PD pulse attenuates as it travels through the stator winding. Hence it is possible that a smaller amplitude PD may be actually arising from a larger PD located further away from the terminals and vice versa.

- *PD detector*

Depending on the bandwidth of the PD detector, a different response may be produced for the same PD event. During PD measurement the frequency spectrum of the stator winding and the frequency spectrum of the PD detector are combined together and the resultant PD spectrum can affect the magnitude of PD pulse.

- *PD types*

Different types of discharges occur at different locations in a machine. The potential for each type of discharge to cause harm to the insulation is different. For example a same magnitude PD occurring in slot region and end-winding region can affect the insulation differently. Hence it is important to consider the type of discharge mechanism along with its magnitude rather than analysing PD solely on the basis of detected magnitude.

- *Differences among machines and measurement conditions*

Machines from various manufacturers differ significantly in terms of construction, design, insulation systems, etc. Even if the machines have the same manufacturer, there will be differences in installation, operation and maintenance and this may result in a different degree of insulation degradation for the same machine. Additionally, other factors like temperature, pressure, humidity, etc can have an effect on PD measurement.

Industrial experience indicates that some machines have high PD magnitudes that do not change over a significant period of time and can sustain them for years without causing any further damage to the insulation. Some machines can have low magnitudes of PD that increases over a period of time indicating the presence of a failure mechanism affecting the insulation.

All the above factors can affect the magnitude of PD measured. Hence the analysis which is based only on PD magnitude cannot be considered reliable.

In order to make a more robust analysis, the PD activity can be trended over a period of time to assess if any insulation degradation mechanisms are causing sustained damage to the insulation <sup>(143,152)</sup>. This involves repeated data collection with a reasonable time gap between each measurement. The process of insulation degradation is a slow process; hence the time gap between each measurement should be sufficiently high for the degrading mechanism to cause a detectable increase in the PD activity which is usually in the range of few months. A typical process cycle used for PD data analysis is shown in figure 9.3.

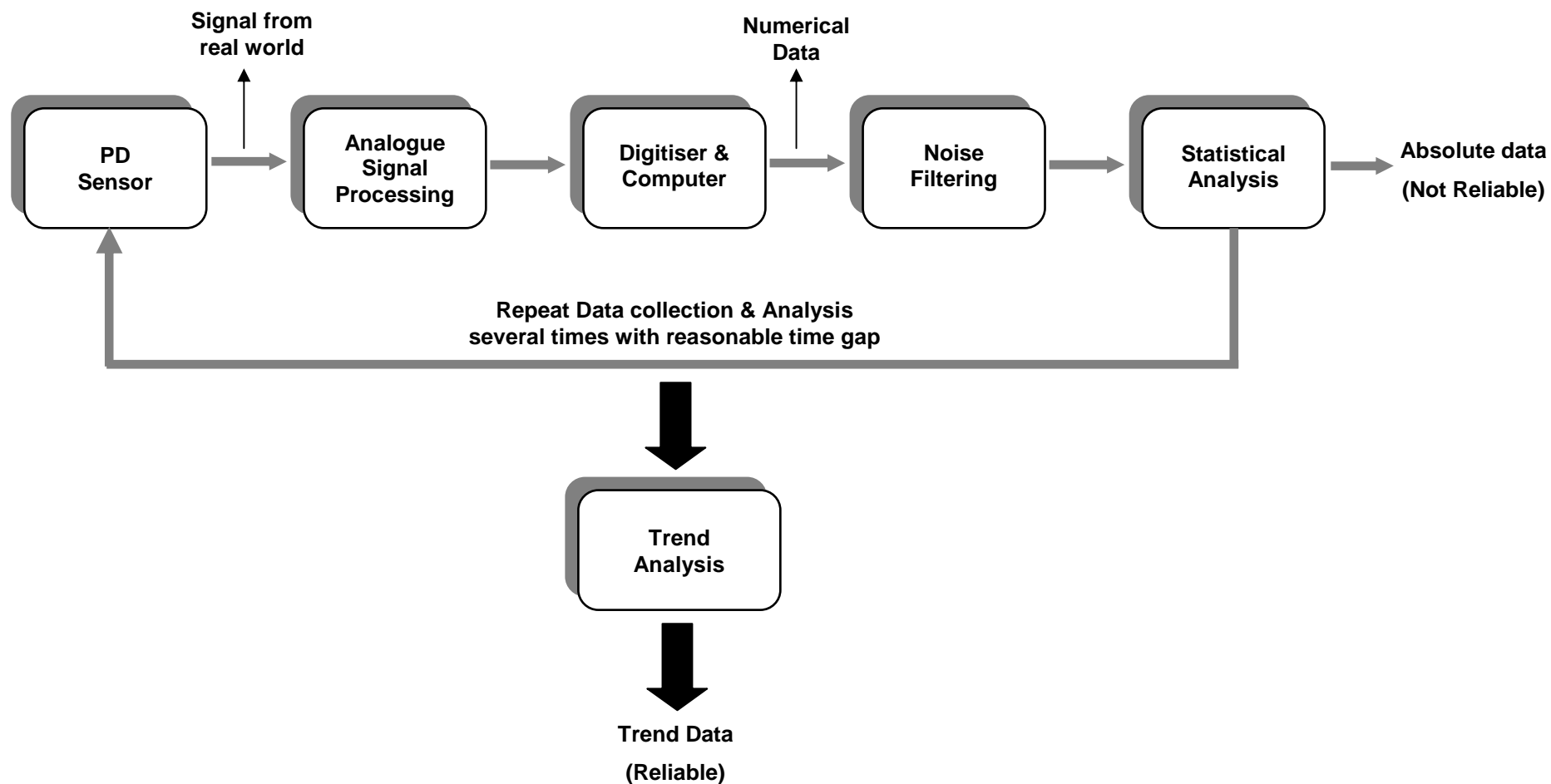


Figure 9.3 Typical process diagram for PD data analysis

The application of neural network for the PD pattern recognition and analysis has been demonstrated by many researchers <sup>(147, 148, 149)</sup> and forms the basis of an expert PD system.

Neural network acts as a classifier for the data fed to it. The capability of a neural network for classifying this data is heavily dependent on the PD test data that was initially used to train the network. Hence, in order to train a neural network it is first necessary to develop a 'defect database'. The defect database will contain a library of defects, failure mechanisms and the corresponding signal patterns. Post training, the neural network will be capable of co-relating a PD pattern to corresponding defect. This forms the basis of an expert PD system. If the system comes across a PD signature which is entirely new, then it can be added to the database for future reference effectively making the system self-learning. A block level representation of such a system is given in figure 9.4.

This of course is a very simplistic view of an expert system and the development of a practical system on similar lines will need a significant amount of research and experimentation.

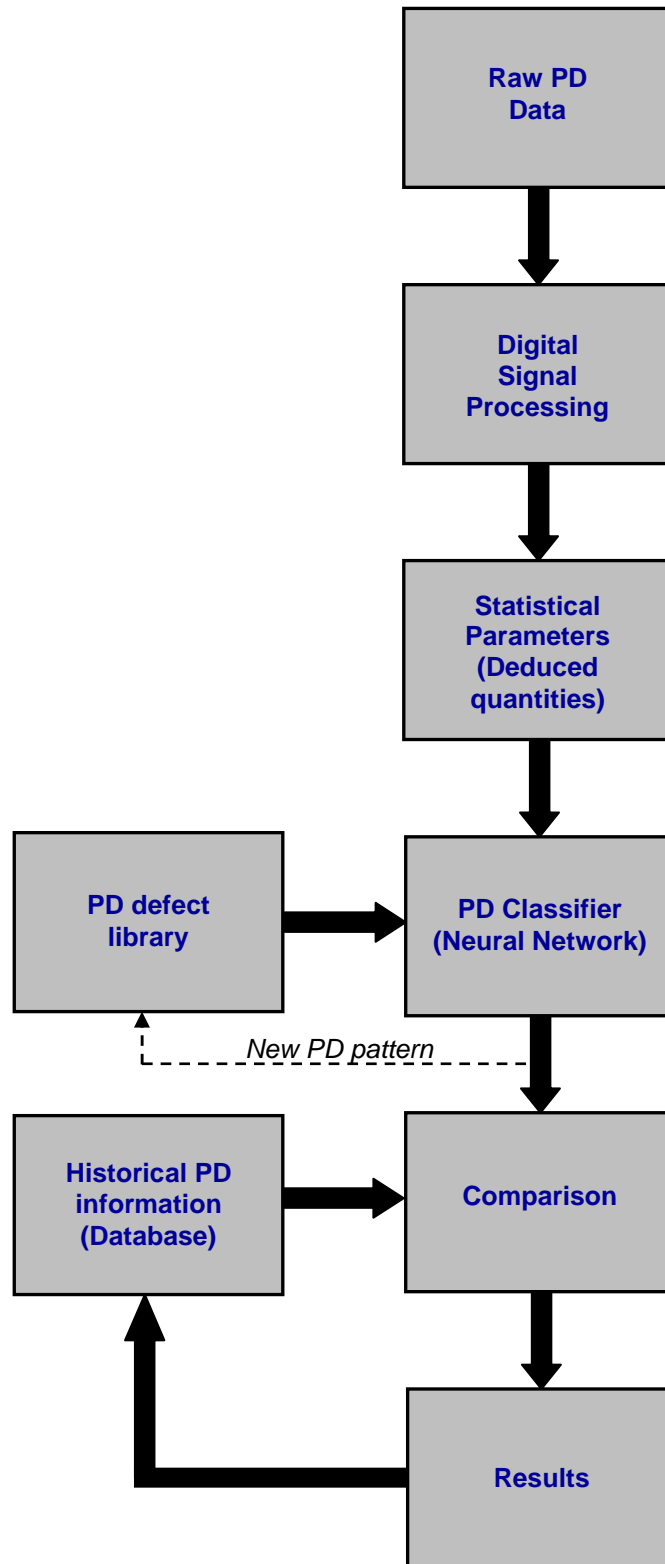


Figure 9.4 Block diagram of an expert PD system

## 9.2 Remote Monitoring System

Most often PD is monitored on a periodic basis as the insulation degradation is a slow process. Continuous monitoring systems are available on the market, but have not been popular, particularly in the North Sea Oil Industry, due to the occurrence of false alarms. False alarms usually occur when a random noise pulse crosses the threshold set by the user for detecting PD. More recently there has been a demand for systems capable of monitoring PD remotely. Remote monitoring of PD has several advantages:

- The problem caused due to a false alarm can be effectively eliminated. If any of the detected pulses exceeds the set threshold, the remote monitoring system can send an alert message to a local host computer or to any computer connected via internet / intranet. An expert can then log on to the remote monitoring unit through the same channel and view the PD data remotely and make an informed decision.
- It can have a significant impact on the cost of maintenance. Presently, a trained personnel travels to the site along with a PD monitoring unit on a periodic basis. This involves substantial costs in travel for personnel, transport of equipment and the man-hours required to test every machine. These problems are particularly acute for the offshore industry where personnel travel costs are significant. If a remote monitoring system is available then the data collection and analysis can be done remotely on an onshore site; eliminating the need for the personnel to travel.
- When the insulation degradation process starts to accelerate, it is required to reduce the monitoring intervals in order to establish the rate of degradation so that a corrective action can be planned. Remote monitoring can lead to efficient maintenance as the machine can be monitored as often as required without significant costs.

Remote monitoring systems are now commercially available from a few manufacturers. The ICM<sup>®</sup> monitor by Power Diagnostix Systems GmbH and PD Check/Scope from Techimp systems are some examples of remote monitoring systems. A generalised scheme of a remote PD monitoring system is shown in figure 9.5.

The PD data from each machine is recorded by individual data collectors at desired frequency intervals. The data collectors usually have basic signal processing and analysis capabilities. The data collectors are connected to a local server through a fibre optic TCP/IP plant intranet (LAN) system. The local server will have some form of PD management software that stores PD data from all machines and handle alarm flags if

any. A PD expert located anywhere in the world can connect through any remote computer to this local server via internet and access the PD data for detailed analysis.

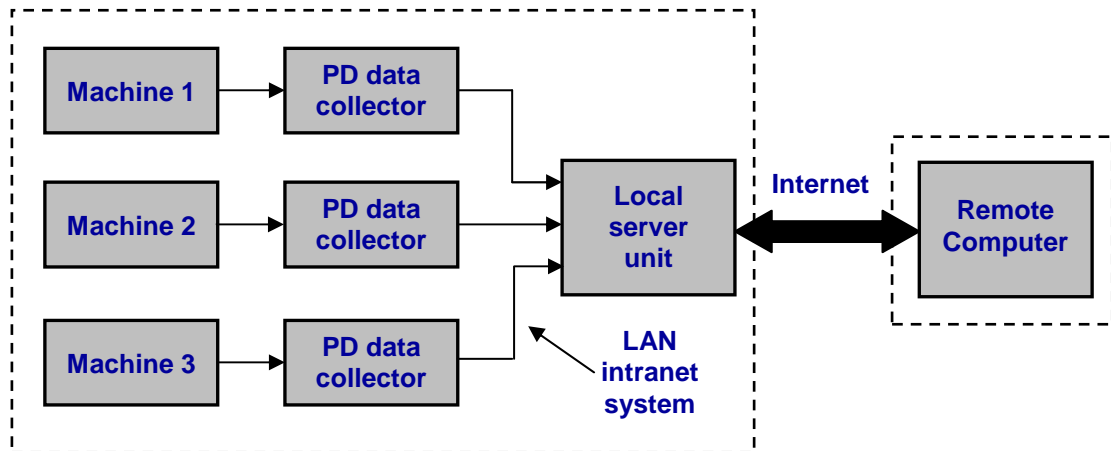


**Figure 9.5 Generalised scheme of a remote monitoring system**

### 9.3 Summary

Any PD monitoring system should have software that is capable of providing options for noise filtering and displaying PD data in different forms that can aid in PD analysis. Some of the standard techniques used for PD data analysis like the ‘pulse height analysis’ and ‘phase resolved PD analysis’ have been discussed. An absolute measurement of PD is often considered unreliable due to various factors. The trending of PD data over a period of time provides a more robust analysis. Hence the software should be capable of storing historical PD in a systematic manner.

Neural networks can be used for developing an expert PD system. Remote monitoring system provides several advantages over the conventional PD monitoring systems and these factors will have to be considered for future development.

# CHAPTER 10: CONCLUSIONS AND FUTURE WORK

## 10.1 Conclusions

The research project described in this thesis is the result of work undertaken through the 'Knowledge Transfer Program' (KTP) scheme in association with 'The Robert Gordon University' as the academic partner and 'Dowding & Mills' as the company based partner.

The on-line condition monitoring of rotating machines is given paramount importance, particularly in industries such as Oil and Gas where the financial implications of machine shut-down is very high. The project work was directed towards the on-line condition monitoring of high voltage rotating machines by detection of partial discharges. Monitoring of partial discharge activity in high voltage rotating machines is considered to be an important tool for maintaining the insulation health of the motor.

The degradation of HV stator insulation occurs due to operating stresses that can be classified into mechanical, thermal, electrical and environmental. Chapter 2 outlines the cause and effect of each of these stresses and can lead to the generation of PDs. In a rotating machine different types of discharges can occur either in the slot region or in the endwinding region and each have their own characteristics. When a PD event occurs, it manifests itself in different forms i.e. heat, light, noise, electromagnetic pulse, current pulse, etc. Accordingly they can be detected using an appropriate PD sensor. The electrical detection of PD using Rogowski coils provides a completely non-intrusive method and was investigated in this work.

Initially, a single channel prototype hardware was designed along with a basic software (using LabVIEW) for detecting and storing PD pulses from a single phase of a machine. The field-testing of this unit provided an opportunity to acquire real PD data in an industrial environment. PD data is often superimposed with noise from extraneous sources making it difficult to analyse the PD pattern. This was practically experienced during this visit. Two algorithms for filtering noise were developed as discussed in chapter 6. It was found that the 'amplitude based' filtering was not really suitable; however the frequency based filtering did show some encouraging results.

In the next stage of prototype development a complete three channel data acquisition system was developed along with the associated software required to store PD data from all three channels. The performance of this system was benchmarked against the

existing StatorMonitor® system which is an already proven system in the industry; but the design is becoming obsolete. The performance of the new three channel system was found to be satisfactory.

The software was further modified for acquiring PD data continuously for 50 cycles. This is necessary for the statistical processing of PD signals. As the data was sampled with a high sampling rate of 5 Ms/S, the resultant file size for a complete data set for 50 cycles was very high and impracticable. A data compression technique was developed to reduce the file size while preserving the important PD data.

The DAQ card used for the design was interfaced with a laptop computer using the PCMCIA bus which is now obsolete. A new DAQ program has been developed for use with USB DAQ cards. The program was also modified to make the PD storage format compatible to the existing StatorMonitor analysis software which will again help to benchmark the performance of the new system.

Although the progress of the project was hampered due to the lack of high voltage test-facilities, the opportunity for conducting practical site-test was considered advantageous. Albeit, arranging for site-tests was tedious and time consuming.

During the course of this project, most efforts were concentrated on acquisition and storage of PD data rather than the actual analysis. However it was learnt through literature review and practical on-site experience that the interpretation of PD data is not a straightforward process. More often, a skilled personnel's intervention is required for the interpretations of PD data. Developing software for PD analysis is considered as a challenging task due to the fact that the PD signals are erratic in nature and are dependent on multiple factors. A simple rule based analysis is not directly applicable for PD interpretation and most times is a call of judgement.

The results obtained from all the experiments undertaken during this project have produced encouraging results. Most importantly, a hardware data acquisition platform for the detection of PD pulses has been successfully established which can now be developed further to improve its performance. Dowding & Mills is now considering building a high voltage test facility within its premises and this will provide a great boost for the future development of this project.

It is finally considered that a great deal of work is still required for the development of a commercially viable PD monitoring and detection system, in particular in the areas relating to software used for PD data analysis.

## **10.2 Future Work**

The main objective of the work undertaken through this project was to develop a data acquisition system for PD detection in high voltage rotating machines and evaluate its feasibility. The site testing of the three channel system has demonstrated that the PD pulses can be effectively detected by using Rogowski coils and the associated signal conditioning circuitry. However, the ultimate objective would be to develop a complete system that is not only capable of acquiring PD pulses and displaying them but also capable of analysing the PD data and diagnosing the condition of high voltage stator insulation. This by no means is an easy task and will require a considerable amount of research work.

It is a known fact that a high bandwidth system is not necessarily needed for the condition monitoring of rotating machines. As discussed in the section 4.3.3, a bandwidth of around 500KHz or less is known to be sufficient. With a vast array of electronic modules readily available in the market, it is practically feasible to build the complete digitising electronics using readily available components. One such solution is presented in section 9.1.2. However, the signal conditioning unit still may need a customised design.

### **10.2.1 Hardware Development**

The existing hardware design of the prototype system was constrained by the budget requirements for the project. Most of the electronics was developed using the available facilities by designing circuit boards with basic Dual-In-Line packaged (DIP) ICs (integrated circuits). Many modern ICs (like monolithic filters, amplifiers) are only available in surface mount packages. The use of surface mount devices will help in making the design more versatile and compact. In particular, the design of the amplifier can be improved by using a Voltage Gain controlled Amplifiers (VGA).

### *Immediate development*

The configuration of the existing amplifier design limits the number of gain settings achievable to '12'. However the use of VGAs will significantly enhance the number of possible gain settings providing a greater flexibility. Also if VGAs with digital gain control are used then the gain control accuracy may be improved as the gain control logic is implemented within the IC.

A new system using VGA (AD600) is currently being developed. The AD600 is a dual channel VGA and each independent channel of AD600 provides a gain of 0dB to +40dB. The block diagram of this system is shown in figure 10.1. The gain of the VGA is varied by controlling the reference voltage and the scaling factor of AD600 is internally trimmed to 31.25mV/dB. The reference voltage is varied by means of a digital potentiometer (AD7376). The AD7376 is a 128 position digital potentiometer and the slider position is controlled by a microcontroller. A 2 volt precision reference is divided into 128 steps providing a resolution of 15.625mV/step i.e. 2 steps will change the reference voltage by 31.25mV. Thus each independent channel of AD600 provides a gain of 0dB to +40dB in 64 different steps. With two channels cascaded together the maximum achievable gain will be +80dB with a variety of gain settings, thus making the system more flexible. The same design can be easily translated into a three channel system by simply replicating various blocks. The use of digital potentiometers can be avoided if VGAs with digital gain control is used (e.g. LMP8100).

The microcontroller also handles the user input interface. A 12-bit DAQ card can be considered for improving the amplitude resolution.

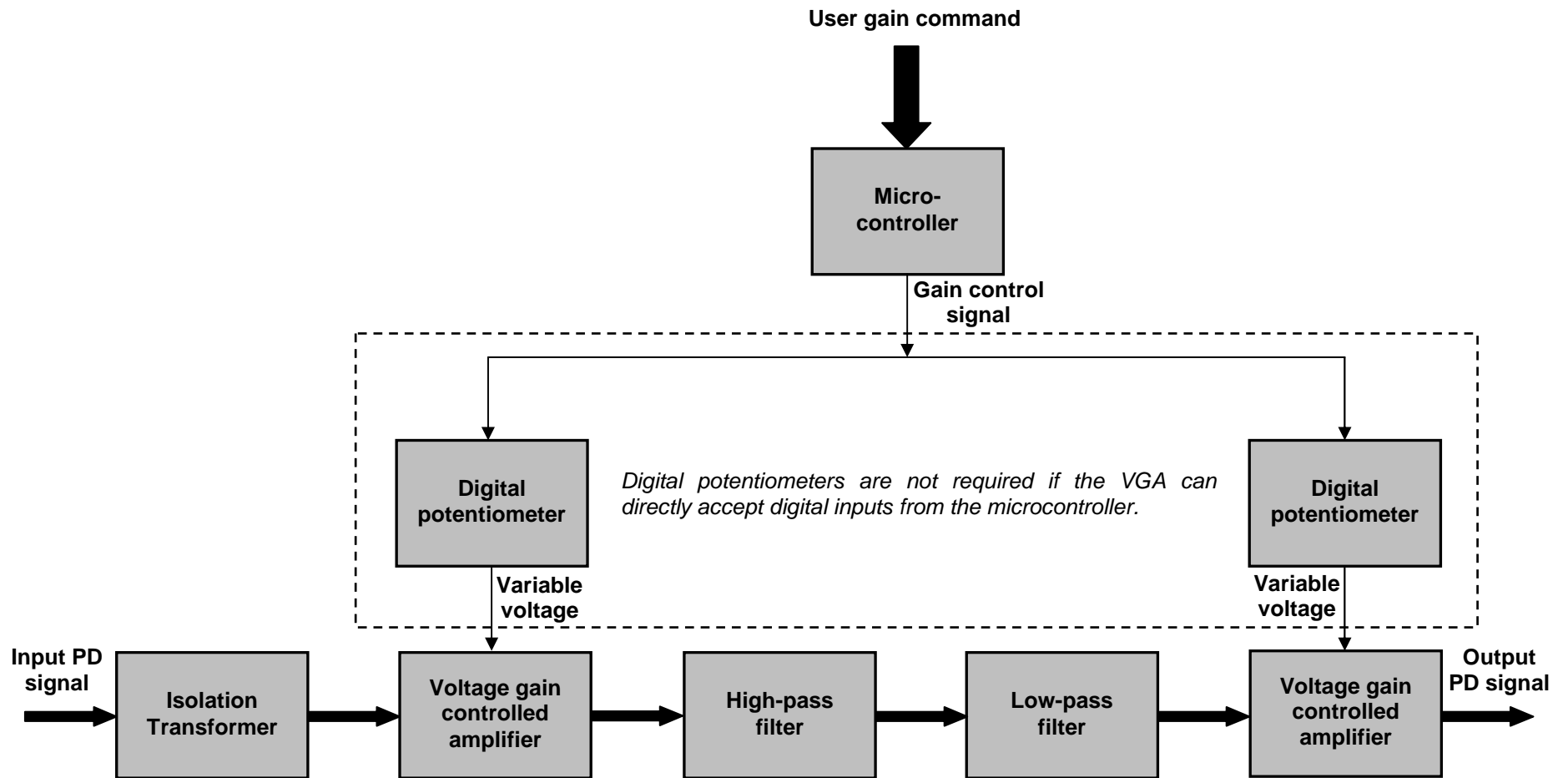
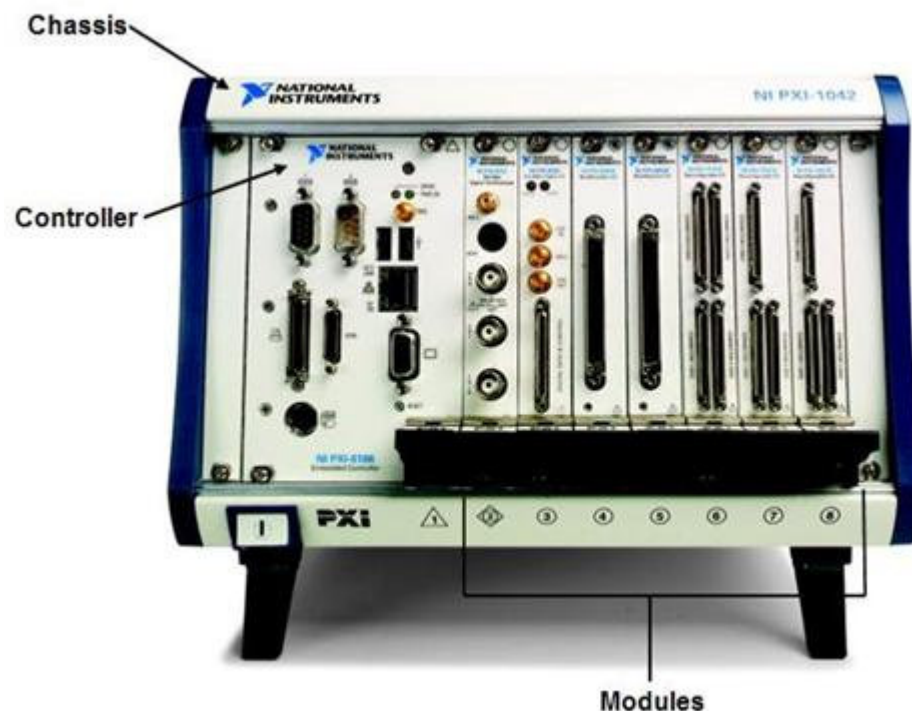


Figure 10.1 New design for signal conditioning unit

## PXI system

The PD detector is intended for use in industrial applications. Hence the design of the detector needs to be portable and robust to withstand the rigors of an industrial environment. The PXI system by National Instruments is one such possible solution. The PXI system is a configurable system available in a robust chassis and comes with an industrial computer (embedded controlled). This computer can be interfaced with various other DAQ modules through a high speed PXI bus that is capable of speeds up to 132 Mega bits per second (Mb/s). The PXI bus connections are located on the back plane of the chassis making it easy to slot-in various PXI modules that are readily available in the market. Figure 10.2 shows a picture of a basic PXI module with 8 slots for expansion. The current estimated cost of such a system is given in table 10.1. An 8-bit DAQ card with 4 simultaneous inputs and a sampling frequency of 3Ms/s is not available with a PXI interface. A better DAQ card with a resolution of 12-bit and a sampling frequency of 10Ms/s has been selected for the design.



**Figure 10.2 Standard 8 slot PXI chassis with controller** <sup>(131)</sup>

At a future stage the customised signal conditioning unit can be designed as a plug-in module with PXI bus compatibility and the embedded controller can be used to control all the gain settings along with other DAQ processes.

**Table 10.1 Estimate costing for PXI DAQ system**

No.	Model	Description	Cost
1	NI-PXI 8183	Embedded Controller	£1,199
2	N/A	15" Flat panel touch screen	£1,149
3	NI - PXI 6115	4 channel DAQ; 12 bit; 10 Ms/S	£3,199
4	NI- PXI 1031	4U PXI Chassis	£779
5	N/A	Accessories	£675
<b>Total</b>			<b>£7,001</b>

*Note: The pricing information shown in table 10.1 was obtained from the National instruments website [www.ni.com](http://www.ni.com) on 15<sup>th</sup> May2010.*

## **10.2.2 Software Development**

The existing system displays the PD pulses in time domain like a traditional oscilloscope-type display. This type of display does provide some information regarding the phase position of the discharges. But it is difficult to determine the repetition rates of the highest discharges. A 'pulse height distribution' display (as described in chapter 8) can be used to determine the repetition rates of various discharge amplitudes.

The phase resolved PD pattern (' $\phi$ -q-n' pattern) provides vast amount of information like the predominance of PD pulses in +ve and -ve cycles, Skewness and Kurtosis. The development of a software system capable of displaying phase resolved PD pattern will prove useful in PD data analysis.

For permitting trend analysis, it is necessary to develop a database to store historical PD data of various machines in a systematic manner. A rudimentary database to store raw PD is currently under progress.

Statistical analysis techniques still depend on the user's expertise for PD analysis. But researchers have proposed techniques for an automated analysis of PD data <sup>(144, 145, 146)</sup>. The application of neural networks for pattern recognition is well known. Numerous studies have been published demonstrating the potential of neural networks for PD pattern recognition and analysis <sup>(147, 148, 149)</sup>. As demonstrated by Yang *et.al.* <sup>(150)</sup> the wavelet analysis is another technique that can be used for PD pattern recognition. These areas can be investigated further to achieve an automated analysis.

More recently there has been a demand for systems capable of monitoring PD remotely. The advantages of a remote monitoring system over the conventional periodic monitoring have been discussed in Chapter 8. However, implementation of a remote monitoring system demands a substantial investment in terms of having a fibre optic or Ethernet TCP/IP intranet system. Currently there are not many plants that have a fibre optic TCP/IP intranet system that is readily available throughout the plant. Secondly, each machine will need its own individual PD data collector unit installed. Due to these factors the commercial implementation of such a system is currently not a financially viable option. However, as time progresses, most industrial plants are bound to modernise and the cost of data acquisition systems will reduce, making remote monitoring an attractive practical solution. Hence including options for remote monitoring in the future PD system design should be strongly considered.

## References

1. Mobley R.; 'An Introduction to predictive maintenance'; 2002; Available at: <http://books.google.com/books?id=SjgXzxpAzSQC&dq=predictive+maintenance>. Accessed 18<sup>th</sup> May 2009.
2. Stephens Matthew P., 'Productivity and Reliability – Based maintenance management' ; Pearson Prentice Hall, pp.66
3. Howarth W.; 'Predictive Maintenance saves money, Improves plant reliability', May 2004. Available at: [http://www.emersonprocess.com/home/library/articles/pharmprocess/pharmprocess0405\\_predmaint.pdf](http://www.emersonprocess.com/home/library/articles/pharmprocess/pharmprocess0405_predmaint.pdf) . Accessed 28<sup>th</sup> May 2009.
4. Failure Identification and analysis for high voltage induction motors in petrochemical industry – O.V. Thorsen, M.Dalva., IEEE transactions on industry applications, vol35, no. 4, July / August 1999. pp. 814
5. W. T. Thomson : "A Review of On-Line Condition Monitoring Techniques for Three-Phase Squirrel-Cage Induction Motors -Past Present and Future" Keynote address at IEEE Symposium on Diagnostics for Electrical Machines, Power Electronics and Drives, Gijon, Spain, Sept. 1999 pp 3-18.
6. Greg C. Stone, Edward A. Boulter, Ian Culbert, Hussein Dhirani: "Electrical Insulation For Rotating Machines: Design, Evaluation, Aging, Testing and Repair", Wiley – IEEE Press, Jan 2004.
7. Haddad A., Warne D., "Advances in High Voltage Engineering", Institute of Electrical Engineers, Power and Energy Series 40, Published 2004.
8. Bengtsson Marcus, *et.al.*, 'Technical design of condition based maintenance system – A case study using sound analysis and case-based reasoning', Maintenance and Reliability conference - Proceedings of the 8<sup>th</sup> Congress, 2<sup>nd</sup> - 5<sup>th</sup> May 2004.
9. K. Hatakeyama, Rui Fransisco Martins: "Managing Incipient Faults in Rotating Machines based on Vibration Analysis and Fuzzy Logic", presented at International Symposium on Management Engineering Conference (March 2006).
10. Ron Barron: "Engineering Condition Monitoring – Practice, methods and applications", Addison Wesley Longman, Published 1996.
11. Price, J.T.. 'Vibration analysis methods for preventative maintenance [of cement plants]', IEEE – IAS/PCA Cement industry technical conference, 29 April – 3 May 2001, pp 333-341.
12. Mendel, E.; Mariano, L.Z.; Drago, I.; Loureiro, S.; Rauber, T.W.; Varejao, F.M.; Batista, R.J., 'Automatic bearing fault pattern recognition using vibration signal analysis', 5<sup>th</sup> IEEE International symposium on Diagnostics for electrical machines, power electronics and drives, 30<sup>th</sup> June – 2<sup>nd</sup> July 2008, pp 955-960.

13. Braun, S.G. 'The Signature Analysis of Sonic Bearing Vibrations', IEEE transactions on Sonics and ultrasonics, Vol.27, No.6, Nov 1980, pp 317-327.
14. Breen, T.B.; Kliman, G.B.; Patel, S.C., 'New developments in noninvasive on-line motor diagnostics', Conference record of 43<sup>rd</sup> Annual petroleum and chemical industry conference, 23-25 September 1996, pp 231-236.
15. Nandi, S.; Toliyat, H.A.; Xiaodong Li, 'Condition monitoring and fault diagnosis of electrical motors-a review', IEEE transactions on energy conversion, Vol.20, No.4, Dec 2004, pp 719-729.
16. El Hachemi Benbouzid, M., 'A review of induction motors signature analysis as a medium for faults detection', IEEE transactions on industrial electronics, Vol.47, No.5, October 2005, pp 984-993.
17. Cusido, J.; Rosero, J.; Aldabas, E.; Ortega, J.A.; Romeral, L., 'Fault detection techniques for induction motors', Electrical Power Quality and Utilisation Magazine, Vol. II, No.1, 2006, pp 36-46.
18. Stone, G.; Culbert, I., 'The testing tools', IEEE Industry applications magazine, Vol.14, No.6, Nov-Dec 2008, pp 48-53.
19. Lorand, S.; Barna D. J.; Agoston B.K.; 'Rotor faults detection in squirrel-cage induction motors by current signature analysis', IEEE-TTTC International conference on Automation, Quality and Testing, Robotics, May 13- 15, 2004, Romania.
20. Bikfalvi, P.; Imecs, M., 'Rotor Fault Detection in Induction Machines: Methods and Techniques - State-of-the-Art' IEEE International conference on Automation, Quality and Testing, Robotics, 25-28 May 2006, Vol.1, pp 199-204.
21. Jee-Hoon Jung; Jong-Jae Lee; Bong-Hwan Kwon, 'Online Diagnosis of Induction Motors Using MCSA', IEEE transactions on Industrial electronics, Vol.53, No.6, Dec 2006, pp 1842-1852.
22. Thomson, W.T.; Fenger, M., 'Current signature analysis to detect induction motor faults', IEEE Industry Applications magazine, Vol.7, No.4, Jul-Aug 2001, pp 26-34.
23. Bonnett, A.H., Soukup, G.C., 'Cause and analysis of stator and rotor failures in three phase squirrel-cage induction motors', IEEE transactions on Industry Applications, Vol.28, No.4, July/August 1992, pp 921-937.
24. Buchan, J.G., 'Partial discharge measurements in high voltage motors', PhD thesis, Robert Gordon's Institute of Technology, September 1987.
25. Stone, G.C., Lyles, J.F., Braun, J.M., Kaul, C.L., 'A thermal cycling type test for generator stator winding insulation', IEEE Transactions on energy conversion, Vol.6, No.4, December 1991, pp 707-713.
26. Stone, G.C., Gupta, B.K., Lyles, J.F., Sedding, H.G., 'Experience with accelerated ageing tests on stator bars and coils', Conference record of the 1990 IEEE International Symposium on Electrical Insulation, Toronto, Canada, 3-6 June, 1990, pp 356-360.

27. Montsinger, V.M., 'Loading transformers by temperature', AIEE transactions, Vol. 49, No.2, April 1930, pp 776-790.
28. 'Life expectancy of motors in mild nuclear plant environments', EPRI report NP3887, Feb. 1985.
29. Dakin, T.W., 'Electrical insulation deterioration treated as a chemical rate phenomenon', AIEE transactions, Vol. 67, No.1, Jan 1948, pp 113-122.
30. Kutz, M., Lyles, J.F., Stone G.C., 'Application of partial discharge testing to hydro generator maintenance', IEEE transactions on power apparatus and systems, Vol. PAS-103, No.8, Aug. 1984, pp 2588-2597.
31. Edwards, D.G., 'Planned maintenance of high voltage rotating machine insulation based upon information derived from on-line discharge measurements', International conference on life management of power plants, Edinburgh, 12-14 Dec, 1994, pp 101-107.
32. Maughan, C.V., Gibbs, E.E., Giaquinto, E.V., 'Mechanical testing of high voltage stator insulation systems', IEEE transactions on power apparatus and Systems, Vol.89, No.8, 1970, pp 1946-1970.
33. Kai Wu; Kanegami, M.; Takahashi, T.; Suzuki, H.; Ito, T.; Okamoto, T.; Yano, H, 'Effect of mechanical vibration on the behaviour of partial discharges in generator windings', IEEE Transactions on Dielectrics and Electrical Insulation, Vol.13, No.1, Feb 2006, pp 345-352.
34. Forster, J.A.; Klataske, L.F., 'IEEE Working Group Report of Problems with Hydrogenerator Thermoset Stator Windings Part II-Detection, Correction and Prevention', IEEE transactions on power apparatus and systems, Vol.PAS-100, No.7, 1981, pp 3292-3300.
35. Dymond, J.H.; Stranges, N.; Younsi, K.; Hayward, J.E., 'Stator winding failures: contamination, surface discharge, tracking', IEEE transaction on Industry Applications, Vol.38, No.2, Mar-Apr 2002, pp 577-583.
36. Campbell, S.R.; Stone, G.C.; Sedding, H.G.; Klempner, G.S.; McDermid, W.; Bussey, R.G., 'Practical on-line partial discharge tests for turbine generators and motors', IEEE transactions on energy conversion, Vol.9, No.2, June 1994, pp 281-287.
37. Kouadria, D., 'The ageing and breakdown characteristics of electrical machine insulation materials', PhD thesis, The University of Brighton in collaboration with Dowding & Mills, March 1998.
38. Fenger, M.; Stone, G.C., 'Investigations into the effect of humidity on stator winding partial discharges', IEEE transaction on Dielectrics and electrical insulation, Vol.12, No.2, April 2005, pp3 341-346.
39. Naprasert, S.; Chongchaikit, S.; Puthwattana, S., 'The Effect of Humidity on Partial Discharge Measurement', Conference record of 2006 8<sup>th</sup> International conference on properties and application of dielectric materials, June 2006, pp 57-60.

40. Binder, E.; Draxler, A.; Muhr, M.; Pack, S.; Schwarz, R.; Egger, H.; Hummer, A., 'Effects of air humidity and temperature to the activities of external partial discharges of stator windings', Conference record of 1999 11<sup>th</sup> international symposium on high voltage engineering', Vol.5, Aug 1999, pp 264-267.
41. Nawawi, Z.; Muramoto, Y.; Hozumi, N.; Nagao, M., 'Effect of humidity on Partial Discharge characteristics', Conference proceedings of 7<sup>th</sup> international conference on properties and applications of dielectric materials', Nagoya, June1-5, 2003, Vol.1, pp 307-310.
42. Soltani, Reza; David, Eric; Lamarre, Laurent, 'Study on the effect of humidity on dielectric response and partial discharges activity of machine insulation materials', Conference record of 2009 IEEE Electrical insulation conference, Montreal, QC, Canada, 31 May – 3 June 2009, pp 343-347.
43. Nurse, J.A., 'Development of modern high-voltage insulation systems for large motors and generators', Power engineering journal, Vol. 12, No.3, June 1998, pp 125-130.
44. Farahani, M.; Borsi, H.; Gockenbach, E.; Kaufhold, M., 'Partial discharge and dielectric response behaviour of insulation systems for high voltage rotating machines under electrical stress', Conference record of 2004 CEIDP, 17-20 Oct 2004, pp 271-274.
45. Persson, E., 'Transient effects in application of PWM inverters to induction motors', IEEE transaction on industry applications, Vol. 28, No.5, Sept-Oct 1992, pp 1095-1101.
46. Gupta, B.K.; Lloyd, B.A.; Sharma, D.K, 'Degradation of turn insulation in motor coils under repetitive surges', IEEE transactions on energy conversion, Vol. 5, No. 2, June 1990, pp 320-326.
47. Stone, G.C.; van Heeswijk, R.G.; Bartnikas, R, 'Investigation of the effect of repetitive voltage surges on epoxy insulation', IEEE Transactions on energy conversion, Vol. 7, No. 4, December 1992, pp 754-760.
48. Ward, B.E.; Stone, G.C.; Kurtz, M., 'A Quality Control Test for High Voltage Stator Insulation', IEEE Electrical insulation magazine, Vol.3, No.5, September 1987, pp 12-17.
49. Cygan, P., Laghari, J.R., 'Models for insulation ageing under electrical and thermal multistress', IEEE transactions on electrical insulation, Vol. 25. No.5, October 1990, pp 923-933.
50. Brancato, E.L., 'A pathway to multifactor aging', IEEE transactions on electrical insulation, Vol.28, No.5, October 1993, pp 820-825.
51. Simoni, L., 'A General Approach to the Endurance of Electrical Insulation under Temperature and Voltage', IEEE transactions on electrical insulation', Vol.16, No.4, August 1981, pp 277-289.
52. Simoni, L., 'General Equation of the Decline in the Electric Strength for Combined Thermal and Electrical Stresses', IEEE transactions on electrical insulation', Vol.19, No.1, February 1984, pp 45-52.

53. Agarwal, V.K.; Banford, H.M.; Bernstein, B.S.; Brancato, E.L.; Fouracre, R.A.; Montanari, G.C.; Parpal, J.L.; Seguin, J.N.; Ryder, D.M.; Tanaka, J., 'The Mysteries of Multifactor Ageing', IEEE Electrical Insulation Magazine, Vol. 11, No. 3, May-June 1995, pp 37-43.
54. Simoni, L.; Mazzanti, G.; Montanari, G.C.; Lefebvre, L., 'A general multi-stress life model for insulating materials with or without evidence for thresholds', IEEE transactions on electrical insulation, Vol. 28, No. 3, June 1993, pp 349-363.
55. Mazzanti, G.; Montanari, G.C.; Simoni, L. 'Study of the synergistic effect of electrical and thermal stresses on insulation life', IEEE Annual report of the conference on electrical insulation and dielectric phenomena, 20-23 Oct 1996, Vol. 2, pp 684-687.
56. Mazzanti, G.; Montanari, G.C.; Simoni, L.; Srinivas, M.B, 'Combined electro-thermo-mechanical model for life prediction of electrical insulating materials', IEEE Annual report of the conference on electrical insulation and dielectric phenomena, 22-25 Oct 1995, pp 274-277.
57. Bartnikas, R.; Morin, R., 'Multi-stress aging of stator bars with electrical, thermal, and mechanical stresses as simultaneous acceleration factors', IEEE transactions on energy conversion, Vol. 19, No.4, December 2004, pp 702-714.
58. Paloniemi, P., 'Theory of Equalization of Thermal Ageing Processes of Electrical Insulating Materials in Thermal Endurance Tests I: Review of Theoretical Basis of Test Methods and Chemical and Physical Aspects of Ageing, Part 1, 2 and 3', IEEE transactions on electrical insulation, Vol. EI16, No.1, February 1981, pp 1-30.
59. Kimura, K., 'Multistress aging of machine insulation systems', IEEE Annual report of the conference on electrical insulation and dielectric phenomena, 22-25 Oct 1995, pp 205-210.
60. Kaufhold, M.; Schafer, K.; Bauer, K.; Bethge, A.; Risse, J., 'Interface phenomena in stator winding insulation - challenges in design, diagnosis, and service experience', IEEE Electrical insulation magazine, Vol.18, No.2, March/April 2002, pp 27-36.
61. Kreuger, F.H., 'Partial discharge detection in high-voltage equipment', Butterworth, 1989; pp 7.
62. Kang, S.H.; Park, Y.G.; Lee C.; Park, J.N.; Lim, K.J.; 'Voltage-time characteristics of PD patterns in void discharges', Proceedings of 2001 International symposium Electrical Insulating Materials, 19<sup>th</sup> -22<sup>nd</sup> Nov, 2001, pp 25-28.
63. Mason, J.H., 'The deterioration and breakdown of dielectric resulting from partial discharges', IEEE proceedings 1951, 98, Pt 1, pp 44-59.
64. Ryder, D. ; 'The interpretation of partial electrical discharge measurements with insulation damage and ageing'; Conference on Electrical Insulation and Dielectric Phenomena; 17-20 October 1993; pp 642-647.

65. Kurimsky J.; Kolcunova I.; Cimbala R.; 'Partial discharge analysis for insulation systems of electric rotating machines with various voltage stress', Acta Electrotechnica et Informatica, Vol. 8, No. 4, 2008, pp 64-67.
66. Davies, N.; Yuan Tian; Tang, J.C.Y.; Shiel, P.; 'Non-intrusive partial discharge measurements of MV switchgears', International conference on Condition Monitoring and Diagnosis, Beijing, 21-24 April 2008, pp 385-388.
67. Nindra, B.S.; Kogan V.; Dawson F.; 'Surface corona suppression in high voltage stator winding end-turns', Proceedings of Electrical Insulation Conference and Electrical manufacturing expo, 1995, pp 411-415
68. Cargill, S.M.; Edwards D.G.; 'Corona screen effectiveness in large rotating machines under high voltage, high frequency transient conditions', IEE proceedings on Electric power applications, 1998, Vol. 145, pp 469-474.
69. Bonnett, A.H.; 'Analysis of winding failures in three phase squirrel cage induction motors', IEEE transactions on industry applications, Vol. IA-14, No. 3, May-June 1978, pp 223-226.
70. Stranges, M.K.W.; Stone, G.C.; Bogh, D.L.; 'Progress on IEC 60034-18-42 for qualification of stator insulation for medium-voltage inverter duty applications', IEEE technical conference on Petroleum and chemical industry, 17<sup>th</sup>-19<sup>th</sup> Sept 2007, pp 1-7.
71. Boulter, E.A.; Stone, G.C.; 'Historical development of rotor and stator winding insulation materials and systems', IEEE Electrical insulation magazine, May-June 2004, Vol. 20, Issue 3, pp-25-39.
72. Jackson, R.J.; Wilson, A; 'Slot discharge activity in air cooled motors and generators', IEE proceedings of Electric power applications, Vol. 129, Issue 3, May 1982, pp 159-167.
73. Culbert, I.M.; 'A review of cleaning methods for motor winding', Cement industry technical conference, 18-22 May 2008, Miami, pp 291-296.
74. Walker, P; Champion J.N.; 'Experience with turn insulation failures in large 13.2 kV synchronous motors', IEEE transactions on energy conversion, 1991, Vol. 6, Issue 4, pp 670-678.
75. Kusumoto, S.; Itoh, S. ; Tsuchiya, Y. ; Mukae, H. ; Matsuda, S. ; Takahashi, K.; 'Diagnostic Technique of Gas Insulated Substation by Partial Discharge Detection'; IEEE transactions on Power Systems and Apparatus; July1980, Vol. 99, No. 4; pp 1456-1465.
76. Pearson, J.S. ; Farish, O. ; Hampton, B.F. ; Judd, M.D. ; Templeton, D. ; Pryor, B.W. ; Welch, I.M. ; 'Partial discharge diagnostics for gas insulated substations'; IEEE transactions on Dielectrics and Insulation,1995, Vol. 2, No. 5, pp 893-905.
77. Griffin, G.D.; Sauers, I.; Kurka, K.F.; Easterly, C.E.; 'Spark decomposition of SF<sub>6</sub>: chemical and biological studies'; IEEE transactions on Power Delivery; 1989, Vol. 4, No. 3, pp 1541-1551.

78. Imad-U-Khan ; Zhongdong Wang ; Cotton, I. ; Northcote, S.; 'Dissolved gas analysis of alternative fluids for power transformers'; IEEE Electrical Insulation Magazine; 2007, Vol. 23, No.5, pp 5-14.
79. Ferrito, S.J.; 'A comparative study of dissolved gas analysis techniques: the vacuum extraction method versus the direct injection method'; IEEE transactions on Power Delivery; 1990; Vol. 5; No.1; pp 20-25.
80. Khan, I. ; Zhongdong Wang ; Jie Dai ; Cotton, I. ; Northcote, S.; 'Fault gas generation in ester based transformer fluids and dissolved gas analysis (DGA)'; International conference on condition monitoring and diagnosis; 21-24<sup>th</sup> April 2008; pp 909-913.
81. Emsley, A.M. ; Stevens, G.C. ; 'Review of chemical indicators of degradation of cellulosic electrical paper insulation in oil-filled transformers'; IEE Proceedings Science, Measurement & Technology, 1994, Vol. 141, No. 5, pp 324-334.
82. Unsworth, J.; Mitchell, F.; 'Degradation of electrical insulating paper monitored with high performance liquid chromatography'; IEEE transactions on electrical insulation; 1990, Vo. 25, No. 4; pp 737-746.
83. M. Muhr; R. Schwarz; 'Partial discharge measurement as a Diagnostic Tool for HV-Equipments'; 8<sup>th</sup> International conference on Properties and Applications of Dielectric Materials'; Bali; June 2006, pp 195-198.
84. Kemp, I.J.; 'Partial discharge plant-monitoring technology: present and future developments'; IEE Proceedings Science, Measurement & Technology; 1995; Vol. 142, No. 1; pp 4-10.
85. Lundgaard, L.E.; 'Partial discharge. XIV. Acoustic partial discharge detection-practical application'; IEEE Electrical Insulation Magazine; Vol. 8, No. 5, Sept/Oct 1995, pp 34-43.
86. Lundgaard, L.E. ; Runde, M. ; Skyberg, B.; 'Acoustic diagnosis of gas insulated substations: a theoretical and experimental basis'; IEEE Transactions on Power Delivery, 1990, Vo. 5; No. 4, pp 1751-1759.
87. <http://www.plant-maintenance.com/articles/partialdischarge.pdf> - accessed on 24th July 2008.
88. [http://scholar.lib.vt.edu/theses/available/etd-05122003-161802/unrestricted/thesis\\_fin.pdf](http://scholar.lib.vt.edu/theses/available/etd-05122003-161802/unrestricted/thesis_fin.pdf) - accessed on 6th September 2008.
89. Deheng Zhu ; Kexiong Tan ; Xianhe Jin; 'The study of acoustic emission method for detection of partial discharge in power transformer'; Second International Conference on Properties and Applications of Properties and Applications of Dielectric Materials, Beijing, China, 1988, Vol. 2, pp 614-617.
90. Schwarz, R.; Muhr, M.; 'Modern technologies in optical partial discharge detection'; Conference on Electrical Insulation and Dielectric Phenomena, 2007, pp 163-166.

91. Xn Yang; Yn Ming; Cao Xiaolong; Qiu Changrong; Chen, G.; 'Comparison between optical and electrical methods for partial discharge measurement'; Proceeding of 6<sup>th</sup> International Conference on Properties and applications of Dielectric Materials; 21-26<sup>th</sup> June 2000; Vol. 1; pp 300-303.
92. Cosgrave, J.A. ; Vourdas, A. ; Jones, G.R. ; Spencer, J.W. ; Murphy, M.M. ; Wilson, A. ; 'Acoustic monitoring of partial discharges in gas insulated substations using optical sensors'; IEE Proceedings on Science, Measurement and Technology, Sep 1993, Vol. 140, No. 5, pp 369-374.
93. Blackburn, T.R. ; Phung, B.T. ; James, R.E. ; 'Optical fibre sensor for partial discharge detection and location in high-voltage power transformer'; Sixth International Conference on Dielectric Materials, Measurements and Applications, 7-10 Sep 1992 ; Manchester; pp 33-36.
94. Sang Bin Lee ; Jinkyu Yang ; 'An on-line groundwall and phase to phase insulation quality assessment technique for AC machine stator windings'; Conference Record of Industry Applications Conference, 2-6 Oct 2005; Vol. 1; pp 10-19.
95. Nelson, R.L. ; 'Bridge measurement of very low dielectric loss at low temperatures'; Proceedings of Institution of Electrical Engineers; July 1974, Vol. 121; No. 7; pp 764-770.
96. IEEE Recommended Practice for Measurement of Power Factor Tip-Up of Electric Machinery Stator Coil Insulation; 2001.
97. Kelen Andreas; 'Critical Examination of the Dissipation Factor Tip-up as a Measure of Partial Discharge Intensity'; IEEE transactions on Electrical Insulation, Feb 1978, Vol. 13; No. 1; pp 14-24.
98. Petersons, O. ; 'A Transformer-Ratio-Arm Bridge for Measuring Large Capacitors Above 100 Volts'; IEEE transactions on Power Apparatus and Systems; May 1968; Vol. 87, No. 5, pp 1354-1361.
99. <http://www.eltelindustries.com/webadmin/PDFs/22042009105422732.pdf> -  
accessed on 15th Jan 2010.
100. Stephenson J. N. ; 'Measurement of Partial Discharge Pulses in a High Voltage System'; BSc Thesis; Robert Gordon's Institute of Technology, April 1987; pp - 36.
101. Simons, J.S.; 'Diagnostic testing of high-voltage machine insulation. A review of ten years' experience in the field'; IEE Proceedings on Electric Power Applications, May 1980, Vol. 127; No. 3; pp 139 - 154.
102. Kouadria, D., 'The ageing and breakdown characteristics of electrical machine insulation materials', PhD thesis, The University of Brighton in collaboration with Dowding & Mills, March 1998.

103. Kreuger, F.H. ; Gulski, E. ; Krivda, A. ; 'Classification of partial discharges'; IEEE transactions on Electrical Insulation; Dec 1993; Vol. 28; No. 26; pp 917-931.
104. Gulski, E. ; Kreuger, F.H. ; 'Diagnostics of insulating systems using statistical tools'; Conference record of IEEE International Symposium on Electrical Insulation; Baltimore MD, 7-10 June 1992; pp 393-396.
105. Hudon, C. ; Belec, M. ; 'Partial discharge signal interpretation for generator diagnostics'; IEEE Transactions on Dielectrics and Electrical Insulation; April 2005; Vol. 12; No. 2; pp 297-319.
106. Gross, D.W.; 'On-line partial discharge diagnosis on large motors'; Conference Proceedings on Electrical Insulation and Dielectric Phenomena; Mexico; October 2002; pp 474 – 477.
107. Stone, G.C. ; Sedding, H.G. ; Costello, M.J. ; 'Application of partial discharge testing to motor and generator stator winding maintenance'; IEEE Transactions on Industry Applications; Mar-Apr 1996; Vol. 32; No. 2; pp 459 – 464.
108. Stone, G.C. ; Sedding, H.G. ; 'New technology for partial discharge testing of operating generators and motors'; Proceedings of Electrical Electronics Insulation Conference and Electrical Manufacturing & Coil Winding Conference; Chicago; 4-7 Oct1993; pp 667 – 672.
109. Watt, G. ; Kouadria, D. ; 'The practical use of a computerised partial discharge measuring system for online condition monitoring of high voltage stator windings'; Ninth International Conference on Electrical Machines and Drives; (Conf. Publ. No. 468) ; 1999; pp 112 – 117.
110. Kouadria, D. ; Watt, G. ; 'Partial discharge patterns and the identification of defects in high voltage stator windings insulation' ; Eighth International Conference on Dielectric Materials, Measurements and Applications; (IEE Conf. Publ. No. 473); 2000; pp 236 – 240.
111. Stone, G.C. ; Sedding, H.G. ; Fujimoto, N. ; Braun, J.M. ; 'Practical implementation of ultrawideband partial discharge detectors'; IEEE Transactions on Electrical Insulation; Feb 1992; Vol. 27; No. 1; pp 70 – 81.
112. Wilson, A.; Jackson, R.J.; Wang, N.; 'Discharge detection techniques for stator windings'; IEE Proceedings on Electric Power Applications; 1985; Vol. 132, No.5, pp 234 – 244.
113. Beggs, B.J. ; Kemp, I.J. ; Wilson, A. ; 'Characterisation of discharge phenomena in voids'; Conference Record of IEEE International Symposium on Electrical Insulation; Toronto, Canada; 3-6 June 1990; pp 145-148.
114. Sedding, H.G. ; Stone, G.C. ; 'A discharge locating probe for rotating machines'; Proceedings of the 19<sup>th</sup> Electrical Electronics Insulation Conference; Chicago; 25-28 Sep 1989; pp 225 – 227.
115. Hudon, C. ; Torres, W. ; Belec, M. ; Contreras, R.; 'Comparison of discharges measured from a generator's terminals and from an antenna in front of the

- slots'; Conference Proceedings of Electrical Insulation Conference and Electrical Manufacturing & Coil Winding; Cincinnati; 16-18 Oct 2001; pp 533 – 536.
116. Zhu, H.; Kemp, I.J.; 'Pulse propagation in rotating machines and its relationship to partial discharge measurements'; Conference Proceedings of IEEE International Symposium on Electrical Insulation; Baltimore, USA; 7-10 June 1992; pp 411 – 414.
  117. HV Testing, Monitoring and Diagnostic Workshop (2000, Alexandria, Virginia, 13 & 14 September 2000) – paper no. 4.
  118. Robles, G. ; Argueso, M. ; Sanz, J. ; Giannetti, R. ; Tellini, B. ; 'Identification of parameters in a Rogowski coil used for the measurement of partial discharges'; Proceedings of IEEE Conference on Instrumentation and Measurement Technology; 1-3 May 2007; pp 1 – 4.
  119. Ramboz, J.D.; 'Machinable Rogowski coil, design, and calibration'; IEEE Transactions on Instrumentation and Measurement; April 1996; Vol. 45, No. 2, pp 511 – 515.
  120. Brown, A.J.; 'Condition monitoring of HV electrical rotating plant-on-line partial discharge techniques'; IEE Colloquium on Understanding your Condition Monitoring; Chester; April 1999; pp 1/1 – 1/3.
  121. Harrold, R.T. ; Emery, F.T. ; 'Radio Frequency Diagnostic Monitoring of Electrical Machines'; IEEE Electrical Insulation Magazine; March 1986; Vol. 2; No. 2; pp 18-24.
  122. Smith, W. R.; 'Online condition monitoring of HV electrical rotating plant. A comparison of techniques'; IEE/ImechE international conference on Power Station Maintenance – Profitability through Reliability; Edinburgh; 30 Mar-1 Apr 1998; pp 71-74.
  123. Zhu, H. ; Green, V. ; Sasic, M. ; Haliburton, S. ; 'Sensitivity improvement of capacitive couplers for on-line partial discharge testing in rotating machines'; IEEE Conference on Electrical Insulation and Dielectric Phenomena; Minneapolis; 19-22 Oct 1997; Vol. 2; pp 534 – 537.
  124. Green, V.; Sasic, M.; Wright, B.; 'Summary of industry practices, guides and standards related to on-line partial discharge monitoring of stator insulation condition'; Conference proceedings of 52<sup>nd</sup> Annual Petroleum and Chemical Industry Conference, Industry Applications Society; Denver, Colorado; 12-14 Sept 2005; pp 359 – 365.
  125. Sedding, H.G. ; Campbell, S.R. ; Stone, G.C. ; Klempner, G.S. ; 'A new sensor for detecting partial discharges in operating turbine generators'; IEEE Transactions on Energy Conversion; Dec 1991; Vol. 6; No. 4; pp 700 – 706.
  126. Austin, J. ; James, R.E. ; 'On-Line Digital Computer System for Measurement of Partial Discharges in Insulation Structures'; IEEE Transactions on Electrical Insulation; 1976; Vol. EI 11; No. 4; pp 129-139.

127. James, R.E.; Phung, B.T.; 'Development of computer-based measurements and their application to PD pattern analysis' ; IEEE Transactions on Insulation & Dielectrics;1995; Vol. 2; No. 5; pp 838 – 856.
128. Bonnie C. Baker; 'Anti-Aliasing, Analogue Filters for Data Acquisition Systems'; Microchip Technology Inc. Application Note AN699; [http://www.microchip.com/stellent/idcplg?IdcService=SS\\_GET\\_PAGE&nodeId=1824&appnote=en011696](http://www.microchip.com/stellent/idcplg?IdcService=SS_GET_PAGE&nodeId=1824&appnote=en011696). Accessed 15<sup>th</sup> May 2009.
129. Karki Jim; 'Active Low-Pass Filter Design'; Texas Instruments Application Report; Sep 2002; <http://focus.ti.com/lit/an/sloa049b/sloa049b.pdf>. Accessed 25th May 2009.
130. LabVIEW User Manual. April 2003 edition. Austin, Texas, USA. National Instruments Corporation USA; 2003.
131. PXI tutorial by National Instruments; <http://zone.ni.com/devzone/cda/tut/p/id/4811> - accessed on 15th May 2010.
132. Stone, G.C.; 'Partial discharge. VII. Practical techniques for measuring PD in operating equipment'; Electrical Insulation Magazine, IEEE ; Jul-Aug 1991; Vol. 7, No. 4; pp 9–19.
133. Borsi H.; Gockenbach E.; Schichler; ' Partial discharge (PD) Measurements under noisy condition – possibilities and limits of digital noise rejection'; Proceedings of 8<sup>th</sup> International Symposium on High Voltage Engineering; Yokohama, Japan; 23 -27 August 1993; pp 17-20.
134. Zaman S. *et.al.* ' An adaptive digital system to reduce periodical noise in on-line partial discharge monitoring'; Proceedings of 8<sup>th</sup> International Symposium on High Voltage Engineering; Yokohama, Japan; 23 -27 August 1993; pp 77-80.
135. Borsi, H.; Gockenbach, E.; Wenzel, D.:' Separation of partial discharges from pulse-shaped noise signals with the help of neural networks ' ;Science, Measurement and Technology, IEE Proceedings -;1995; Vol. 142; No. 1; pp 69 - 74.
136. Kopf. U; Feser K.; 'Noise suppression in partial discharge measurements'; 8<sup>th</sup> International Symposium on High Voltage Engineering; Yokohama, Japan; 23 - 27 August 1993; pp 81 - 84.
137. Ma, X. ; Zhou, C. ; Kemp, I.J. ; 'Interpretation of wavelet analysis and its application in partial discharge detection'; IEEE Transactions on Dielectrics and Electrical Insulation; June 2002; Vol. 9; No. 3; pp 446 – 457.
138. Shim, I.; Soraghan, J.J.; Siew, W.H.:' Detection of PD utilizing digital signal processing methods. Part 3: Open-loop noise reduction ' ;Electrical Insulation Magazine, IEEE ; 2001; Vol. 17; No. 1; pp 6 – 13.
139. Zhu, H. ; Green, V. ; 'Diagnosis of stator insulation of generators and motors using in-service partial discharge testing'; Proceedings of International Conference Power System Technology, 1998; Vol. 1; pp 76-80.

140. James *et.al.* 'Computer-based measurements and their applications to PD pattern analysis'; IEEE transactions on Dielectrics and Insulation; Oct 1995; Vol. 2; No. 5; pp 838 – 856.
141. Gross, D.W.; 'Partial discharge measurement and monitoring on rotating machines'; Conference Record of the IEEE International Symposium on Electrical Insulation, 2002; pp 570-574.
142. Gross, D.W.; 'On-line partial discharge diagnosis on large motors'; Conference on Electrical Insulation and Dielectric Phenomena, 2002 Annual Report; Mexico; pp 474 -477.
143. Zhu, H.; Green, V.; Sasic, M.; 'Identification of stator insulation deterioration using on-line partial discharge testing'; IEEE Electrical Insulation Magazine; 2001; Vol. 17; No. 6; pp 21-26.
144. Satish, L. ; Zaengl, W.S.; 'Artificial neural networks for recognition of 3-d partial discharge patterns'; IEEE Transactions on Dielectrics and Electrical Insulation; April 1994; Vol.1; No.2; pp 265 – 275.
145. G. C. Montanari ; 'Insulation Diagnosis of High Voltage Apparatus by Partial Discharge Investigation'; 8th International Conference on Properties and applications of Dielectric Materials; Bali, Indonesia; June 2006; pp 1 – 11.
146. Krivda A, *et.al.* 'The use of fractal features for recognition of 3-D partial discharge patterns'; IEEE Transactions on Dielectrics and Electrical Insulation; October 1995; Vol. 2 ; No. 5; pp 889 – 892.
147. Salama, M.M.A.; Bartnikas, R.; 'Determination of neural-network topology for partial discharge pulse pattern recognition'; IEEE Transactions on Neural Networks; 2002; Vol. 13; No. 2; pp 446-456.
148. Candela, R.; Mirelli, G.; Schifani, R.; 'PD recognition by means of statistical and fractal parameters and a neural network'; IEEE Transactions on Dielectrics and Electrical Insulation; 2000; Vol. 7; No. 1; pp 87-94.
149. Jeong-Tae Kim; *et.al.* 'Partial Discharge Pattern Recognition Using Fuzzy-Neural Networks (FNNs) Algorithm'; Proceedings of the IEEE International Power Modulators and High Voltage Conference; Las Vegas, USA; 2008; pp 272-275.
150. Ji Yang; Lin Du; You Yuanwang; 'Wavelet Multi-Resolution Analysis Used for Partial Discharge Pattern Recognition'; Conference Record of Twenty-Seventh International Power Modulator Symposium; Arlington, USA; 2006; pp 108-111.
151. <http://www.deltaresearch.com/triangle.htm> - accessed on 15<sup>th</sup> October 2010.
152. Stone, G.C.; Kantardziski, P; 'Partial discharge testing of motor and generator windings: An absolute or a comparison test?'; Proceeding of International Symposium on Electrical Insulating Materials; 1998; Toyohashi, Japan; Sept 27-30; pp 63-66.

**Appendix A-1 Comparison of various market available discharge detectors**

Model	Brand	Type of monitoring				Type of Equipment					Sensor Type					Connectivity						Data Display			Other Parameters						
		Offline	On-line	Cont.	Periodic	Motor	Generator	GIS	Tx	Cable	SSC	CC	RC	HFCT	ACC	Serial	USB	FO	GPIB	Ethernet	Modem	Mag.	2D	3D	Inputs	Alarm	Analog O/P	Analog I/P	Stand Alone	PC Based	B/W
PDA IV	IRIS		✓		✓		✓					✓			✓	✓			✓		✓	✓								✓	
TGA-B	IRIS		✓		✓	✓	✓					✓			✓	✓			✓		✓	✓								✓	
TGA-S	IRIS		✓		✓		✓					✓			✓	✓			✓		✓	✓								✓	
PD Trac	IRIS		✓	✓		✓	✓		✓	✓					✓				✓		✓	✓		3	✓	✓	✓	✓			
Hydro Trac	IRIS		✓	✓			✓								✓				✓		✓	✓		12	✓	✓		✓			
Bus Trac	IRIS		✓	✓		✓	✓								✓				✓		✓	✓		9	✓	✓		✓			
Hydro Guard	IRIS		✓	✓		✓	✓									✓			✓		✓	✓	✓	24	✓	✓	✓	✓			
Bus Guard	IRIS		✓	✓		✓	✓									✓			✓		✓	✓	✓	24	✓	✓	✓	✓			
Turbo Guard	IRIS		✓	✓		✓	✓				✓					✓			✓		✓	✓	✓	24	✓	✓	✓	✓			
PDA Premium	ADWEL		✓		✓	✓	✓								✓	✓						✓	✓	6					✓	150MHz	
STB	ADWEL		✓	✓		✓	✓								✓				✓		✓	✓		3	✓	✓	✓	✓			
COPA	ADWEL		✓	✓		✓	✓								✓		✓		✓		✓	✓		96	✓	✓	✓	✓			
PPM-97	ADWEL	✓			✓	✓	✓				Uses ferrite probe																	✓		10MHz	
ICM system	PDD		✓		✓	✓	✓	✓	✓			✓		✓	✓		✓			✓	✓	✓	✓	8					✓	2GHz	
ICM compact	PDD		✓		✓			✓	✓	✓		✓		✓	✓					✓	✓	✓	✓						✓	2GHz	
ICM monitor	PDD		✓	✓		✓	✓	✓	✓	✓		✓		✓	✓		✓			✓	✓	✓	✓	32	✓	✓	✓	✓			
AIA monitor	PDD		✓		✓			✓	✓	✓				✓	✓						✓	✓	✓						✓	2GHz	
TDA compact	PDD	✓			✓				✓	✓	Tan δ Analyser										✓							✓			
HVS 1000	M&B	✓	✓		✓	✓	✓	✓				✓	✓	✓							✓	✓								✓	
PDD/T	M&B		✓		✓	✓	✓	✓					✓	✓	✓						✓	✓							✓		
HVS 2000	M&B	✓	✓		✓	✓	✓	✓					✓	✓	✓						✓	✓							✓		
DD/T	Others		✓		✓														✓		✓	✓		1				✓			
DDX 9101	Others		✓		✓										✓				✓		✓	✓		6+					✓		
DDX 9121	Others		✓		✓										✓				✓		✓	✓							✓		
PD Solver	TECHIMP		✓	✓		✓	✓	✓	✓	✓					✓			✓			✓	✓									1GHz
PD Base	TECHIMP		✓		✓	✓	✓	✓	✓	✓					✓				✓		✓	✓								✓	100MHz
PD Monitor	TECHIMP		✓		✓	✓	✓	✓	✓	✓					✓				✓	✓	✓	✓		9	✓				✓		

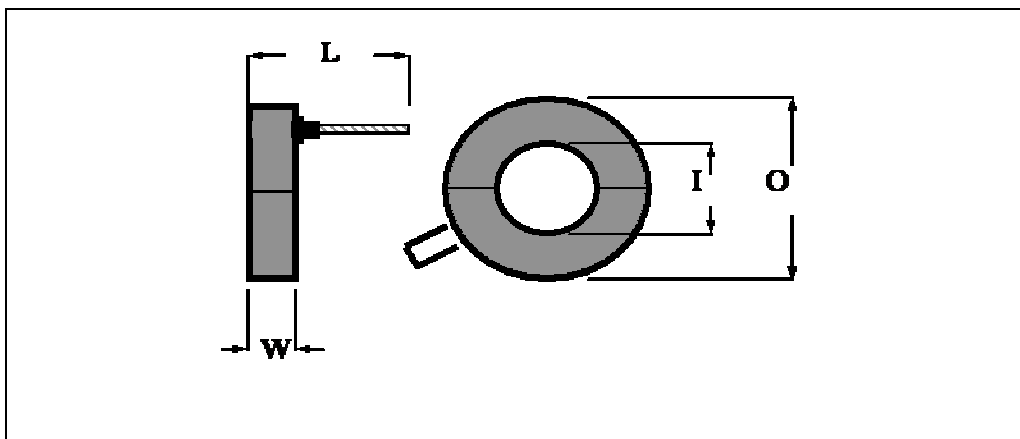
Cont. - Continuous  
 GIS - Gas Insulated Switchgear  
 Tx - Transformer  
 SSC - Stator slot coupler  
 CC - Capacitive coupler  
 RC - Rogoeski coil  
 HFCT - High Frequency Current Transformer  
 ACC - Acoustic sensor  
 FO - Fiber optic  
 Mag. - Magnitude (Qm / NQN / PD value)  
 2D - Pulse height graph / PD against time  
 3D - Phase resolved graph  
 B/W - Bandwidth  
 PDD - PD Diagnostix Systems GmbH  
 M&B - M&B Systems Power Test Equipment  
 Others - Hipotronics / Haefely / Robinson Instruments / Tettex instruments

## Appendix A-2 PDC-85 Rogowski coil datasheet



**DOWDING & MILLS**  
ENGINEERING SERVICES

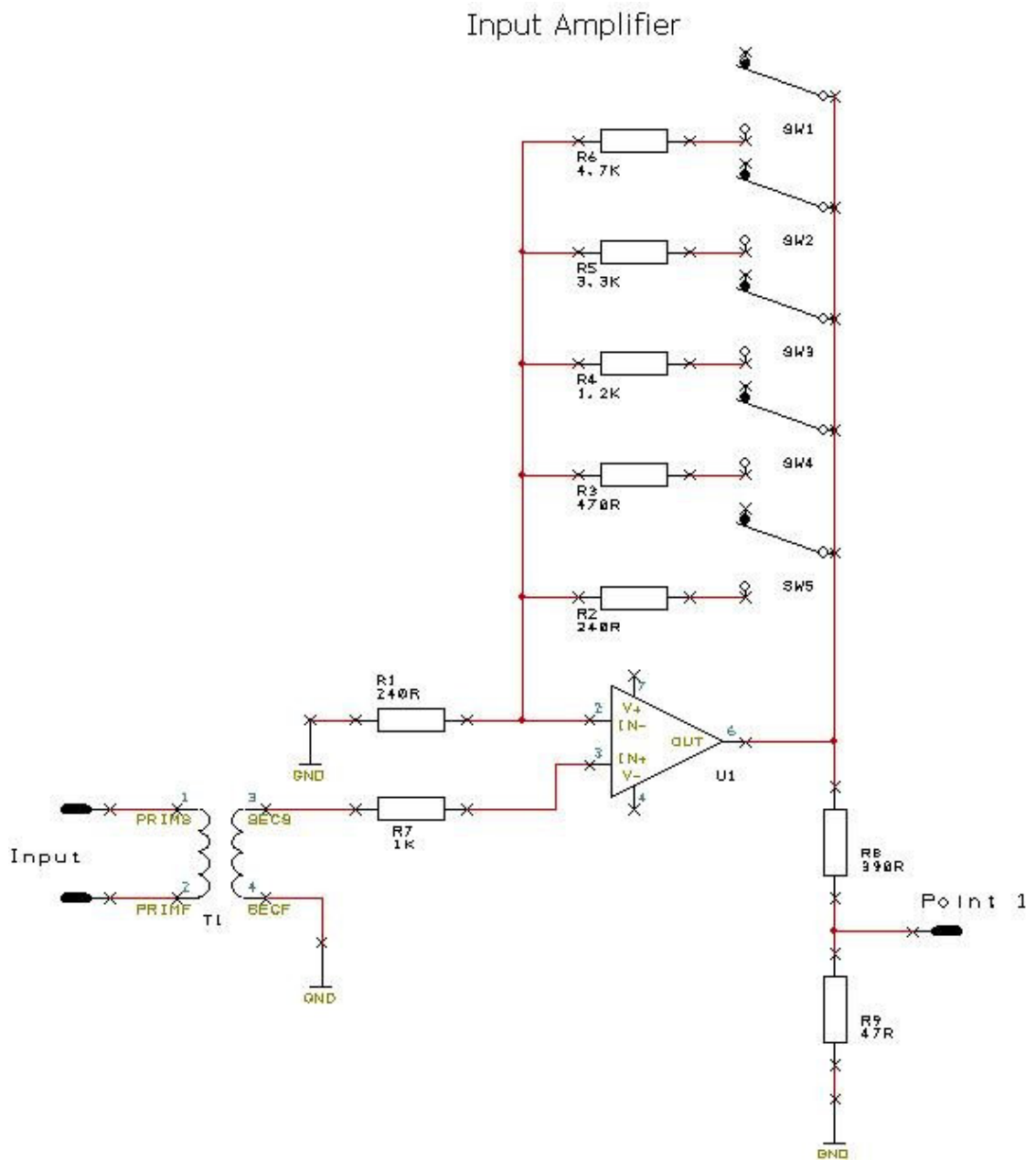
Kirkton Avenue  
Pitmedden Road Ind. Estate  
Dyce. ABERDEEN  
AB21 0BF  
Tel: (44) (0)1224 427200  
Fax: (44) (0)1224 723560



### Rogowski Coil Data Sheet

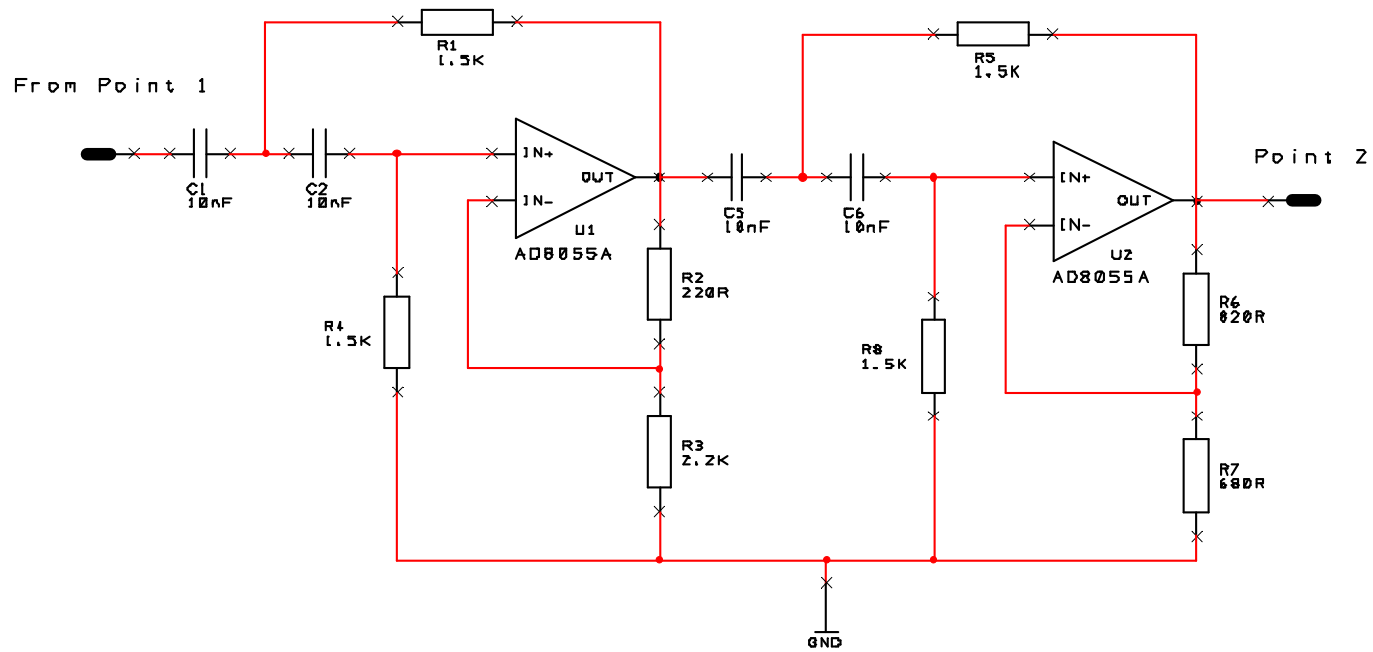
Part No.	PDC - 85
Protection	Ex II 2 G EExe II T6
Operating Temperature Range	-20 to +60°C
Design Approval	BAS00ATEX2051
Standards	BSEN(IEC) 60079-0, 7, 14
Housing Material	Aluminium
Diameter O (outer)	159mm
Dimension I (window)	85mm
Dimension W (depth)	40mm
Dimension L ( Cable Loop)	250mm (Max)
Weight (inc. Cable)	2.3kg
Protection Degree	IP54
Earthing	6mm External Connection
Signal Cable	RG59 GSWB/CSP Cover
Standard Signal Cable Length	3M
Signal Cable Gland	E1XF M16 (Bicc473AA51)
Maximum Current	1000A Primary
Maximum Current	53.8ma Secondary
Open Circuit Voltage	250mV
Sensitivity	0.1mV/A
System Operating Voltage	> 4000v
Energy Dissipation (Worst case)	295J (Short Circuit, 1sec)
Terminating Impedance	50Ω
CTI	800

## Appendix A-3 Circuit diagrams for single channel system



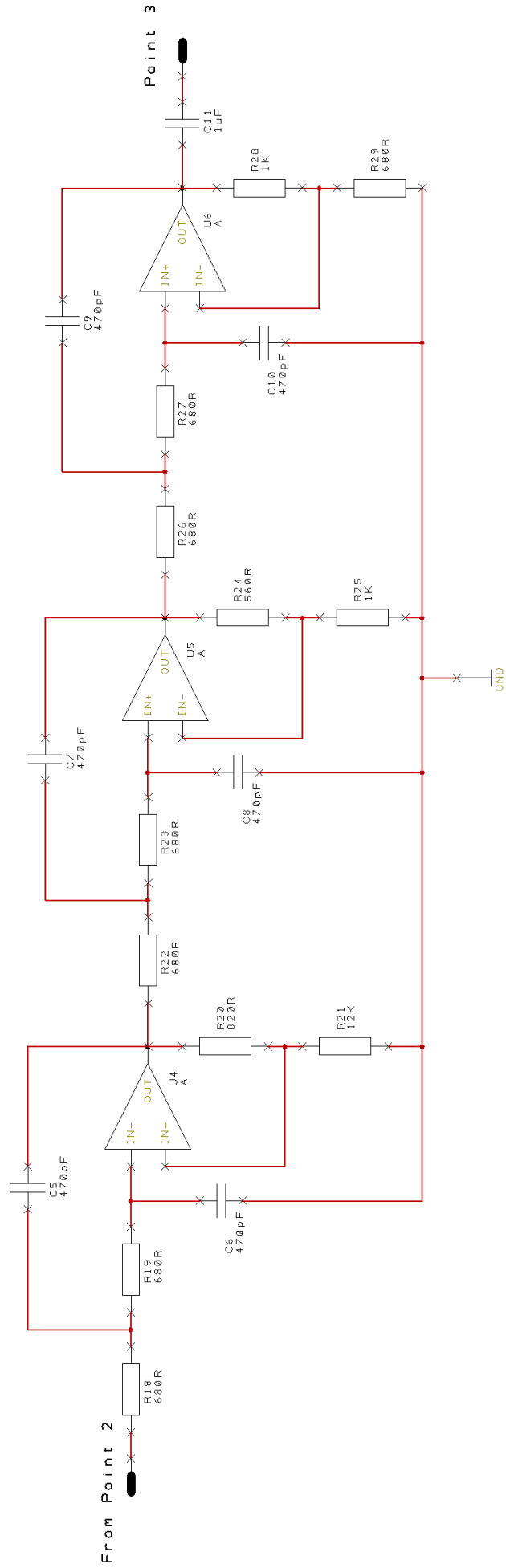
A-3.1 Input amplifier

### 4th Order High Pass Filter



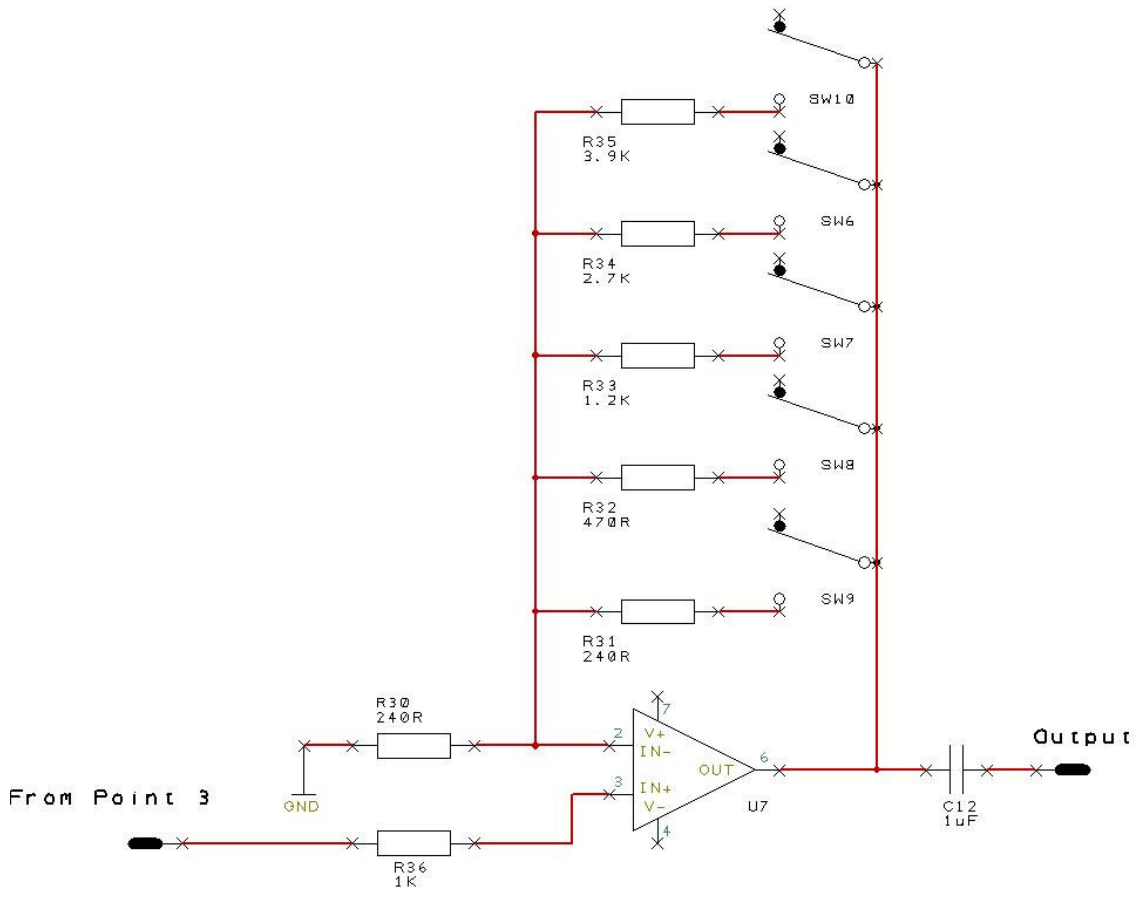
A-3.2 4<sup>th</sup> Order high-pass filter

### 6th Order Low Pass Filter



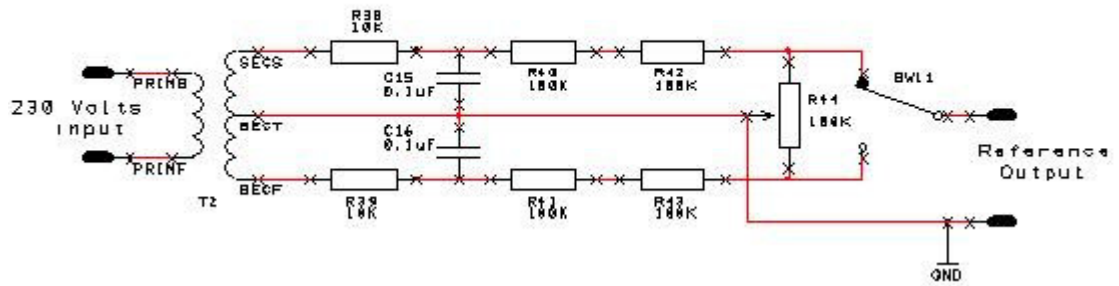
### A-3.3 6th Order low-pass filter

### Output Amplifier



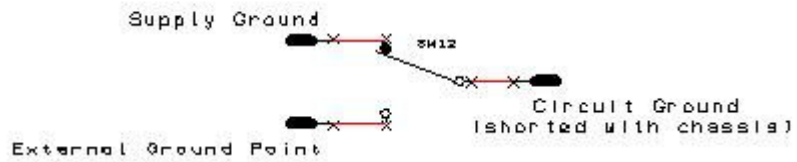
A-3.4 Output amplifier

Reference Signal Circuit



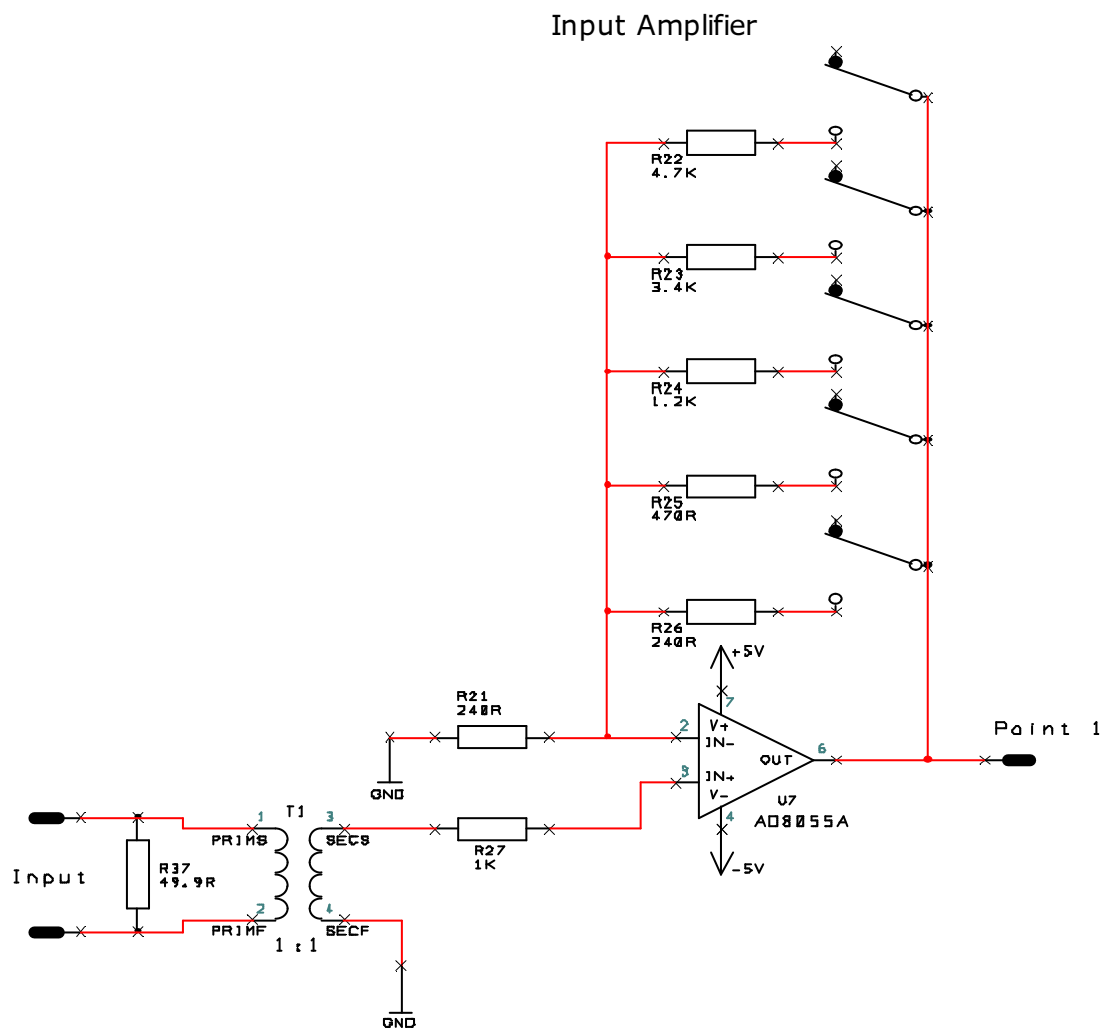
A-3.5 Reference Signal Circuit

Ground Connections



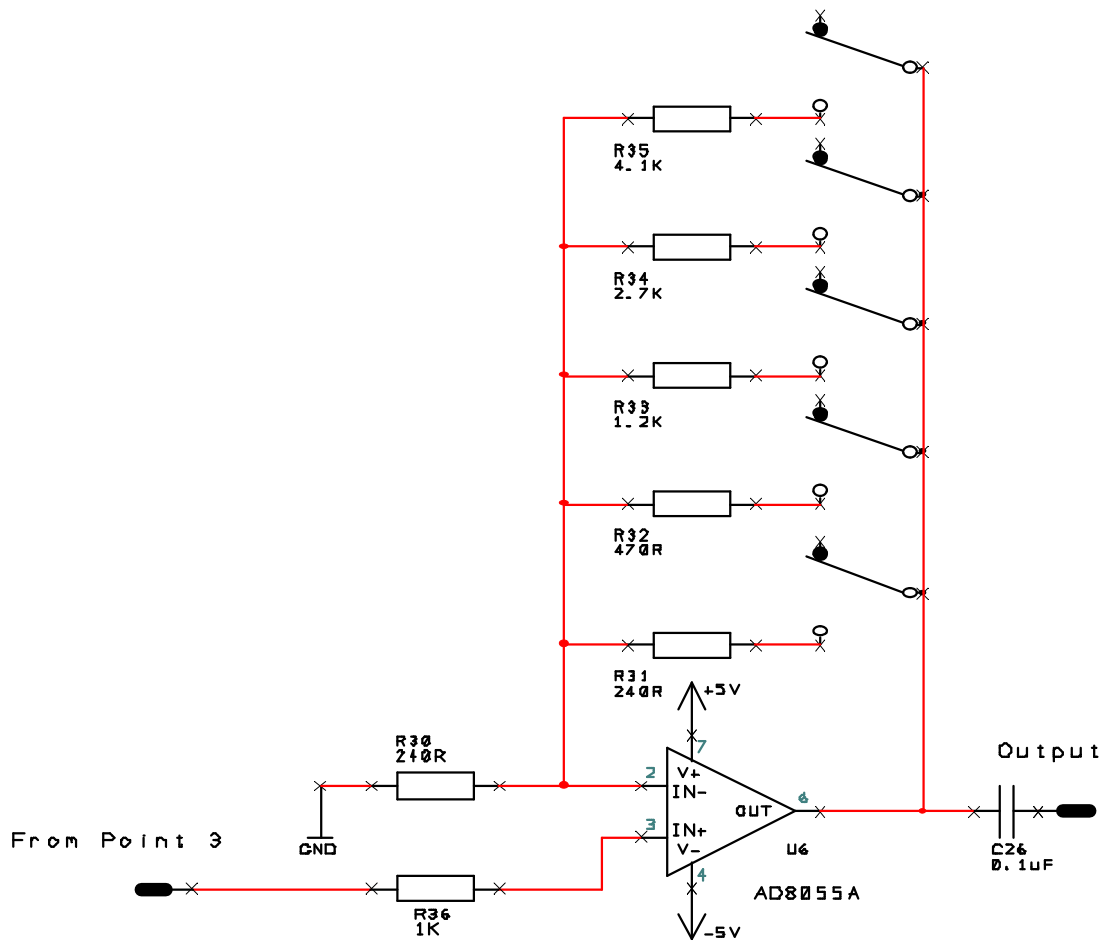
A-3.6 Ground connections

## Appendix A-4 Circuit diagrams for three channel system



A-4.1 Input amplifier

## Output Amplifier



A-4.2 Output amplifier

## Appendix A-5 LabVIEW program details

## A-5.1 Single channel DAQ program

This program is used for acquiring PD data from a single channel along with the reference sine wave for a period of 1 cycle (i.e. 20 ms). The data is acquired with a sampling frequency of 5 Ms/S with a vertical resolution of 8-bits. The Pseudo code for the program is given below.

### Pseudo code

#### ***'Acquire' state***

- i. Configure the DAQ card with acquisition parameters like sampling frequency, no. of samples to be acquired, voltage range, etc.
- ii. Read the voltage input on both channels (i.e. reference channel and PD data channel).
- iii. Display the data from both channels on the graph.

#### ***'Write' state***

- i. Prompt user for a file path and name to store 'reference signal data'.
- ii. Write the reference signal data to the selected location.
- iii. Prompt user input for a file path and name to store 'PD phase data'.
- iv. Write the PD phase data to the selected location.

#### ***'Read' state***

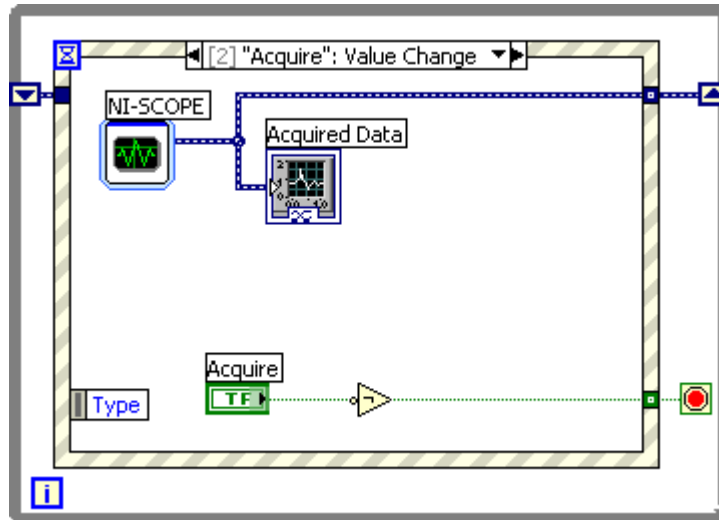
- i. Prompt user to select a file to read the reference signal data.
- ii. Prompt user to select a file to read the PD phase data.
- iii. Read the data from selected files and display them on the same graph.

#### ***'Stop' state***

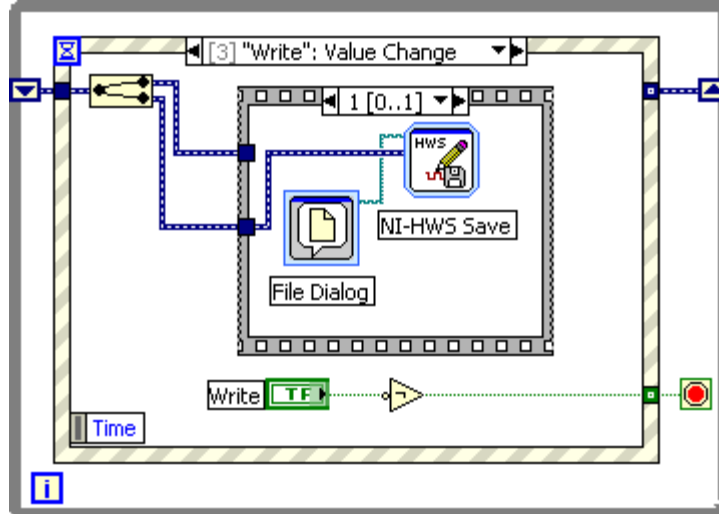
- i. Stop waiting for any user input and exit the program.

The LabVIEW block diagram is shown in figure A-1. The program uses an 'even structure' to detect user input.

### 'Acquire' State



### 'Write' State



### 'Read' State

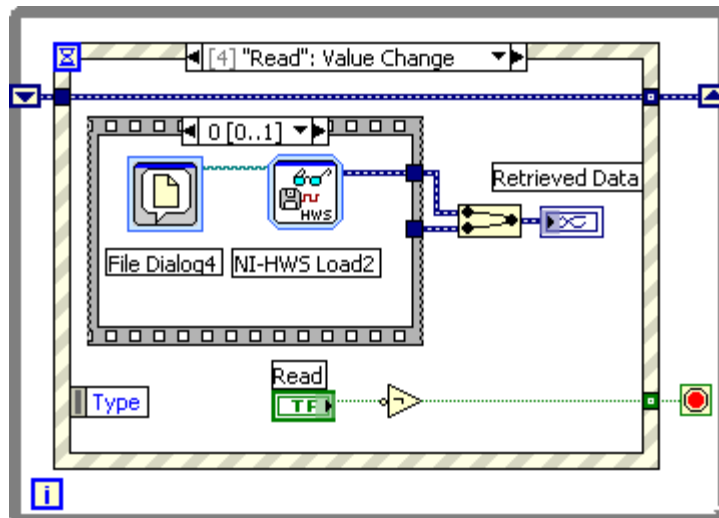


Figure A-1 LabVIEW block diagram - Single channel DAQ program

## **A-5.2 Amplitude based filtering**

This program is used to filter-out any pulses whose amplitudes are beyond the user set threshold. The effectiveness of filtering process can be seen from the time-domain and frequency domain graphs provided. The pseudo code for this program is given below. The LabVIEW block diagram is shown in figure A-2.

### Pseudo code

- i. Prompt user to select a data file to read.
- ii. Read the file and display the original time-domain graph.
- iii. Calculate the Fast Fourier Transform (FFT) of the signal and display the frequency spectrum on the graph.
- iv. Strip the waveform array for analysis.
- v. Compare each element of the array with the set '+ve' & '-ve' threshold limits. If data is within limits then retain the original value else convert the value to '0'.
- vi. Build a new waveform array with the modified values.
- vii. Display the time-domain waveform on the graph.
- viii. Calculate FFT of the new waveform and display the frequency spectrum on graph for comparison.

The original and filtered waveforms are plotted on separate graphs for comparison.

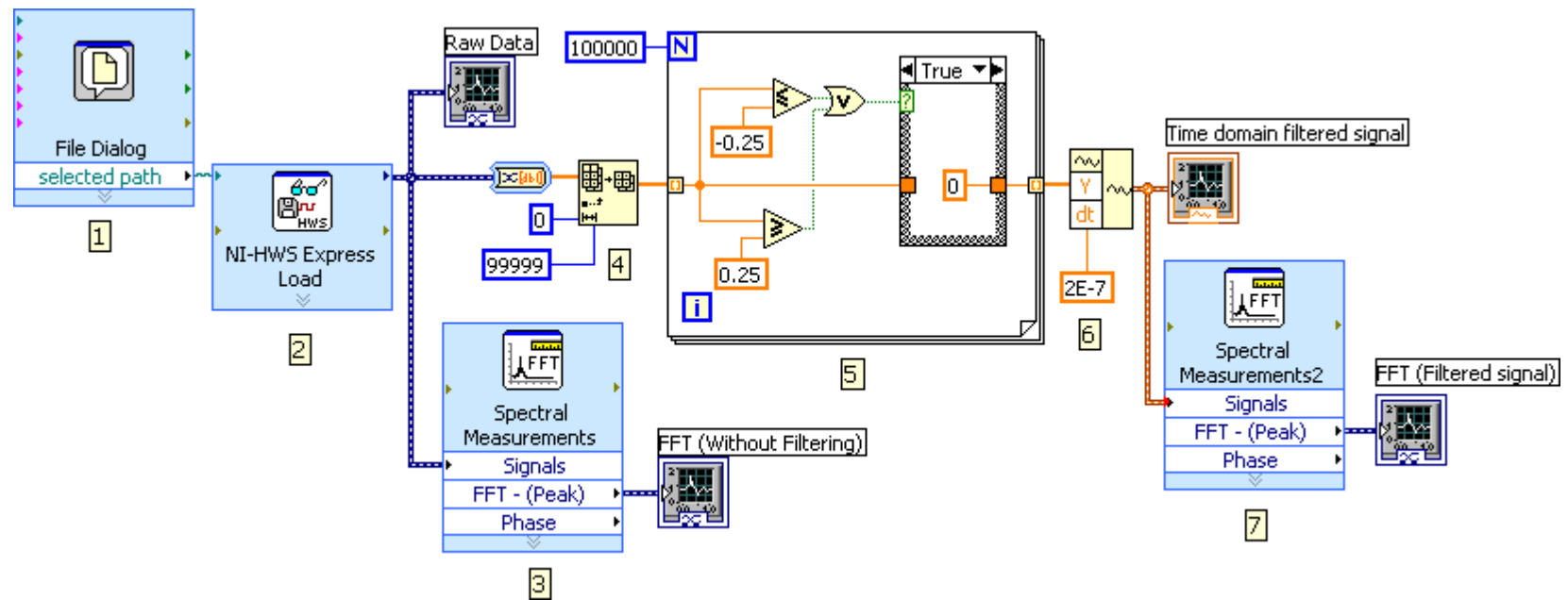


Figure A-2 LabVIEW block diagram for amplitude based filtering technique

### A-5.3 Frequency based filtering

This program calculates the Fast Fourier Transformer of the signal to detect the various frequency components. The highest frequency component (and its harmonics) are thought to be external interference and are filtered out using a series of band-reject filters. The signal also undergoes band-pass filtering (30-300KHz) to eliminate any signals beyond the frequency of interest. The LabVIEW block diagram is shown in figure A-3.

#### Pseudo code

- i. Prompt user to select a data file to read.
- ii. Read the file and display the original time-domain graph.
- iii. Calculate the Fast Fourier Transform (FFT) of the raw signal and display the frequency spectrum on the graph.
- iv. Implement Band-pass filtering (30-300KHz).
- v. Display the band-pass filtered signal in time-domain.
- vi. Calculate FFT of the filtered waveform and display the frequency spectrum on graph for comparison.
- vii. Implement a series of band-reject filters with a bandwidth of 2KHz (up to 7<sup>th</sup> harmonic).
- viii. Display the filtered waveform in time-domain.
- ix. Calculate FFT of the filtered waveform and display the frequency spectrum on graph for comparison.

The original and filtered waveforms are plotted on separate graphs for comparison.

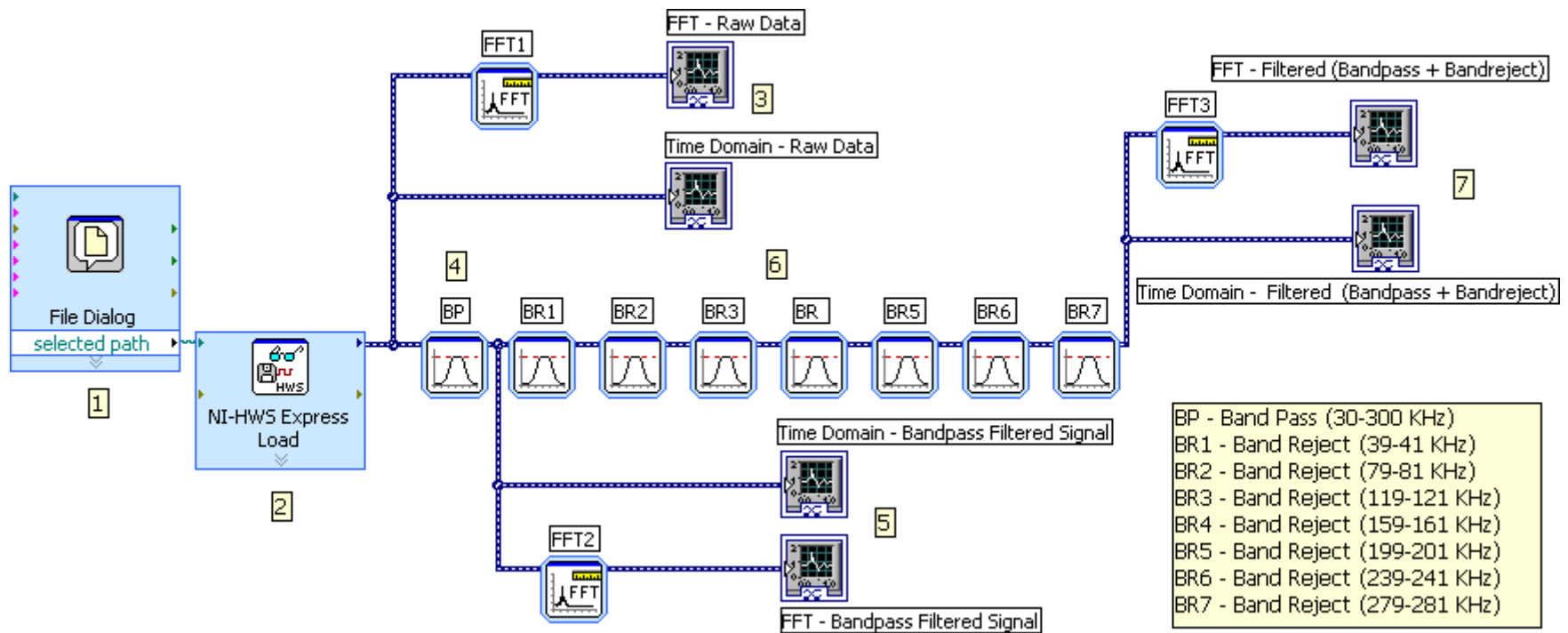


Figure A-3 LabVIEW block diagram for frequency based filtering technique

## **A-5.4 Three phase DAQ program for continuous acquisition**

This program is used for acquiring PD data from all three phases of a machine along with the reference sine wave for a period of 50 cycles (i.e. 1sec). The data is acquired with a sampling frequency of 5 Ms/S with a vertical resolution of 8-bits. The Pseudo code for the program is given below.

### Pseudo code

#### ***'Acquire' state***

- i. Configure both the DAQ cards with acquisition parameters like sampling frequency, no. of samples to be acquired, voltage range, etc.
- ii. Read the voltage input from all four channels for a period of 20ms and display the waveforms on the graphs.
- iii. Continuously keep acquiring and displaying the data (like an oscilloscope) until user presses any other button on the front panel.

#### ***'Write' state***

- i. Acquire data from all four channels for a period of 20 ms.
- ii. Prompt user to provide a file path and name to store reference signal data, followed by red, yellow and blue phase data in a chronological order.
- iii. Write data for 1 cycle for all four channels in the selected file.
- iv. Acquire the next set of PD data (for 20ms) on all four channels and append it to the respective files. Repeat the process 49 times to complete the data set of 50 cycles. (The repeated acquisition takes place automatically and does not require any user input. The acquired cycles are not necessarily consecutive cycles).

#### ***'Read' state***

- i. Prompt user to select files to read in the chronological order of reference signal followed by red, yellow and blue phase data.
- ii. Read the data from selected files and display them on the graph.

#### ***'Stop' state***

- ii. Stop waiting for any user input and exit the program.

The LabVIEW block diagram is shown in figure A-4.

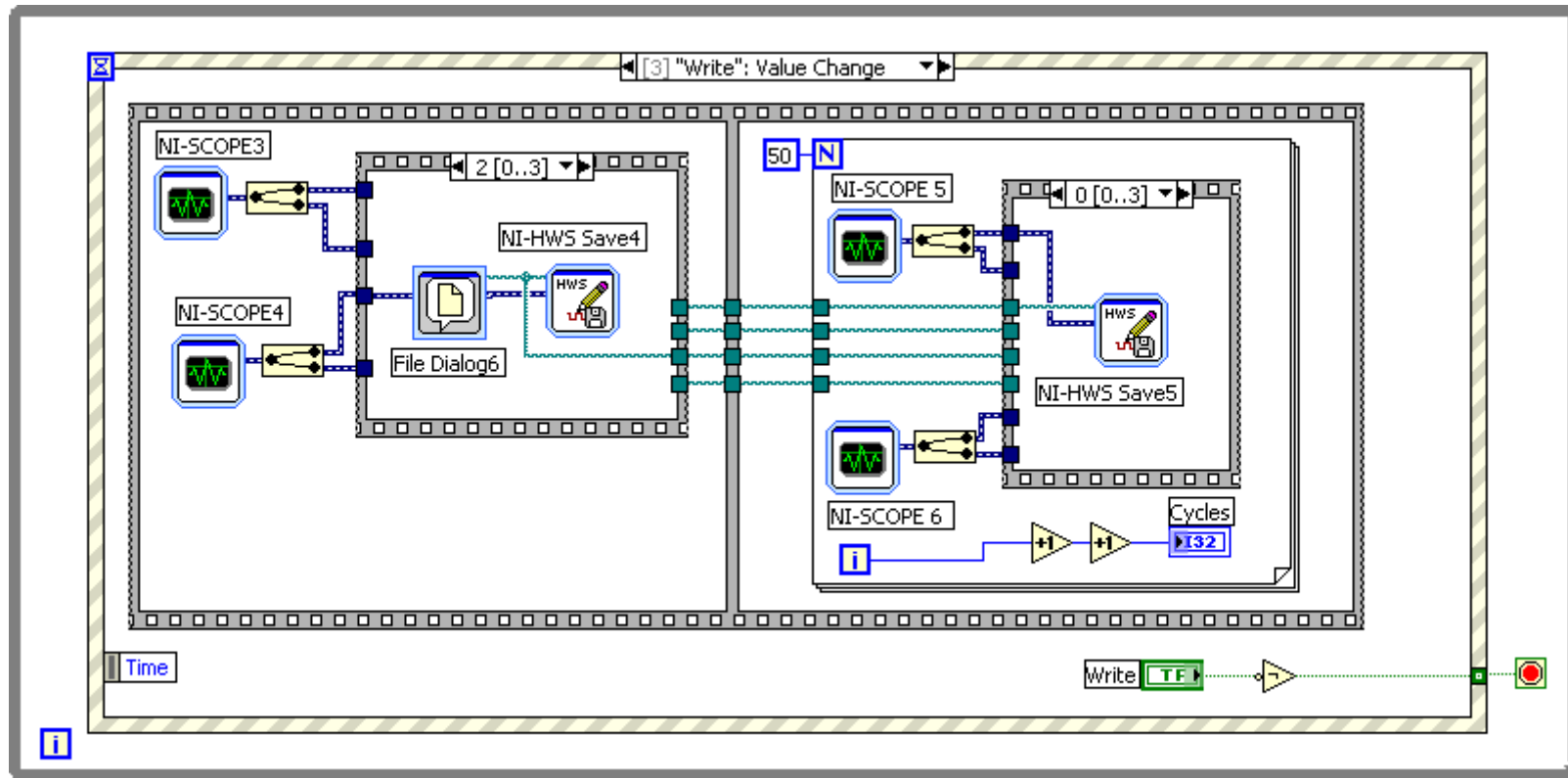


Figure A-4 LabVIEW block diagram - Three phase continuous data acquisition

## **A-5.5 Data compression program**

The original raw data is acquired with a sampling resolution of 5 Ms/S resulting in very large file size. This program compresses the data by selecting the highest sample value in a window of 98 samples. The resultant array is reduced from 100,000 samples to 1024 samples for a period of 20 ms. The reduction factor of 98 is chosen in order to make the data compatible with the existing StatorMonitor® PD analysis software. The LabVIEW block diagram is shown in figure A-5.

### Pseudo code

- i. Prompt user to select a data file to read the reference signal.
- ii. Read the file and display the original waveform on the graph.
- iii. Convert all values from the waveform array to absolute values.
- iv. Divide the complete array into individual sub-arrays with 98 elements in each sub-array. Obtain the index value of the highest element in each sub-array.
- v. Adjust the index values to address the highest values in the original array (i.e. add 98 to second value, 196 to third value and so on).
- vi. Using the index value array, obtain the highest values in every 98 elements of the original array (data resolution reduced by 98 times).
- vii. Build a waveform array with the new 1024 elements and plot them on the graph.
- viii. Repeat steps i-vii for red phase, yellow phase and blue phase.

The original and compressed waveforms are plotted on separate graphs for comparison.

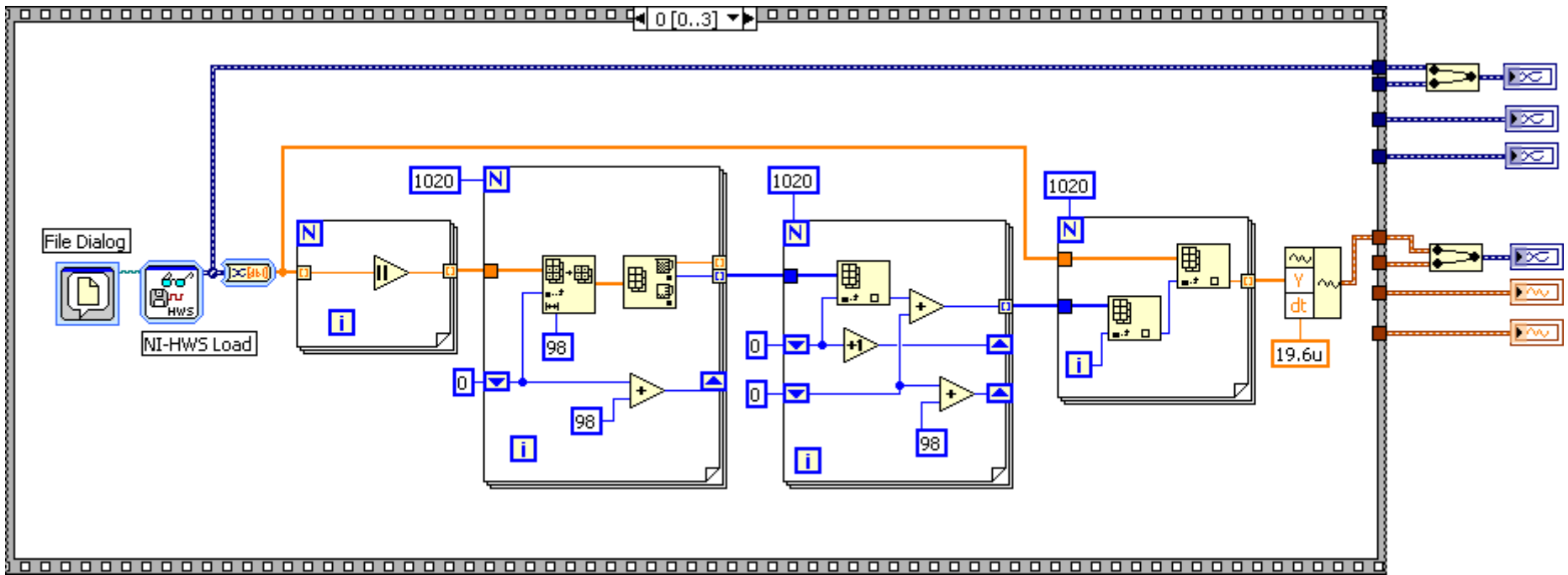


Figure A-5 LabVIEW block diagram – Data compression program

## A-5.6 Three phase USB DAQ program

This software is used to acquire PD data from all three phases of the machine using the NI-USB 5132 DAQ devices. The data is compressed and stored in a format that is compatible with the StatorMonitor PD analysis software. The software consists of a main VI program that calls other sub-VI programs during its execution. The hierarchal diagram of the main VI and sub-VI programs is shown in Figure A-6.

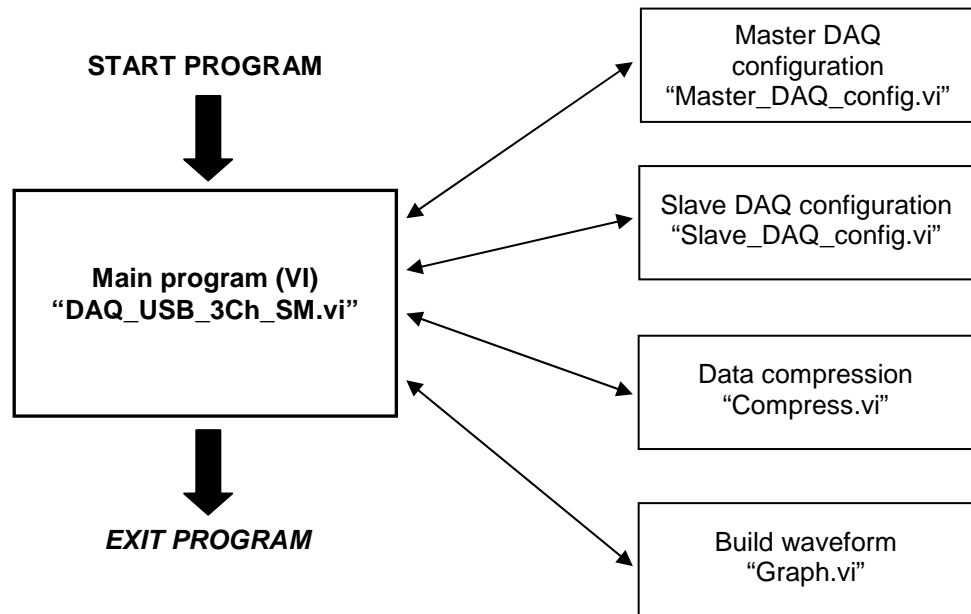


Figure A-6 Software hierarchy diagram for USB DAQ

### Main program ("DAQ\_USB\_3Ch\_SM.vi")

The main program controls the complete execution of the DAQ process based on the user inputs. The program uses the 'state machine architecture' and uses the 'event structure' loop for detecting any user command. The program has four states i.e. 'Acquire', 'Save', 'Read' and 'Exit'. The 'Acquire' function continuously acquires and displays the data like an oscilloscope. The 'Save' function acquires and saves the PD data for 100 cycles. The 'Read' function reads the data from a file for 100 cycles and the 'Exit' function closes the program. The pseudo code for each of the states is given in the following sections.

Pseudo code:

**'Acquire' state**

- i. Configure all the data acquisition channels using 'Master\_DAQ\_config.vi' and 'Slave\_DAQ\_config.vi'.
- ii. Disable all user inputs except 'Stop' button.
- iii. Initiate acquisition and read the voltage input from all four channels for a period of 20ms.
- iv. Convert the waveform array from each channel to numerical scalar array and compress the data using 'Compression.vi'.
- v. Convert the numerical scalar array to waveform array using 'Graphs.vi' and display the compressed data on the graphs.
- vi. Continuously keep acquiring and displaying the data (like an oscilloscope) by repeating steps (iii – v) until user presses the 'Stop' button or an error occurs.
- vii. If user presses 'Stop' button, stop the acquisition process, enable all the user controls and wait for user command.

The LabVIEW block diagram for 'Acquire' state is shown in figure A-7.

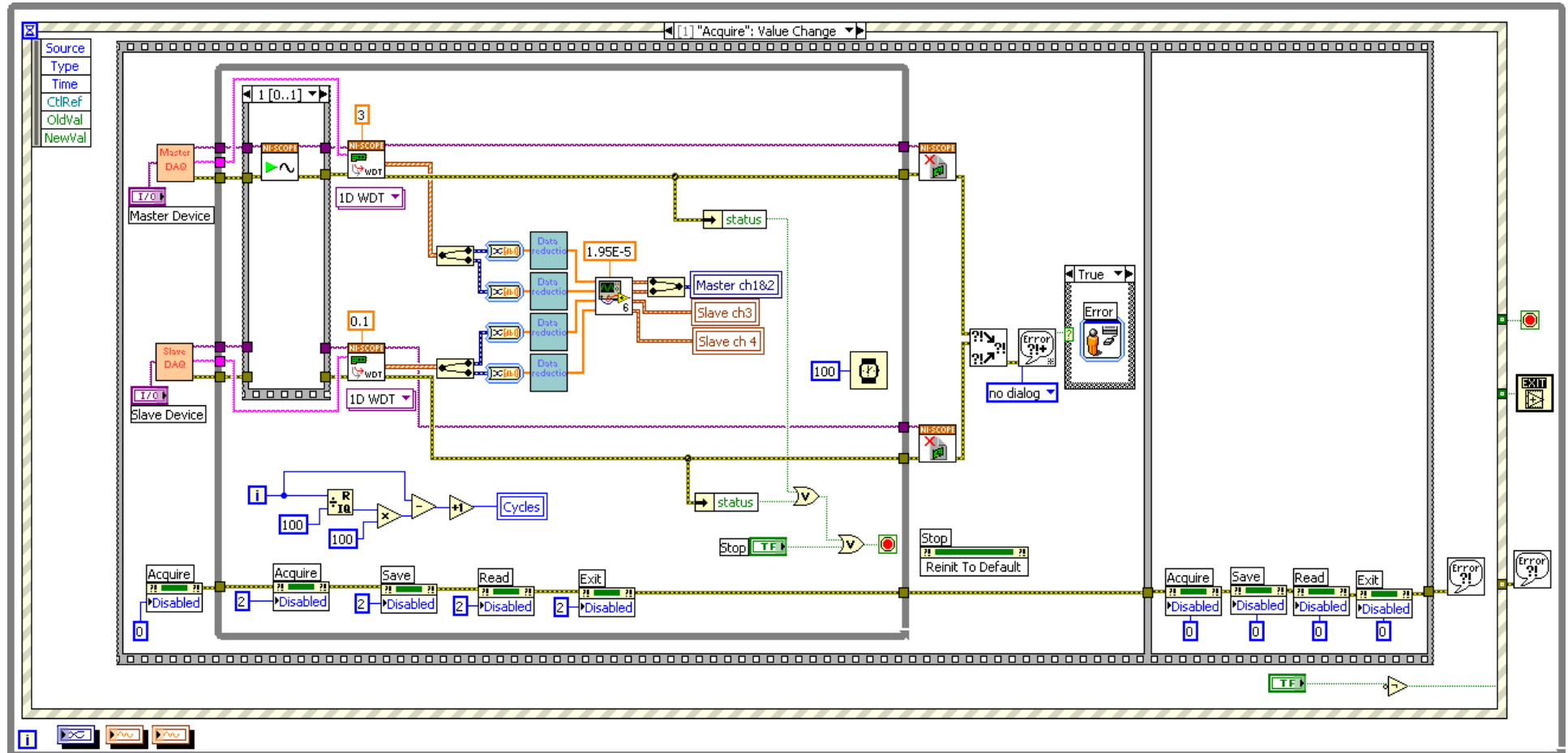


Figure A-7 LabVIEW block diagram – 'Acquire' state for three phase USB DAQ program

Pseudo code:

**'Save' state**

- i. Reinitialise front panel controls to default values. Configure all the data acquisition channels using 'Master\_DAQ\_config.vi' and 'Slave\_DAQ\_config.vi'.
- ii. Disable all user controls until 100 cycles of data is recorded into a file.
- iii. Initiate acquisition and read the voltage input from all four channels for a period of 20ms.
- iv. Convert the waveform array from each channel to numerical scalar array and compress the data using 'Compression.vi'.
- v. Write / append the numerical scalar data from all four channels to a single 2D array in a format compatible to StatorMonitor software.
- vi. Convert the numerical scalar array to waveform array using 'Graphs.vi' and display the compressed data on the graphs.
- vii. Continue the process (steps iii – vi) for 100 cycles; update 'cycles' variable for every iteration of the loop.
- viii. Prompt user to provide a file path and name to store the data in a file.
- ix. Write the data (100 cycles) from the 2D array to the designated file in a binary format (compatible to StatorMonitor system).
- x. On completing file-write, enable all the user controls and wait for user command.

The LabVIEW block diagram for 'Save' state is shown in figure A-8.

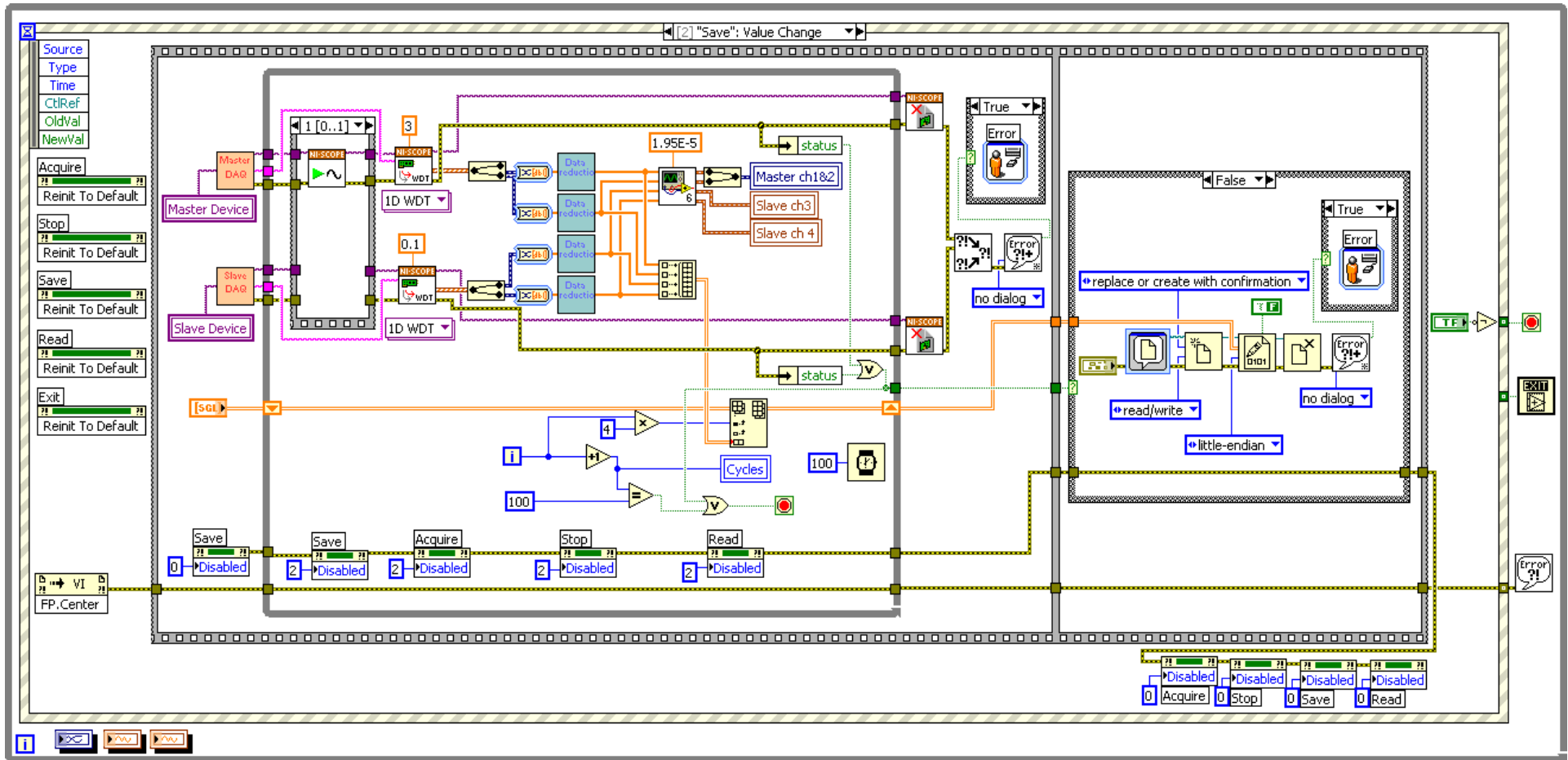


Figure A-8 LabVIEW block diagram – ‘Save’ state for three phase USB DAQ program

Pseudo code:

***'Read' state***

- i. Prompt user to select a binary file to read and load the selected file in the memory.
- ii. Disable all user controls until complete data is read from a file.
- iii. Split the data into four different numerical arrays; each array containing data for 1 channel for a period of 20ms (1 cycle).
- iv. Convert the numerical scalar array to waveform array using 'Graphs.vi' and display the data on the graphs.
- v. Continue the process (steps iii – iv) until all the 100 cycles of data are read from the file.
- vi. On completing data-read, enable all the user controls and wait for user command.

The LabVIEW block diagram for 'Read' state is shown in figure A-9.

***'Exit' state***

- i. Stop all process and exit LabVIEW.

The code for this state is relatively simple and not given here for brevity.

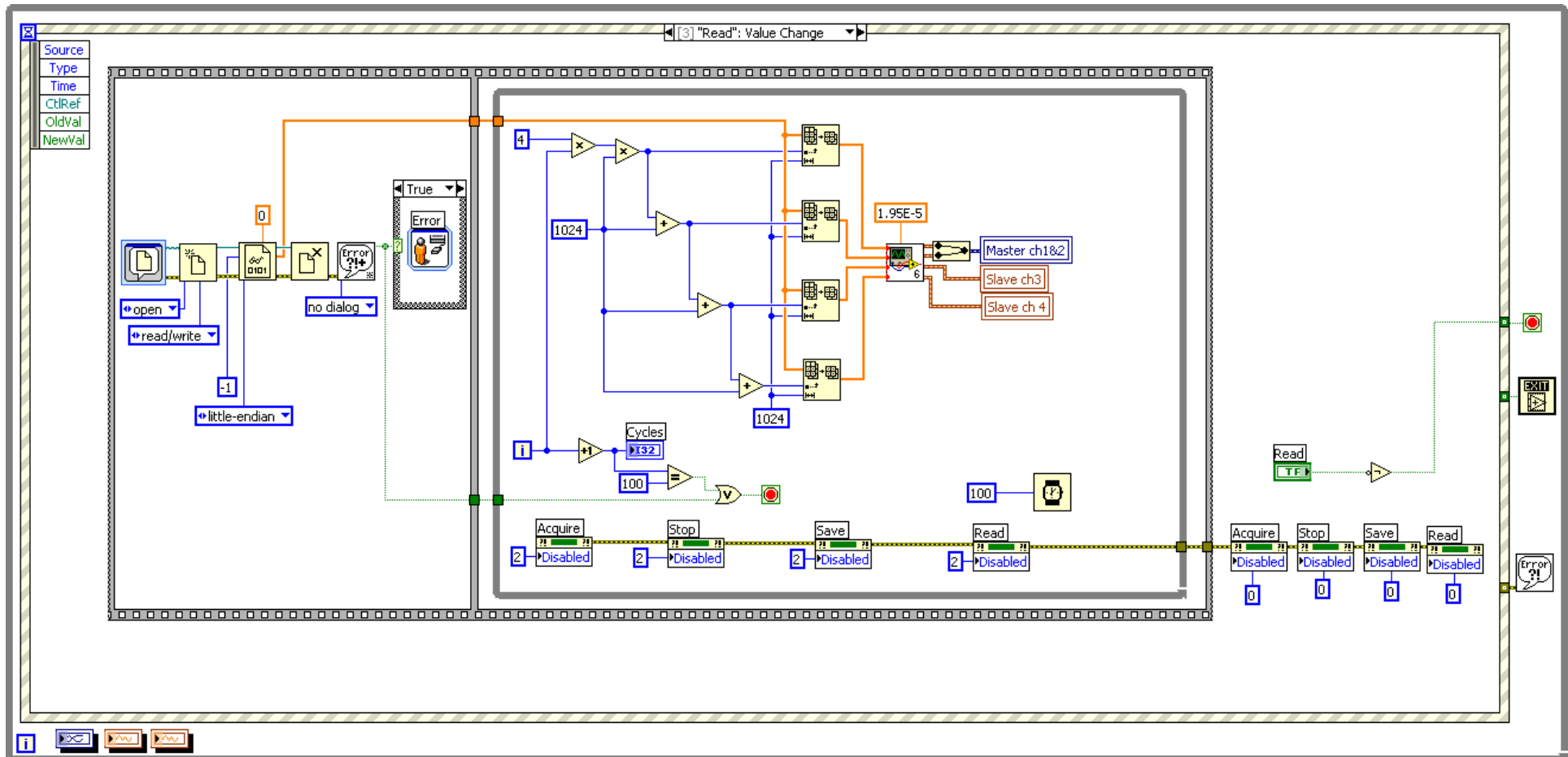


Figure A-9 LabVIEW block diagram – 'Read' state for three phase USB DAQ program

## Master DAQ configuration (“Master\_DAQ\_config.vi”)

The ‘PFI1’ lines on both DAQ are connected together for the purpose of synchronisation. The two USB DAQs are configured in a Master-Slave configuration and synchronized through PFI lines. Both the USB DAQs don’t start the data acquisition simultaneously and there is a small delay between the Master and the Slave. A successful trigger on Channel ‘0’ of Master DAQ card initiates the acquisition on both its channels and also sends a trigger signal to the Slave through PFI line. The Slave initiates the acquisition on receiving a signal on its PFI line. There is a delay (2 sample clock cycles) before the Slave starts to acquire the data. However, this delay is insignificant for the application.

The LabVIEW block diagram for this program is shown in figure A-10. The pseudo code is given below.

### Pseudo code:

- i. Create a new DAQ task for both the channels.
- ii. Configure vertical parameters - coupling and voltage range.
- iii. Configure sampling parameters – no. of samples, sampling frequency, etc.
- iv. Configure trigger parameters – trigger source, trigger level, delay, etc.
- v. Configure ‘PFI1’ as output channel to export trigger signal to slave device.

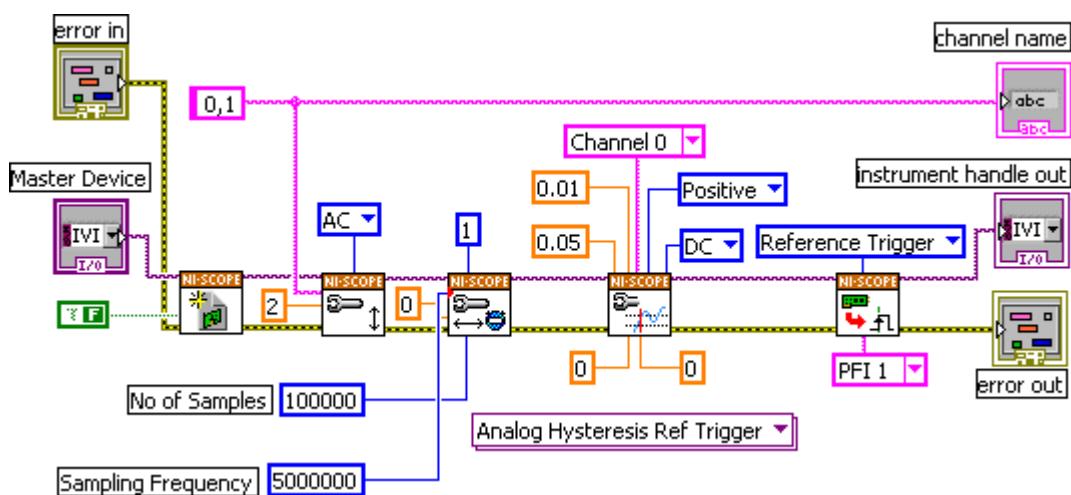


Figure A-10 LabVIEW block diagram for Master\_DAQ\_config.vi

## Slave DAQ configuration (“Slave\_DAQ\_config.vi”)

The slave DAQ card is configured to start the acquisition process on both channels when it receives a trigger signal from the master DAQ card on the 'PFI1' line. The settings for the vertical and horizontal parameters for both the channels are same as that of the Master DAQ channels. As stated earlier there is a small delay (2 sample clock cycles) between the Master and Slave to start the data acquisition. The data is acquired with a sampling rate of 5Ms/s i.e. 100,000 samples/cycle. The data is further compressed by a factor of 98 (preserving the highest value in the dataset of 98) to convert the 100,000 samples/cycle to 1024 samples/cycle. In a worst case scenario, there only will be an error in the first compressed value of the 1024 samples. Again, this can only happen if the highest value in the first 98 samples were to occur in the first two samples. Hence the jitter is considered insignificant for the application.

The LabVIEW block diagram for this program is shown in figure A-11. The pseudo code is given below.

Pseudo code:

- i. Create a new DAQ task for both the channels.
- ii. Configure vertical parameters - coupling and voltage range.
- iii. Configure sampling parameters – no. of samples, sampling frequency, etc.
- iv. Configure trigger parameters – trigger source, trigger level, delay, etc. The trigger source is set to 'PFI1' channel.

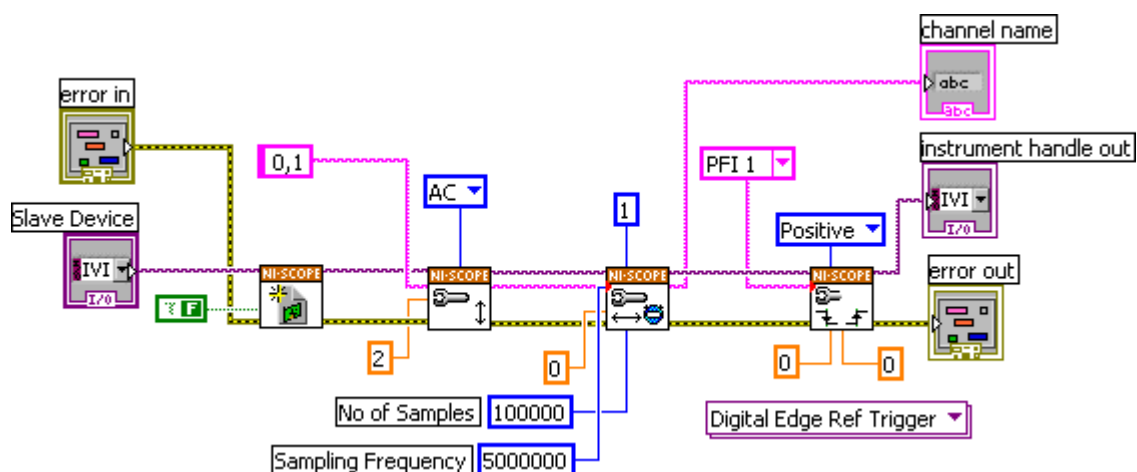


**Figure A-11 LabVIEW block diagram for Slave\_DAQ\_config.vi**

**Data Compression (“Compress.vi”)**

The 'Compress.vi' program is very similar to the data compression program described in Appendix A-5.5; hence is not repeated here.

### Graph display (“Graphs.vi”)

When a waveform data array is converted to numerical scalar array, the amplitude information of the data is preserved but the timing information is lost. In order to display the numerical scalar array on a time base graph, it is necessary to have the timing information. This program adds the timing information to every sample in the scalar numerical array. The LabVIEW block diagram for this program is shown in figure A-12. The pseudo code is given below.

#### Pseudo code:

- i. Read the amplitude value (y-axis) from the numerical scalar array.
- ii. Add the timing information ( $\Delta t$ ) to each element in the array (  $\Delta t = 19.6\mu\text{S}$  in this case to display 1024 values over a period of 20 mS.
- iii. Output the waveform array with timing information added to every element.

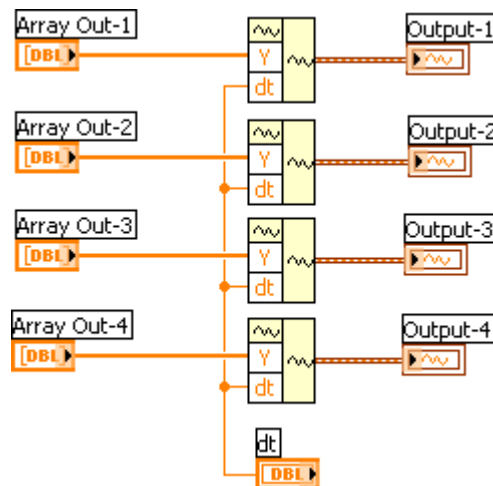
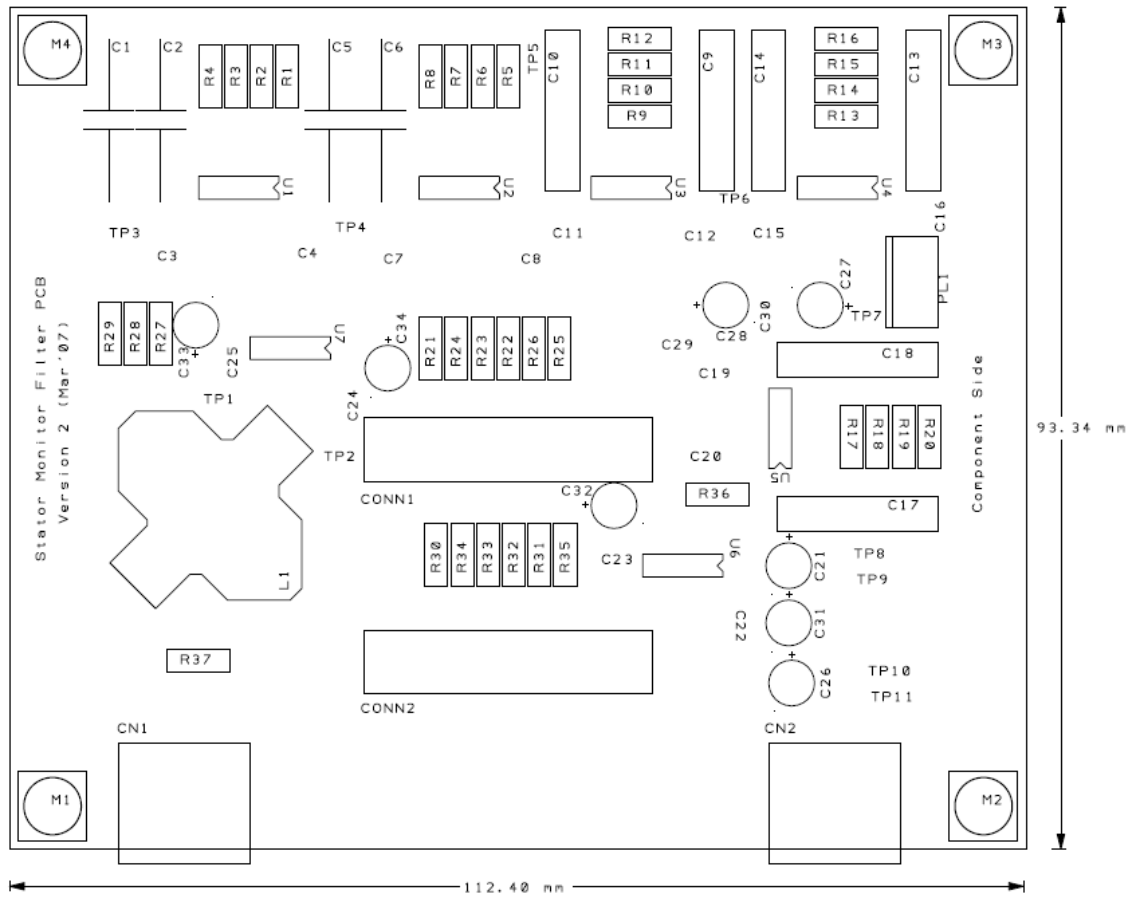


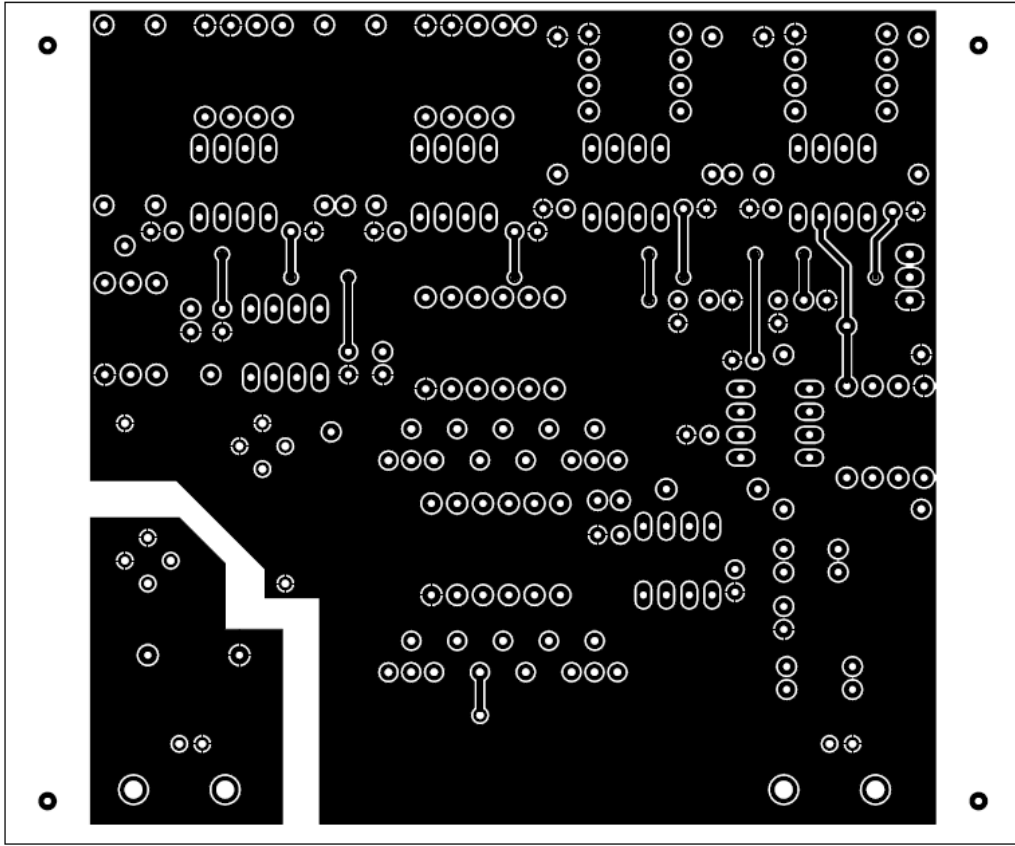
Figure A-12 LabVIEW block diagram – Graph.vi

## Appendix A-6 Printed Circuit Board Details

## A-6.1 Top Silk Layer of PCB



## A-6.2 Top Copper Layer (component side) of PCB



### A-6.3 Bottom Copper Layer (solder side) of PCB

